TECHNISCHE UNIVERSITÄT MÜNCHEN

TUM School of Life Sciences

Metabolomics and bioassay-guided fractionation: integrated strategies to characterize bioactive metabolites secreted by probiotic bacteria

Juliano Roldan Fonseca

Vollständiger Abdruck der von der TUM School of Life Sciences der Technischen Universität München zur Erlangung des akademischen Grades eines

Doktors der Naturwissenschaften

genehmigten Dissertation.

Vorsitzender:	Prof. Dr. Erwin Grill
Prüfer der Dissertation:	1. apl. Prof. Dr. Philippe Schmitt-Kopplin
	2. Prof. Dr. Wilfried Schwab

Die Dissertation wurde am 26.09.2022 bei der Technischen Universität München eingereicht und durch die TUM School of Life Sciences am 06.02.2023 angenommen.

“Whether you think you can, or you think you can't…you're right.”
— Henry Ford

Acknowledgments

First of all, I would like to express my profound gratitude to my supervisor apl. Prof. Dr. Philippe Schmitt-Kopplin for giving me the amazing opportunity to work in his group and use state-of-art instruments and laboratories, for his excitement about science and infinite curiosity, for his guidance, and specially for being a positive force of motivation during tough times. The journey was long and not always like a delightful day of surf in a tropical beach; there were frustrating days, many failed attempts, and disappointing times. Still, what seemed an overwhelming journey – i.e., dealing with multiple and interdisciplinary topics (different from my academic background), failure, managing subprojects, negotiating with people, and in my case learning new languages – turned out to be the most important personal and professional development stage of my life. I did not become a better analytical chemist only, but a Scientist and a better person. Again, thanks immensely.

Having said that, I want to thank Dr. Norbert Hertkorn for sharing his knowledge, creative ideas, and for providing support in NMR spectroscopy. Also, many thanks to Dr. Istvan Gebefugi for taking his time for scientific discussions and, together with Dr. Agnes Fekete, for making sure I was feeling at home when I arrived in Munich.

My sincere thanks go to all BGC colleagues who shared their student time with me (I really mean all). You became my friends and family and were the only ones who really understood what I was doing in Germany (non-academic friends and family used to ask: are you still a student? Do you have a salary? Are you developing a new drug? How do you survive winter?). You probably know what I mean. They are Alesia Walker, Jenny Uhl, Michael Witting, Franco Moritz, Sara Forcisi, Dimitris Tziotis, Kilian Wörmann, Constanze Müller, Lemia Boutegrabet, and Yu He. I apologize if I forgot to mention some of you.

Special thanks to Dr. Marianna Lucio for her friendship and dedication to help me on statistical data analysis, as well as Dr. Mourad Harir for his kind scientific support and special attention given to the treatment of my FT-ICR MS data. Thanks to Dr. Basem Kanawati for his guidance and support during FT-ICR MS measurments, and to Brigitte Look for her the technical assistance.

Also great thanks to all reserach partners: Prof Dr. Anton Hartmann, Prof. Dr. Susanne Krauss-Etschmann, Inge Kepert, Kerstin Hochwind, and all scientists and students that collaborated with me directly or indirectly in projects and publications, including everyone involved in the “Chemostat Project” and bacterial quorum sensing research – topic which is

not the focus of this thesis but have generated two scientific publications and a nice work on sample preparation using magnetic nanoparticles.

Many thanks for the financial and professional support from Helmholtz Zentrum München and to Winclove Probiotics B.V. for providing bacteria strains, scientific information, and financial support to go to conferences.

My most significant thanks go to my life partner Raffaela as she held on with me through many of the ups and downs of the PhD process, shared in the anxieties and hopes while not understanding my work and what I was trying to do. The same is valid for my parents Cida and David whom I also thanks for their unconditioned love and hard work to make sure their children (my brother Luciano and I) succeed in school and in the world of higher education. It is not easy for them to have a son living far away from home (approx. 11.000 km), but they gave me the freedom to pursue what I want.

Summary

Allergies, inflammatory bowel disease and type 1 diabetes are highly prevalent in industrialized countries and are expected to increase for the next decades. Since autoimmune diseases are treatable but hardly curable, there has been a clear market demand for alternative therapies to pharmaceuticals products such as probiotic bacteria cocktails. Added to foods and drinks, or taken as supplement in capsules, powder or liquid formulations, probiotic products are widely consumed and their health benefits have been continuously claimed. At the same time, due to ambiguous scientific findings, such claims have been challenged by health authorities.

Due to the lack of information about probiotic derived substances on which heath claims are based, the aim of this work was to chemically characterize probiotic culture supernatants from different commercial strains and to identify potential bioactive compounds present in supernatants that showed immunomodulatory activity *in vitro*. For that, a combination of holistic metabolomics using Fourier Transform Ion Cyclotron Resonance Mass Spectrometry and classical bioassay-guided fractionation followed by chemical characterization of bioactive fractions was applied.

The work described in this thesis shows the potential of non-target metabolomics to reveal differences between immunomodulatory active and non-active probiotic culture supernatants. Based on unique and statistically relevant detected mass features, it was possible to identify the most populated metabolic pathways in each class of samples, where the tryptophan pathway was overrepresented in the class of bioactive supernatants. Following that, classical bioassay-guided fractionation revealed D-tryptophan as a newly identified secreted molecule that showed bioactivity not only *in vitro* but also *in vivo*, where it ameliorated allergic airway inflammation and hyperresponsiveness in mice. This discover generated a patent granted to Helmholtz Zentrum München and two scientific publications.

Motivated by that result, an enantioseparation method with selective detection (UHPLC-MS) was established to simultaneously quantify a wide range of D- and L-amino acids in biological samples, which was published and can be used by the scientific community to support future research on the unexplored applications of D-amino acids.

The findings presented here are just the “tip of the iceberg” and reinforce the importance of gut microbiome to the body, contributing to more than a century of research on probiotics. After proper safety investigation, tailored bacterial products could be exploited as an

alternative therapy not only for chronic immune diseases but also for a broader spectrum of diseases. I encourage deeper research on probiotics secreted components, which might be the source of new pharmacological substances and consequently, boost acceptance from health authorities on probiotic health claims.

Zusammenfassung

Allergien, chronisch-entzündliche Darmerkrankungen (CED) und Diabetes sind in den Industrieländern weit verbreitete Krankheiten und werden in den nächsten Jahrzehnten voraussichtlich weiter stark zunehmen. Da Autoimmunerkrankungen zwar behandelbar, aber kaum heilbar sind, gibt es eine starke Nachfrage nach alternativen Behandlungstherapien zu pharmazeutischen Produkten, wie beispielsweise den weit verbreiteten probiotischen Bakterienkulturen. Probiotika werden in (sehr) großem Umfang als Zusatz in Nahrungsmitteln und Getränken, oder als Kapseln, Pulver oder Flüssigformulierungen konsumiert, und es werden Ihnen kontinuierlich gesundheitsfördernde Wirkungen zugeschrieben. Gleichzeitig werden diese positiven Auswirkungen auf die menschliche Gesundheit aufgrund ambivalenter Forschungsergebnisse von den Gesundheitsbehörden in Frage gestellt.

Da es an Informationen zu Wirkstoffen mangelt, die aus Probiotika stammen und auf denen gesundheitsfördernde Wirkungen basieren, war das Ziel dieser Arbeit, probiotische Zellkulturüberstände verschiedener kommerzieller Stämme chemisch zu charakterisieren und potenzielle bioaktive Verbindungen, die *in vitro* eine immunmodulatorische Aktivität zeigen, zu identifizieren. Dafür wurde eine Kombination aus holistischen Metabolom Analysen mittels Fourier-Transform Ionenzyklotronresonanz Massenspektrometrie und klassischer wirkungsorientierter Fraktionierung mit anschließender chemischer Charakterisierung der bioaktiven Fraktionen angewandt.

Die Ergebnisse dieser Arbeit verdeutlichen das Potenzial von Non-Target-Metabolomics, um Unterschiede zwischen immunmodulatorisch aktiven und nicht-aktiven probiotischen Kulturüberständen aufzudecken. Anhand von einzigartigen und statistisch relevanten Massensignalen war es möglich, die am dichtesten besiedelten/Hauptstoffwechselwege/am häufigsten vorkommenden Stoffwechselwege in jeder Klasse von Überständen zu identifizieren. Dabei war in der Klasse der bioaktiven Überstände der Tryptophan-Stoffwechselweg überrepräsentiert. Die klassische wirkungsorientierte Fraktionierungsstrategie ergab, dass D-Tryptophan ein sekretiertes Molekül ist, das in unserem In-vitro-Screeningsystem Bioaktivität zeigte und auch allergische Atemwegsentzündungen und Hyperreagibilität bei Mäusen verbesserte. Für diese Entdeckung wurde ein Patent an das Helmholtz Zentrum München vergeben und zudem wurden die Ergebnisse in zwei wissenschaftlichen Publikationen veröffentlicht.

Motiviert durch diese Erkenntnisse wurde eine Enantiomerentrennungsmethode mit selektiver Detektion (UHPLC-MS) entwickelt, die es ermöglicht ein breites Spektrum von D- und L-Aminosäuren in biologischen Proben gleichzeitig zu quantifizieren. Diese Methode wurde ebenfalls veröffentlicht und kann die zukünftige Erforschung neuer Anwendungsbereiche von D-Aminosäuren unterstützen.

Die hier vorgestellten Ergebnisse stellen nur die „Spitze des Eisbergs“ dar und unterstreichen die Bedeutung des Darmmikrobioms für den menschlichen Körper, wodurch Sie einen wichtigen Beitrag zur der mehr als ein Jahrhundert langen Erforschung von Probiotika leisten. Nach gründlicher Unbedenklichkeitsprüfung könnten maßgeschneiderte bakterielle Produkte als alternative Therapie nicht nur für chronische Immunerkrankungen, sondern auch für ein breiteres Spektrum von anderen Krankheiten genutzt werden. Ich ermutige zu einer vertieften Forschung an sekretierten Substanzen aus Probiotika, die der Ursprung für neue pharmakologische Wirkstoffe sein können, und möchte daher die Akzeptanz von gesundheitsbezogenen Angaben zu Probiotika bei Gesundheitsbehörden erhöhen.

Table of Contents

List of Tables

List of supplementary tables

List of Figures

List of supplementary figures

List of abbreviations

AA	*Amino acid*
AAI	*Allergic airway disease*
ACN	*Acetonitrile*
AHL	*N-acylhomoserine lactone*
ANOVA	*Analyse of variance*
CDM	*Chemically defined media*
CV	*Coefficient of variance*
DC	*Dendritic cells*
EIC	*Extracted ion chromatogram*
ESI+ / ESI–	*Electrospray ionization positive / negative mode*
FAO	*Food and Agriculture Organization of the United Nations*
FLD	*Fluorescence detector*
Foxp3	*Forkhead box p3*
FT-ICR MS	*Fourier transform ion cyclotron resonance mass spectrometry*
HPLC	*High performance liquid chromatography*
HMDB	*Human Metabolome Database*
IDO	*Indoleamine 2,3-dioxygenase*
KEGG	*Kyoto Encyclopedia of Genes and Genomes*
LGG®	*Lactobacillus rhamnosus GG*
MS	*Mass spectrometry*
m/z	*Mass-to-charge ratio*
MeOH	*Methanol*
MNPs	*Magnetic nanoparticles*
NMR	*Nuclear magnetic resonance*
NP	*Natural Products*
OPLS-DA	*Orthogonal Partial least square discriminative analysis*
PCA	*Principle component analysis*
PDA	*Photodiode Array Detector*
PFP	*Pentafluorophenyl stationary phase (chromatography)*
ppm	*Parts per million*
R^2	*Coefficient of determination*
RP	*Reversed phase (chromatography)*
SLC6A14	*Solute carrier family 6 amino acid transporter member 14*
SPE	*Solid phase extraction*

S/N	*Signal-to-noise ratio*
Suppl.	*Supplementary information*
TIC	*Total ion chromatogram*
Treg	*Regulatory T*
Trp	*Tryptophan*
tR	*Retention time (chromatography)*
UHR-TOF MS	*Ultra-high resolution time of flight mass spectrometry*
UPLC®	*Ultra performance liquid chromatography*
UV	*Ultraviolet*
WHO	*World Health Organization*
w/w	*weight/weight*

Scientific Communication

Publications

1. **Juliano Fonseca,** Marianna Lucio, Mourad Harir, Philippe Schmitt-Kopplin (2022). Mining for Active Molecules in Probiotic Supernatant by Combining Non-Targeted Metabolomics and Immunoregulation Testing. *Metabolites* 12: 35.

2. **Juliano Fonseca**, Inge Kepert, Constanze Müller, Katrin Milger, Kerstin Hochwind, Matea Kostric, Maria Fedoseeva, Caspar Ohnmacht, Stefan Dehmel, Petra Nathan, Sabine Bartel, Oliver Eickelberg, Michael Schloter, Anton Hartmann, Philippe Schmitt-Kopplin, Susanne Krauss-Etschmann (2017). D-Tryptophan from probiotic bacteria influences the gut microbiome and allergic airway disease. *Journal of Allergy and Clinical Immunology* 139: 1525-35.[1]

3. **Fonseca JR**, Müller C, Rock TM, Krauss-Etschmann S & Schmitt-Kopplin P (2014) Enantioseparation and selective detection of D-amino acids by ultra-high-performance liquid chromatography/mass spectrometry in analysis of complex biological samples. *Journal of Chromatography A* 1324: 109–114.

4. Buddrus-Schiemann, Katharina, Martin Rieger, Marlene Mühlbauer, Maria Vittoria Barbarossa, Christina Kuttler, Burkhard A. Hense, Michael Rothballer, Jenny Uhl, **Juliano R. Fonseca**, Philippe Schmitt-Kopplin, Michael Schmid, Anton Hartmannet. (2014). Analysis of N-Acylhomoserine Lactone Dynamics in Continuous Cultures of Pseudomonas Putida IsoF by Use of ELISA and UHPLC/qTOF-MS-Derived Measurements and Mathematical Models. *Analytical and Bioanalytical Chemistry* 406: 6373–83.

5. Cataldi TRI, Bianco G, **Fonseca J** & Schmitt-Kopplin P (2013). Perceiving the chemical language of Gram-negative bacteria: listening by high-resolution mass spectrometry. *Analytical and Bioanalytical Chemistry* 405: 493–507.

[1] Patent granted to Helmholtz Zentrum München Deutsches Forschungszentrum für Gesundheit und Umwelt (GmbH). Krauss-Etschmann, S.; Hartmann, A.; Schmitt-Kopplin, P.; Schloter, M. Methods and compositions for treating inflammatory diseases. US patent 10,857,128. December 8, 2020.

1

General introduction

It has been estimated that human body contains about 100 trillion microbe cells, including viruses, microbial eukaryotes and prokaryotes, which encode more than 150-fold unique genes than our own genome. Ninety-nine per cent of those microorganisms are bacteria and the majority resides in the gut (~500-1000 species) - followed by the skin - living in mutualistic and symbiotic relationship, playing a vital role in human nutrition, physiology, and health (Sommer and Bäckhed 2013). Besides recent criticism on how those numbers were calculated and were over cited in the literature, the new claim that the ratio of bacteria to human cells in our body is more likely to be 1:1 rather than 10:1 (or even 100:1 sometimes stated) does not change the importance of the subject host-microbiota interactions (Sender et al. 2016). Bacteria genes encode metabolic pathways that are important for human life, involving degradation of indigestible polysaccharides, fermentation of sugars into short-chain fatty acids, and provision of amino acids and vitamins (Qin et al. 2010; Gill et al. 2006 ; Eckburg et al. 2005). Additionally, our microflora protects intestinal epithelial cells against injury (Zhan et al. 2013), influence host gene expression involved in fat storage (Delzenne et al. 2011), and occupy potential pathogens attachments sites competing for nutrients preventing infections and diseases (Keeney and Finlay 2011). For all these reasons, it seems appropriate to view humans as a “super-organism” representing a combination of human and microbial DNAs and whose metabolism depends on bacteria contributions, sharing an immense diversity of substances and beneficial relationships (Goodacre 2007; Sekirov and Finlay 2006).

The colonization of our body by microbes occurs immediately after birth, mainly due contact with the flora present in the mother´s birth canal and through breast milk. The sterile infant gut begins to be colonised by facultative anaerobes and strict anaerobes bacteria such as enterobacteria and bifidobacteria - although differences in composition occurs due infections, sanitary conditions, or formula-fed diet for example (O'Hara and Shanahan 2006; Mountzouris et al. 2002) - and develops during a lifetime been affected by age, diet, health status, use of medication, life style, among others (**Figure 1.1**). By tracking two individuals daily over the period of 1 year, David et al. observed the overall microbial community in gut, i.e., 75-90% bacteria, last stable for months, but the intake of fiber-rich foods, citrus, yogurt, infections, and travels can shape the gut microbiota within a single day (David et al. 2014).

Bacteria living in the human gastrointestinal tract (GI) achieve the highest cell densities recorded for any ecosystem rising to an estimated 10^{11} –10^{12} bacteria per gram of colonic content in the large intestine, which comprises approximately 60% of faecal mass. The most common genera are *Bifidobacterium, Clostridium, Bacteroides, Eubacterium, Escherichia, Enterococcus, Streptococcus, and Klebsiella.* This complex microworld has a profound effect in human health being associated with a variety of disease states (O'Hara and Shanahan 2006).

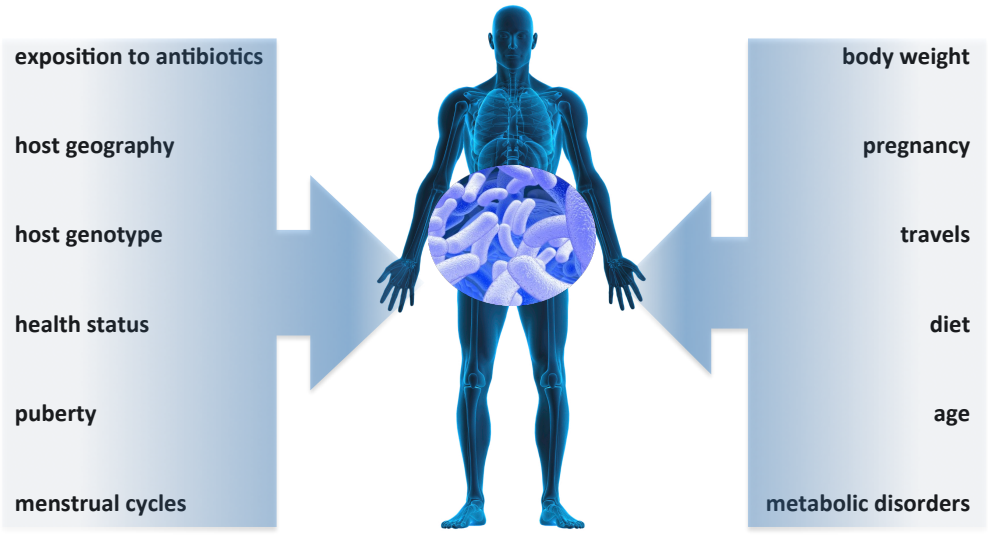

Figure 1.1. Major factors that can affect microbial composition in the human body.

The understanding of our microbiota is in its infancy and multimillion projects such as The Human Microbiome Project (HMP) (Turnbaugh et al. 2007) and MetaHIT (Qin et al. 2010) were launched given the importance of this essential "organ". Since most species cannot be culture in laboratory, advanced molecular techniques for sequencing total DNA and 16S ribosomal RNA allowed scientists to characterize our diverse bacterial community out of feces or biopsies extracts. From those projects, gene catalogues were established, association microbial gene-human phenotype were proposed, and hundreds of studies were published linking microbiota composition with diseases such as bowel disorders, allergies, obesity, cancer, and diabetes, setting the foundation for further research on human-bacteria relationship in health (http://commonfund.nih.gov/publications?pid=16).

Collins et al. reviewed animal-model studies that describe the bidirectional communication between intestinal microbiota and host brain. Bacterial products may reach the brain via the bloodstream or influence host cells, e.g., immune and enteroendocrine cells, to produce hormones and neutransmitters such as serotonin (5-hydroxytryptamine), a tryptophan derivative found mainly in the GI but also present in the central nervous system where it contributes to mood; or gastrin and cholecystokinin which controls appetite. On the other hand, stress and emotions can alter the physicochemical properties of intestinal habitat through the release of corticosterone, adrenaline and noradrenaline for example, changing gut microbial composition (Collins et al. 2012). To add to this subject, mass spectrometry-based analysis showed the influence that microbiome has on mice blood and plasma biochemistry, reporting specific indole-containing molecules, amino acids, phenyl derivatives, and flavones detected in conventional mice samples but not in germ-free animals (Wikoff et al. 2009).

Gut-flora-dependent metabolism and its link to cardiovascular diseases risk have also been reported. After plasma analysis of multiple individuals in a clinical cohort, increasing levels of lipid phosphatidylcholine (PC) dietary metabolites such as choline, trimethylamine N-oxide, and betaine were associated to the presence of peripheral artery disease, coronary artery disease, and history of myocardial infarction phenotypes. Further feeding experiments with deuterated-PC in mice confirmed the necessary biochemical step performed by the gut-flora to generate those pro-atherosclerotic metabolites, suggesting the manipulation of microbial composition may be a novel therapeutic approach to prevent heart diseases (Wang Z. et al. 2011). A complementary study done by Koeth et al. concluded that microbiota can also metabolize carnitine - structurally similar to choline and abundant in red meat and food additives – producing trimethylamine N-oxide which modulates cholesterol and sterol

metabolism, awakening about the safety of chronic L-carnitine supplementation (Koeth et al. 2013).

Individual diversity in human gut microbiota can be immense, but besides the challenge, Jansson et al. studied fecal samples of a twin cohort in order to search biomarkers for Crohn´s disease (CD) and correlated them to bacterial population within the same samples (Jansson et al. 2009). Bacterial species abundant in individual with ileal CD (i.e., *B. vulgatus, B. ovatus* and *E. coli*) were strongly correlated with bile acids and fatty acids metabolites; while bacteria abundant in samples of healthy individual (i.e., *F. prausnitzii* and *B. uniformis*) showed correlation to phospholipids and flavin mononucleotide. Greenblum et al. used a similar approach to identify microbiome enzymes enriched in obese individuals and patients diagnosed with inflammatory bowel disease (Greenblum et al. 2012).

Research done by our group using high-fat diet-induced obesity and genetically driven Type-2 Diabetes animal models, showed alteration in mouse gut community and metabolism. Higher abundances of *Firmicutes* and *Deferribacteres* were observed in obese animals while *Proteobacteria* and *Bacteroidetes* were abundant in non-obese ones. Regarding bacterial-derived metabolites, endocannabinoid-like molecules, and several bilirubin degradation compounds were increased in cecal content of obese animals while enterolactone and enterodiol were increased in non-obese ones (Walker, Pfitzner, et al. 2014). Unsaturated fatty acids such as arachidonic acid (C20:4), icosapentanoic acid (C20:5), and docosahexanoic acid (C22:6), and several sulfur-containing metabolites detected in fecal samples of diabetic animal models showed to be significantly elevated compared to samples from wild-type mice (Walker, Lucio, et al. 2014). Nowadays over 25 diseases, syndromes, or functional aberrations have been linked to an altered intestinal microbiome (de Vos and De Vos 2012).

Among all diseases typically increasing in industrialized societies, sensitization rates to allergens in children are currently approaching 40%-50% worldwide according to the World Allergy Organization (Pawankar et al. 2013). The exact cause of this increase is still unknown but an environmental change together with familial predisposition seems to contribute to the high incidence of this pathology. The influence of our commensal flora in the activation and response of mammalian immune system, and its implication for the development of atopic disorders like allergy and asthma, will be further discussed in this dissertation.

1.1 Intestinal microbiota and the activation of immune system

The adult human intestine is a 10 m long tube, and a single layer epithelial cell covers its irregular inner surface representing a surface area of approximately 200 m^2 populated by 10^4 to 10^7 microbial cells per gram of colonic content in the ileum and reaching 10^{11} to 10^{12} cells per gram of colonic content in the colon (~60% of faecal mass). Host–microbe interactions occur along the intestinal mucosa and the presence of bacteria plays an important role in the development of intestinal epithelium and intestinal immune system (O'Hara and Shanahan 2006). The biofilm-like architecture of the mucosal layer limits access of bacteria to epithelium and facilitates nutrient exchange (**Figure 1.2**). In this environment, dendritic cells (DCs) play a key role in the initiation of primary immune response. They monitor the inner intestine content and act as messengers of immune system. DCs sample microbes by extending long dendrites between tight junctions of epithelial cells into the gut lumen and carry them alive to the lymph nodes, major sites of other immune cells. They convert microbes into smaller pieces and display the antigenic fragments (co-stimulatory molecules) on their cell surfaces, activating B cells to produce protective IgA antibodies, which are distributed throughout all mucosal surfaces. In doing so, the immune system shapes the composition of the resident microbial community (Hooper, Littman, and Macpherson 2012; Round and Mazmanian 2009). It is important to mention that DCs are not only present in the intestinal mucosa but also in tissues that are in contact with the external environment, such as the skin, inner nose, lungs, and stomach, and they participate in allergic manifestations.

Dendritic cells do not exist in just one state. Immature DCs are either poor stimulators or unable to induce immunity but once they receive activation signals from pathogens, lymphocytes, antigens, or commensal bacteria, they undergo morphological changes (e.g. formation of dendrites) and molecular changes (e.g. surface expression of costimulatory molecules and cytokine production) being able to initiate immune responses (Münz, Steinman, and Fujii 2005; Mazmanian et al. 2005; Lanzavecchia and Sallusto 2001) - Steinman was honoured with the 2011 Nobel Prize in Physiology or Medicine due his discovery of dendritic cells in the `70s[2].

[2] The Nobel Prize in Physiology or Medicine 2011. Available at: http://www.nobelprize.org/nobel_prizes/medicine/laureates/2011/ (Accessed: December 2019)

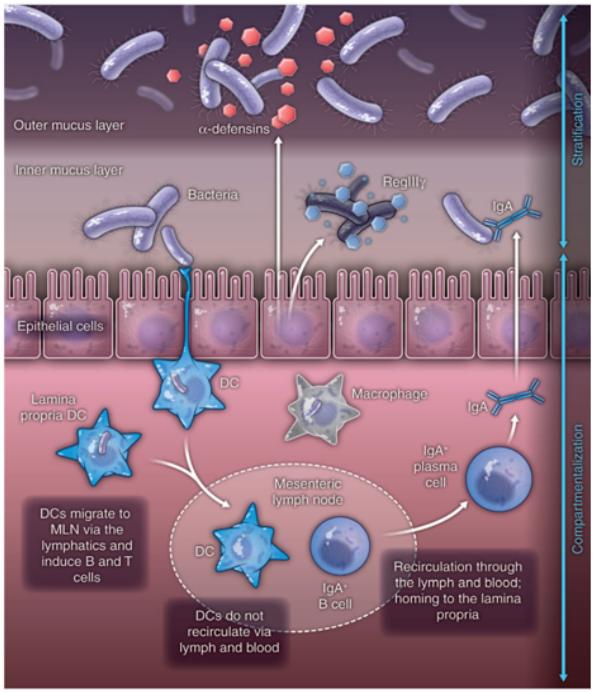

Figure 1.2. Looking inside-out: immune system control of the microbiota. (From Hooper LV, Littman DR & Macpherson AJ 2012. Interactions between the microbiota and the immune system. Science 336: 1268–73. Reprinted with permission from AAAS).

Mature dendritic cells produce different types of cytokines and induce lymphocytes differentiation such as naïve T cells, a type of white blood cell that presents several subsets with distinct functions, e.g., assist maturation of B cells (Helper), bind to virus and tumour cells to destroy them (Cytotoxic), maintain immunologic self-tolerance by suppressing T cell activation triggered by weak stimuli (Regulatory - Treg), and generate "memory" cells for future protection (Lanzavecchia and Sallusto 2001).

The maturation status of DCs depends on the nature of the stimulus and will determine whether a T cell polarizes towards T helper (Th1, Th2) or T regulatory (**Figure 1.3**). Although its molecular mechanism is poorly understood, T cell differentiation into Th2 cell type will result in allergic inflammation but its differentiation into Treg will be critical for continued immune tolerance to foreign antigens. Thus, inhibit DCs signals that leads to Th2 lineage can be a potential therapeutic strategy. The complexity of allergic manifestation and the role of dendritic cells is nicely reviewed elsewhere (Gill M.A. 2012; Reiner 2007).

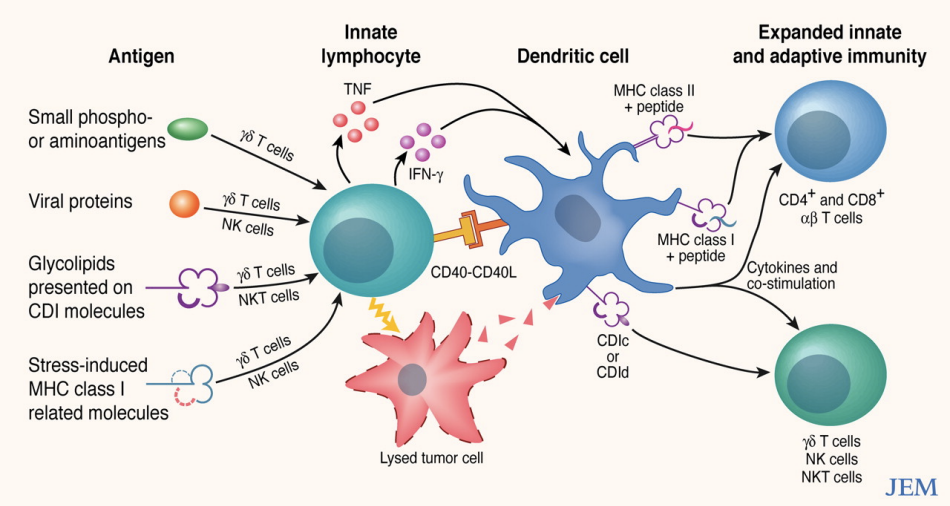

Figure 1.3. Activation signals from the microenvironment leads to DCs maturation. The DCs expand the innate response producing cytokines that differentiate additional innate and adaptive lymphocytes. (from Münz et al. J Exp Med 2005; 202: 203-207. Reprinted with permission).

1.2 The hygiene hypothesis

The hygiene hypothesis suggests that the increase of atopic diseases in the modern civilization, i.e., asthma, allergic rhinitis, and atopic dermatitis, may be due the decreased exposure to microbes during our children's first year of life, particularly in developed countries. High hygiene standards, use of antibiotics, less breastfeeding, and processed-food diets may prevent the normal development of baby's immune system by not challenging it to respond to different threats during its maturation (Buchen 2010).

Strachan proposed in 1989 the original concept of the "hygiene hypothesis" by reporting his observations in two British cohorts that showed an inverse association between family/household size and the incidence of atopic disease and hay fever (Strachan 1989). A decade later, he not only concluded that declining family size does not appear to explain the increase in asthma and hay fever prevalence, but also that data available (till 1990s) relating earlier childhood infections and later development of atopic diseases were inconsistent, even though no alternative explanation emerged so far and the "hygiene hypothesis" was considered immunologically plausible (Strachan 2000).

There are some difficult on this type of research since it requires longitudinal studies with follow up over several years, but besides conflicting findings, the "hygiene hypothesis", or now called "microbiota hypothesis", still drives research and open discussions. A study involving 6 to 13 years old children from southern Germany, Austria and Switzerland compared those individuals living full-time on farms with a reference group who lived in the

same regions, but not in rural areas. The results showed that personal exposure to a greater variety of fungi and bacteria in farming environment decreases the risk of developing atopic diseases (Ege et al. 2011). Furthermore, experiments using germ-free animals showed that those mice have a deficient antibody production, imperfect intestine tissues and epithelial cells - which increases permeability, and higher mortality after infections compared to colonized animals (Mazmanian et al. 2005; Round and Mazmanian 2009).

Based on this hypothesis, interest has surged regarding the possibility to manipulate our gut microbiome by the administration of microbes or microbial metabolites in order to prevent and treat atopic diseases not only in adults but also infants at greater risk for developing illness.

1.3 Probiotics

The word “probiotics” can be better explained as a combination of the Latin preposition *pro* ("for") and the Greek adjective *βιοτος*, the latter deriving from *βίος* ("life"). The theory proposed by Metchnikoff in the beginning of the 20th century was the basis for the concept of probiotic bacteria, suggesting that Bulgarian peasants had long and healthier life span due to their high consumption of fermented milk containing the bacterium "Bulgarian Bacillus", today called *Lactobacillus delbrueckii subsp. bulgaricus* (Metchnikoff 1908). He shared the Nobel prize of medicine in 1908 with Paul Erhlich in recognition to their work on immunity and the discovery of phagocytosis[3]. In 1920, Cheplin and Rettger did not succeed in proving the survival of “Bacillus bulgaricus” in man intestine, but provided scientific evidences about the intestine´s rapid colonization by “Bacillus acidophilus”; a strain that showed several advantages over the “B. bulgaricus” with regard to milk culture, e.g., better taste, smell, and creamy consistency (Cheplin and Rettger 1920).

Despite earlier historic facts, the word “probiotic” has been used since the 1950s, attributed to organic and inorganic supplements administered to patients suffering malnutrition and after, to fermented products. Only in the ‘70s probiotics was referred to “micro-organisms or substances that contribute to intestinal microbial balance”. Definitions of probiotics have been refined as more scientific knowledge has been gained in this field

[3] The Nobel Prize in Physiology or Medicine 1908. Available at: http://www.nobelprize.org/nobel_prizes/medicine/laureates/1908/ (Accessed: December 2019)

(Hamilton-Miller et al. 2007). Nowadays, probiotics are defined by the World Health Organization (WHO) as "live microorganisms which when administered in adequate amounts confer a health benefit on the host" (FAO/WHO 2002).

Applied to humans and animals, the global market for probiotic products grow exponentially year-by-year. In 2006, Western Europe consumed more than 1.4 billion euros in probiotic foods (Saxelin 2008) and the global probiotic market was expected to reach US$ 44.9 billion in 2018 (Pedretti 2013). Interest in probiotics is high all over the world and studies showing their efficacy as potential therapeutics or in disease prevention hold great promise (Gill H.S. and Guarner 2004). Many peer-reviewed scientific journals are given special attention to the topic, e.g., "Beneficial Microbes", Journal of Dairy Science®, "The American Journal of Gastroenterology Supplements", "Applied and Environmental Microbiology", "The International Journal of Food Microbiology", among others.

1.3.1 Probiotics as therapeutic agents against atopic disease

Atopic diseases occur due an exaggerated and imbalanced immune response to environmental or food allergens. The treatment of allergic diseases based on pharmacological interventions with antihistamines, glucocorticoids, steroids, or bronchodilators provide sufficient relief of symptoms but no cure. Is there any agent that fine-tunes immune response and therefore could provide a new therapeutic strategy for patients with atopic diseases? On this matter, many claims in relation to probiotics bacteria have been made. In a double-blinded, placebo-controlled trial, *Lactobacillus rhamnosus* GG (LGG) was given to pregnant women who had at least one first-degree relative suffering of this disease during four weeks prior to delivery, and then to the new-borns for six months. The results showed the frequency of atopic eczema in neonates was lower in the probiotic-treated group compared to the placebo-treated control group (Kalliomäki et al. 2001). Isolauri et al. studied the use of the strains *Bifidobacterium lactis* BB-12 and LGG to control allergic inflammation in 27 new-borns that manifested atopic eczema during breast-feeding; describing an improvement in skin condition after 2 months in all the infants receiving probiotics but only improved in half of the babies that received placebo. The observations were supported by experimental measurements of samples of the probiotic-supplemented group showing a decrease of soluble CD4 glycoprotein concentration in serum (a marker of T-cell activation) and eosinophil protein X (EPX) in urine - a marker for inflammatory activity (Isolauri et al. 2000). Similar results were observed in another clinical trial that evaluated a combination of *Bifidobacterium bifidum, Lactobacillus acidophilus,*

Lactobacillus casei, and Lactobacillus salivarius administered during 8 weeks to 40 children suffering from atopic dermatitis where the total Immunoglobulin E (IgE) level in serum decreased for the probiotic treated group; an antibody that triggers 'immediate hypersensitivity' reactions (Yeşilova et al. 2012). The called "PandA study" reported a reduced incidence of infant eczema in the probiotic-administered group (6 weeks prenatally to mothers and 12 months postnatally to offsprings). The mixture of *Bifidobacterium bifidum*, *Bifidobacterium lactis*, and *Lactococcus lactis* showed beneficial effects at 3 months of age, persisting to a lesser degree through 1 and 2 years. Likewise the reduction in the Th2-associated cytokines IL-5 and IL-13 *in vitro*, subsequently *in vivo* and *ex vivo* in whole blood cells obtained from probiotic-supplemented infants was observed (Niers et al. 2009).

Nevertheless, inconsistency in clinical outcome has challenged the role of probiotics in allergy prevention. An Australian group tested daily supplementation of *Lactobacillus acidophilus* in newborns´ first 6 months of life and despite higher intestinal colonization in supplemented babies, no association with reduced risk of early allergic disease was found (Taylor et al. 2007). Another group failed to prove the beneficial effects of oral supplementation of *Lactobacillus rhamnosus* and *Lactobacillus GG* in infants with atopic dermatitis (Brouwer et al., 2006).

Two review articles draw attention to the lack of robustness among several published studies. Differences on probiotic product or strain used in the experiments, viability of the cells (live probiotic administration versus heat-inactivated cells), small sample size and targeted population, duration of treatment as well as the timing of probiotic introduction (pre- or postnatal) can be the reason of controversial results (Osborn and Sinn 2007; Michail 2009). According to De Roock and colleagues, it seems essential to do well-founded choices on the probiotic strains to be used in clinical trials. Their *in vitro* study showed that the capacity of bacteria to modulate immune response and promote T cells subtypes differentiation is strain specific and cannot be extrapolated even at the species level, i.e., not any probiotic strain will have a beneficial effect on a given disease and earlier laboratory high throughput screening methods may give a good indication of a possible positive response to treatment in clinical tests later (De Roock et al. 2011).

Misleading conclusions in probiotics research show the complexity of the molecular crosstalk between probiotic bacteria, the gut microflora, and the immune system of the individual host. Apart supplemented microorganisms, the molecular basis at which our commensal bacteria regulate immune responses beyond gut environment is only beginning

to be elucidated. It is suggested that symbiotic bacteria-derived metabolites such as carbohydrate binding proteins, short-chain fatty acids, long-chain fatty acids, and biogenic amines might affect host immune maturation, activation, and functions leading to tolerance or pro-inflammatory responses (Frei et al. 2012; Arpaia et al. 2013).

The European Food Safety Authority issued unfavourable opinions on Health Claims on probiotic neutraceuticals while manufactures have the opportunity to market products to ill people without conducting costly clinical trials required for pharmaceuticals to proof safety and efficacy of new drugs (Katan 2012). Although *in vitro* evaluations of probiotic cell-free supernatants as targeted therapies have demonstrated its potential as a source of antipathogenic, anticarcinogenic, or anti-inflammatory compounds (reviewed in Howarth 2010), only few probiotic derived bioactive molecules and cell-wall structures have been identified so far – most often proteins (Kleerebezem et al. 2010; Sánchez et al. 2010), and even less with preclinical evidence for therapeutic effects were characterized, such as the p40 protein derived from LGG cell culture that prevents and treat intestinal inflammation (Yan et al. 2011 ; Yan and Polk 2012). Consequently, in addition to the evidence of microorganism's efficacy in clinical trials, it is of interest to elucidate the molecular nature of probiotic-derived compounds that positive influence host health anticipating the concerns of regulatory bodies and helping to fulfil the "probiotic promise". This type of research may provide innovative therapeutic agents and is therefore explored in the work presented in this thesis.

1.4 The search for natural bioactive compounds: traditional laboratory methods and modern metabolomics technology

Uncultivated or cultivated microorganisms serve as an enormous reservoir of novel natural products (NP) and potent bioactive molecules that can be used in medical applications, also called postbiotics (Wegh at al. 2019). Successful microbial derived compounds such as the revolutionary antibiotic Penicillin discovered by Alexander Fleming in the 1920s, to modern Lovastatin used to reduce the risk of developing heart disease and to decrease the amount of cholesterol in the blood, and Romidepsin – an anticancer agent obtained from the bacteria *Chromobacterium violaceum*, are just few examples of microbes potential as a source of bioactive compounds (Fleming 1929; Caporale 1995).

Microbial communities are highly competitive environments and organisms depend mainly on small molecules for survival and growth (primary metabolites) as well for defence

and communication (secondary metabolites). They can transform molecules and release an extremely complex mixture of molecular entities and isomers into the surrounding biota, which can display positive or deleterious responses in a targeted organism (Lechtenfeld et al. 2015; Josefa et al. 2013; Leao et al. 2010). Chemically mediated interactions between organisms are the focus of many of our medicines and natural products research might capture small compounds that affect any step in a metabolic or biochemical signalling pathway. While the chances of those compounds becoming a drug on the market are very low, small bioactive molecules can originate libraries of "inspired NP structures" – compounds synthetically modified by the introduction of drug-like functionality (Pascolutti and Quinn 2014). Despite the fact that many pharmaceutical companies have deemphasized classic NP research by introducing cost-effective and time-efficient High-Throughput Screening (HTS) technologies, natural compounds or derivatives can cover a much vaster chemical space relevant to biology than synthetic compounds and still represented ca. 50% of new approved drugs in 2010 including the majority of antitumor agents (Newman and Cragg 2012; Harvey et al. 2015).

1.4.1 Bioassay-guided fractionation

Traditionally, bioassay-guided fractionation has dominated novel bioactive NP discovery. In this approach, scientists start with a complex crude extract of plants, microorganisms, marine organisms, invertebrates, cell cultures, etc.; and divide it into fractions based on components physicochemical properties such as solubility, molecular polarity, size, charge, or chirality. The effect caused by each fraction is evaluated in a given *in vitro* biological system (bioassay) to identify the source of potential bioactive substances. Alternating between further fractionation and bioassay responses, it is possible to isolate and identify the compound/s that shows biological activity.

Before the introduction of chromatography, fractionation techniques using solvent partitioning were extensively used. Still applied to plant material and higher marine organisms, liquid–liquid extraction (LLE) serves as initial step of NP isolation. It is characterized by using large volumes of solvents and long extraction times but produces low extraction yields of bioactive molecules. Crude material can be treated with solvents of different polarity, e.g., hexane, diethyl ether, chloroform, methanol, or ethanol, originating crude extracts. The extract is then further fractionated in a separation funnel by adding an immiscible solvent so that compounds can be partitioned based on their differential solubility

in each solvent, governed by the partition constant K ($K = C_A/C_B$, where C_A and C_B represent the concentration of the solute in solvents A and B) (Sarker et al. 2006).

Since the discovery of chromatography by Tswett in the early 1900s, chromatographic techniques have been predominantly used in NP research and are closely linked with the advances reached in novel bioactive compound discovery. The need of better purification of biomolecules forced the development of solid phase materials used in chromatography and vice versa (Ettre and Sakodynskii 1993a; Ettre and Sakodynskii 1993b). The classic preparative open-column liquid chromatographic is a standard choice to separate components of a complex extract. Suitable to laboratory- and industrial-scale, and to large a quantity of material, this technique consists in applying the crude extract at the top of a column (normally made of glass) densely packed with fine adsorbent particles such as silica, alumina, florisil ($MgSiO_3$), graphitized carbon, cellulose, and divinilbenzene. The extract components are then separated and eluted by a flow of liquid mobile phase using the force of gravity and are collected at the exit of the column (**Figure 1.4**). Depending on the choice of packing material and solvent, different separation mechanisms will take place through selective distribution of compounds between the mobile and solid phases due, e.g., hydrogen-bridge, hydrophobic interactions, dipole-dipole or ion-dipole interactions, van-der-Waals-forces, among others. Almost any material that does not react with matrix compounds and the mobile phase can be used as an adsorbent (Sarker et al. 2006).

The Green Chemistry movement has been exploring ways to reduce the risk of chemical exposure to humans and environment and new forms of extraction were developed. The most successful is the Solid-Phase Extraction (SPE) technique, which significantly decreased the amount of solvent used in isolation procedures but still provides high extraction yield and selectively (Raynie and Essel 2013). SPE employs a wide range of stationary phases such as silica gel, reversed- and normal-phases, ion-exchange resins, chiral phases, or polymeric mixed-mode materials that are pre-packed in small plastic cartridges where compounds are separated by a slow flow of solvent under vacuum or positive pressure conditions. The most popular adsorbents used are bonded-silica based materials – not only for SPE but also for other separation techniques (**Table 1**) (Snyder et al. 2009; Supelco 1998). The interaction mechanisms already mentioned above apply also to SPE.

Different strategies can be used in Solid-Phase Extraction: either the compounds of interest are adsorbed in the stationary phase while the solvent elutes impurities, or impurities are retained while compounds are eluted and collected in one step. Moreover, scientists can fractionate complex mixtures using more than one cartridge packed with different adsorbents

or by applying stepwise gradient elution in a single cartridge using a sequence of solvents with increasing eluting power (Månsson et al. 2010).

Another advantage of SPE besides its Green Chemistry principles is that it offers possibilities for robotic process automation and for coupling to hyphenate instruments such as Liquid Chromatography–Mass Spectrometry (LC-MS) or Liquid Chromatography–Nuclear Magnetic Resonance Spectroscopy (LC-NMR), delivering cleaned extracts to LC further fractionation that can lead to the identification of compounds in early stages of the bioassay-guided process. In addition to that, the increasing sensitivity of analytical instruments has also contributed to the downscale of natural products isolation and stimulate the use of SPE extraction (Bucar et al. 2013).

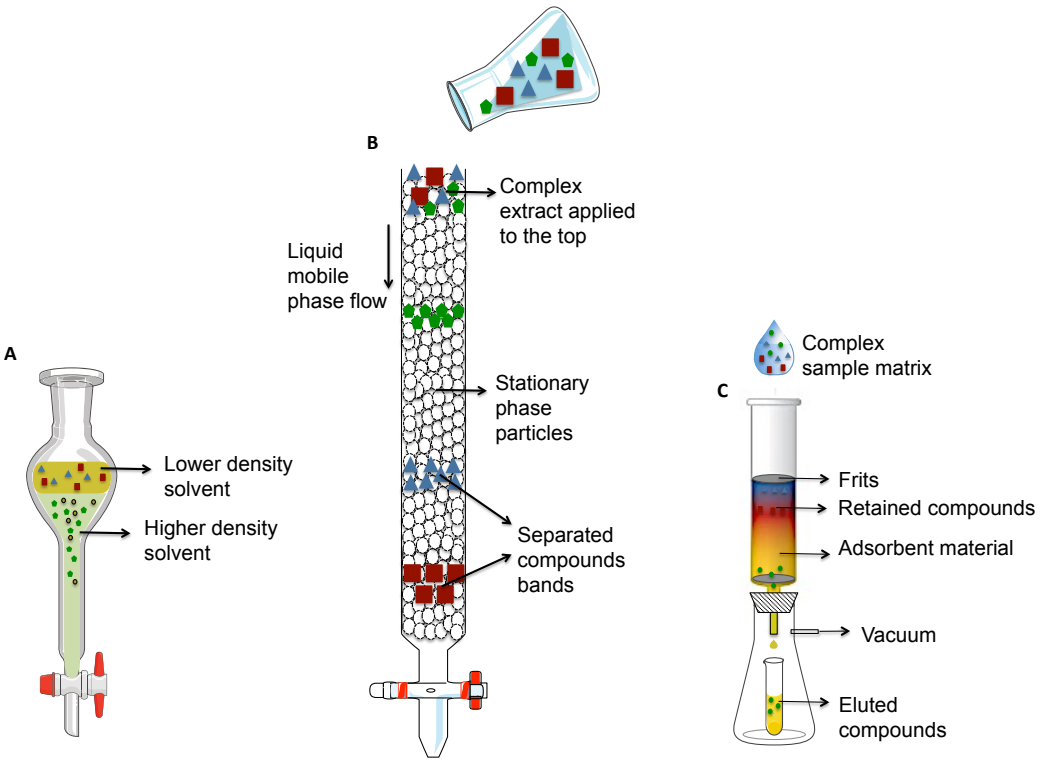

Figure 1.4. Classic natural products extraction techniques. (A) Liquid-liquid extraction separates matrix constituents based on their solubility in immiscible solvents. (B) Preparative chromatography typically uses large glass columns packed with solid material over which the liquid mobile phase is passed at low-pressure. Separation of chemical constituents occurs due the difference between molecules in their degree and strength of interaction with the stationary phase. (C) Solid-phase extraction (SPE) is suitable for small sample amounts and employs a wide range of stationary phases pre-packed into small plastic syringe-shaped cartridges that can be purchased commercially. Forced flow is applied using a vacuum system or positive pressure to isolate compounds of interest based on liquid chromatographic principles.

Table 1: Typical chemically bonded stationary phases used for chromatographic separation and isolation of compounds in SPE.

Stationary Phase	**Ligand**	**Mode**	**Types of Compounds**
Silica gel	Si-OH	Normal phase	Polar non-ionic
Nitro	Si-NO_2	Normal phase	Aromatics and compounds with double bonds
Cyanopropyl	Si-$(CH_2)_3CN$	Reversed phase or normal phase	Slightly polar, polar
Amino Propyl	Si-$(CH_2)_3NH_2$	Reversed phase, normal phase, or weak anion exchange	Carbohydrates, polar non-ionic, anions and organic acids
SAX – Strong anion exchanger - Quaternary amine	Si-$(CH_2)_3N^+(CH_3)_3$	Ion-exchange	Nucleotides, nucleosides, proteins amino acids and organic acids
SCX - Strong cation exchanger - Sulfonic acid	Si-$(CH_2)_3SO_2OH$	Ion-exchange	Organic basis
Octadecylsilane (C18)	Si-$C_{18}H_{37}$	Reversed phase	Non-polar neutral solutes, MW < 2000 Da - widely applied
Octylsilane (C8)	Si-C_8H_{17}	Reversed phase	Non-polar solutes (less retentive than the C18)
Butylsilane (C4)	Si-C_4H_9	Reversed phase	Non-polar solutes, hydrophobic polypeptides and proteins (lower hydrophobicity than C18 or C8)
Phenyl-propyl	Si-$(CH_2)_3Ph$	Reversed phase	Aromatics and compound containing unsaturated bonds
Pentafluorphenyl	Si-$(CH_2)_3C_6F_5$	Reversed phase	Substituted aromatic compounds. Alternative selectivity to phenyl phases, and alkyl phases
LH-20*	Cross-linked dextran	Size exclusion, ion exchange and reversed phase	Steroids, terpenoids, lipids, and low molecular weight peptides.
HLB*	Copolymer of divinylbenzene and N-vinylpyrrolidone.	Reversed phase	Polar and non-polar from aqueous samples

* Non-silica-based stationary phases

1.4.1.1 Modern Liquid Chromatography systems

Once fractions are collected and characterized by bioassay, NP scientists can benefit from the modern generation of High- and Ultra-High Pressure Liquid Chromatography instruments (HPLC and UPLC® / UHPLC) to achieve higher resolution separations of major constituents of bioactive fractions originating less complex sub-fractions, which facilitates structural elucidation of compounds by additional relevant techniques (Guillarme et al. 2010; Snyder et al. 2009). Typically, HPLC instruments operate at a maximum pressure limit of 400 bar and uses closed steel columns of 2–5 mm inner diameter and 5–25 cm length packed with stationary phase particles ranging in average from 3,5 to 10 µm diameter. New age UPLC® hardware can work up to 1000 bar using sub-2 µm fully porous or core-shell particles packed inside 5–15 cm length columns with 1.0–2.1 mm inner diameter - offering higher separation efficiency, i.e., it produces narrower peak widths that enhances resolution between two adjacent peaks and significantly improves fraction collection precision. According to Van Deemter equation Eq. (1), smaller particles increase the column efficiency by lowering the height equivalent of theoretical plates (HETP) as shown in **Figure 1.5** (van Deemter et al. 1956; Oláh et al. 2010). The equation includes the main factors that contribute to band broadening and describes the relation between separation efficiency, average mobile phase linear velocity (u, mm/s), and particle diameter (d_p). In a simplified form, the van Deemter equation is:

$$HETP = A.d_p + \frac{B.D_M}{u} + C\frac{{d_p}^2.u}{D_M} \quad (1)$$

where the term A is the Eddy diffusion and refers to band broadening (peak fronting and tailing) due to infinite number of paths that molecules may take while passing through a column. It is influenced by the nature of column (length, diameter) and by the nature of particles being used. The term B is the longitudinal diffusion and refers to the diffusion of molecules from a place of high concentration to areas of lower concentration to achieve equilibrium, being affected by the mobile phase flow rate. C refers to molecules mass transfer between mobile- and stationary-phase, and D_M is the analyte diffusion coefficient into the mobile phase.

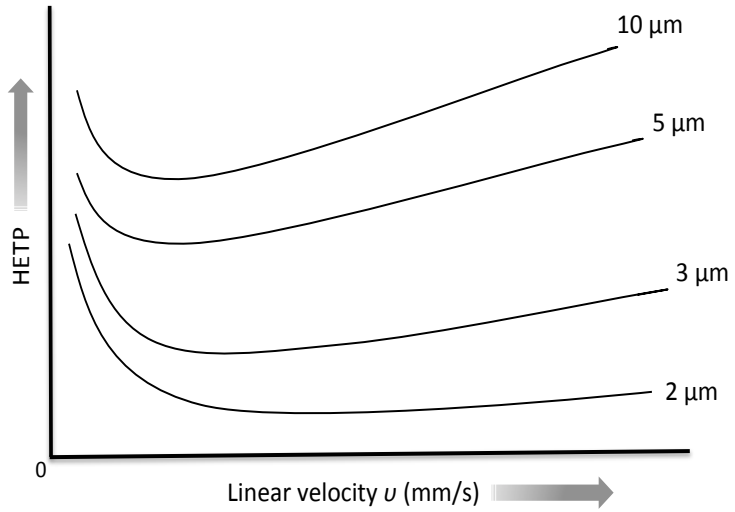

Figure 1.5. Theoretical van Deemter plot comparing different particle sizes. The lower value of HETP at the curve represents the optimal flow rate to obtain the maximum efficiency of a chromatographic column (adapt from Nguyen et al. 2006; copyright policy: open access).

Theoretical plates do not really exist but serve as a model to understand column efficiency. HETP as well as theoretical plate number N (Eq.2) are empirically determined, and columns behave as if they have different numbers of plates for each different compound in a mixture.

$$N = 16\left(\frac{t_R}{W}\right)^2 \quad (2)$$

where t_R is the retention time, i.e., the time it takes a solute to travel through the column; and W is the peak width at the base of the chromatogram originated with a detector device (UV/Vis, photodiode array, fluorescence, infrared radiation, MS, etc.). Again, a column is considered to be more efficient when it produces sharp symmetrical peaks that are baseline resolved from each other, and consequently gives high N values and low HETP.

Scientists can choose from a wide variety of equipment, column size, solid phase materials, and extraction methods to separate their mixture and no single strategy will lead to novel bioactive compounds discovery. Bioassay-guided fractionation is clearly a well-established approach to uncover new chemical entities, but it has some limitations as well. The process may sound trivial but can be surprisingly time-consuming and laborious. It is possible to automate fractionation, and yet, the incompatibility of the fast separation timescale (few milliseconds) and the bioassay response step (reaction times of seconds, minutes, or even days) makes real online hyphenation not straightforward. Also, liquid chromatography often uses organic solvents and other additives that are rarely compatible with biochemical assays, adding a fraction evaporation step to the process prior its dilution

in a suitable medium (Weller 2012). The long procedure can degraded unstable compounds, mask the real source of bioactivity, or provide insufficient concentration of compounds to show bioeffect or to carry out structural characterization in different instruments (Prince and Pohnert 2010). In some cases, individual fractions or compounds may have no effect on bioassay but when combined they show biological activity (Helfer et al. 2014). It also happens that scientists find out the bioactive compound identified has already been discovered or that the bioactivity is due to false positives.

To overcome those limitations and explore the amazing chemodiversity offered by nature, holistic approaches such as metabolomics have emerged as a new complementary solution to the reductionist bioassay-guided structure elucidation.

1.4.2 Metabolomics

The concept of metabolomics has arise from NMR spectroscopy studies of metabolic composition of biofluids, cells and tissues in the mid-1980s, and was formally defined in the late ‘90s as “metabonomics - the quantitative measurement of the dynamic multiparametric metabolic response of living systems to pathophysiological stimuli or genetic modification” (Nicholson et al. 1999). It joined the “omics” revolution in molecular biology (genomics, transcriptomics, and proteomics) offering a cheaper and high-throughputer technology than its mature 'omics' cousins, allowing the analysis of a larger numbers of samples. The term “metabonomics” was lately separated from the terminus “metabolomics”; defined as “a comprehensive analysis, in which all the metabolites of a biological system are identified and quantified” (Fiehn 2002). Nowadays, due the great overlap in philosophies and analytical methodologies, the scientific community mostly uses the terminology “metabolomics”.

While genes and proteins are subject to regulatory epigenetic processes and post-translational modifications, metabolites are not encoded in the genome and represent precursors, intermediates and end products of enzymatic reactions being the closest link to the phenotype. They are small molecules (< 1000Da) with enormous variation of chemical and physical properties (molecular weight, polarity, solubility, and volatility), concentration ranges, and are subject to continuous change influenced by a number of external factors (Krug et al. 2012). Thus extraction, separation, and analytic techniques that work for one class of metabolites are often ineffective for others and scientists must rely on many modern instruments to obtain relevant data, such as capillary electrophoresis–mass spectrometry (CE-MS), liquid chromatography–mass spectrometry (LC-MS), gas chromatography–mass

spectrometry (GC-MS), nuclear magnetic resonance (NMR), among others (Baker 2011; Alonso et al. 2015).

Metabolomics experiments analyse and compare samples to identify possible biomarkers for diseases, environmental and lifestyle markers, therapeutics targets, new biochemistry pathways and unknown compounds, or to correlate genotype with phenotype at molecular level (Lindon et al. 2007). The first step in metabolomics studies is to clearly define its objectives. It will influence the decision regarding sampling and metabolite extraction procedures, the number of biological and technical replicates (samples) needed, as well as the analytical instrument to be used (Nicholson and Lindon 2008). In some cases, it may be of interest to measure pre-defined set o metabolites that are involved in specific biochemical pathways to confirm a hypothesis or answer a research question. This approach is called "targeted metabolomics" and although it sounds conflicting with the original definition of metabolomics, the term is widely accepted by the community. Targeted approaches focus on quantitative or semi-quantitative analysis, method validation, and require analytical standards. It has contributed to the development of highly sensitive and robust methods for measuring biologically important metabolites in high-throughput manner. Non-targeted (or untargeted) metabolomics, in contrast, aims to simultaneously measure as many metabolites as possible (including unknown ones) in multiple samples resulting in inferior sensitivity and quantitation capabilities. Experiments are often hypothesis generating rather than hypothesis driven and originates complex data sets, with file sizes on the order of gigabytes per sample for some new high-resolution mass spectrometry instruments (Patti et al. 2012).

When instrumental analysis is done and data is acquired, there are a number of pre-processing steps prior to data interpretation. The complexity of cellular metabolism, chemical and physical sample variations, or analytical platform temporal drifts might challenge metabolite identification/quantification. Spectra are typically treated for noise reduction, baseline correction and normalization, peak picking, and spectrum alignment prior to statistical analysis. Then, robust statistics is necessary to explore the complex content of the data to find association patterns between sample groups. In the next step, discriminative signals are identified (i.e., possible metabolites) and translated into biological relevant conclusion. **Figure 1.6** presents the workflow differences between the classical bioassay-guided fractionation and metabolomics approach.

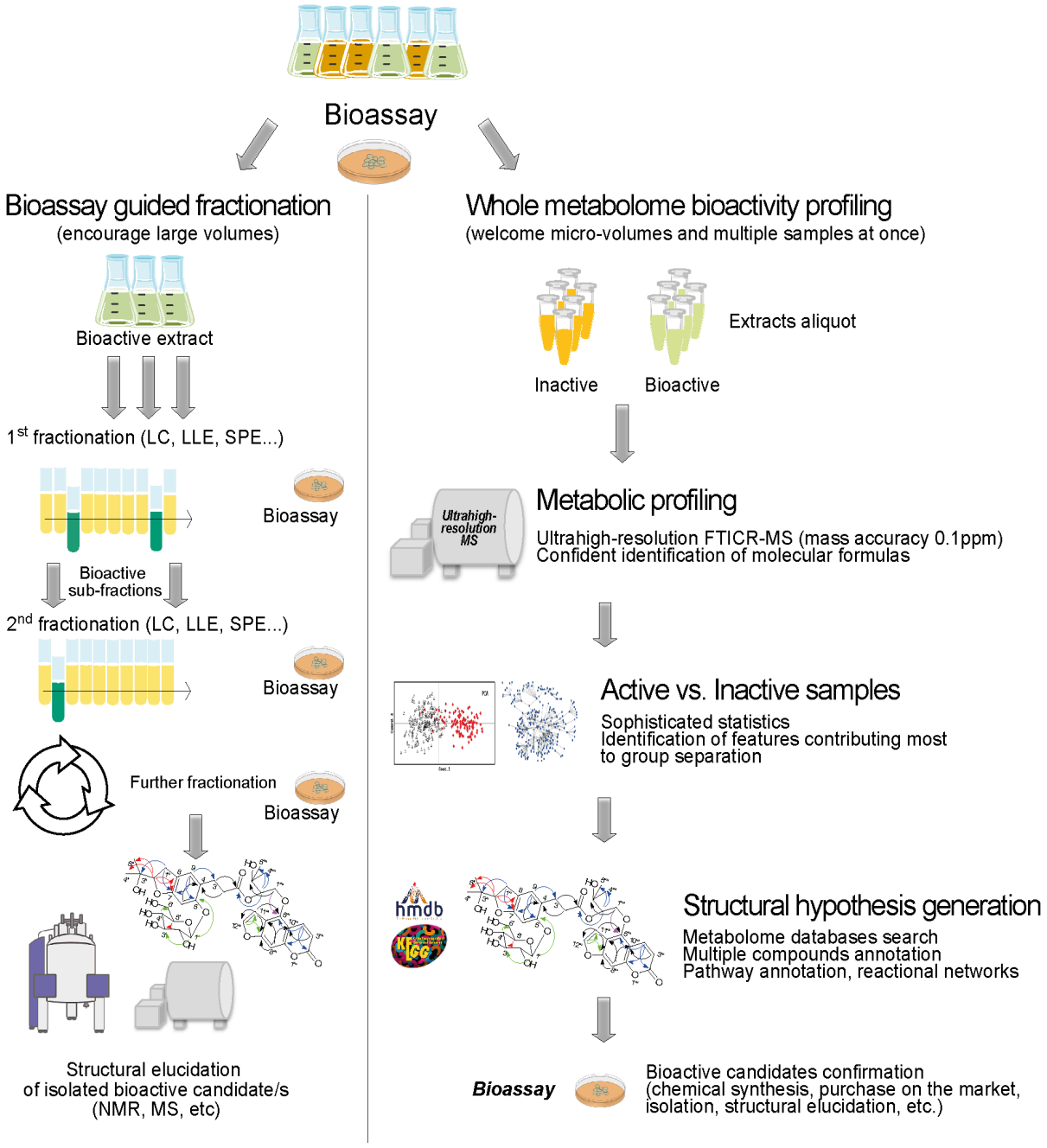

Figure 1.6. Schematic representation of two approaches to new bioactive compound discovery. (Left panel) Traditional bioassay-guided fractionation is time and labor intensive due to its step-by-step separation using chromatographic techniques followed by biological activity assessments. It removes most of the interfering matrix compounds but may lead to losses of active compounds. (Right panel) Holistic metabolomics approach deals with complexity, requires high level of expertise in instrumentation and data analysis, but offers scientists a broader picture of the biological system in study (Fonseca et al. 2022).

Natural Products scientists can take advantage of state-of-the-art analytical instruments combined with the power of bioinformatics to study natural samples in a more holistic way. Metabolomics strategies, specially those base on mass spectrometry, can be a valuable approach to discover new bioactive molecules (Havlícek and Spízek 2014; Harvey et al. 2015; Antón et al. 2013). Because all compounds are measure at once, unstable ones are likely to be detected as well as synergic effects arising from two or more agents in combination. Pre-analytical and sample preparation is in general simpler and faster compared to bioassay-guided isolation. Qualitative and quantitative differences in the intracellular or extracellular metabolite profile (metabolic fingerprinting / footprinting, respectively) of the organisms in study can help to elucidate behavioural or physiological responses (bioassay) and to assign organisms to groups accordingly. Additionally, NP crude extract metabolic profiles can be correlated to their modes of action and then be compared to other profiles through libraries of bioactive extracts helping to predict the identities of potential biologically active molecules directly from the complex mixture, accelerating discovery (Kurita et al. 2015; Ito et al. 2011; Prince and Pohnert 2010).

Enormous molecular diversity and biological functionality are two important features metabolomics can cover. However, samples are most subject to “noise” and signal interference in instrumental analysis than bioassay-guided fractions. As mentioned above, metabolomics studies (specially non-targeted approaches) produce lots of data that challenge analysis and interpretation; the most time-consuming step in metabolomics (Kuhlisch and Pohnert 2015). High-resolution instruments, e.g., Fourier transform ion cyclotron resonance mass spectrometry (FT-ICR MS), and NMR spectrometers are very expensive and require highly skilled professionals as well as fast computer memory. As any other young discipline and technology, the continued development of metabolomics and analytical platforms might outspread its application, making metabolomics cheaper and automated.

1.4.2.1 Cell culture metabolomics

Optimized laboratory condition allows scientists to study microorganisms and cells as individuals and serve as a good model for the investigation of cellular processes or to predict a drug effect, also allowing miniaturization and automation for high-throughput screenings. It clearly differs from natural environments where microorganisms coexist in complex social communities and highly organized biofilms interacting with each other at intra- and interspecies level trough extracellular signalling molecules. In nature they cope with

temperature and humidity variations, change in the pH of their surroundings, and adapt their rate of metabolism according to nutrient supply. Only a small proportion (1%) of known microorganisms can be grown in a laboratory and in the case of bacteria, studies are typically done during a relatively small period of their life cycle called exponential grow phase (Palková 2004). But, laboratory cell culture conditions can be physico-chemically and physiologically optimized (e.g. temperature, pH, pressure, O_2 and CO_2 concentration, hormones, and nutrients) to stimulate cell growth and production of molecules of applied interest, a particular sustainable source for natural product scientists (Valenzuela et al. 2015).

Metabolomics studies of cell cultures are less expensive and easier to perform than animal models or human studies where individual variations, age, gender, heath status, or strict ethical norms must be considered. *In vitro* models simplifies natural systems allowing scientist to explore cell metabolic capabilities and molecular interactions in a highly accessible way, being the best choice experiments for proof of concept and hypothesis generating in early-stage research (Sixt et al. 2013; Cuperlović-Culf et al. 2010). Even so, development of cell culture metabolomics faces some challenges. Studies involving comparison of different cell lines or species of microorganism might require different grow medium formulation and conditions (expected to faithfully represent *in vivo* essential aspects) adding an obstacle to experimental results interpretation. Culture characteristics affect cell density, growth rate, and may induce variation in the metabolic profile (Huang et al. 2015; Bonarius et al. 2000; Tweeddale et al. 1998). Additionally, metabolite sampling is a two-step process: quenching and extraction. The goal of quenching is to rapid stop cell metabolism by adding a cold solvent to the culture (60% methanol solution at -40 °C is currently preferred) to maintain *in vivo* concentration constant and avoid leakage of intracellular metabolites into the medium. Only then, cells can be harvested by centrifugation or fast filtration. The overall procedure should be done as rapidly as possible because results showed that cold solvent quenching does not gives 100% prevention of cell membrane damage and the longer cells are in contact with the solvent, the higher are the chances of metabolite leakage. It means that executing an extra washing step to the resulting cell pellet to remove interstitial fluid, which contains medium components and extracellular metabolites, will increase the chances of loss of intracellular metabolites. Another limitation for quenching is the degree of dilution of supernatant samples which can make it difficult to assess extracellular metabolites (Sellick et al. 2011; Villas-Bôas et al. 2005).

The follow challenging step aims to efficiently extract metabolites from the cell cytoplasm and subcellular compartments with minimal losses by degradation or further

reactions, avoiding large biomolecules (e.g., proteins, DNA, RNAs), and being compatible with the analytical method of choice. The total number of distinct cell or microbial metabolites is yet unknown and there is no universal extraction method that will cover all classes of molecules. Several intracellular extraction solutions have been described so far (e.g. chloroform, methanol, ethanol, buffered solutions, acid or alkaline solution) but methanol or chloroform is preferred since analysts can perform extractions at quenching conditions, i.e., at very low temperatures, collecting a more analytical instrument-friendly samples. The study approach (targeted or non-targeted, intra- or extracellular metabolomics) will define the most suitable procedure.

When the analysis of cell-free culture supernatants (also called exometabolome analysis, or "metabolic footprinting") is the focus of the study, the sampling procedure is less technical demanding. Cold centrifugation or fast filtration at low temperatures can separate culture medium from cells in suspension (da Luz et al. 2014), but it is still important to minimize as much as possible metabolic activity while avoiding that samples get frozen, which induces cell wall rupture. Then, supernatants can be directly analysed or concentrated to dryness to be later re-constituted in appropriate solvent before their injection into the analytical system (León et al. 2013; Dietmair et al. 2010; van der Werf et al. 2005).

Although metabolic footprinting represents only a fraction of the entire cell metabolism, it provides important information for understanding cell-to-cell communication, to monitor growth behaviour, to characterize strains, to study metabolite flux trough uptake and secretion of compounds supporting metabolic engineering and industrial biotechnological processes, and has been successfully applied to bacterial culture supernatants (Pinu and Villas-Boas 2017; Dörries and Lalk 2013; Behrends et al. 2009; Mapelli et al. 2008).

1.4.2.2 Mass spectrometry-based metabolomics

Metabolomics involves not only finding statistically significant variations in metabolites abundance between sample sets but also identifying the correct chemical formula of those confidently. Many analytical platforms are available for such studies, but mass spectrometry has become the instrument of choice due to its sensitivity, selectivity, speed of analysis, and the structural information it provides (e.g., exact mass of molecular ion, fragmentation patterns, isotopic ratios) applicable across a wide range of compound classes. Also, MS can be preceded by a separation technique to reduce sample complexity and enhance its quantitation power - most commonly LC, GC, and CE. The number of MS-based

metabolomics studies grew quickly exceeding NMR-based ones; showing greater clinical potential once instruments require less space and are less costly to maintain (aside from FT-ICR MS). It is important to mention that NMR is generally accepted as the gold standard in metabolomics and provides complementary information to other techniques. It is robust, quantitative, and non-destructive (i.e., samples can be reused); but it suffers from relatively lower sensitivity compared to MS, which limits the number of metabolites measured simultaneously (Mishur and Rea 2012; Scalbert et al. 2009; Büscher et al. 2009).

Mass spectrometers acquire signals in the form of a mass-to-charge ratio (m/z) and plot them versus ions relative abundance to originate a mass spectrum. Thus, compounds first need to be ionized so that they can be moved and manipulated by electric field (in vacuum conditions), be separated in the mass analyser, and then be detected. Charge can be transferred to a molecule using a variety of ionization methods that fall into two categories: "hard" and "soft". Hard ionizations are very energetic and leads to an extensive fragmentation of the molecular ion (the one with the greatest m/z value, and relative to the molecular mass of a compound), while the "soft" ones use a gentle process enhancing the abundance of molecular ions and therefore only few primary fragments are obtained. An example of "hard" method is the electron ionization (EI) commonly used for GC-MS analysis, where the sample in vapour state is introduced perpendicular to an electron bean. During this collision process, an electron from the analyte molecule is expelled converting the molecule to a positive ion, which promptly causes fragmentation into detectable daughter ions providing valuable information for structural elucidation of compounds. A complementary "hard" method but softer than EI is the chemical ionization (CI) where, following similar principle, electrons ionize first reagent gas molecules (e.g., methane, isobutene, ammonia) that will react with analyte molecules and form ions due proton transfer reactions, hydride abstractions, adduct formations, or charge transfers. This technique yields less fragmentation and the molecular ion is easily recognized. Both EI and CI application is limited to sufficiently volatile and thermally stable compounds (Hoffmann and Stroobant 2007).

The development of soft ionization methods has revolutionized biomolecular analysis by mass spectrometry making it possible to analyse non-volatile and thermolabile compounds in liquid phase. Proteins, peptides, sugars, polymers, and metabolites can be now ionized using MALDI (Matrix-Assisted Laser Desorption Ionisation), or by its variations SELDI (Surface Enhanced Laser Desorption Ionisation), and DIOS (Direct Ionisation on Silicon) (Tanaka et al. 1988) as well as using electrospray ionization (ESI), introduced by Fenn in

the late ‘80s (Fenn et al. 1989). In 2002, the Nobel Prize for Chemistry was shared between John Fenn, Koichi Tanaka, and Kurt Wüthrich (an NMR expert) because of their work on analytical methods for identification and structure analyses of biological macromolecules in solution[4] (Kungl. Vetenskapsakademien 2002).

1.4.2.2.1 Electrospray ionization source

While laser desorption techniques require appropriate sample preparation prior MS analyses by embedding the sample in a matrix material which absorb the energy of the laser, ESI allows sample ionization in their liquid native form without any additional preparation steps to enable ions creation. For that reason, ESI is easily coupled with liquid chromatography instruments and is suitable for direct sample injection being the most used ionization method in metabolomics.

In this technique, sample solution is driven at low flow rates into a metal capillary where a high potential difference is applied between it and the sampling cone (typically 2−5 kV, positive or negative). Electrostatic charges are transferred to the solution forcing a fine spray of droplets populated with charges of the same polarity as the one of the needles. The coulombic repulsion on the surface becomes so large relative to the droplet size that they “explode” originating gas-phase ions enabling almost fragment free molecular ion detection - a flow of warm gas is used to favour solvent evaporation (**Figure 1.7**) (Kebarle and Verkerk 2009). The optimal voltage and maximum ionization depends on the characteristics of the analyte (e.g., polar, non-polar, high or low MW), and experimental parameters such as solution flow rate, solvent composition and pH, distance between the needle and counter electrode, temperature, etc. (Cech and Enke 2002). The ionization process takes place at atmospheric pressure and produces not only ions but also neutral or clusters of ions with neutrals. The challenge is to introduce only desolvated free ions into the MS vacuum region and many ESI sources and interface designs were developed in attempt to improve ion transmission - consequently selectivity and sensitivity of detection. It includes ESI source variations like the APPI (atmospheric pressure photo ionization), APCI (atmospheric pressure chemical ionization) (Manisali et al. 2006), nanoelectrospray microchip devices (Lazar et al. 2006) and the desorption electrospray ionization (DESI) applied to solid samples (Cooks et al. 2006); but they all maintain basic features of the original ESI configuration.

[4] The 2002 Nobel Prize in Chemistry. Available at: http://www.nobelprize.org/nobel_prizes/chemistry/laureates/2002/ (Accessed: December 2019)

The mass spectrum obtained in electrospray positive mode (ESI+) for a given molecule (M) is characterized mainly by the presence of protonated ions $[M+nH]^{n+}$, and adducts with cations, e.g., $[M+K]^+$, $[M+Na]^+$, or $[M+NH_4]^+$. Multiple charged ions are also observed (normally for large molecules with several ionisable sites) as well as aggregates like dimers or higher order ones, i.e., $[nM+H]^+$. In electrospray negative mode (ESI–), the predominant ions are formed by abstraction of protons, e.g., $[M-nH]^{n-}$, $[M+FA-H]^-$ (FA=formic acid), or adduct anion formation such as $[M+Cl]^-$ and $[M+F]^-$. Aggregates are rarely observed in ESI– (Hoffmann and Stroobant 2007). ESI+ mode strongly favours the ionization of basic compounds and nitrogen-containing ones like amines and amides; ESI– favours the ionization of acid structures, sugars, and sugar phosphate. Compounds that contain a mixture of functional groups may be detected in both modes but ESI+ produces more features and show higher signal intensities than ESI– (Yuan et al. 2012).

Enormous attention is given to ion-suppression effects: an ionization effect that impacts sensitivity and quantitative performance of a mass detector and one should be aware of. In the ESI process, components of a sample compete for a limited amount of charge and droplet space. Thus, the presence of endogenous matrix components, coeluting compounds and mobile phase additives (e.g., EDTA, TFA, used in chromatography), non-volatile solutes (e.g., salts at high concentration), or surfactants (e.g., PEG and TWEEN) can change the efficiency of droplet formation, solvent evaporation, and may "steal" charges away from the analytes of interest, meaning that less analyte ions reach the MS detector and therefore its signal is significantly reduced (suppressed). Furthermore, given the diversity of metabolites, the degree of ion suppression can vary from compound to compound since they differ in physiologic concentration, polarizability, solubility, or pKa (acid dissociation constant). For example, higher mass molecules with high surface potential and proton affinity may supress low molecular weight metabolites (Annesley 2003; Jessome and Volmer 2006; Oss et al. 2010). Strategies to minimize ion suppression include improvement of sample cleanup to remove interfering substance (e.g., protein precipitation, filtration, SPE extraction, etc.), modification of reagents avoiding the use of non-volatile exogenous additives, dilution of the sample when convenient, and reduction of sample injection volume and ESI flow rate to generate smaller and more highly charged droplets.

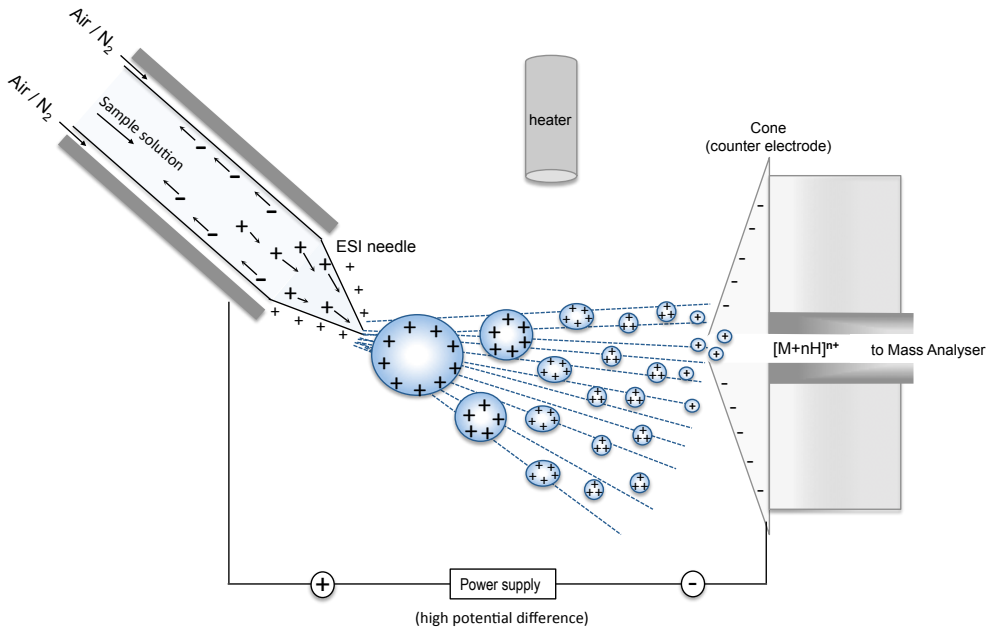

Figure 1.7. Schematic representation of the electrospray process in positive mode. ESI is an atmospheric pressure ionization that occurs in a closed chamber hot environment and in the presence of turbulent auxiliary gas flow. Ion formation involves not only an electrochemical process but also extensive solvent thermal evaporation, which brings droplets charges closer together and increases coulombic repulsion, leading to droplets fission. The applied voltage can be either positive or negative, generating positive ions, e.g., $[M+H]^+$ and $[M+Na]^+$ or negative ions, e.g., $[M-H]^-$ and $[M+Cl]^-$.

1.4.2.2.2 Mass analysers

The ability of a mass analyser to separate ions out of complex mixtures and distinguish closely located signals from each other (i.e., the resolution between two ions with a small m/z difference) plays an important role in metabolomics and structural elucidation of unknown compounds. The development of high-resolution instruments has enabled mass measurement with tremendous accuracy facilitating elemental composition assignment to a single formula instead of a range of possible ones (Schmitt-Kopplin et al. 2010), which can shorter the time for new compound identification. Mass accuracy indicates the deviation observed between the instrument's response (m/z measured) and the theoretical m/z calculated for a given ionazed compound reflecting how precise will be its elemental composition determination. Accuracy is often expressed in parts per million (ppm) (Brenton and Godfrey 2010; Hoffmann and Stroobant 2007):

$$accuracy\ (ppm) = \frac{(measured\ mass - theoretical\ mass)}{theoretical\ mass} \times 10^6 \qquad (3)$$

Modern FT-ICR MS instruments equipped with 7 to 15 Tesla super-conducting magnets can determine molecular formulas for MW ≅500 Da with sub-1 ppm mass accuracy, i.e., corresponding to a mass error of an electron (0.00054858026 Da), being able to separate species with almost same mass (isobars) and resolve isotopologues. In this type of mass analyser, ions are confined in the ICR cell where they are accelerated by the application of a rapidly varying electric field (RF) in the presence of a spatially uniform magnetic field (B). In the ICR cell, ions are subject to the Lorentz magnetic Force and undergoes into circular orbit cyclotron motion of a radius *r* according to:

$$F = mass \times acceleration = m \,.\frac{v^2}{r} = zv \,.B \qquad (4a)$$

in which *m* is mass, *v* velocity of a particle moving in the plane xy, and *z* is charge.

In a rotating or orbiting object going in circles, there is a relation between distance from the axis (*r*), the angular frequency (i.e., $\omega = d\theta / dt$; in radians per second), and magnitude of tangential velocity ($v_r = r \,.\, \omega$). Thus, the tangential velocity formula can be transformed into $\omega = v / r$ and equation $4a$ becomes:

$$m.\omega = z \,.B \quad (4b)\,; \qquad \omega = \frac{z.B}{m} \quad (4c) \qquad \text{or} \qquad \frac{m}{z} = \frac{B}{\omega} \quad (4d)$$

which means that m/z is measure as a *frequency* signal over a period of time and different ions circulate at different orbital frequencies. All ions of a given mass-to-charge ratio are excited to the same orbital radius by the RF field and have the same ICR frequency, amazingly independent of their velocity. Ions of identical m/z value are grouped together before excitation and move together in tight ion packets being detected by a pair of electrodes through the induction of differential current between them as the ions pass nearby - current amplitude is proportional (but not linear) to the number of orbiting ions as well as the number of charges in the ion (**Figure 1.8**). Then, Fourier transformation mathematically converts frequencies spectrum to a mass spectrum (Marshall and Hendrickson 2002). Since ICR cell volume is limited, the detector is susceptible to oversaturation, i.e., the amount of ion exceeds the dynamic range of the instrument.

Mass resolving power (i.e., $m/\Delta m$ - where m represents the mass and Δm the peak width at half-peak height necessary for separation at mass m) increases linearly with increasing applied B field and can achieve more than 1,000,000 in FT-ICR MS. Inside the ICR cell, ions are able to travel kilometres during just 1-second observation getting separated from each other – one reason why ICR instruments have such high resolution. The principles of FT-ICR MS and its developments are nicely described by Marshall (Marshall, Hendrickson, and Jackson 1998; Marshall 2000). Because ions must be confined for extended detection periods, FT-ICR MS scan speed (one per sec) does not match chromatography separation peak entries (e.g., LC and GC, where a higher number of scans to originate a peak is required) and therefore online coupling compromise the high-resolution, mass accuracy and sensitivity potential that this type of mass spectrometer can offer. Most metabolomics applications involving FT-ICR MS instruments are therefore performed by direct sample introduction.

Modern ultrahigh-resolution time-of-flight mass spectrometry (UHR-TOF MS), such as the maXis QqTOF-MS from Bruker Daltonics, can operate at a high resolving power of 60,000 at low-mass range and delivers mass accuracies of 2 ppm. Its lower resolution compared to FT-ICR instruments is sufficient for many application and its fast scanning rates favour coupling to UHPLC instruments, making TOF-MS a widely used mass analyser in the metabolomics and NP research (Forcisi et al. 2013). The TOF analysers separate ions according to their velocities after initial acceleration by an electrostatic field of several keV (elétrons-volt) to a kinetic energy ($E=(mv^2)/2$) towards reflectors in the field-free region flight tube; where they are separated and detected by the detector positioned at the other extremity of tube (**Figure 1.9**). Mass-to-charge ratios are then determined by measuring the time (*tof*) that ions take to travel the distance (L) between the source and the detector (Hoffmann and Stroobant 2007; Bruker Daltonik GmbH 2008), according to the equation:

$$tof = \frac{L}{v} = L\left(\frac{m}{2zeV}\right)^{\frac{1}{2}} \quad (5)$$

where L and eV are instrument constants. Ions of different mass reach different velocities, i.e., lighter ions travel faster than equally charged heavier ones. The increase in the length of the flight path (L) will increase resolution – to illustrate that, the maXis™ UHR-TOF instrument has a 3 meters high flight tube and a 6 m high TOF was build in USA by the team of Dr. Marvin L. Vestal with the objective to reach 200,000 resolving power but the instrument showed to be very sensitive to mechanical vibration in the room, which kept them

from hitting such resolution (Arnaud 2010). Theoretically, a 30-meter flight tube should provide to a TOF-MS the resolving power close to the one of a FT-ICR MS instrument, which is not practical and commercially viable. On the other hand, TOF instruments have much higher speed of scan and detection (which makes its coupling to different separation techniques a very attractive combination for quantitative analysis), it has a simpler and cheaper construction, and are more resistant to ion oversaturation than FT-ICR MS.

The newest high-resolution mass analyser introduced to the market is the orbitrap. It applies and electrostatic voltage to central spindle likes electrode, trapping ions that cycle around it under the influence of an electrostatic field. Similar to FT ICR, frequencies are measured, and Fourier transformation converts signals to obtain mass spectrum. Orbitraps has provided resolving power up to 200,000 with relative small equipment size and cost, but recent advances in its technology showed that this type of instrument is capable of 960,000 resolving power at m/z 400 after some instrument modifications (Denisov et al. 2012) . A detailed description of its fundamental principles and comparison to other mass analysers is presented elsewhere (Zubarev and Makarov 2013; Hoffmann and Stroobant 2007). Further introduction to orbitrap-MS is out of the scope of this thesis.

The appropriate mass analyser to be used in a study depends on many factors such as research question, the need for extreme resolving power to deal with unknown compounds (or not), the need for precise quantification (which involves scan speed), instrument availability, or on the molecular mass of analytes (e.g., typically FT-ICR MS covers the range of molecules between 150 and 1000 Da while TOF is widely applied in proteomics). In this thesis, FT-ICR MS was the instrument of choice for untargeted metabolomics and UHR-TOF for targeted quantitative analysis. Both instruments allow the isolation of an ion and its further fragmentation by collision induced dissociation without loss in accuracy (known as multiple-stage mass spectrometry – MS^n). This process yields valuable information about the structure of the precursor ion.

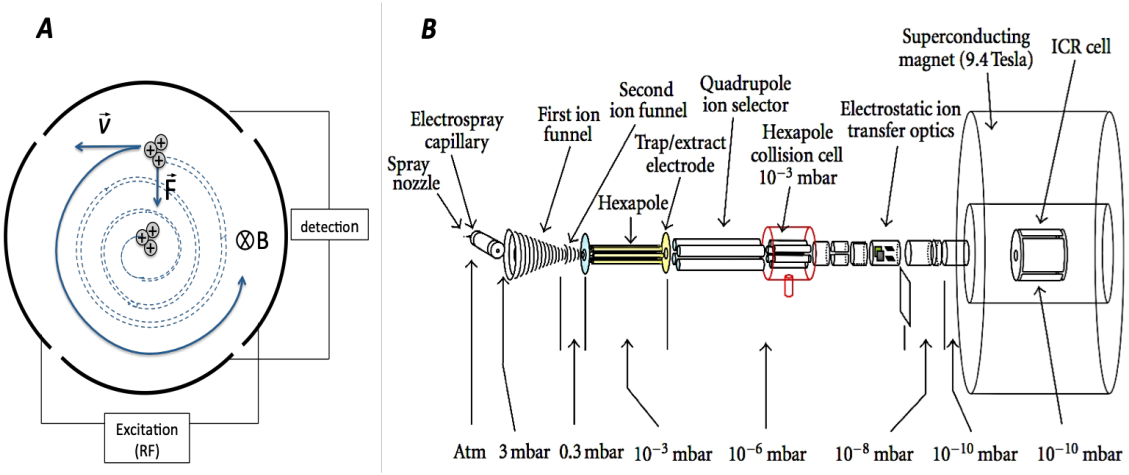

Figure 1.8. Schematic diagram of a cylindrical ICR cell and non-scaled FT-ICR MS system. A: uniform rotating electric field is applied at or near the frequency of ions of particular m/z value (excitation) increasing their moving radius to a detectable region. Detection plates are positioned orthogonal to the excitation plates. The magnetic field B is perpendicular to the plane of the paper and forces ion cyclotron motion in a circle due to the Lorentz force (composed of three ideally harmonic oscillations but cyclotron frequency is the one detected). Positive and negative ions orbit in opposite senses and frequencies are then converted to a mass spectrum using Fourier transformation. B: ESI source, ion transfer section in n-poles and optics, vacuum system, and ICR cell inside the superconducting magnet - based on the APEX Qe FT-ICR from (Bruker Daltonics) and adapt from Bergquist et al. 2012 (Copyright policy : open-access).

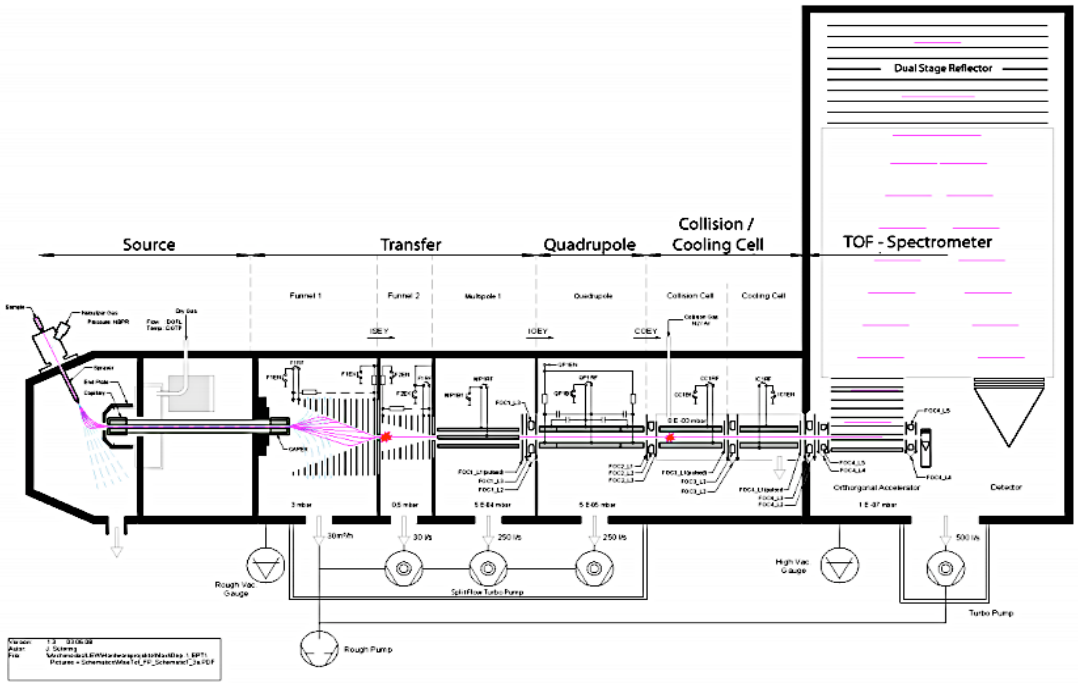

Figure 1.9. Illustration of maXis™ UHR-TOF MS instrument**.** Source (spray chamber and capillary), Ion Transfer Stage (funnel 1, funnel 2, multipole), Quadrupole, Collision/Cooling Cell and TOF spectrometer (orthogonal accelerator, dual stage reflector, detector). Reproduced with permission (Bruker Daltonik GmbH 2008).

1.4.2.3 Data analysis

It is common to display in a chart the important variables of a simple system, e.g., plotting the variation of a specific analyte concentration over time for a single sample. But, the evolving of metabolomics and the ongoing development of high-resolution MS instruments has increased the amount and complexity of the data generated that is not readily comprehensible in its form. For example, how to address thousands of m/z signals intensities across hundreds of samples? Therefore, after correcting MS spectra for baseline effects, smoothing, peak alignment, outlier detection, normalization, and setting up a data matrix (Boccard et al. 2010), mathematical and statistical analyses are needed to extract relevant information from the data that might explain the observed biological phenomena in study - concept often called chemometrics. Multivariate methods such as Principal Component Analysis (PCA) and Hierarchical Cluster Analysis (HCA) are the most known data analysis techniques in metabolomics and are usually applied for exploratory purpose to reveal systematic variations (patterns) in the data, presence of outliers, and identify the features (variables) that are strongly related to those patterns using an unsupervised approach, i.e., without sample group information input. When the number of experiments is small compared to the amount of variables (e.g., m/z signals), supervised techniques such as Partial Least Square-Discriminative Analysis (PLS-DA) can be applied as an extension to PCA to "sharpen" the separation of samples into predefined classes based on priori knowledge (e.g., bioactive x non-bioactive, diseased x health control, etc.) finding the features that most contributed to the grouping (Lucio 2008).

Projection-based methods assume that the system in question is driven by a small number of latent variables (LVs) reducing the dimensionality of data. PCA is a liner transformation that preserves as much of the variance in the original data as possible and converts the multivariate data into few two-dimensional hyperplanes system orthogonal to each other (called principal components) where the largest possible variance within the data is on the first coordinate (PC1), then the second greatest variance on the second coordinate (PC 2), and so on. PCA provides a *score plot* (**Figure 1.10**) that shows the relation among objects (e.g., samples) plotting the ones with similar multivariate profiles close to each other. Then, the *loading plot* shows the influence (weight) that an individual variable has in separating objects into different groups. Thus, PCA is a rapid and powerful view tool that simplifies information-rich datasets into a graph showing the majority of total variance existing in the data (Trygg and Lundstedt 2007).

Since PCA only expose scores (i.e., class separation) when within-group variation is sufficiently less than between-group variation, supervised PLS-DA technique can help to find hidden correlation structures in the data (delivering the same type of plots as PCA does). If a dataset structure is well predictable by PCA, then PLS-DA can verify and test it in more detail. However, PLS-DA requires a minimum sample size for a satisfactory model, which increases substantially with the number of variables monitored - many metabolomics studies involve far too many variables, and perhaps too few samples are available. To effectively evaluate the results obtained by PLS-DA model, cross-validation and permutation tests are necessary (Worley and Powers 2013; Grootveld 2014).

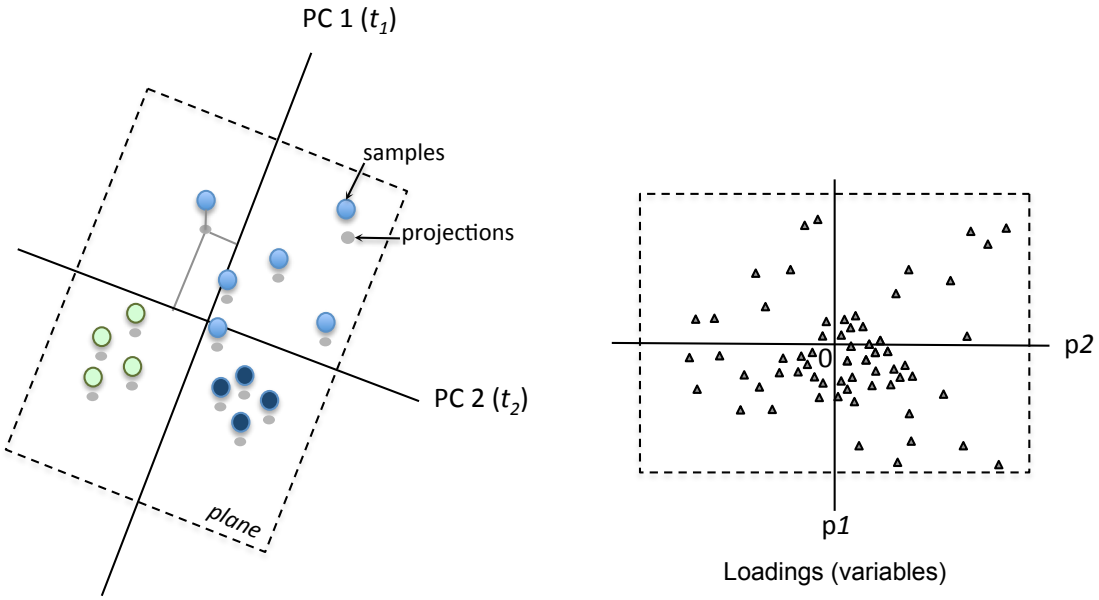

Figure 1.10. Principal component analysis model. Two-dimensional plane projection of original data that leads to a score plot (left) revealing groupings, trends and outliers among objects. The perpendicular distance from each point onto the plane is called residual error. Samples with similar multivariate profile fall close to each other. The loading plot (right) reveals the variables responsible for the discrimination of groups in the corresponding score plots. Highly correlated variables group together relatively far from the origin 0. Variables on opposite sides, with an angle greater than 90 degrees between them, have negative correlation.

1.5 Aim and outline of the thesis

Chronic immune diseases such as allergies, inflammatory bowel disease or diabetes are highly prevalent in industrialized countries. Although the symptoms of chronic immune diseases are treatable to some extent, the underlying pathologies remain incurable. Probiotic bacteria are widely used as food additives in "functional foods" or "neutraceuticals" and have shown clinical evidence of their safety and efficacy for the treatment of diseases. Besides that, there are diverging opinions on study results due to the lack of methodological standardization in selection of patients, study duration, selection of probiotic strains, or choice of appropriate doses for example (as reported by Hempel et al. 2011). The substantial growth of the probiotics market increased awareness of regulatory agencies as consumers might use such microorganisms as "drugs", where probiotics producers don´t have to invest in R&D and manufacturing practices for their products at the level required for pharmaceuticals. In 2010, the European Food Safety Authority issued unfavourable opinions on probiotics health claims and the major reason was the lack of information to identify the substance on which the claim is based. Thus, finding probiotics-derived compounds with functional bioactivity (also called *postbiotics*) and understanding its mechanisms of action may provide the basis for future development of therapeutic substances as well as appropriate probiotic strain selection for specific applications. Within this context, the overall objective of the present research was:

i. to perform FT-ICR MS untargeted metabolomics of cell-free supernatants obtained from probiotic strains *in vitro* cultivation, and to identify differences in the metabolic profile between bioactive and non-bioactive supernatants (Chapter 2).

ii. to stablish a classical bioassay-guided fractionation strategy to isolate and identify bioactive molecules present in cell-free probiotic supernatants (Chapter 3) and to develop and implement an UPLC-MS analytical method for the enantioseparation and quantitative analysis of DL-amino acids in biological matrices (Chapter 4).

iii. to prove D-tryptophan as a probiotic-derived metabolite involved in the modulation of the immune response *in vitro* and *in vivo* (Chapter 5).

Figure 1.11. Multi-institutional and interdisciplinary research collaboration network

This work was made possible thanks to the close cooperation between scientists and PhD students from the different departments and institutions illustrated above. I declare no conflicts of interest.

1.6 References

Alonso A., Marsal S., Julià A., 2015. Analytical Methods in Untargeted Metabolomics: State of the Art in 2015. *Frontiers in Bioengineering and Biotechnology* 3: 23.

Annesley T.M., 2003. Ion Suppression in Mass Spectrometry. *Clinical Chemistry* 49: 1041–44.

Antón J., Lucio M., Pena A., Cifuentes A., Brito-Echeverria J., Moritz F. et al. 2013. High Metabolomic Microdiversity within Co-occurring Isolates of the Extremely Halophilic Bacterium *Salinibacter ruber. PLOS One* 8: e64701

Arnaud C.H., 2010. High-Res Mass Spec. *Chemical & Engineering News* 88: 10–15.

Arpaia N., Campbell C., Fan X., Dikiy S., van der Veeken J., DeRoos P., Liu H., et al., 2013. Metabolites Produced by Commensal Bacteria Promote Peripheral Regulatory T-Cell Generation. *Nature* 504: 451–55.

Baker M., 2011. Metabolomics: From Small Molecules to Big Ideas. *Nature Methods* 8: 117–21.

Behrends V., Ebbels T.M.D., Williams H.D., Bundy J.G., 2009. Time-Resolved Metabolic Footprinting for Nonlinear Modeling of Bacterial Substrate Utilization. *Applied and Environmental Microbiology* 75: 2453–63.

Bergquist J., Baykut G., Bergquist M., Witt M., Mayer F-J., Baykut D., 2012. Human Myocardial Protein Pattern Reveals Cardiac Diseases. *International Journal of Proteomics*, Article ID 342659, 1–17.

Boccard J., Veuthey J.L., Rudaz S., 2010. Knowledge Discovery in Metabolomics: An Overview of MS Data Handling. J*ournal of Separation Science* 33: 290–304.

Bonarius H.P., Houtman J.H., Schmid G., de Gooijer C.D., Tramper J., 2000. Metabolic-Flux Analysis of Hybridoma Cells under Oxidative and Reductive Stress Using Mass Balances. *Cytotechnology* 32: 97–107.

Brenton A.G., Godfrey A.R. 2010. Accurate Mass Measurement: Terminology and Treatment of Data. *Journal of the American Society for Mass Spectrometry* 21: 1821–35.

Brouwer M.L., Wolt-Plompen S.A.A., Dubois A.E.J., Van Der Heide S., Jansen D.F., Hoijer M.A., Kauffman H.F., Duiverman E.J., 2006. No Effects of Probiotics on Atopic Dermatitis in Infancy: A Randomized Placebo-Controlled Trial. *Clinical & Experimental Allergy* 36: 899–906.

Bruker Daltonik GmbH. 2008. *maXis User Manual*. version 1.

Bucar F., Wube A., Schmid M., 2013. Natural Product Isolation - How to Get from Biological Material to Pure Compounds. *Natural Product Reports* 30: 525–45.

Buchen, L. 2010. What Can Microbiologists Who Study Human Bowels Learn from Those Who Study the Bowels of the Earth? *Nature* 468: 492–95.

Büscher J.M., Czernik D., Ewald J.C., Sauer U., Zamboni N., 2009. Cross-Platform Comparison of Methods for Quantitative Metabolomics of Primary Metabolism. *Analytical Chemistry* 81: 2135–43.

Caporale L.H. 1995. Chemical Ecology: A View from the Pharmaceutical Industry. *Proceedings of the National Academy of Sciences of the United States of America* 92:

75–82.

Cech N.B., Enke C.G., 2002. Practical Implications of Some Recent Studies in Electrospray Ionization Fundamentals. *Mass Spectrometry Reviews* 20: 362–87.

Cheplin H.A., Rettger L.F., 1920. Studies on the Transformation of the Intestinal Flora, with Special Reference to Implantation of Bacillus Acidophilus, II. Feeding Experiments on Man. *Proceedings of the National Academy of Sciences of the United States of America* 6: 704–05.

Collins S.M., Surette M., Bercik P., 2012. The Interplay between the Intestinal Microbiota and the Brain. *Nature Reviews Microbiology* 10 (11): 735–42.

Cooks G.R., Ouyang Z., Takats Z., Wiseman J.M., 2006. *Ambient Mass Spectrometry*. Science 311: 1566–70.

Cuperlović-Culf M., Barnett D., Culf A.S., Chute I., 2010. Cell Culture Metabolomics: Applications and Future Directions. *Drug Discovery Today* 15: 610–21.

da Luz J.A., Hans E., Zeng A-P., 2014. Automated Fast Filtration and on-Filter Quenching Improve the Intracellular Metabolite Analysis of Microorganisms. *Engineering in Life Sciences* 14: 135–42.

David L.A., Materna A.C., Friedman J., Campos-Baptista M.I., Blackburn M.C., Perrotta A., Erdman S.E., Alm E.J., 2014. Host Lifestyle Affects Human Microbiota on Daily Timescales. *Genome Biology* 15: R89.

De Roock S., Van Elk M., Hoekstra M.O., Prakken B.J., Rijkers G.T., de Kleer I.M., 2011. Gut Derived Lactic Acid Bacteria Induce Strain Specific CD4 + T Cell Responses in Human PBMC. *Clinical Nutrition* 30: 845–51.

de Vos W.M., De Vos E.J., 2012. Role of the Intestinal Microbiome in Health and Disease: From Correlation to Causation. *Nutrition Reviews* 70 (SUPPL. 1): 45–56.

Delzenne N.M., Audrey N.M., Fredrik B., Cani P.D., 2011. Targeting Gut Microbiota in Obesity: Effects of Prebiotics and Probiotics. *Nature Reviews Endocrinology* 7: 639-46.

Denisov E., Damoc E., Lange O., Makarov A., 2012. Orbitrap Mass Spectrometry with Resolving Powers above 1,000,000. *International Journal of Mass Spectrometry* 325-327: 80–85.

Dietmair S., Timmins N.E., Gray P.P., Nielsen L.K., Krömer J.O., 2010. Towards Quantitative Metabolomics of Mammalian Cells: Development of a Metabolite Extraction Protocol. *Analytical Biochemistry* 404: 155–64.

Dörries K., Lalk M., 2013. Metabolic Footprint Analysis Uncovers Strain Specific Overflow Metabolism and D-Isoleucine Production of Staphylococcus Aureus COL and HG001. *PLoS ONE* 8: e81500.

Ege M.J., Mayer M., Normand A-C., Genuneit J., Cookson W., Phil D., et al., 2011. Exposure to Environmental Microorganisms and Childhood Asthma. T*he New England Journal of Medicine* 364: 701–09.

Eckburg P.B., Bik E.M., Bernstein C.N., Purdom E., Dethlefsen L., Sargent M., Gill S.R., Nelson K.E., Relman D., 2005. Diversity of the human intestinal microbial flora. *Science* 308: 1635–38.

Ettre L.S., Sakodynskii K.I., 1993a. M.S. Tswett and the Discovery of Chromatography I: Early Work (1899-1903). *Chromatographia* 35 (3/4): 223–31.

———. 1993b. M.S. Tswett and the Discovery of Chromatography II: Completion of the Developments of Chromatography. *Chromatographia* 35 (5): 329–38.

FAO/WHO, Joint Working Group on Drafting Guidelines for the Evaluation of Probiotics in Food, 2002. Guidelines for the Evaluation of Probiotics in Food.

Fenn J.B., Mann M., Meng C.K., Wong S.F., Whitehouse C.M., 1989. Electrospray Ionization for Mass Spectrometry of Large Biomolecules. *Science* 246: 64–71.

Fiehn O., 2002. Metabolomics - the Link between Genotyopes and Phenotypes. *Plant Molecular Biology* 48: 155–71.

Fleming A., 1929. On the Antibacterial Action of Cultures of a Penicillium, with Special Reference to Their Use in the Isolation of B. Influenzae. *British Journal of Experimental Pathology* 10: 226–36.

Forcisi S., Moritz F., Kanawati B., Tziotis D., Lehmann R., Schmitt-Kopplin P., 2013. Liquid Chromatography-Mass Spectrometry in Metabolomics Research: Mass Analyzers in Ultra High-Pressure Liquid Chromatography Coupling. *Journal of Chromatography A* 1292: 51–65.

Frei R., Lauener R.P., Crameri R., O'Mahony L., 2012. Microbiota and Dietary Interactions: An Update to the Hygiene Hypothesis? *Allergy* 67: 451–61.

Gill H.S., Guarner F., 2004. Probiotics and Human Health: A Clinical Perspective. *Postgraduate Medical Journal* 80 (947): 516–26.

Gill M.A., 2012. The Role of Dendritic Cells in Asthma. *The Journal of Allergy and Clinical Immunology* 129 (4): 889–901.

Gill S.R., Pop M., Deboy R.T., Eckburg P.B., Peter J., Samuel B.S., Gordon J.I., Relman D.A., Fraser C.M., Nelson K.E., 2006. Metagenomic Analysis of the Human Distal Gut Microbiome. *Science* 312 (5778): 1355–59.

Goodacre R., 2007. Metabolomics of a Superorganism. *The Journal of Nutrition* 137 (1 Suppl): 259S–266S.

Greenblum S., Turnbaugh P.J., Borenstein E., 2012. Metagenomic Systems Biology of the Human Gut Microbiome Reveals Topological Shifts Associated with Obesity and in Fl Ammatory Bowel Disease. *Proceedings of the National Academy of Sciences of the United States of America* 109: 594–99.

Grootveld M., 2014. Introduction to the Applications of Chemometric Techniques in 'Omics' Research: Common Pitfalls, Misconceptions and 'Rights and Wrongs'. In Metabolic Profiling: Disease and Xenobiotics, Chapter 1, 1–34. Royal Society of Chemistry

Guillarme D., Ruta J., Rudaz S., Veuthey J-L., 2010. New Trends in Fast and High-Resolution Liquid Chromatography: A Critical Comparison of Existing Approaches. *Analytical and Bioanalytical Chemistry* 397: 1069–82.

Hamilton-Miller J.M.T., Gibson G.R., Bruck W., 2007. Some Insights into the Derivation and Early Uses of the Word 'probiotic. *British Journal of Nutrition* 90: 845.

Harvey A.L., Edrada-Ebel R., Quinn R.J., 2015. The Re-Emergence of Natural Products for Drug Discovery in the Genomics Era. *Nature Reviews Drug Discovery* 14: 111-29.

Havlícek V., Spízek J., 2014. Natural Products Analysis Intrumentation, Methods, and Applications. Edited by Vladimír Havlícek and Jaroslav Spízek. Hoboken, New Jersey, John Wiley & Sons, Inc.

Helfer M., Koppensteiner H., Schneider M., Rebensburg S., Forcisi S., Müller C., Schmitt-Kopplin P., Schindler M., Brack-Werner R., 2014. The Root Extract of the Medicinal Plant Pelargonium Sidoides Is a Potent HIV-1 Attachment Inhibitor. *PLoS ONE* 9: e87487.

Hempel S., Newberry S., Ruelaz A., Wang Z., Miles J.N.V., Suttorp M.J., Johnsen B., et al. 2011. Safety of Probiotics Used to Reduce Risk and Prevent or Treat Disease. Agency for Healthcare Research and Quality. Evidence Report Technology Assessment.

Hoffmann E., Stroobant V., 2007. Mass Spectrometry Principles and Applications. Third Edition, Chichester, England: John Wiley & Sons Ltd.

Hooper L.V, Littman D.R., Macpherson A.J., 2012. Interactions between the Microbiota and the Immune System. *Science* 336: 1268–73.

Howarth G.S., 2010. Probiotic-Derived Factors: Probiotaceuticals? *The Journal of Nutrition* 140: 229–30.

Huang Z., Shao W., Gu J., Hu X., Shi Y., Xu W., Huang C., Lin D., 2015. Effects of Culture Media on Metabolic Profiling of the Human Gastric Cancer Cell Line SGC7901. *Molecular BioSystems* 11: 1832–40.

Isolauri E., Arvola T., Sütas Y., Moilanen E., Salminen S., 2000. Probiotics in the Management of Atopic Eczema. *Clinical and Experimental Allergy* 30: 1604–10.

Ito T., Odake T., Katoh H., Yamaguchi Y., Aoki M., 2011. High-Throughput Profiling of Microbial Extracts. *Journal of Natural Products* 74: 983–88.

Jansson J., Willing B., Lucio M., Fekete A., Dicksved J., Halfvarson J., Tysk C., Schmitt-Kopplin P., 2009. Metabolomics Reveals Metabolic Biomarkers of Crohn's Disease. *PLoS ONE* 4: e6386.

Jessome L.L., Volmer D.A., 2006. Ion Suppression: A Major Concern in Mass Spectrometry. *LCGC North America* 24: 498–510.

Josefa A., Lucio M., Pena A., Cifuentes A., Brito-Echeverría J., Moritz F., Tziotis D., et al., 2013. High Metabolomic Microdiversity within Co-Occurring Isolates of the Extremely Halophilic Bacterium Salinibacter Ruber. *PLoS ONE* 8: 1–14.

Kalliomäki M., Salminen S., Arvilommi H., Kero P., Koskinen P., Isolauri E., 2001. Probiotics in Primary Prevention of Atopic Disease: A Randomised Placebo-Controlled Trial. *The Lancet* 357: 1076–79.

Katan M.B., 2012. Why the European Food Safety Authority Was Right to Reject Health Claims for Probiotics. *Beneficial Microbes* 3: 85–89.

Kebarle P., Verkerk U.H., 2009. Electrospray: From Ions in Solution to Ions in the Gas Phase, What We Know Now. *Mass Spectrometry Reviews* 28: 898–917.

Keeney K.M., Finlay B.B.. 2011. Enteric Pathogen Exploitation of the Microbiota-Generated Nutrient Environment of the Gut. *Current Opinion in Microbiology* 14: 92–98.

Kleerebezem M., Hols P., Bernard E., Rolain T., Zhou M., Siezen R.J., Bron P., 2010. The Extracellular Biology of the Lactobacilli. *FEMS Microbiology Reviews* 34: 199–230.

Koeth R.A., Wang Z., Levison B.S., Buffa J.A., Org E., Sheehy B.T., Britt E.B., et al. 2013. Intestinal Microbiota Metabolism of L-Carnitine, a Nutrient in Red Meat, Promotes Atherosclerosis. *Nature Medicine* 19: 576–85.

Krug S., Kastenmuller G., Stuckler F., Rist M.J., Skurk T., Sailer M., Raffler J., et al., 2012. The Dynamic Range of the Human Metabolome Revealed by Challenges. *The FASEB Journal* 26: 2607–19.

Kuhlisch C., Pohnert G., 2015. Metabolomics in Chemical Ecology. *Natural Product Reports* 32: 937–55.

Kungl. Vetenskapsakademien, The Royal Swedish Academy of Sciences. 2002. Mass Spectrometry (MS) and Nuclear Magnetic Resonance (NMR) Applied to Biological Macromolecules. Advanced Information on the Nobel Prize in Chemistry 2002. Available at: https://www.nobelprize.org/uploads/2018/06/advanced-chemistryprize2002.pdf (Accessed: 23 Mar 2020).

Kurita K.L., Glassey E., Linington R.G., 2015. Integration of High-Content Screening and Untargeted Metabolomics for Comprehensive Functional Annotation of Natural Product Libraries. *Proceedings of the National Academy of Sciences of the United States of America* 112: 11999–12004.

Lanzavecchia A., Sallusto F., 2001. Regulation of T Cell Immunity by Dendritic Cells. *Cell* 106: 263–266.

Lazar I.M., Grym J., Foret F., 2006. Microfabricated Devices: A New Sample Introduction Approach to Mass Spectrometry. *Mass Spectrometry Reviews* 25: 573–94.

Leao P.N., Pereira A.R., Liu W-T., Ng J., Pevzner P.A., Dorrestein P.C., König G.M., et al., 2010. Synergistic Allelochemicals from a Freshwater Cyanobacterium. *Proceedings of the National Academy of Sciences of the United States of America* 107: 11183–88.

Lechtenfeld O.J., Hertkorn N., Shen Y., Witt M., Benner R., 2015. Marine Sequestration of Carbon in Bacterial Metabolites. *Nature Communications* 6: 6711.

León Z., García-Cañaveras J.C., Donato M.T., Lahoz A., 2013. Mammalian Cell Metabolomics: Experimental Design and Sample Preparation. *Electrophoresis* 34: 2762–75.

Lindon J.C., Nicholson J.K., Holmes E., 2007. Handbook of Metabonomics and Metabolomics. First Edition, Amsterdam, The Netherlands: Elsevier B.V.

Lucio M. 2008. Datamining Metabolomics: The Convergence Point of Non-Target Approach and Statistical Investigation (Doctoral dissertation). Fakultät Wissenschaftszentrum Weihenstephan, Technischen Universität München.

Manisali I., Chen D.D.Y., Schneider B.B., 2006. Electrospray Ionization Source Geometry for Mass Spectrometry: Past, Present, and Future. *TrAC Trends in Analytical Chemistry* 25: 243–56.

Månsson M., Phipps R.K., Gram L., Munro M.H.G., Larsen T.O., Nielsen K.F., 2010. Explorative Solid-Phase Extraction (E-SPE) for Accelerated Microbial Natural Product Discovery, Dereplication, and Purification. *Journal of Natural Products* 73: 1126–32.

Mapelli V., Olsson L., Nielsen J., 2008. Metabolic Footprinting in Microbiology: Methods and Applications in Functional Genomics and Biotechnology. *Trends in Biotechnology* 26: 490–97.

Marshall A.G., Hendrickson C.L., Jackson G.S., 1998. Fourier Transform Ion Cyclotron Resonance Mass Spectrometry: A Primer. *Mass Spectrometry Reviews* 17: 1–35.

Marshall A.G., 2000. Milestones in Fourier Transform Ion Cyclotron Resonance Mass Spectrometry Technique Development. *International Journal of Mass Spectrometry*

200: 331–56.

Marshall A.G., Hendrickson C.L., 2002. Fourier Transform Ion Cyclotron Resonance Detection: Principles and Experimental Configurations. *International Journal of Mass Spectrometry* 215: 59–75.

Mazmanian S.K., Liu C.H., Tzianabos A.O., Kasper D.L., 2005. An Immunomodulatory Molecule of Symbiotic Bacteria Directs Maturation of the Host Immune System. *Cell* 122: 107–18.

Mazmanian S.K., Round J.L., Kasper D.L., 2008. A Microbial Symbiosis Factor Prevents Intestinal Inflammatory Disease. *Nature* 453: 620–25.

Metchnikoff, E.; Mitchell, P.C. The Prolongation of Life. Optimistic Studies. G.P. Putnam´s Sons: London, UK, 1908.

Michail S., 2009. The Role of Probiotics in Allergic Diseases. *Allergy, Asthma & Clinical Immunology* 5: 5.

Mishur R.J., Rea S.L., 2012. Applications of Mass Spectrometry to Metabolomics and Metabonomics: Detection of Biomarkers of Aging and of Age-Related Diseases. *Mass Spectrometry Reviews* 31: 70–95.

Mountzouris K.C., McCartney A.L., Gibson G.R., 2002. Intestinal Microflora of Human Infants and Current Trends for Its Nutritional Modulation. *British Journal of Nutrition* 87: 405–20.

Münz C., Steinman R.M., Fujii S-i., 2005. Dendritic Cell Maturation by Innate Lymphocytes: Coordinated Stimulation of Innate and Adaptive Immunity. *The Journal of Experimental Medicine* 202: 203–07.

Newman D.J., Cragg G.M., 2012. Natural Products as Sources of New Drugs over the 30 Years from 1981 to 2010. *Journal of Natural Products* 75: 311–35.

Nguyen D.T.T., Guillarme D., Rudaz S., Veuthey J-L., 2006. Fast Analysis in Liquid Chromatography Using Small Particle Size and High Pressure. *Journal of Separation Science:* 1836–48.

Nicholson J.K., Lindon J.C., 2008. Metabonomics. *Nature* 455: 1054–56.

Nicholson J.K., Lindon J.C., Holmes. E., 1999. Metabonomics: Understanding the Metabolic Responses of Living Systems to Pathophysiological Stimuli via Multivariate Statistical Analysis of Biological NMR Spectroscopic Data. *Xenobiotica* 29: 1181–89.

Niers L., Martín R., Rijkers G., Sengers F., Timmerman H., Van Uden N., Smidt H., Kimpen J., Hoekstra M., 2009. The Effects of Selected Probiotic Strains on the Development of Eczema (the PandA Study). *Allergy* 64: 1349–58.

O'Hara A.M., Shanahan F., 2006. The Gut Flora as a Forgotten Organ. *EMBO Reports* 7: 688–93.

Oláh E., Fekete S., Fekete J., Ganzler K., 2010. Comparative Study of New Shell-Type, Sub-2 Micron Fully Porous and Monolith Stationary Phases, Focusing on Mass-Transfer Resistance. *Journal of Chromatography A* 1217: 3642–53.

Osborn D.A., Sinn J.K., 2007. Probiotics in Infants for Prevention of Allergic Disease and Food Hypersensitivity. Cochrane Database Systematic Reviews, No. 4.

Oss M., Kruve A., Herodes K., Leito I., 2010. Electrospray Ionization Efficiency Scale of Organic Compounds. *Analytical Chemistry* 82: 2865–72.

Palková Z., 2004. Multicellular Microorganisms: Laboratory versus Nature. *EMBO Reports* 5: 470–76.

Pascolutti M., Quinn R.J., 2014. Natural Products as Lead Structures: Chemical Transformations to Create Lead-like Libraries. *Drug Discovery Today* 19: 215–21.

Patti G.J., Yanes O.,Siuzdak G., 2012. Metabolomics: The Apogee of the Omics Trilogy. *Nature Reviews, Molecular Cell Biology* 13: 263–69.

Pawankar R., Canonica G.W., Holgate S.T., Lockey R.F., Blaiss M.S., 2013. WAO White Book on Allergy. World Allergy Organization.

Pedretti S., 2013. Probiotic Market : Up or Down? *Nutrafoods* 12: 18–19.

Pinu F.R., Villas-Boas S.G., 2017. Extracellular Microbial Metabolomics: The State of the Art. *Metabolites* 43: 1-15, doi:10.3390/metabo7030043.

Prince E.K, Pohnert G., 2010. Searching for Signals in the Noise: Metabolomics in Chemical Ecology. *Analytical and Bioanalytical Chemistry* 396: 193–97.

Qin J., Li R., Raes J., Arumugam M., Burgdorf K.S., Manichanh C., Nielsen T., et al. 2010. A Human Gut Microbial Gene Catalogue Established by Metagenomic Sequencing. *Nature* 464: 59–65.

Raynie D.E., Essel V., 2013. Green Chemistry Perspectives on Analytical Extractions. *LC GC North America* 31: 18–21.

Reiner S.L., 2007. Development in Motion: Helper T Cells at Work. *Cell* 129: 33–36.

Round J.L., Mazmanian S.K., 2009. The Gut Microbiome Shapes Intestinal Immune Responses during Health and Disease. *Nature Reviews Immunology* 9: 313–23.

Sánchez B., Urdaci M.C., Margolles A., 2010. Extracellular Proteins Secreted by Probiotic Bacteria as Mediators of Effects That Promote Mucosa-Bacteria Interactions. *Microbiology* 156: 3232–42.

Sarker S.D., Latif Z., Gray A.I., 2006. Natural Products Isolation. Second edition: Totowa, New Jersey, Humana Press Inc.

Saxelin M., 2008. Probiotic Formulations and Applications, the Current Probiotics Market, and Changes in the Marketplace: A European Perspective. *Clinical Infectious Diseases* 46 (Suppementary article 2): S76–79.

Scalbert A., Brennan L., Fiehn O., Hankemeier T., Kristal B.S., van Ommen B., Pujos-Guillot E., et al., 2009. Mass-Spectrometry-Based Metabolomics: Limitations and Recommendations for Future Progress with Particular Focus on Nutrition Research. *Metabolomics* 5: 435–58.

Schmitt-Kopplin P., Gelenscér A., Dabek-Zlotorzynka E., Kiss G., Hertkorn N., Harir M., Hong Y., Gebefügi I., 2010. Analysis of the Unresolved Organic Fraction in Atmospheric Aerosols with Ultrahigh-Resolution Mass Spectrometry and Nuclear Magnetic Resonance Spectroscopy: Organosulfates As Photochemical Smog Constituents. *Analytical Chemistry* 82: 8017–26.

Sekirov I., Finlay B.B., 2006. Human and Microbe: United We Stand. *Nature Medicine* 12: 736–37.

Sellick C.A., Hansen R., Stephens G.M., Goodacre R., Dickson A.J., 2011. Metabolite Extraction from Suspension-Cultured Mammalian Cells for Global Metabolite Profiling. *Nature Protocols* 6: 1241–49.

Sender R., Fuchs S., Milo R., 2016. Are We Really Vastly Outnumbered? Revisiting the Ratio of Bacterial to Host Cells in Humans. *Cell* 164: 337–40.

Sixt B.S., Siegl A., Müller C., Watzka M., Wultsch A., Tziotis D., Montanaro J., Richter A., Schmitt-Kopplin P., Horn M., 2013. Metabolic Features of Protochlamydia Amoebophila Elementary Bodies - A Link between Activity and Infectivity in Chlamydiae. *PLoS Pathogens* 9: e1003553.

Snyder L.R., Kirkland J.J., Dolan J.W., 2009. Introduction to Modern Liquid Chromatography. Third Edition, Hoboken, New Jersey, USA. John Wiley & Sons, Inc.

Sommer F., Bäckhed F., 2013. The Gut Microbiota-Masters of Host Development and Physiology. Nature Reviews, *Microbiology* 11: 227–38.

Strachan, D.P. 1989. Hay Fever, Hygiene, and Household Size. *The BMJ* 299: 1259–60.

Strachan, David P. 2000. Family Size , Infection and Atopy : The First Decade of the Hygiene Hypothesis . *Thorax* 55 (Suppl 1): 2–10.

Supelco 1998. Guide to solid hase extraction. Bulletin 910. Sigma-Aldrich Co.

Tanaka K., Waki H., Ido Y., Akita S., Yoshida Y., Yoshida T., Matsuo T., 1988. Protein and Polymer Analyses up to M/z 100 000 by Laser Ionization Time-of-Flight Mass Spectrometry. *Rapid Communications in Mass Spectrometry* 2: 151–53.

Taylor A.L., Dunstan J., Prescott S.L., 2007. Probiotic Supplementation for the First 6 Months of Life Fails to Reduce the Risk of Atopic Dermatitis and Increases the Risk of Allergen Sensitization in High-Risk Children: A Randomized Controlled Trial. *Journal of Allergy and Clinical Immunology* 119: 184–91.

Trygg J., Lundstedt T., 2007. Chemometrics Techniques for Metabonomics. The Handbook of Metabonomics and Metabolomics, edited by John C. Lindon, Jeremy K. Nicholson, and Elaine Holmes. First edition 171–199. Amsterdam, The Netherlands: Elsevier B.V.

Turnbaugh P.J., Ley R.E., Hamady M., Fraser-Liggett C., Knight R., Gordon J.I., 2007. The Human Microbiome Project: Exploring the Microbial Part of Ourselves in a Changing World. *Nature* 449: 804–10.

Tweeddale H., Notley-McRobb L., Ferenci T., 1998. Effect of Slow Growth on Metabolism of Escherichia Coli, as Revealed by Global Metabolite Pool ('metabolome') Analysis. *Journal of Bacteriology* 180: 5109–16.

Valenzuela J.F., Pinuer L., Cancino A.G., Yánez R.B., 2015. Effect of pH and Dilution Rate on Specific Production Rate of Extra Cellular Metabolites by Lactobacillus Salivarius UCO_979C in Continuous Culture. *Applied Microbiology and Biotechnology* 99: 6417–29.

van Deemter J.J., Zuiderweg F.J., Klinkenberg A. 1956. Longitudinal Diffusion and Resistance to Mass Transfer as Causes of Nonideality in Chromatography. *Chemical Engineering Science* 5: 271–89.

van der Werf M.J., Jellema R.H., Hankemeier T., 2005. Microbial Metabolomics: Replacing Trial-and-Error by the Unbiased Selection and Ranking of Targets. *Journal of Industrial Microbiology & Biotechnology* 32: 234–52.

Villas-Bôas S.G., Højer-Pedersen J., Akesson M., Smedsgaard J., Nielsen J., 2005. Global Metabolite Analysis of Yeast: Evaluation of Sample Preparation Methods. *Yeast* 22: 1155–69.

Walker A., Lucio M., Pfitzner B., Scheerer M.F., Neschen S., de Angelis M.H., Hartmann

A., et al. 2014. The Importance of Sulfur-Containing Metabolites in Discriminating Fecal Extracts between Normal and Type 2 Diabetic Mice. J*ournal of Proteome Research* 13: 4220–31.

Walker A., Pfitzner B., Neschen S., Kahle M., Harir M., Lucio M., Moritz F., et al. 2014. Distinct Signatures of Host-Microbial Meta-Metabolome and Gut Microbiome in Two C57BL/6 Strains under High-Fat Diet. *The ISME Journal* 8: 2380–96.

Wang Z., Klipfell E., Bennett B.J., Koeth R., Levison B.S., Dugar B., Feldstein A.E., et al. 2011. Gut Flora Metabolism of Phosphatidylcholine Promotes Cardiovascular Disease. *Nature* 472: 57–63.

Wegh C.A.M., Geerlings S.Y., Knol J., Roeselers G., Belzer C., 2019. Postbiotics and Their Potential Applications in Early Life Nutrition and Beyond. *International Journal of Molecular Sciences* 20: 4673; doi:10.3390/ijms20194673.

Weller M.G., 2012. A Unifying Review of Bioassay-Guided Fractionation, Effect-Directed Analysis and Related Techniques. *Sensors* 12: 9181–9209.

Wikoff W.R., Anfora A.T., Liu J., Schultz P.G., Lesley S., Peters E.C., Siuzdak G., 2009. Metabolomics Analysis Reveals Large Effects of Gut Microflora on Mammalian Blood Metabolites. *Proceedings of the National Academy of Sciences of the United States of America* 106: 3698–703.

Worley B., Powers R., 2013. Multivariate Analysis in Metabolomics. *Current Metabolomics* 1: 92–107.

Yan F., Cao H., Cover T.L., Washington M.K., Shi Y., Liu L., Chaturvedi R., et al., 2011. Colon-Specific Delivery of a Probiotic-Derived Soluble Protein Ameliorates Intestinal Inflammation in Mice through an EGFR-Dependent Mechanism. *The Journal of Clinical Investigation* 121: 2242–53.

Yan F., Polk D.B., 2012. Characterization of a Probiotic-Derived Soluble Protein Which Reveals a Mechanism of Preventive and Treatment Effects of Probiotics on Intestinal Inflammatory Diseases. *Gut Microbes* 3: 25–28.

Yeşilova, Yavuz, Ömer Çalka, Necmettin Akdeniz, and Mustafa Berktaş. 2012. Effect of Probiotics on the Treatment of Children with Atopic Dermatitis. *Annals of Dermatology* 24: 189–93.

Yuan M., Breitkopf S.B., Yang X., Asara J.M., 2012. A Positive/negative Ion-Switching, Targeted Mass Spectrometry-Based Metabolomics Platform for Bodily Fluids, Cells, and Fresh and Fixed Tissue. *Nature Protocols* 7: 872–81.

Zhan Y., Chen P-J, Sadler W.D., Wang F., Poe S., Núñez G., Eaton K., Chen G.Y., 2013. Gut Microbiota Protects against Gastrointestinal Tumorigenesis Caused by Epithelial Injury. *Cancer Research* 73: 7199–210.

Zubarev R.A., Makarov A., 2013. Orbitrap Mass Spectrometry. *Analytical Chemistry* 85: 5288–96.

2
Mining for Active Molecules in Probiotic Supernatant by Combining Non-Targeted Metabolomics and Immunoregulation Testing

Published as: *Juliano Roldan Fonseca, Marianna Lucio, Mourad Harir and Philippe Schmitt-Kopplin (2022). Metabolites 12:35.*

Author contributions

Juliano R. Fonseca proposed the research question, experimental design, and performed untargeted metabolomics analysis using FT-ICR-MS and data interpretation under the guidance of Philippe Schmitt-Kopplin. Juliano R. Fonseca conducted the literature search and wrote the first draft. Mourad Harir has performed MS spectra clean-up, data processing and molecular formula annotation. Marianna Lucio has performed multivariate statistics. All contributed to the review of the manuscript. Juliano R. Fonseca edited the final version.

Abstract

Chronic respiratory diseases such as asthma, are highly prevalent in industrialized countries. As cases are expected to rise, there is a growing demand for alternative therapies. Our recent research on the potential benefits of probiotics suggests that they could prevent and reduce the symptoms of many diseases by modulating the host immune system with secreted metabolites. This article presents the first steps of the research that led us to identify the immunoregulatory bioactivity of the amino acid D-Trp reported in our previous study. Here we analyzed the cell culture metabolic footprinting of 25 commercially available probiotic strains to associate metabolic pathway activity information with their respective immune modulatory activity observed in vitro. Crude probiotic supernatant samples were processed in three different ways prior untargeted analysis in positive and negative ionization mode by direct infusion ESI-FT-ICR-MS: protein precipitation, and solid phase extraction (SPE) using HLB and CN-E sorbent cartridges. The data obtained was submitted to multivariate statistical analyses to distinguish supernatant samples into the bioactive and non-bioactive group. Pathway analysis using discriminant molecular features showed an overrepresentation of the tryptophan metabolic pathway for the bioactive supernatant class, suggesting that molecules taking part in that pathway may be involved in the immunomodulatory activity observed in vitro. This work showcases the potential of metabolomics to drive product development and novel bioactive compound discovery out of complex biological samples in a top-down manner.

This chapter fully reproduces the content of the publication but includes some adaptations to align with the format of this thesis.

2.1 Introduction

The hygiene hypothesis suggests that the increase of atopic diseases in the modern civilization (e.g., asthma, allergic rhinitis, and atopic dermatitis) may be due the decreased exposure to microbes during the children's first year of life, particularly in developed countries and urban areas. High hygiene standards, use of antibiotics, less breastfeeding, and processed-food diets may prevent the normal development of baby's immune system by not challenging it to respond to different threats during its maturation (Buchen 2010; Strachan 1989). A comparable theory was proposed by Metchnikoff at the beginning of the 20th century, considered to be the precursor of the concept of probiotic bacteria. He suggested that the Bulgarian rural population had longer and healthier life span due to their high consumption of fermented milk containing the bacterium "Bulgarian Bacillus", today called *Lactobacillus delbrueckii subsp. Bulgaricus* (Metchnikoff 1908). However, it was only in the mid-1990s that "probiotics" received proper attention from the medical community as potential therapeutic agents (Podolsky 2012). Today, probiotics represent a serious research field where health claims have been made on a variety of diseases and a multibillion dollar global market has emerged around it, full of popular products that are now part of our daily life (Raghuwanshi et al. 2018).

Atopic diseases occur due an exaggerated and unbalanced immune response to environmental or food allergens, and treatment is based on interventions with antihistamines, glucocorticoids, steroids, or bronchodilators that provide relief of symptoms but no cure (Holgate & Lack 2005). In this context, probiotics have been studied as a therapeutic alternative. *Lacticaseibacillus rhamnosus* GG (LGG) was given to pregnant women prior to delivery who had at least one first-degree relative with atopic eczema, allergic rhinitis, or asthma, and then to the new-borns for six months. The results showed the frequency of atopic eczema in neonates was lower in the probiotic-treated group than in the placebo-treated control group (Kalliomaki et al. 2001). The use of the strains *Bifidobacterium lactis* BB-12 and LGG to control allergic inflammation was studied in 27 new-borns that manifested atopic eczema during breast-feeding and an improvement in skin condition after 2 months in all the infants receiving probiotics was reported, supported by a decrease of soluble CD4 glycoprotein concentration in serum (a marker of T-cell activation) and eosinophil protein X in urine (a marker for inflammatory activity) (Isolauri et al. 2000). Similar results were observed in another clinical trial where combination of probiotic strains was administered for 8 weeks to 40 children with atopic dermatitis. The total Immunoglobulin E (IgE) level in

serum decreased for the probiotic treated group; an antibody that triggers 'immediate hypersensitivity' reactions (Yeşilova 2012). The called "PandA study" reported a reduced incidence of infant eczema in the probiotic-administered group (6 weeks prenatally to mothers and 12 months postnatally to offspring) with positive effects persisting through 1 and 2 years. Reduction of cytokines that regulate many aspects of allergic inflammation was observed in whole blood cells obtained from probiotic-supplemented infants (Niers et al. 2009).

Nevertheless, inconsistency in clinical outcome has challenged the role of probiotics in allergy prevention. Two reviews articles have drawn attention to the lack of robustness of several published studies challenging the positive results observed after administration of probiotics to infants for the prevention of allergic disease (Osborn & Sinn 2007; Michail 2009). The Food and Drug Administration (FDA) has already defined probiotics as live biotherapeutic products and requires a more adequate clinical investigation following the principles of drug-like development (U.S. Food and Drug Administration 2013, p.10). The European Food Safety Authority has issued unfavorable opinions on health claims for probiotic and one of its major reasons was the lack of information on the substances causing the effect on which the claim is founded (Katan 2012).

Besides the efforts of the scientific community, the interaction between probiotics, diet and host remains only partially understood. The controversial results from probiotics research show how complex molecular crosstalk could be between probiotic bacteria, the gut microflora, and the immune system of the host. The ability of probiotics to regulate host immune system using several bacteria derived genes and proteins have been described (Yan 2011). Our own commensal bacteria also regulate immune responses beyond gut environment. It is suggested that symbiotic bacteria-derived metabolites such as carbohydrate binding proteins, short-chain fatty acids, long-chain fatty acids, and biogenic amines might affect host immune maturation, activation, and functions leading to tolerance or pro-inflammatory responses (Frei et al. 2012; Arpaia et al. 2013; Zheng et al. 2020).

Studies on microbiome-related treatments for immunological disorders using supplemented microorganisms are still needed. However, rational selection of which probiotic strain(s) may be submitted to non-clinical or clinical trials based on derived extracellular metabolites with potential host immunoregulatory activity is not a common practice so far.

Traditionally, bioassay-guided fractionation has dominated the discovery of new bioactive compound. The work starts with a complex crude extract from a source of potential

bioactive chemical entities (i.e., plants, fungi, marine organisms, microorganism cell cultures, etc.), and components are separated into fractions based on compounds physicochemical properties using different techniques such as chromatography, liquid-liquid extraction (LLE), supercritical fluid extraction (SFE), solid phase extraction (SPE), distillation, among others. An *in vitro* biological system (bioassay) tests for the effect caused by each fraction. Alternating between further fractionation and bioassay responses will likely lead to the isolation and identification of the compound/s with biological activity (Prince & Pohnert 2010). However, it is a time-consuming process and sometimes the bioactive effect of a fraction is lost after successive fractionation steps due to, e.g., dilution of the bioactive components to an inactive level, lack of long-term stability of components, or lack of synergistic activity of more than one component once each of them are separated into different fractions.

Enormous molecular diversity and biological functionality are two important features that metabolomics can cover at once, revealing potential bioactive compounds or at least leading to hypothesis that will set the ground for further investigations. We recently integrated targeted and non-targeted metabolomics strategies based on mass spectrometry into a clinical intervention trial using probiotics (Bazanella et al. 2017). Metabolomics was shown to be a valuable approach to the discover of new bioactive molecules in biosamples (Harvey et al. 2015; Anton et al. 2013; Kremb et al. 2017; O'Rourke et al. 2016), and out of extremely complex organic environmental samples (Mueller et al. 2020; Zhernov et al. 2017). *In vitro*, metabolomics can provide important information on cell-to-cell communication, on cell growth behavior, on metabolite flux supporting metabolic engineering and industrial biotechnological processes and has been successfully applied to study bacterial culture supernatants (Pinu & Villas-Boas 2017; Dörries & Lalk 2013; Behrends et al. 2009; Mapelli et al. 2008). **Figure 1.6** (Chapter 1) shows the workflow differences between the classical bioassay-guided fractionation and the metabolomics approach in the discovery of new bioactive compounds.

Here we want to highlight the first research steps we followed before our discovery of D-tryptophan as a modulator of the gut microbiome and allergic airway disease (Kepert et al. 2017; Krauss-Etschmann et al. 2020). This study presents our rapid screening approach via direct infusion of 25 samples derived from probiotic supernatant in high resolution Fourier Transform Ion Cyclotron Resonance Mass Spectrometry (FT-ICR-MS), with the objective to simultaneously screen as many metabolites as possible, and to discriminate supernatants that showed immunomodulatory properties from inactive ones by applying

multivariate statistical analysis to the acquired data. For that, aliquots of each probiotic culture supernatant were subjected in parallel to three different sample cleaning procedures prior to FT-ICR-MS analysis: a simple protein precipitation from the crude supernatant, and solid-phase extraction (SPE) with the HLB hydrophilic polymeric phase and cyano-propyl sorbent (CN-E) phase, i.e., each strain supernatant generated three samples (Crude Supernatant, HLB-SPE extract and CN-E-SPE extract) that were analyzed after electrospray ionization (ESI) in positive and negative modes.

2.2 Materials and Methods

2.2.1 Probiotic strains cultivation and supernatant collection

A total of 20 probiotic strains were obtained from Winclove Probiotics B.V. (Amsterdam, The Netherlands) whereas 5 other ones were purchased from three different sources (**Table 2**). The bacteria were cultivated using chemically defined medium CDM1 (based on Savijoki et al. 2006); consisting of 20 L-amino acids, ten vitamins, eight salts and four nucleobases (Suppl. **Table S 1**). The surfactant Tween® 80, a polysorbate, is known to cause interferences in mass spectrometry analyses and was therefore omitted from the medium (Tong et al. 2002). Cells were growth under sterile microaerobic/anaerobic conditions at 37 °C and bacteria concentration was followed by optical density of the medium (OD) at 600 nm. Supernatants were collected only after cells had reached stationary phase and a minimum cell number of 10^8 colony-forming units/mL. Fast filtration method was applied to separate cells from medium and cell-free supernatants were stored at -20 °C right after filtration and then at -80 °C until analysis. A portion of each supernatant was saved for bioassay screening as well.

2.2.2 Bioassays for immunomodulatory activity in probiotic supernatants

Results of two biological assays previously performed were used in this study to assign probiotic supernatants into the group of bioactive or non-bioactive one. The bioactivity screenings were based on probiotic supernatants ability decrease the CC chemokine ligand 17 (CCL17) secretion in a human Hodgkin lymphoma cell line (approx. 70% decrease relative to untreated cells and to supernatant from the non-probiotic Lacticaseibacillus rhamnosus DSM-20021; negative control), and to concordantly prevent upregulation of costimulatory molecules in LPS stimulated human dendritic cells, both assays are described in detail elsewhere (Kepert et al. 2017)

2.2.3 Sample pre-treatment prior to chemical analysis

Probiotic strains were cultivated in water-based and highly salted media, which may also contain lipids and proteins produced by the bacteria. These are potential interferes that must be removed from the samples prior to MS analysis. Thus, Oasis® HLB SPE cartridges (100 mg, 1 mL; Waters, Milford, MA, USA) and Bond Elut™ Cyano (CN-E) SPE cartridges (100 mg, 1 mL, Agilent, Inc., Walnut creek CA, USA) were first conditioned with 1 mL methanol and then equilibrated with 1 mL of water each. Cell-free culture supernatant of each strain and sterile CDM1 medium (Blank) were treated as follow: a portion of 5 mL were first centrifuged at 5000 rpm for 10 min at 10 °C, 2 mL of the upper layer were carefully taken and submitted to HLB-SPE and 2 mL to CN-E SPE purification. Each cartridge was then cleaned with 1 mL water and metabolites were eluted with 1 mL MeOH. Methanolic extracts were stored at -80 °C until analysis. It was also of interest to analyse crude supernatants as well, i.e., without being submitted to SPE extraction. Thus, 2 mL of each strain cell-free supernatant were transferred to Falcon™ tubes and were subject to protein precipitation with 4 mL cold acetonitrile (previously stored at -20 °C) during 20 min in ice bath immersion. Then, solutions were centrifuged at 11000 rpm for 10 min at 10 °C and the upper layer of each sample were carefully taken and stored until analysis.

All solvents and water were LC-MS grade quality (CROMASOLVE®, Fluka® Analytical, Sigma-Aldrich-Aldrich, St. Louis, USA).

2.2.4 FT-ICR-MS chemical analyses

Ultrahigh resolution mass spectra were acquired on a Fourier Transform Ion Cyclotron Resonance Mass Spectrometry (Solarix™, Bruker Daltonics GmbH, Bremen, Germany) equipped with a 12 Tesla super conducting magnet (magnex scientific Inc., Yarnton, GB). An Apollo II electrospray source (Bruker Daltonics GmbH, Bremen, Germany) was used for ionization. Prior sample analysis, the instrument was calibrated with on arginine clusters (m/z 173.10440, 347.21607, 521.32775 and 695.43943) by injecting 1 mg/L arginine solution - calibration errors in this mass range were below 0.1 ppm. SPE extracted samples were diluted 1:10 (v:v) for ESI positive mode analyses and 1:50 for negative mode. Non-extracted supernatants were diluted 1:10 for both ESI positive and negative mode analyses. Dilutions were done with 70% MeOH aqueous solution containing 0.1% FA and these dilution factors were defined after preliminary MS detection testes. Supernatant samples were injected with Gilson autosampler (223 Sample Changer, Gilson Inc., Middleton, USA) where samples were kept cooled at 8 °C during the analysis. Samples were analysed by

blocks of sample types: HLB extracts, CN-E extracts, and crude supernatants. The sample analysis order has been randomized between bioactive and non-bioactive supernatants inside each block. After the analysis of a group of 10 samples, three spectra of pure methanol were acquired to minimize cross-contamination and ion memory effects. MS data was acquired using the program ApexControl 1.5 (Bruker Daltonics) and the instrument has been tuned to obtain highest sensitivity for metabolites detection in each type of sample in a 10 min run time (Suppl. **Table S 2**).

2.2.5 Data processing and data analysis

Data processing of FT-ICR-MS spectra is an important step to originate meaningful data matrices used in multivariate statistical analyses and data interpretation. The spectra have been extracted and processed using the software DataAnalysis 4.0© (Bruker Daltonics GmbH, Bremen, Germany). Internal calibration of positive mode spectra was done according to a mass list of endogenous abundant metabolites such as amino acids and cell-growth medium components, where spectra acquired in negative mode were internally calibrated with a reference mass list of fatty acids. The mass lists files (.asc) were exported with a signal-to noise ratio (S/N) of 4 for ESI[+] and 3 for ESI[-] spectra, and were aligned within a 1 ppm window with the software Matrix Generator 0.4, an in-house written software (Lucio et al. 2011). Further mass filtering was performed in each data matrix and the masses occurred in less than 10% of samples (of each class) were excluded from further analysis. Sterile CDM1 medium samples and pure solvents spectra were equally treated. Possible elemental formulas were assigned for each peak in batch mode using in-house software (FormulaCalculator) (Green and Perdue 2015). The formulae generated were validated by setting chemical constraints (N rule, O/C ratio ≤ 1, H/C $\leq 2n+2$, elements count: C0-100, H0-∞, O0-80, N0-7, S0-1) in conjunction with an automated theoretical isotope pattern comparison (Kind and Fiehn 2007; Hertkorn et al. 2008). The different datasets were analyzed by multivariate data analysis. The data were scaled using the unit variance method. The first model, PCA (principal component analysis), gave an overview of the main relations between samples and variables, without any prior information on the diverse classes. The models revealed the first separation between the molecular signatures. For each model we presented the amount of variance explained by the first two components R^2Y(cumulative). A discriminatory strategy, using orthogonal partial least squares discriminant analysis (OPLS-DA), was then applied to all data matrices. The classification method drove the separation between bioactive and non-bioactive samples, increasing the likelihood of

producing biologically relevant results. The lists of the most important masses were listed choosing the highest loadings values. The goodness of the fit and of the prediction were evaluated with the R^2Y and Q^2 values. To exclude overfitting, we computed the p-value of the Cross-Validation Analysis of Variance (CV-ANOVA). All the multivariate modelling has been done in SIMCA-P© 13 (Umetrics, Umea, Sweden). Discriminant mass features that originated OPLS DA models were uploaded into MetaboAnalyst web-based platform with a search range of 1.0 ppm for metabolic pathway analysis (Chong et al. 2018).

2.3 Results and discussion

2.3.1 Probiotic strains and their respective supernatant immunomodulatory response

Each individual probiotic culture supernatant was harvested at early stationary phase since bacteria are at their maximum size and cell density and in theory, have maximized production of metabolites (Chubukov & Sauer 2014). These supernatants previously showed a concordant immune response in two different bioassay screenings (Kepert et al. 2017), i.e., it downmodulated costimulatory molecules (bioactive) or it was inactivity. The outcome was not specie dependent (**Table 2**).

Table 2: Probiotic strain supernatants subjected to metabolite screening and their respective immunomodulatory response previously observed in vitro.

			Effect on	
Bacterial strain	**Code**	**Source**	**DC[a]**	**KM-H2[b]**
Bifidobacterium animalis subsp.lactis	BB-12[c]	Chr. Hansen, Horsholm, Denmark	+	+
Bifidobacterium animalis	W53	Winclove Bioindustries BV, The Netherlands	-	-
Bifidobacterium breve	W9	Winclove Bioindustries BV, The Netherlands	+	+
Bifidobacterium breve	W25	Winclove Bioindustries BV, The Netherlands	-	-
Bifidobacterium lactis	BB-420	Danisco, Niebüll, Germany	+	+
Bifidobacterium lactis	W51	Winclove Bioindustries BV, The Netherlands	-	-
Enterococcus faecium	W54	Winclove Bioindustries BV, The Netherlands	-	-
Lactobacillus acidophilus	LA-5	Chr. Hansen, Horsholm, Denmark	+	+
Lactobacillus acidophilus	W12	Winclove Bioindustries BV, The Netherlands	-	-
Lactobacillus acidophilus	W33	Winclove Bioindustries BV, The Netherlands	+	+
Lactobacillus acidophilus	W74	Winclove Bioindustries BV, The Netherlands	-	-
Lacticaseibacillus casei	LC-01	Chr. Hansen, Horsholm, Denmark	+	+
Lacticaseibacillus casei	W20	Winclove Bioindustries BV, The Netherlands	-	-
Lacticaseibacillus casei	W56	Winclove Bioindustries BV, The Netherlands	+	+
Lacticaseibacillus casei	W79	Winclove Bioindustries BV, The Netherlands	+	+
Lactobacillus helveticus	W60	Winclove Bioindustries BV, The Netherlands	-	-
Lacticaseibacillus paracasei	W7	Winclove Bioindustries BV, The Netherlands	+	+
Lactiplantibacillus plantarum	W21	Winclove Bioindustries BV, The Netherlands	-	-
Lactiplantibacillus plantarum	W62	Winclove Bioindustries BV, The Netherlands	-	-
Lacticaseibacillus rhamnosus	LGG	Valio Ltd, Helsinki, Finland	+	+
Lacticaseibacillus rhamnosus	W102	Winclove Bioindustries BV, The Netherlands	-	-
Ligilactobacillus salivarius	W24	Winclove Bioindustries BV, The Netherlands	-	-
Lactococcis lactis	W32	Winclove Bioindustries BV, The Netherlands	-	-
Streptococcus salivarius	W122	Winclove Bioindustries BV, The Netherlands	-	-
Streptococcus thermophilus	W69	Winclove Bioindustries BV, The Netherlands	-	-

[a] Ability to decreased the percentages of human derived dendritic cells (DCs) expressing costimulatory molecules CD83-, CD80-, CD86-, and CD40 after lipopolysaccharide (LPS)-induced maturation, by at least 30% relative to untreated DCs and DCs treated with supernatant from the non-probiotic *Lacticaseibacillus rhamnosus* DSM-20021 (negative controls).

[b] Ability to lower CCL17 secretion by KM-H2 cells in a dose-dependent manner to concentrations of approx. 30% of those observed in untreated cells and in cells treated with supernatant of the non-probiotic *Lacticaseibacillus rhamnosus* DSM-20021 (negative controls).

[c] Apart from BB-12, probiotics providers did not disclose further details on subspecies

2.3.2 FT-ICR-MS analysis and data processing prior statistics

Prior FT-ICR-MS analysis, each individual probiotic supernatant was subjected to three different desalting extraction procedures to generate three organic extracts using methanol: two after solid phase extraction (HLB-SPE and CN-E SPE) and one after a simple protein precipitation of crude supernatant. These extracts also correspond to differential chromatographic fractionations leading to chemical mixtures with various biological responses. Analysis of each extract by FT-ICR-MS in both electrospray ionization (ESI) modes (i.e., positive and negative) resulted in an ASCII file containing the mass to charge (m/z) and their respective signal abundance. To investigate differences in the metabolome data between bioactive and non-bioactive probiotic supernatants, individual sample ASCII data files were combined according to sample type and ESI mode resulting in six data matrix: crude supernatant/ESI[+], crude supernatant/ESI[-], HLB-SPE extract/ESI[+], HLB-SPE extract/ESI[-], CN-E-SPE extract/ESI[+], and CN-E-SPE extract/ESI[-]. After mass signal alignment, mass filtering and molecular formula assignment, each data matrix showed several molecular features. The highest number of features was observed for the data matrix HLB-SPE extract followed by the matrix CN-E-SPE extract, both in ESI negative mode (**Table 3**)

Table 3: Number of m/z features present in each data matrix after data processing and molecular formula annotation

	Sample pretreatment applied		
ESI mode	**Crude Supernatant***	**HLB-SPE extract**	**CN-E-SPE extract**
Positive**	344	2658	1367
Negative	1970	3932	3353

* Crude supernatant was subject to protein precipitation with cold acetonitrile, followed by centrifugation (the upper layer of each sample was carefully taken and diluted prior analysis). No solid phase extraction was applied.

** Signal-to noise ratio (S/N) of 4 was applied as substantial amount of noise signals was not excluded with S/N 3. The significant lower amount of m/z annotated features presented in crude-supernatant analysis compared to SPE-extracts can be a result of ion suppression caused by growth medium components at high concentration; while SPE extracts concentrate metabolites and remove, to a certain extent, medium ingredients from the sample.

2.3.3 Principal Component Analysis and Orthogonal Partial Least Square Discriminative Analysis

Unsupervised principal component analysis (PCA) was applied to each individual data matrix without any input on sample classification to the model. The score plots obtained from these analyses are shown in **Figure 2.1**. Green and blue dots represent samples belonging to one of the two different groups for better visualization only, i.e., immunomodulatory active supernatants and inactive ones. Only two models showed a group separation trend (Plots D and F). The data obtained in ESI negative ionization mode for samples submitted to CN-E-SPE extraction showed a more homogenous grouping of bioactive supernatants when compared to other models suggesting that this model has predictive relevance. The strong homogeneity between the bioactive groups in that model is underlined through the presence of some outliers (samples from W32, W54, and W53). This could suggest more unique character of these inactive samples. Data matrix PCA analysis for HLB-SPE extracts/ESI[-] (model D) describes a particular pattern on correlated samples belonging to the group of non-bioactive supernatants in the lower-left quadrant. Samples in this cluster were originated from cell culture of different probiotic species (Bifidobacterium, Lactobacillus, Streptococcus, and Enterococcus), but those samples may share some similarities in their detected metabolic profile. This model also suggests predictive relevance.

Figure 2.2 shows the OPLS-DA score scatter plots for the six calculated models after 7-fold cross validation. The values that indicate the goodness of the fit (R2) and the different levels of predictability (Q2) are reported in the plots. We also added the p-values referred to the CV-ANOVA. We could achieve for the models B, E and F a Q2 value closer to 0.5. This could suggest that the model has predictive relevance for a particular reflective endogenous latent variable (Q2 = 0.5 indicates a good model; a threshold of 0.5 is generally admitted for metabolomics (Triba et al. 2015)). Highly divergent values of R2 and Q2 values would indicate model over fitting, i.e., poor prediction power (Hair et al. 2017; Worley & Powers 2013). Examining the results, we could infer that only 3 out of 6 models had a robust classification power: model F (CN-E-SPE extracts/ESI[-]), which showed already a separation of groups in unsupervised PCA even though 3 inactive samples were misclassified to the bioactive class (W60, W102 and W122); model **D** (HLB-SPE extract/ESI[-]) with its high classification power without misclassification of samples; and model **C** (HLB-SPE extract/ESI[+]) which showed also a good classification power although CV-Anova p value was higher for this model (p=0.046) than for the models **D** and **F**.

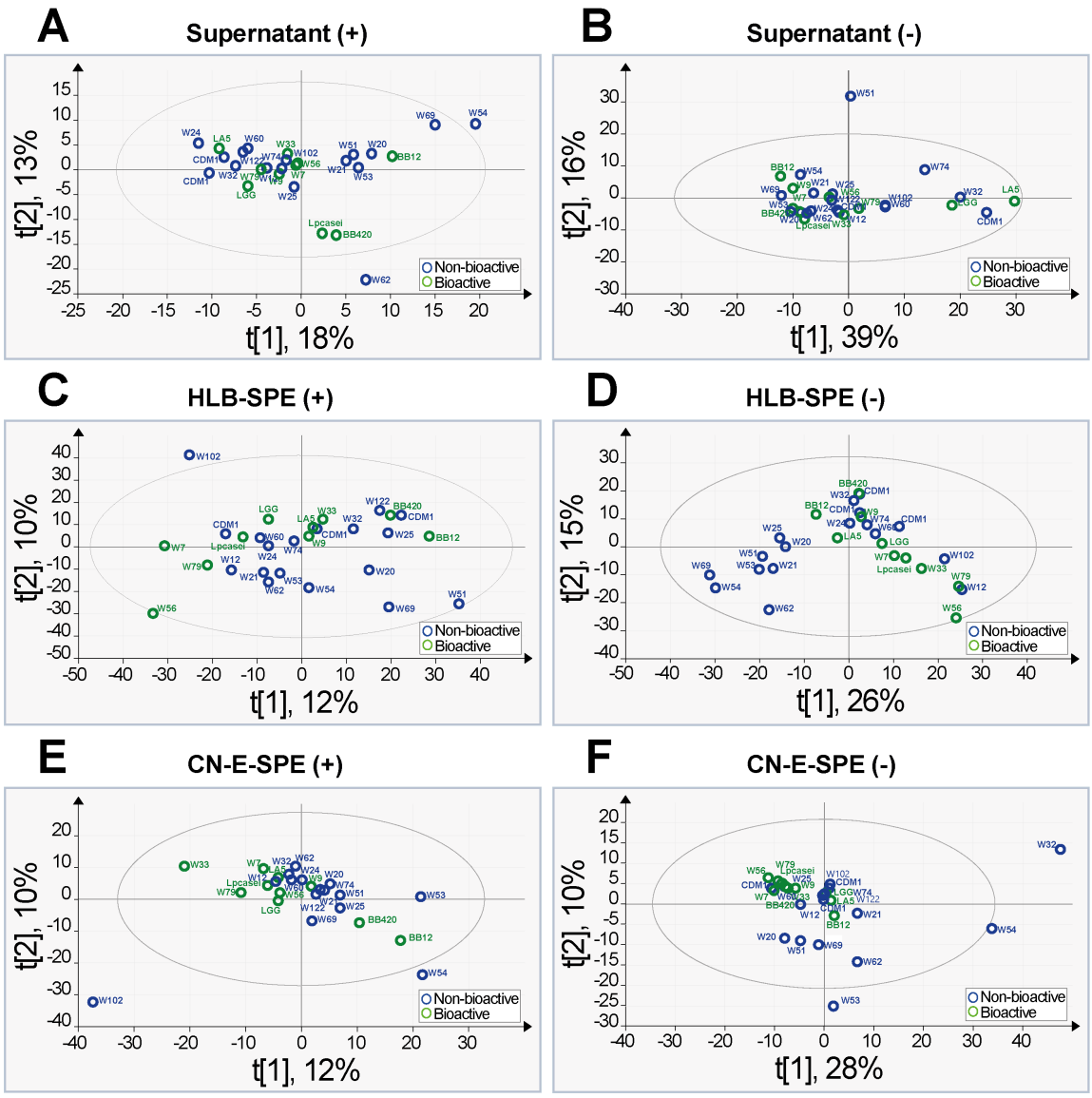

Figure 2.1. Unsupervised PCA scores plots obtained from the data matrix of samples of crude probioticotic supernatants (A,B), HLB-SPE extracts (C,D), and CN-E-SPE extracts (E,F). The left side displays results obtained from FT-ICR-MS analyses in ESI positive mode and the right side in ESI negative mode. Only models D and F showed a group separation trend with predictive relevance.

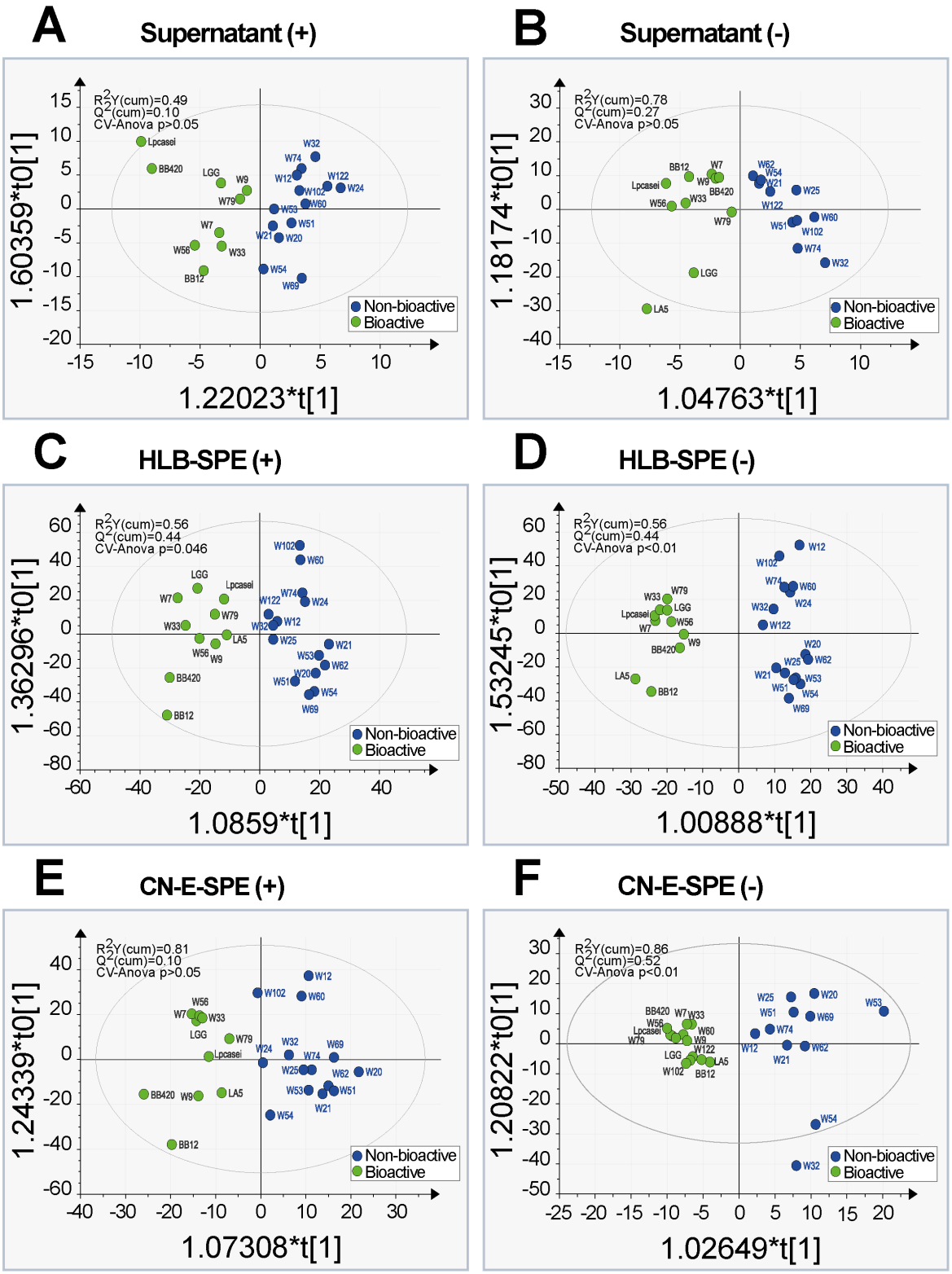

Figure 2.2. Supervised OPLS-DA scores plots. Models C, D and F are robust and have a high classification power. Discriminant molecular features (m/z) observed in these three models were submitted to metabolic pathway analysis thereafter. The left side displays results obtained from FT-ICR-MS analyses in ESI positive mode (A,C,E) and the right side in ESI negative mode (B,D,F).

2.3.4 Metabolic pathway assessment

The most discriminant masses revealed by OPLS-DA for each class in all robust models (**Figure 2.2 C,D,F**), were submitted to MetaboAnalyst web-based platform for metabolic pathway analysis using the "MS Peaks to Pathways" software feature; specially designed for untargeted metabolomics (Chong et al. 2018). As no library of bacteria species was available in MetaboAnalyst by the time of this assessment, *Homo sapiens* was chosen as specie to perform pathway analysis since it has the most comprehensive organism library in the KEGG metabolic network database (Kanehisa et al. 2000; Kanehisa et al. 2006). The resulting pathways activity listed by MetaboAnalyst was compared to the reference pathways represented in the KEGG database for species of bacteria analogous to those investigated in this study. Only bacteria pathways listed in KEGG which were the most populated with hits, and pathways reflecting the conditions of the experiment were considered for the data interpretation (e.g., nicotine and caffeine metabolism were excluded). **Figure 2.3** shows that unique pathways were populated for each class of supernatants in the three models, with little overlap between the two classes and between the results of the three data sets.

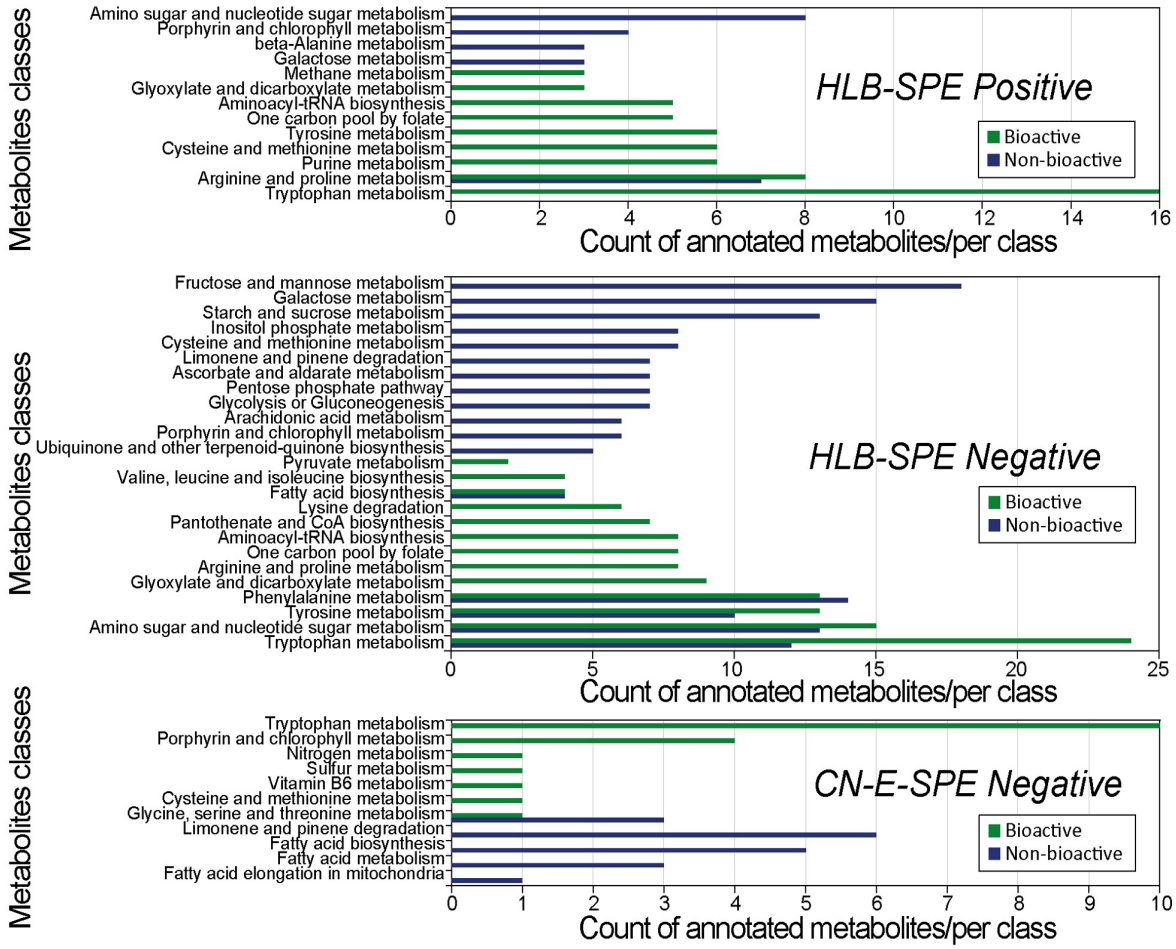

Figure 2.3. Description of the most populated KEGG metabolic pathways and their respective number of hits. Pathway analysis was originated from the most discriminant mass features of each class derived from the OPLS DA models that showed robust classification power.

2.3.5 Tryptophan Metabolism

Remarkably, the tryptophan (Trp) metabolic pathway was overrepresented in the bioactive supernatant class in all three models; especially in the HLB-SPE extract/ESI[+] and CN-E-SPE extract/ESI[-] ones, where no hits related to Trp metabolism were observed for the non-bioactive class. Metabolite hits predicted in the Trp pathway were compared between models and classes (**Table 4**). A comparison visualization using Venn diagrams is shown in (**Figure 2.4**). In fact, only 16 hits were observed from the data of HLB-SPE extract/ESI[+], but no unique one. A total of 24 hits were observed from the data of HLB-SPE extract/ESI[-], where 7 hits were unique. Ten hits were observed from the data of CN-E-SPE extract/ESI[-], being one hit unique. A total of 25 different hits related to tryptophan metabolism was counted for the class of bioactive supernatants combined. Discriminant features for the non-bioactive class of supernatants showed only three unique hits related to Trp metabolism while nine hits were shared with the bioactive class. Out of these nine shared

hits, six were present in all evaluated data matrices, two were present in HLB-SPE extracts but not in the CN-E extract, and one was only present in the HLB-SPE/ESI[-] matrix. Trp amino acid was annotated as discriminant feature only in the bioactive supernatant data set of HLB-SPE extracts in both positive and negative ionization mode.

Table 4: Tryptophan metabolism pathway activity prediction (hits) directly from mass peaks of the most discriminant features (KEGG compound codes).

Bioactive Supernatants SPE Extract			**Non-Bioactive Supernatants Extract**	**Metabolite Hit Prediction ***
HLB-SPE/ESI[+]	**HLB-SPE/ESI[-]**	**CN-E-SPE/ESI[-]**	**HLB-SPE/ESI[-]**	
C00078	C00078	NP	NP	Tryptophan
C00331	C00331	C00331	NP	Indolepyruvic acid
C00643	C00643	C00643	C00643	5-Hydroxy-L-tryptophan
C01598	C01598	NP	C01598	Melatonin
C00978	C00978	NP	NP	N-Acetylserotonin
C00780	C00780	C00780	NP	Serotonin
C02298	C02298	C02298	C02298	N-Acetylindoxyl
C02700	C02700	C02700	C02700	L-Formylkynurenine
C00328	C00328	C00328	NP	L-Kynurenine
C03227	C03227	NP	NP	3-Hydroxy-L-kynurenine
C00637	C00637	C00637	C00637	Indole-3-acetaldehyde
C02693	C02693	NP	NP	Indole-3-acetamide
C00954	C00954	C00954	C00954	Indole-3-acetic acid
C02937	C02937	NP	NP	Indole-3-acetaldehyde oxime
C03230	C03230	C03230	C03230	3-Indoleglycolaldehyde
C02043	C02043	NP	C02043	Indolelactate
NP	C00955	NP	C00955	Indole-3-ethanol
		C02470		Xanthurenic acid
	C01987			2-Aminophenol
	C01249			7,8-Dihydro-7,8-dihydroxykynurenate
	C01717			Kynurenic acid
	C00398			Tryptamine
	C02172			N-Acetylisatin
	C01252			4-(2-Aminophenyl)-2,4-dioxobutanoate
	C00463			Indole; 2,3-Benzopyrrole
			C02775	Dihydroxyindole
			C02938	3-Indoleacetonitrile
			C03574	2-Formylaminobenzaldehyde

* Metabolites are not structurally elucidated by mean of FT-ICR-MS but displayed as hit prediction based on high accuracy mass (<1.0 ppm mass error).
NP: not present

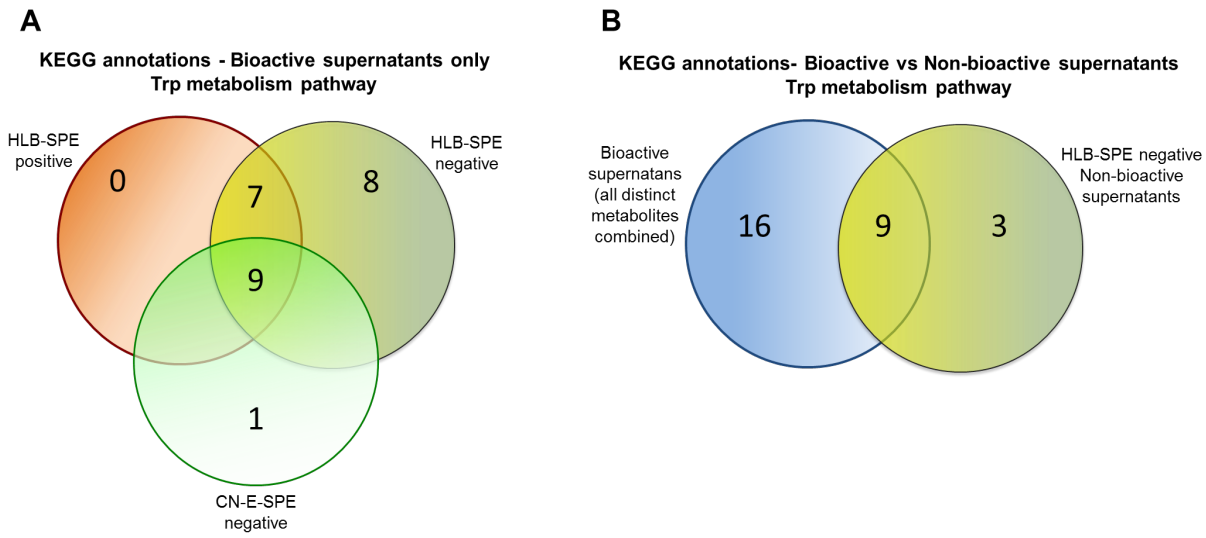

Figure 2.4. Venn diagram and the relationship between datasets for the trypthopan pathway. A: counts of unique and shared m/z features presented in each sample type data matrix of bioactive supernatants. B: unique Trp pathway metabolites of bioactive supernatans compared to ones of non-bioactive supernatans; where from the 9 common annotations, 6 were present in all data matrices, 2 were presente in HLB-SPE extracts but not in the CN-E extract, and 1 was present only in the HLB-SPE negative matrix.

2.4 Discussion

2.4.1 The approach to sample generation and untargeted metabolomics

The pretreatment of biological samples is usually required prior instrumental analysis to reduce matrix complexity and remove salts. The number of m/z features present in each data matrix reflects that (**Table 3**). Solid-phase extraction was more effective in producing a cleaner sample than a simple protein precipitation, lowering baseline noise and improving MS detection. The influence of different sample extraction techniques and different electrospray ionization mode on the chemical diversity detected by FT-ICR-MS was also demonstrated, even if pathway activity assessment was performed on statically discriminant m/z features only (**Figure 2.3**). Based on our experience and on information provided by SPE suppliers, the HLB-SPE and CN-E SPE extraction was chosen in an attempt to cover a significant wide range of metabolite classes (Li et al 2017; Jha et al. 2013). Due to its non-polar and polar functional groups (the hydrophilic N vinylpyrrolidone and the lipophilic divinylbenzene), the HLB hydrophilic polymeric phase can retain a much broader range of polar to non-polar, neutral and acidic to basic compounds than traditional reversed-phase C18-silica-based SPEs. HLB phases are also very resistant to over-drying, making extraction methods more reproducible and robust (Buszewski & Szultka 2012). As a supplementary phase, the medium polar cyano propyl sorbent (CN-E) can extract from aqueous matrices

moderately polar to non-polar compounds that would be irreversibly retained on non-polar sorbents such as C8- and C18-based phases.

Overlapping of discriminant metabolic pathways and metabolite hits were observed between different data matrices, as shown in **Figure 2.3** and **Table 4**. The shared hits between the bioactive and non-bioactive class in the tryptophan metabolism pathway may be explained by the presence of structural isomers and stereoisomers (e.g., N-Acetylindoxyl, Indole-3-acetic acid and 3-Indoleglycolaldehyde (C10H9NO2); Indolelactate and 5-Methoxyindoleacetate (C11H11NO3); L/D-Formylkynurenine and 5-Hydroxy-L/D-tryptophan). We believe that these predicted metabolites would still deserves a test in bioassays. Additionally, it is expected that some metabolites are retained by both HLB and CN-E solid phases and/or can be ionized in ESI positive and negative modes, and we acknowledge the redundancy potential in the data obtained from a single probiotic supernatant that was subjected to these different techniques. However, each individual supernatant extract originated a data set that was combined into a data matrix, and some metabolite hits were predicted across different matrices for the group of bioactive supernatants only (trypthopan, indolepyruvic, serotonin, etc.). Results of a single data matrix validate the ones of other matrices as each individual probiotic sample validates the group (bioactive or non-bioactive), reinforcing hypothesis towards potential bioactive metabolites. Yet, it should be noted that the data generated from both SPE fractions and ionizations modes clearly differed from each other and this piece of information can be useful to drive the isolation and identification of a specific class of metabolites by using the proper technique. We did not want to miss that by combining different data sets prior data processing and statistics.

2.4.2 Immunomodulatory supernatants and bioactive pathways

The results of pathway analysis suggest that tryptophan related metabolites produced by probiotic bacteria may be involved in the underlying biological processes of immunomodulation observed in our *in vitro* test systems. This study was followed by another one where bioassay-guided fractionation was applied to the two most bioactive supernatants and structural elucidation using instrumental analysis (enantiomeric chromatography separation, NMR and FT-ICR-MS) revealed that D-tryptophan has been the immunomodulator compound present in a bioactive fraction, which was confirmed in *in vitro* and *in vivo* experiments (Chapter 5). In this case, the classical strategy validated the hypothesis originated with our high throughput nontargeted FT-ICR-MS based

metabolomics towards the importance of tryptophan metabolic pathway to immunomodulation.

In vivo, the balance between activation and suppression of the immune response depends on various regulatory mechanisms, where the impact of microbiome and Trp metabolism on immune tolerance has been much investigated (Gao et al. 2018; Gostner et al. 2016). Two enzymes are well known to drive the first step of the amino acid Trp into the kynurenine pathway. In the human body, the rate-limiting enzyme Trp 2,3-dioxygenase (TDO) converts L-Trp into N-formyl-L-kynurenine in the liver, while indoleamine 2,3-dioxygenase (IDO) does the same but is primarily expressed in epithelial cells, stem cells, and cells of the immune system such as monocytes, macrophage, and dendritic cells (DCs). Thus, IDO has been studied and recognized to have immunoregulatory roles (Pallotta et al. 2011; Aldajani et al. 2016). Overexpression of IDO was correlated with immunosuppression and tolerance *in vitro* and in animal models, likely, due to the depletion of tryptophan and production of bioactive metabolites such as kynurenine, 3-hydroxy-kynurenine, or xanthurenic acid which seems to suppress T-cell responses, induces regulatory T cells and facilitates the development of regulatory DCs (Van der Leek et al. 2017; Mellor & Munn 2004; von Bubnoff & Bieber 2012). However, the effect of Trp degradation on human DCs is still unclear. For instance, it has been demonstrated *in vitro* that human DCs increased the expression of inhibitory receptors and showed significantly lower stimulatory capacity toward T cells under low Trp concentration conditions, but no difference on the stimulatory capacity was observed when a mixture of the metabolites anthranilic acid, 3-hydroxykynurenine, 3-hydroxyanthranilic acid, and quinolinic acid was added a prior to the medium; contrarily of what was observed for T-cells (von Bubnoff et al. 2011). On the other hand, Belladonna et al. showed that nearby produced kynurenines and derived metabolites can be taken up by murine DCs inducing a tolerogenic phenotype, independently of Trp availability and IDO activity, i.e., IDO-competent cells can “transfer” tolerogenic potential to DCs lacking functional IDO by producing Trp metabolites (Belladonna et al. 2006). Manni et al. (2020) confirmed those findings showing that exogenous L-kynurenine induced endotoxin tolerance on mice DCs that were submitted to a lipopolysaccharide (LPS) induced hyperresponsiveness. Together with Trp metabolism, immunomodulation related to L-arginine metabolism (also well populated in the bioactive group of supernatants) has been well described in the literature (Murray 2016). Co-expression and co-activity of both IDO and Arginase 1 enzymes was shown to promote a metabolite network (intra- and inter-cellular) that induces DCs immunosuppressive properties (Mondanelli et al. 2017).

Gut microbiome can direct utilize the amino acid Trp limiting its availability to the host. This per se may affect host immune system. Besides using IDO activity to generate kynurenine or hydroxykynurenine, intestinal microorganisms can also transform Trp into several indoles that are ligands for aryl hydrocarbon receptors (AHR) (Agus et al. 2018; Neavin et al. 2018). Such ligands activate AHR, which was demonstrated to induce IDO expression in LPS stimulated DCs, promoting immune tolerance and differentiation of naïve T cells into T regulatory cells (Nguyen et al. 2010). It is also known that bacteria synthesize diverse D-amino acids that are then enantioselectively recognized by some receptors and enzymes in mammals and may mediate adaptive immunity (Sasabe & Suzuki 2018; Aliashkevich et al. 2018). Synthesis of D-amino acids by bacteria involves mechanisms catalyzed by racemase, epimerase or aminotransferase enzymes, resulting in direct interconversion of the L- and D- stereoisomers (Radvok & Moe 2014). *In vivo*, IDO can catabolize D-Trp into D-kynurenine which is further metabolized to kynurenic acid by D-amino acid oxidase (D-AAO) or kynurenine aminotransferase (KAT); or it is converted into D-3-hydroxykynurenine by kynurenine 3-monooxygenase (Notarangelo et al. 2016). The results presented here paved the way for our research that identified the D-form of the amino acid tryptophan, isolated from supernatants of LGG and W56 culture, as an immunomodulator *in vitro* and *in vivo*, while its L-form and other D-amino acids were inactive. Whether D-metabolites derived from D-Trp induce tolerogenic DCs or not, has yet to be discovered.

Metabolic pathways involving other amino acid also characterized the group of bioactive supernatants, especially aromatic ones such as phenylalanine and tyrosine which are suggested to be putative precursors of bioactive bacterial metabolites (Sridharan et al. 2014). Another example of a pathway distinguishing the group of bioactive supernatants, which plays a crucial role in the development of immune cells (inducing immunity or tolerance) and in many autoimmune diseases, is the Aminoacyl-tRNA biosynthesis (ARS) (Nie et al. 2019). The identification of probiotic derived metabolites belonging to theses pathways and the assessment of their potential as immunomodulators, is a stimulus for future studies. Overall, the advantage of the FT-ICR-MS metabolomics-based supernatant screening strategy for our probiotic research is that predicted hits (or identified bioactive compound candidates) are often commercially available or are easy to synthetize and can be directly tested in bioassays prior or without laborious bioassay-guided fractionation investigation.

2.4.3 Implications and limitations of the study

To reasonably compare the supernatants samples using FT-ICR-MS spectra, differences in cell culture had to be as limited as possible, as well as the number of medium components that could potentially cause MS detection interferences. As such, a simple chemically defined medium (CDM1) was preferred to cultivate all 25 probiotic strains under the same conditions whilst recognizing the fact that some strains initially available did not grow adequately in this minimal essential medium and had to be excluded from the screening experiment, and also the fact that a full growth medium with various sources of compounds could potentially spark a different metabolic footprint if it was applied (Kell et al. 2005). On the other hand, each of the 25 probiotic supernatants harvested from CDM1 medium showed a concordant immunomodulatory response with supernatants harvested from the same strains cultivated in complex de Man Rogosa-Sharpe (MRS) medium (Kepert et al. 2017)

Centrifugation followed by fast filtration was a quick and simple method to harvest cell-free supernatants (aliquots of supernatants were incubated after that and no cell growth was observed proving that those supernatants were cell-free). The loss of certain set of metabolites during this procedure due to, e.g., binding to the filter material or lack of stability was not investigated, as well as leakage of bacteria cells intracellular metabolites into the supernatant. However, further investigation of the drawbacks of the fast filtration method was beyond the scope of this study once immunomodulatory activity could be proven in the harvest of cell-free supernatants thereafter, i.e., the compound/s responsible for the immunomodulatory effect in our bioassay was/were present in the collected supernatant sample.

The loss of metabolites during sample preparation using SPEs may not be excluded as well. It is possible that some metabolites were not retained in the solid phase during the first SPE step (sample load) or subsequently washed out during the washing step. Only the eluted samples (MeOH extract) were analyzed by FT-ICR-MS. To overcome that, aliquots of bacteria supernatants were taken crude and analyzed without being subjected to SPE extraction, which unfortunately did not generate a robust separation in OPLS.

FT-ICR-MS analysis by direct infusion enabled us to rapidly screen the probiotic stains of highest bioactive activity, which led to important pathway information. This analytical approach did not enable isomer's differentiation, but neither a classical non-targeted LC/MS method would have been able to achieve that. Due to the well-known importance of stereochemistry in biological processes, follow-up *in vitro* assays to test isomers activity and sample analysis using complementary techniques such as enantioselective chromatography

and NMR was essential to distinguish D-tryptophan as a chiral molecule within the most bioactive compound candidates in our follow-up study.

2.5 Conclusion

Although probiotic strains were cultivated in a closed and controlled environment and immunomodulation was tested in vitro – which may not reflect the *in vivo* conditions in the human body – untargeted analysis using direct infusion FT-ICR-MS followed by multivariate statistical analysis enabled the distinction between the group of immunomodulatory supernatants and inactive ones offering a broad overview into possible secreted bioactive compounds and the most significant metabolic pathways that differentiates the two classes of supernatants.

The results suggest that tryptophan metabolism may play an important role in regulating DCs immune tolerance and can be used to foster follow-up experiments. For example, discriminant hits can be seen as potential candidate compounds to undergo bioassay screenings which may accelerate the identification of bioactive metabolites or at least, give scientists an indication of potential bioactive classes of compounds to be explored next. This does not apply only to Trp metabolism but also to other discriminant pathways yet to be explored. Often, metabolites hits are commercially available or are easy to synthetize, but their immunomodulatory properties have been not investigated.

The findings and strategy presented here can support the selection of the most appropriate strains that should go through a more expensive and complex animal or/and human study posteriorly. It may help scientists and manufactures to better design probiotic cocktail products tailored to a special treatment and disease, and to improve interactions with regulatory agencies based on the characterization of strains metabolic footprinting. The emerging trend of postbiotics is another field that can benefit from the research approach described in this work. Studies using probiotic derived bioactive metabolites may overcome obstacles when, for example, oral administration of probiotics is not feasible, or a specific therapeutic dose of a metabolite is needed.

.

2.6 References

Agus, A.; Planchais, J.; Soko, H., 2018. Gut Microbiota Regulation of Tryptophan Metabolism in Health and Disease. *Cell Host Microbe*, 23, 716-724.

Aldajani, W. A.; Salazar, F.; Sewell, H. F.; Knox, A.; Ghaemmaghami, A. M., 2016. Expression and regulation of immune-modulatory enzyme indoleamine 2,3-dioxygenase (IDO) by human airway epithelial cells and its effect on T cell activation. *Oncotarget*, *7*, 57606–57617.

Aliashkevich, A.; Alvarez, L.; Cava, F., 2018. New Insights Into the Mechanisms and Biological Roles of D-Amino Acids in Complex Eco-Systems. *Frontiers in Microbiology*, 9, Article 683.

Antón J.; Lucio, M.; Pena, A.; Cifuentes, A.; Brito-Echeverria, J.; Moritz, F.; Tziotis, D.; López, C.; Urdiain, M.; Schmitt-Kopplin, P.; Rosselló-Móra, R., 2013. High metabolomic microdiversity within co-occurring isolates of the extremely halophilic bacterium salinibacter ruber. *PLoS One*, 8, e64701.

Arpaia, N.; Campbell, C.; Fan, X.; Dikiy, S.; van der Veeken, J.; DeRoos, P.; Liu, H., Cross, J.R.; Pfeffer, K.; Coffer, P.J.; Rudensky, A.Y., 2013. Metabolites produced by commensal bacteria promote peripheral regulatory T-cell generation. *Nature*, 504, 451–455.

Bazanella, M.; Maier, T.V.; Clavel, T.; Lagkouvardos, I.; Lucio, M.; Maldonado-Gòmez, M.X.; Autran, C.; Walter, J.; Bode, L.; Schmitt-Kopplin, P.; Haller, D., 2017. Randomized controlled trial on the impact of early-life intervention with bifidobacteria on the healthy infant fecal microbiota and metabolome. *The American Journal of Clinical Nutrition*, 106, 1274–1286.

Belladonna, M.L.; Grohmann, U.; Guidetti, P.; Volpi, C.; Bianchi, R.; Fioretti, M.C.; Schwarcz, R.; Fallarino ,F.; Puccetti, P., 2006. Kynurenine Pathway Enzymes in Dendritic Cells Initiate Tolerogenesis in the Absence of Functional IDO. *The Journal of Immunology*, 177, 130-137.

Behrends, V.; Ebbels, T.M.D.; Williams, H.D.; Bundy, J.G., 2009. Time-resolved metabolic footprinting for nonlinear modeling of bacterial substrate utilization. *Applied and Environmental Microbiology*, 75, 2453–63.

Buchen, L., 2010. The new germ theory: What can microbiologists who study human bowels learn from those who study the bowels of the earth? *Nature*, *468*, 492–495.

Buszewski, B.; Szultka, M., 2012. Past, Present, and Future of Solid Phase Extraction: A Review. *Critical Reviews in Analytical Chemistry*, 42, 198-213

Chong J., Soufan O., Li C., Caraus I., Li S., Bourque G., Wishart D.S. and Xia J., 2018 MetaboAnalyst 4.0: towards more transparent and integrative metabolomics analysis. *Nucleic Acids Research* 46: W486-494.

Chubukov V., Sauer U., 2014. Environmental Dependence of Stationary-Phase Metabolism in *Bacillus subtilis* and *Escherichia coli*. *Applied and Environmental Microbiology* 80: 2901–09.

Dörries, K.; Lalk, M., 2013. Metabolic footprint analysis uncovers strain specific overflow metabolism and D-isoleucine production of staphylococcus aureus COL and HG001. *PLoS One*, 8, e81500.

Frei, R.; Lauener, R.P.; Crameri, R.; O'Mahony, L., 2012. Microbiota and dietary

interactions: An update to the hygiene hypothesis? *Allergy*, 67: 451–461.

Gao, J.; Xu, K; Liu, H.; Liu, G.; Bai, M.; Peng, C.; Li, T.; Yin, Y., 2018. Impact of the Gut Microbiota on Intestinal Immunity Mediated by Tryptophan Metabolism. *Frontiers in Cellular and Infection Microbiology*, 8, Article 13.

Green, N.W.; Perdue, E.M. Fast Graphically Inspired Algorithm for Assignment of Molecular Formulae in Ultrahigh Resolution Mass Spectrometry. *Analytical Chemistry* 2015, 87, 5086–5094.

Gostner, J.M.; Becker, K.; Kofler, H.; Strasser, B.; Fuchs, D., 2016. Tryptophan Metabolism in Allergic Disorders. *International Archives of Allergy and Immunology*, 169, 203-215.

Hair J.F., Hult G.T.M., Ringle C.M., Sarstedt M., 2017. A Primer on Partial Least Squares Structural Equation Modeling (PLS-SEM), Second Edition. SAGE Publications Inc., Los Angeles, USA.

Harvey, A.L.; Edrada-Ebel, R.; Quinn, R.J., 2015. The re-emergence of natural products for drug discovery in the genomics era. *Nature Reviews Drug Discovery*, 14, 111 29.

Hertkorn, N.; Frommberger, M.; Witt, M.; Koch, B.P.; Schimitt-Kopplin, P.; Perdue, E.M. Natural organic matter and the event horizon of mass spectrometry. *Analytical Chemistry* 2008, 80, 8908–8919.

Holgate, S.T.; Lack, G., 2005. Improving the management of atopic disease. *Archives of Disease in Childhood* 90, 826-831.

Isolauri, E.; Arvola, T.; Sütas, Y.; Moilanen, E.; Salminen, S., 2000. Probiotics in the management of atopic eczema. *Clinical & Experimental Allergy*, 30, 1604–1610.

Jha, B.; Kavita, K.; Westphal, J.; Hartmann, A.; Philippe Schmitt-Kopplin, P., 2013. Quorum Sensing Inhibition by Asparagopsis taxiformis, a Marine Macro Alga: Separation of the Compound that Interrupts Bacterial Communication. *Marine Drugs*, 11, 253-265.

Kanehisa M., Goto S., 2000. KEGG: Kyoto Encyclopedia of Genes and Genomes. *Nucleic Acids Research* 28: 27–30.

Kanehisa M., Goto S., Hattori M., Aoki-Kinoshita K.F., Itoh M., et al., 2006. From genomics to chemical genomics: new developments in KEGG. *Nucleic Acids Research* 34: 354–357.

Kalliomäki, M.; Salminen, S.; Arvilommi, H.; Kero, P.; Koskinen, P.; Isolauri, E., 2001. Probiotics in primary prevention of atopic disease: a randomised placebo-controlled trial. *The Lancet*, 357, 1076–1079.

Katan, M.B., 2012. Why the European Food Safety Authority was right to reject health claims for probiotics. *Beneficial Microbes*, 3, 85–89.

Kepert, I.; Fonseca, J.; Müller, C.; Milger, K.; Hochwind, K.; Kostric, M.; Fedoseeva, M.; Ohnmacht, C.; Dehmel, S.; Nathan, P.; Bartel, S.; Eickelberg, O.; Schloter, M.; Hartmann, A.; Schmitt-Kopplin, P.; Krauss-Etschmann, S. D-Tryptophan from probiotic bacteria influences the gut microbiome and allergic airway disease. *Journal of Allergy and Clinical Immunology* 2017, 139, 1525-1535.

Kell, D.B.; Brown, M.; Davey, H.M.; Dunn, W.B.; Spasic, I.; Oliver, S.G., 2005. Metabolic footprinting and Systems Biology: The medium is the message. *Nature Reviews Microbiology*, 3, 557–565.

Kind, T.; Fiehn, O. Seven Golden Rules for heuristic filtering of molecular formulas

obtained by accurate mass spectrometry. *BMC Bioinformatics* 2007, 8, 105.

Krauss-Etschmann, S.; Hartmann, A.; Schmitt-Kopplin, P.; Schloter, M. Methods and compositions for treating inflammatory diseases. US patent 10,857,128. December 8, 2020.

Kremb S.; Mueller, C.; Schmitt-Kopplin, P.; Voolstra, C.R., 2017. Bioactive potential of marine macroalgae from the Central Red Sea (Saudi Arabia) assessed by high throughput imaging-based phenotypic profiling. *Marine Drugs*, 15, 80.

Li, Y.; Harir, M.; Uhl, J.; Kanawati, B.; Lucio, M.; Smirnov, K.S.; Koch, B.P.; Schmitt-Kopplin, P.; Hertkorn, N., 2017. How representative are dissolved organic matter (DOM) extracts? A comprehensive study of sorbent selectivity for DOM isolation. *Water Reserach*, 116, 316-323.

Lucio, M.; Fekete, A.; Frommberger, M.; Schmitt-Kopplin, P. Metabolomics: High-resolution tools offer to follow bacterial growth on a molecular level. In: de Brujin, F.J. Handbook of Molecular Microbial Ecology I: Metagenomics and Complementary Approaches; John Wiley & Sons Inc.: Hoboken, New Jersey, USA, 2011; Chapter 72.

Manni, G.; Mondanelli, G.; Scalisi, G.; Pallotta, M.T.; Nardi, D.; Padiglioni, E.; Romani, R.; Talesa, V.N.; Puccetti, P.; Fallarino, F., Gargaro, M. Pharmacologic Induction of Endotoxin Tolerance in Dendritic Cells by L-Kynurenine. *Frontiers in Immunology*, 11, Article 292.

Mapelli, V.; Olsson, L.; Nielsen, J., 2008. Metabolic footprinting in microbiology: methods and applications in functional genomics and biotechnology. *Trends in Biotechnology*, 26, 490–947.

Mellor, A.L.; Munn, D.H., 2004. IDO expression by dendritic cells: tolerance and tryptophan catabolism. *Nature Reviews Immunology*, 4, 762-774.

Metchnikoff, E.; Mitchell, P.C. The Prolongation of Life. Optimistic Studies. G.P. Putnam´s Sons: London, UK, 1908.

Michail, S., 2009. The role of probiotics in allergic diseases. *Allergy, Asthma & Clinical Immunolog.*, 5, 5.

Mondanelli, G.; Bianchi, R.; Pallotta, M.T.; Orabona, C.; Albini, E.; Lacono, A.; *et al., 2017.* A Relay Pathway between Arginine and Tryptophan Metabolism Confers Immunosuppressive Properties on Dendritic Cells. *Immunity*, 46, 233-244.

Mueller, C.; Kremb, S.; Gonsior, M.; Brack-Werner, R.; Voolstra, C.R.; Schmitt-Kopplin, P., 2020. Advanced identification of global bioactivity hotspots via screening of the metabolic fingerprint of entire ecosystems. *Scientific Reports*, 10, article 1319.

Murray, P.J., 2016. Amino acid auxotrophy as a system of immunological control nodes. *Nature Immunology*, 17, 132-139.

Neavin, D.R.; Liu, D.; Ray, B.; Weinshilboum, R.M., 2018. The Role of the Aryl Hydrocarbon Receptor (AHR) in Immune and Inflammatory Diseases. *International Journal of Molecular Sciences*, 19, 3851.

Nguyen, N.T.; Kimura, A.; Nakahama, T.; Chinen, I.; Masuda, K.; Nohara, K.; Fujii-Kuriyama, Y.; Kishimoto, T., 2010. Aryl hydrocarbon receptor negatively regulates dendritic cell immunogenicity via a kynurenine-dependent mechanism. *Proceedings of the National Academy of Sciences of the United States of America*, 107, 19961–19966.

Nie, A.; Sun, B.; Fu, Z.; Yu, D., 2019. Roles of aminoacyl-tRNA synthetases in immune

regulation and immune diseases. *Cell Death and Disease*, 10, 901.

Niers, L.; Martín, R.; Rijkers, G.; Sengers, F.; Timmerman, H.; Van Uden, N.; Smidt, H.; Kimpen, J.; Hoekstra M., 2009. The effects of selected probiotic strains on the development of eczema (the PandA Study). *Allergy*, 64, 1349–1358

Notarangelo, F.M.; Wang, C-D., Horning, K.J.; Schwarcz, R., 2016. Role of D-amino acid oxidase in the production of kynurenine pathway metabolites from D-tryptophan in mice. *Journal of Neurochemistry*, 136, 804-814.

O'Rourke, A.; Kremb, S.; Bader, T.M.; Helfer, M.; Schmitt-Kopplin, P.; Gerwick, W.H.; Brack-Werner, R.; Voolstra, C.R. Alkaloids from the sponge Stylissa carteri present prospective scaffolds for the inhibition of Human immunodeficiency Virus 1 (HIV-1). *Marine Drugs* 2016, 14, 28.

Osborn, D.A.; Sinn, J.K.H., 2007. Probiotics in infants for prevention of allergic disease and food hypersensitivity. *Cochrane Database of Systematic Reviews,* 4, CD006475.

Pallotta, M., Orabona, C., Volpi, C.; Vacca, C.; Belladonna, M.L.; Bianchi, R.; *et al.,* 2011. Indoleamine 2,3-dioxygenase is a signaling protein in long-term tolerance by dendritic cells. *Nature Immunology*, 12, 870–878.

Pinu, F.R.; Villas-Boas, S.G., 2017. Extracellular microbial metabolomics: the state of the art. *Metabolites*, 43, 1-15.

Prince, E.K.; Pohnert, G. Searching for signals in the noise: metabolomics in chemical ecology. *Analytical and Bioanalytical Chemistry*, 2010, 396, 193-197.

Podolsky, S.H, 2012. Metchnikoff and the microbiome. *The Lancet*, 380, 1810-1811.

Radvok, A.D.; Moe, L.A., 2014. Bacterial synthesis of D-amino acids. *Applied Microbiology and Biotechnology*, 98, 5363-5374.

Raghuwanshi, S.; Misra, S.; Sharma, R.; Bisen P.S., 2018. Probiotics: nutritional therapeutic tool. *Journal of Probiotics & Health*, 6, 1000194.

Savijoki K., Suokko A., Palva A., Varmanen P., 2006. New convenient defined media for [(35)S] methionine labelling and proteomic analyses of probiotic lactobacilli. Letters in *Applied Microbiology* 42(3): 202–9.

Sasabe, J.; Masataka Suzuki, M., 2018. Emerging Role of D-Amino Acid Metabolism in the Innate Defense. *Frontiers in Microbiology*, 9, Article 933.

Sridharan, G.V.; Choi, K.; Klemashevich, C.; Wu, C.; Prabakaran, D.; Pan, L.B.; Steinmeyer, S.; Mueller, C.; Yousofshahi, M.; Alaniz, R.C.; Lee, K.; Jayaraman, A., 2014. Prediction and quantification of bioactive microbiota metabolites in the mouse gut. *Nature Commun*ications, 5, article 5492.

Strachan, D.P.,1989. Hay fever, hygiene, and household size. *The BMJ*, *299*: 1259–1260

Tong X.S., Wang J., Zheng S., Pivnichny J.V., Griffin P.R., Shen X., Donnelly M., et al. 2002. Effect of Signal Interference from Dosing Excipients on Pharmacokinetic Screening of Drug Candidates by Liquid Chromatography/mass Spectrometry. *Analytical Chemistry* 74: 6305–13.

Triba, M.N.; Le Moyec, L.; Amathieu, R.; Goossens, C.; Bouchemal, N.; Nahon, P.; Rutledge, D.N.; Savarin, P.,2015. PLS/OPLS models in metabolomics: the impact of permutation of dataset rows on the K-fold cross-validation quality parameters. *Molecular BioSystems*, 11, 13-19.

U.S. Food and Drug Administration. Guidance for clinical investigators, sponsors, and IRBs: Investigational New Drug Applications (INDs) - Determining whether human research studies can be conducted without an IND, 2013, p. 10.

Van der Leek, A.P.; Yanishevsky,Y.; Kozyrskyj, A.L., 2017. The Kynurenine Pathway as a Novel Link between Allergy and the Gut Microbiome. *Frontiers in Immunology*, 8, article 1374.

von Bubnoff, D.; Bieber T.,2012. The indoleamine 2,3-dioxygenase (IDO) pathway controls allergy. *Allergy*, 67, 718-725.

von Bubnoff, D.; Wilms, H.; Scheler, M.; Brenk, M.; Koch, S.; Biber, T., 2011. Human myeloid dendritic cells are refractory to tryptophan metabolites. *Human Immunology*, 72, 791-797.

Zhernov, Y.V.; Kremb, S.; Helfer, M.; Schindler, M.; Harir, M.; Mueller, C.; Hertkorn, N.; et al., 2017. Supramolecular combinations of humic polyanions as potent microbicides with polymodal anti-HIV-activities. *New Journal of Chemistry*, 41, 212-224.

Zheng, D.; Liwinski, T.; Elina, E., 2020. Interaction between microbiota and immunity in health and disease. *Cell Research*, 30, 492–506.

Yan F., Polk D.B., 2011. Probiotics and immune health. *Current Opinion Gastroenterology* 27: 496–501.

Yeşilova, Y.; Çalka, Ö; Akdeniz, N.; Berktaş, M., 2012. Effect of probiotics on the treatment of children with atopic dermatitis. *Annals of Dermatology*, 24, 189–193

Worley B., Powers R., 2013. Multivariate Analysis in Metabolomics. *Current Metabolomics* 1: 92–107.

3
Classical strategies for the isolation and identification of probiotic-derived bioactive compounds

3.1 Introduction

The results presented in this chapter are fruit of a close collaboration between the Research Unit Analytical BioGeoChemistry and Research Unit Microbe-Plant Interactions at Helmholtz Zentrum München, and the Comprehensive Pneumology Center (CPC) at Ludwig-Maximilians University Hospital. The systematic study design, assumptions, and methods described in this chapter were the heart of the work that originated two scientific publications, which are shown in Chapters 4 and 5 of this dissertation. The aim of Chapter 3 is to describe in more detail the fundamental analytical chemistry work involved throughout the discovery process.

Supernatants of the best studied probiotic bacterium, *Lactobacillus rhamnosus* GG (LGG), and the *Lactobacillus casei* W56 were selected and screened due to their ability to concordantly lower the constitutive CCL17 secretion of a human Hodgkin lymphoma cell line and prevent upregulation of costimulatory molecules of LPS-stimulated human dendritic cells. A bioassay-guided fractionation scheme was set up to isolate a secreted bacterial molecule that mediates bioactivity where chromatography, mass spectrometry and nuclear magnetic resonance spectroscopy were used to identify the bioactive compound chemical structure. Additionally, an analytical method was established for enatioseparation and quantification of DL-amino acids as a platform for future studies.

3.2 Materials and Methods

3.2.1 Bioassay-guided fractionation of probiotic bacterial supernatants

To detect immune modulatory activity in probiotic cell culture supernatants, two biological screening systems were developed using human monocyte derived dendritic cells and human Hodgkin lymphoma T cell line (KM-H2). These biological assays are well described in the form of a PhD thesis (Kepert 2013) as well as in the publication mentioned in Chapter 5 (Fonseca et al. 2017). For in depth information about bioassay methods and results, please consider reading those references.

Supernatants from LGG and *L. casei* W56 showed high immune modulatory activity in both screening assays and were therefore selected for further bioassay-guided fractionation (**Chapter 5**). Both strains were grown in modified defined medium CDM1 as already described in the previous Chapter, without surfactants since it is known to interfere with the chemical analysis in mass spectrometry.

Six mL of *L. casei* W56 and LGG cell-free supernatants, as well CDM1 medium were applied in parallel to previous conditioned silica gel SPE-C_{18} cartridges (1g, Mega Bond Elut, Varian). This SPE-C_{18} cartridge was chosen due to its bigger size compared to other ones available in the laboratory and therefore, it allowed higher sample load volume. The C18 sorbent is also the most used sorbent in separation and extraction of both natural and synthetic chemicals due to its extreme retention of most organic compounds from aqueous matrices.

The elution procedure was done in eleven linear gradient steps using 2 mL of water/methanol (v/v) mixtures, increasing from 0% to 100% in methanol content. Each resulting eluate was divided in two equal aliquots into Eppendorf® tubes and were dried at 4 ºC using a speed vacuum concentrator (Savant SPD121P SpeedVac Concentrator, Thermo Fisher Scientific) once it was essential to maintain a reference sample of each fraction obtained to test for immunomodulatory effects in vitro. The resulting dried eluates were stored at -20 ºC until start of bioassay experiments or chemical characterization. All MeOH/water extracts that showed bioactive properties in the biological screening systems, had their respective dried aliquot resuspended in 500 µL of 10% MeOH/water solution and were subjected to a second fractionation using a column packed with pentafluorophenylpropyl stationary phase (Kinetex PFP 1.7 µm, 2.1 x 150 mm, Phenomenex). Thus, an Ultra Performance Liquid Chromatography system (UPLC-PDA, Waters) was coupled to an automatic fraction collector (TriVersaNanoMate®, Advion BioSciences) to originate new sub-fractions into 96 well plate devices (**Figure 3.1**). Collection methods were defined for the bioactive extracts according to their chromatogram at the UV wavelength detection that showed the highest number of peaks (i.e., 200 nm). To obtain large volumes of each sub-fraction, the separation and collection process was repeated 15 times (20 uL injection volume). Special care was taken to divide each sub-fraction into two aliquots to allow biological screening, as in the procedure described above in this paragraph. Finally, bioassay results drove the chemical characterization of the new bioactive sub-fractions by NMR and FT-ICR MS. An overview of the bioassay-guided fractionation procedure is presented in **Figure 3.2**.

3.2.2 Structural elucidation of a bioactive compound present in the 20% MeOH/water extracts

Bioactive sub-fractions collected during fractionation in PFP column and their nearest sub-fractions were analysed by UPLC® coupled to high resolution TOF Mass Spectrometer

(MaXis URH-TOF, Bruker Daltonics, Bremen, Germany). To identify the candidate bioactive compound, reversed phase chromatography was applied using a ACQUITY UPLC BEH C18, 1.7 µm, 2.1 x 150 mm column (Waters) with gradient elution from 0 to 100% B in 8 min at 40 °C (Mobile Phase A: 10% MeOH/0.1% formic acid/water; and B: 0.1% formic acid/MeOH) at flow rate of 0.400 ml/min. Total Ion Chromatograms were obtained in electrospray ionization (ESI) positive mode in which peak retention time and m/z values were compared between sub-fraction chromatograms. The peak present only in bioactive sub-fractions chromatograms was carefully isolated and concentrated after repeated chromatographic runs in order to purify as much as possible the candidate bioactive compound for further molecular formula assignment by high resolution FT-ICR MS (APEX-Qe 12 Tesla, Bruker Daltonics, Bremen, Germany) and structural elucidation by proton NMR (UltraShield Plus 800 MHz, Bruker Biospin, Rheinstetten, Germany).

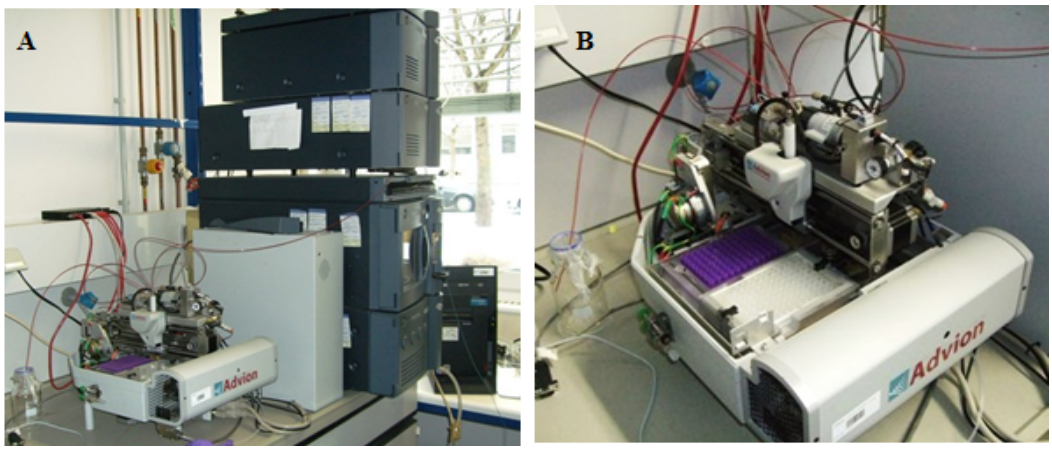

Figure 3.1. Coupling of UPLC® system with an automatic fraction collector. (A) UPLC system and fraction collector robot used for the second step fractionation of bioactive supernatants. (B) TriVersa NanoMate® instrument programmed to collect "time fractions" synchronized with the UPLC run. Sub-fractions were collected into 96 well plate devices (500 µL well volume) according to UV response chromatogram.

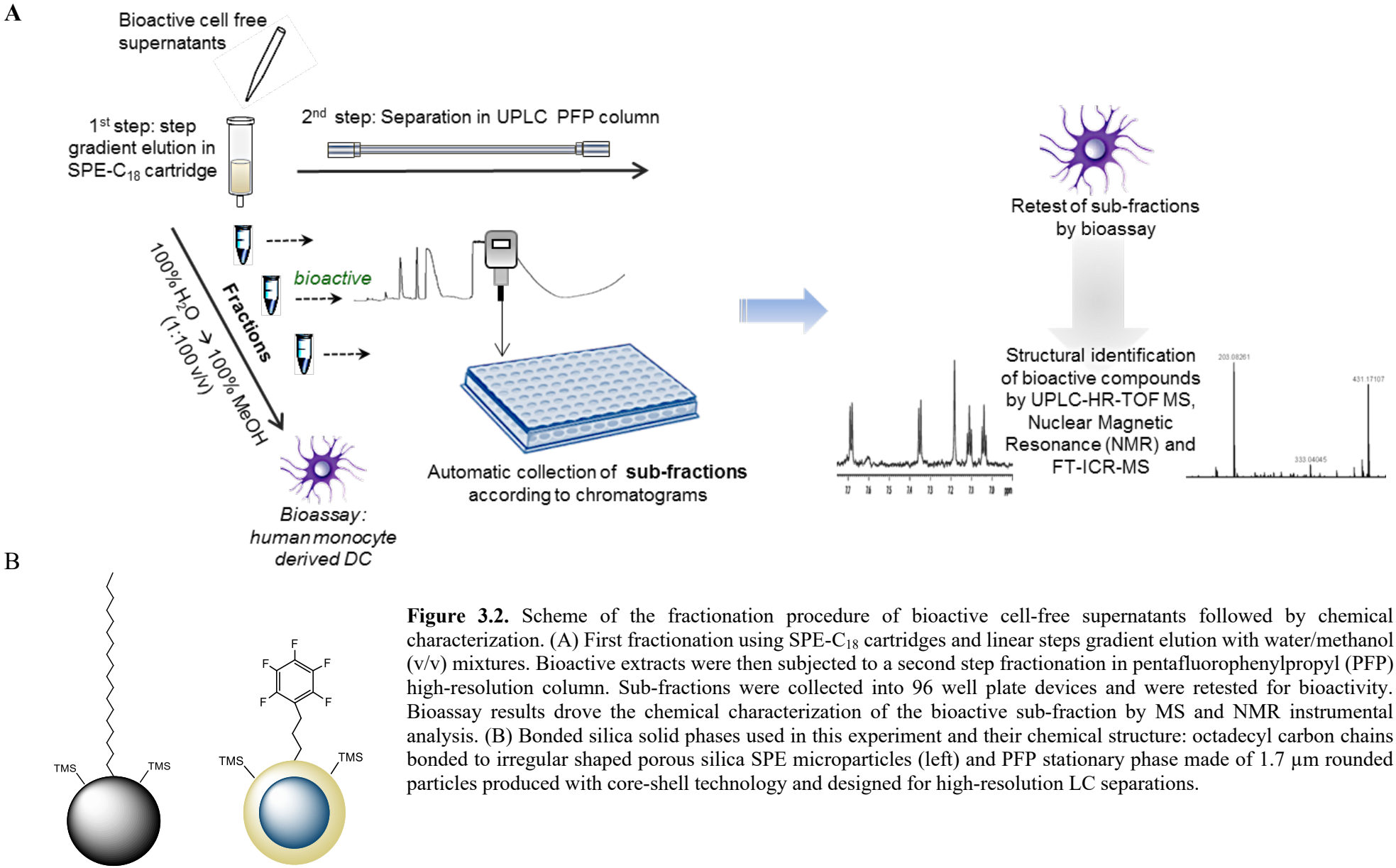

Figure 3.2. Scheme of the fractionation procedure of bioactive cell-free supernatants followed by chemical characterization. (A) First fractionation using SPE-C_{18} cartridges and linear steps gradient elution with water/methanol (v/v) mixtures. Bioactive extracts were then subjected to a second step fractionation in pentafluorophenylpropyl (PFP) high-resolution column. Sub-fractions were collected into 96 well plate devices and were retested for bioactivity. Bioassay results drove the chemical characterization of the bioactive sub-fraction by MS and NMR instrumental analysis. (B) Bonded silica solid phases used in this experiment and their chemical structure: octadecyl carbon chains bonded to irregular shaped porous silica SPE microparticles (left) and PFP stationary phase made of 1.7 µm rounded particles produced with core-shell technology and designed for high-resolution LC separations.

3.2.3 Identification of the bioactive compound

After MS and NMR chemical characterization of the bioactive sub-fractions and identification of a possible bioactive compound, it was of great importance to understand whether the D-stereoisomer of it was present in those fractions since the L-form was a component of the cell culture medium. Thus, methods for chiral separation and detection of AA were reviewed and retested. Derivatization using o-phthaldialdehyde (OPA) and N-isobutyryl-L-cysteine (IBLC) followed by liquid chromatography coupled with fluorescence detection (LC-FLD) analysis was the method of choice to be applied to bioactive sub-fraction samples (Brückner et al. 1995; Brückner and Westhauser 2003). OPA powder was dissolved in methanol and IBLC in 0.1M-borate buffer to generated two reagent stock solutions both at 200 mM concentration. The reagents could be stored separated at 4 ºC for a period of 5 days and therefore only a small volume needed for sample analysis was prepared.

The borate buffer (0.1M) described above was obtained by dissolving 3.0915g of boric acid in 450 mL Milli-Q H_2O. A pH electrode, previously calibrated with reference standards, was then placed into the solution and the pH was carefully adjusted to ~ 9.6-10 by adding small drops of 1M NaOH while stirring the solution using a magnetic stirrer and stirring bar. The volume was then brought to 500 mL with Milli-Q H_2O. This buffer is very stable at room temperature and can be stored for long periods of time, but its pH was always re-assessed before each use.

Derivatization of DL-Trp in standard solutions and samples was carefully carried out under a fume hood. Prior each batch of UPLC-FLD analysis, 1 volume of OPA solution was mixed with 3 volumes of N-isobutyryl-L/D-cysteine to originate a stable OPA/IBLC reagent (Molnar-Perl, 1999; Mengerink et al., 2002). Due the small volume of bioactive sub-fraction available, 10 µL of sample was mixed with 20 µL OPA/IBLC or IBDC inside LC glass vial with conical interior. The derivatization reaction took place in 2 minutes at 25 ºC inside the UPLC® auto-sampler compartment. Thereafter, 10 µL was injected into an Acquity UPLC BEH-C18 2.1 x 150 mm and 1.7 µm particle size column (Waters) at 30 ºC for enantionseparation. Mobile phase A consisted of 20 mM sodium acetate buffer adjusted to pH 6.2 with acetic acid, and mobile phase B was composed of 7% acetonitrile in MeOH. The fluorescence detector was set at λ=300 nm for the excitation and λ= 445 nm for the emission and chromatographic separation was carried out in isocratic elution mode at 45% solvent B.

LC-MS quality Methanol (Chromasolv, Sigma–Aldrich, St. Louis, USA), acetonitrile (Chromasolv, Sigma–Aldrich) and water (MilliQ) were used in this work. The reagents IBLC and IBDC (enantiomeric purity of ≥ 97%) as well OPA (≥ 99%) were purchased from Sigma Aldrich as well as boric acid and enantiomer pure standards of tryptophan.

3.3 Results and discussion

Bacteria-free supernatants of LGG and *L. casei* W56 chromatographed in solid phase extraction cartridges (SPE-C_{18}), as well as the CDM1 medium (control), yielded to a pure water extract and 10 methanol/water extracts. High immune modulatory activity was found concordantly in both screening systems for the 20% MeOH/water extracts along with the 40% and 50% MeOH/water extracts from probiotic cell cultures only, but not in control medium ones. Since the 20% MeOH/water extract showed the highest bioactivity, it was taken to further investigation at first.

The same UPLC separation and fraction collection methods were applied to LGG and *L. casei* W56 extracts as they showed very similar UV chromatogram profiles (which suggests that components of the medium at high concentration contributed significantly to such similar UV response) (**Figure 3.3 - A**). The PFP column stationary phase was chosen since it incorporates fluorine atoms on the phenyl ring and provides unique aromatic and polar selectivity, complementary to the Si-C_{18} SPE phase used in the first step fractionation. Both UPLC and separation column technologies delivered a very consistent chromatography along the 15 repeated runs (of each probiotic strain and medium extract), that could be observed by the reproducibility of chromatograms after each sample injection (data not shown). Consequently, it allowed a high reproducible automated fraction collection. As a result, 10 sub-fractions of the 20% MeOH/water extract of each strain were originated (**Figure 3.3 - B**) where two of them collected in the chromatographic retention time frame of 7-9 min manifested bioactivity in both biological screen systems.

After further analysis of all bioactive sub-fractions and their closest sub-fractions via reversed phase UPLC-High Resolution TOF MS, it was possible to identify a peak at t_R 4.2 minutes only present in the bioactive sub-fractions (**Figure 3.4**), suggesting that this peak would hide the information about the immune modulatory substance. The bioactivity concentration dependence could be assigned in bioassay indicating that *L. casei* W56-7 and LGG-6 sub-fractions had the higher immune modulatory activity. Those results were in good agreement with the peak areas obtained in the TIC chromatograms, in which sub-fractions of W56-7 and LGG-6 had the largest peak.

Extracted mass spectrum at t_R 4.1 - 4.3 min range showed intense signals at m/z 409.1875, 205.0971 and 188.0702 in all chromatograms where the peak was present, strongly suggesting tryptophan ions $[2M+H]^+$, $[M+H]^+$ and its fragment $[M+H-NH_3]^+$ once compared to mass spectrum available at MassBank free web spectral data base (former *http://www.massbank.jp*).

A

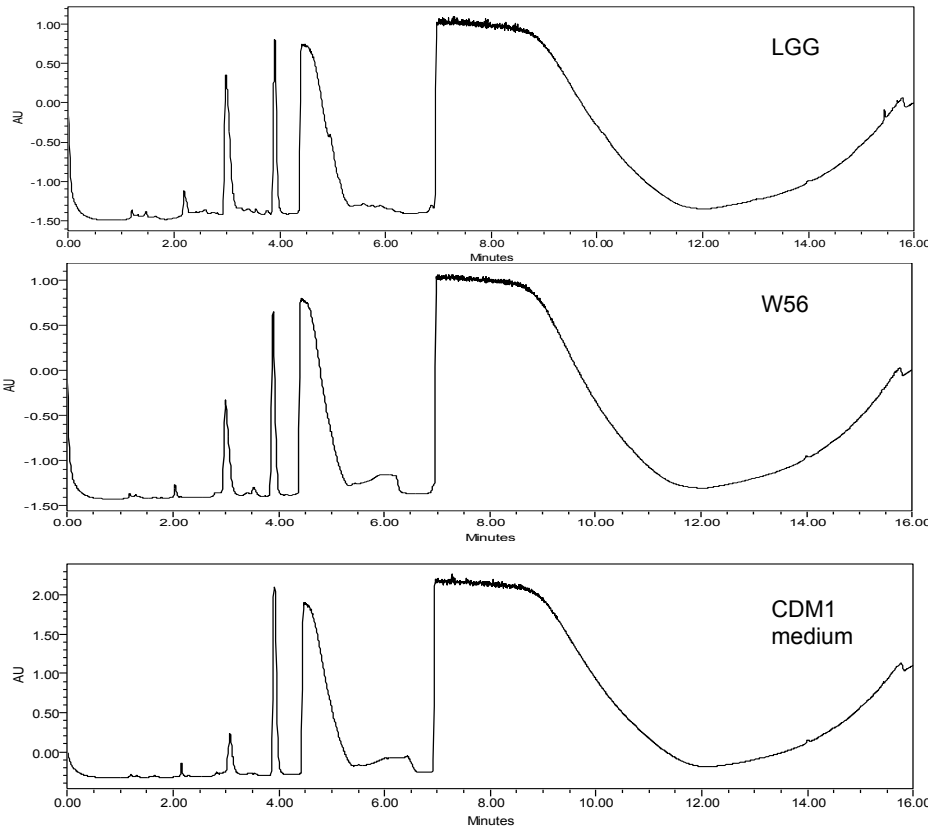

B

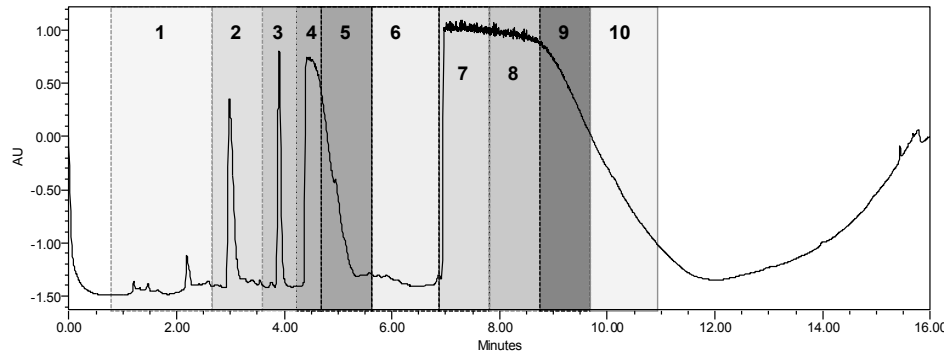

Figure 3.3. Chromatograms of 20%MeOH/Water extract after UV detection at 200 nm. A: comparison between chromatograms obtained after analysis of both strains and medium extracts showing similar profile, probably caused by components of the medium. B: sub-fraction collection windows applied to all 3 extracts (described also in Chapter 4).

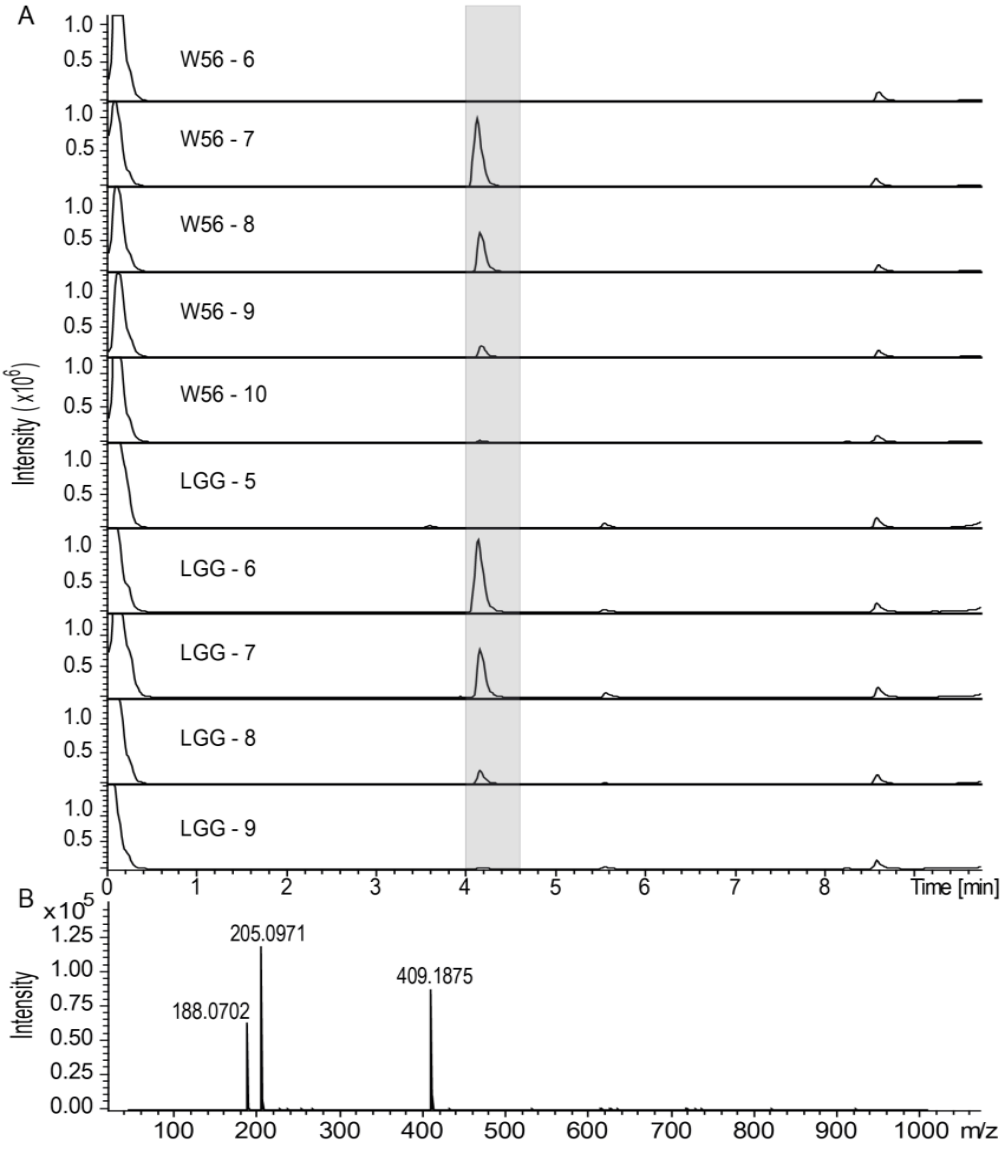

Figure 3.4. UPLC-URH-TOF MS analyses of *L. casei* W56 and LGG bioactive sub-fractions and their nearest neighbors. (A) Total ion chromatograms in ESI+ using reversed phase chromatography (BEH C18 column: 1.7 µm, 2.1 x 150 mm) showing a peak at t_R 4.2 min for all bioactive sub-fractions. (B) Extract mass spectra corresponding to the chromatographic time range of 4.1-4.3 min. The same signal profile was observed for all bioactive sub-fractions (*L. casei* W56-7, -8, -9, and LGG-6, -7, -8), where m/z 409.1875, 205.0971, and 188.0702 strongly agree with the tryptophan ions $[2M+H]^+$, $[M+H]^+$, and its fragment $[M+H\text{-}NH3]^+$.

After careful enrichment of the potential bioactive compound by repeated chromatographic runs and manual fraction collection around the t_R 4.2 min, the isolated candidate compound of both strains was submitted to high resolution mass spectrometry analyses in FT-ICR-MS, where a intense signal at m/z 205.09714 in ESI positive mode and m/z 203.08261 in ESI negative mode indicates with high accuracy the molecular formula of tryptophan $C_{11}H_{12}N_2O_2$ (error <0.01 ppm) as shown in **Figure 3.5**.

Further analyses by proton Nuclear Magnetic Resonance (NMR) provided detailed information on the functional group distribution and molecular structure. It was observed a close agreement between the ^{1}H-NMR spectra of standard tryptophan (Trp) and the bioactive sub-fraction (**Figure 3.6**). The doublets and triplets (δ7.8-7.0) indicated the occurrence of an indole ring. Resonance signals at the region of δ3.9-3.8 and δ3.2-3.1 could also be assigned to β-CH and α-CH protons respectively, although the concentration of the bioactive substance was very low for applying this technique.

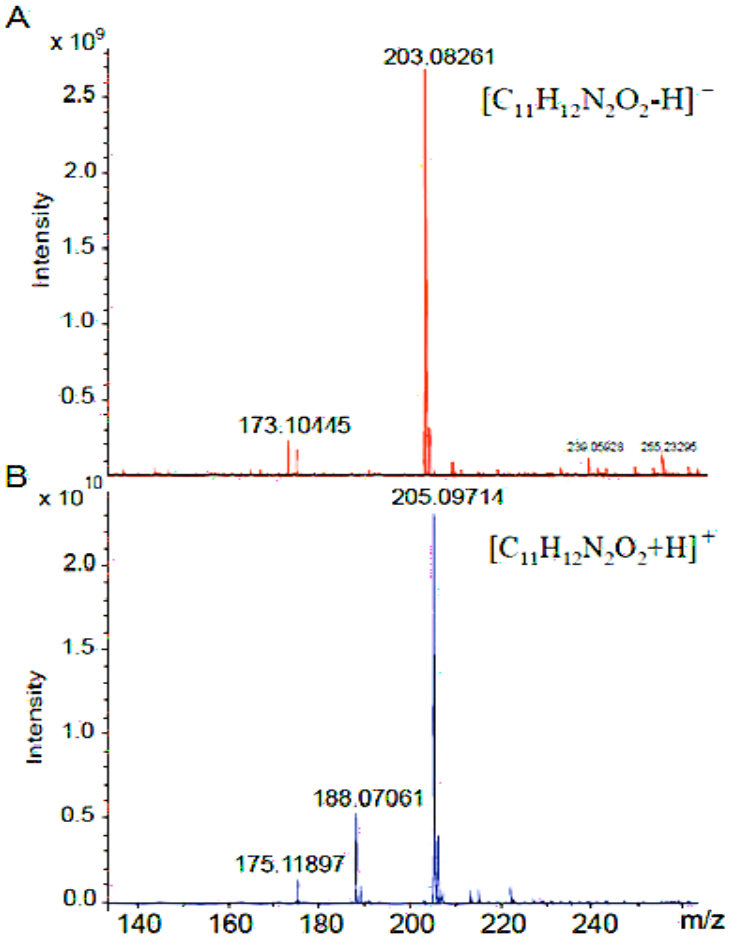

Figure 3.5. FT-ICR-MS spectra a purified bioactive sub-fraction**.** Analysis of *L. casei* W56-7 sub-fraction in ESI negative mode (A) and ESI positive mode (B). The assigned molecular formula is $C_{11}H_{12}N_2O_2$ with an error <0.01 ppm.

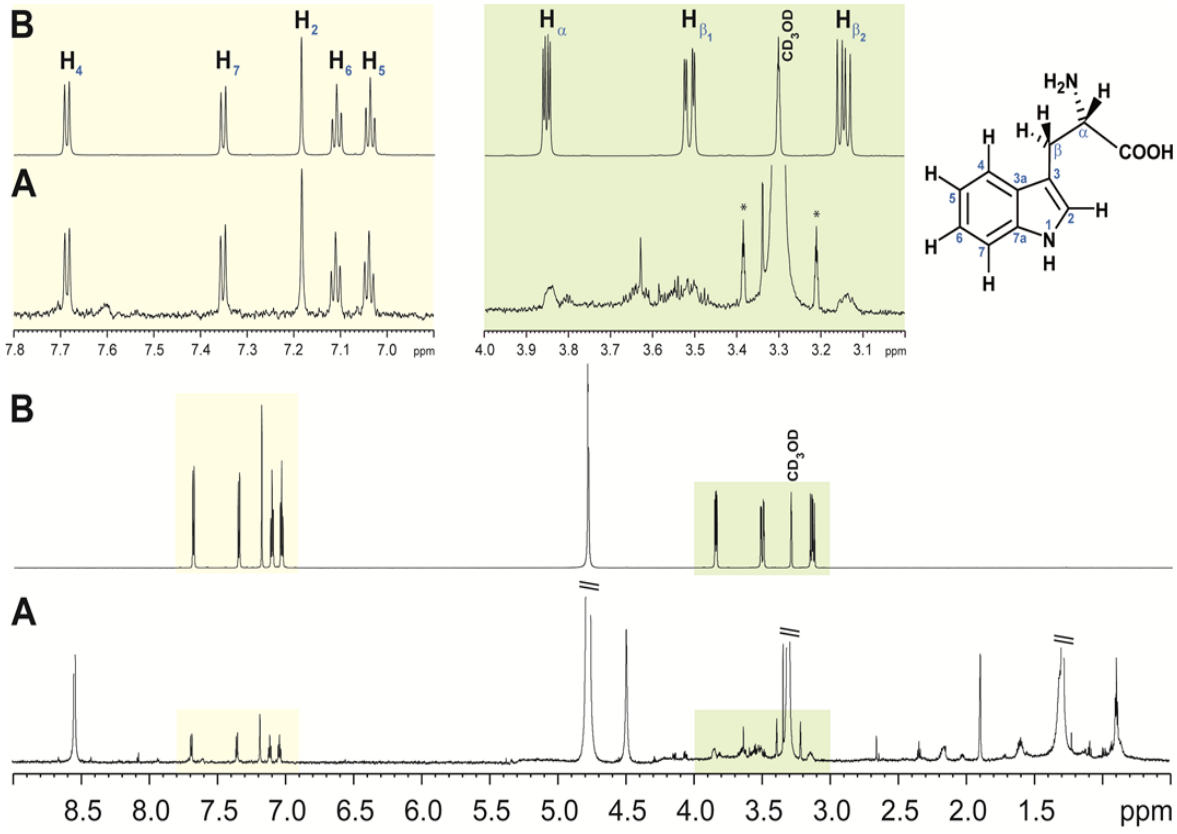

Figure 3.6. 800 MHz 1H NMR spectrum of isolated bioactive compound candidate. Panel A: note the low sample concentration (asterisk: ^{13}C satellites at 0.5 % intensity of HCD_2OD with 99.95 % ^2H). Aromatic spin systems are well recognized including J-couplings, whereas aliphatic nuclei show partial splitting because of low S/N ratio. Panel B: 800 MHz ^1H NMR spectrum of L-tryptophan standard in CD_3OD with aromatic (yellow) and aliphatic (green) spin systems indicated (note: D- and L-tryptophan produce identical NMR spectra in achiral solvents).

Since L-tryptophan was a component of the defined growth medium CDM1, it was reasonable to hypothesized that the bioactive property could be related to the D-form of this amino acid. Therefore, enantiomeric separation was applied to the same purified bioactive sub-fraction used in MS and NMR analyses to verify the presence or not of D-tryptophan. After comparison with standard solutions of L and D-Trp, a likely D-tryptophan peak was observed in the bioactive sub-fraction W56-7 chromatogram (**Figure 3.7**) while the L-form was unique in the corresponding sub-fraction of the control cell-free CDM1 (the culture medium was submitted to the same fractionation steps and bioassay tests and did not show any immune modulatory activity for any fraction). All other bioactive *L. casei* W56 and LGG sub-fractions were saved for further tests in case it was needed.

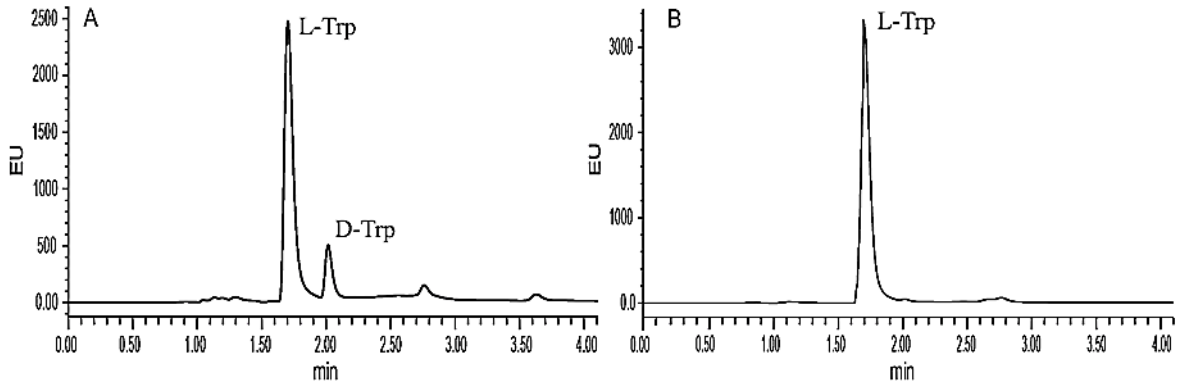

Figure 3.7. Comparative UPLC-FLD chromatogram of a purified bioactive sub-fraction. (A) *L. casei* W56-7 and (B) CDM1 medium respective sub-fraction. OPA-IBLC amino acid derivatization followed by separation in BEH-C18 1.7 µm, 1.0 x 150 mm column using isocratic elution at 45% B in 3 min at 30 ºC (A: 20 mM sodium acetate water solution. B: 7% acetonitrile in MeOH). Flow rate at 100 µL/min. Detection at λ=300 nm excitation and λ=445 nm emission.

Note:

To confirm that bioactivity was restricted to one of Trp isomers, I suggested testing synthetically L- and D-tryptophan standard solutions at different concentrations in both biological screen systems. Only D-tryptophan showed immunomodulatory activity in vitro in a dose dependent manner, whereas L-tryptophan failed to show any effect. Furthermore, other D-amino acids were tested and were inert. Results are nicely described in Chapter 5.

This one-step AA derivatization reaction was easy to perform, and enantiomeric separation could be achieved using a traditional reversed phase C18 column, which avoids the use of more expensive and less robust chiral columns that yet, do not support the ultra-high pressure of UPLC systems. Fluorescence detection is fast, sensitive, easier to operate and significantly cheaper than a mass spectrometer (Waters Corporation, 2007-2009). Then, this simple DL-AA enantio determination technique that has been studied and developed by analysts since the 1990s, was adapted to the current UPLC technology and helped to answer the research question in place: D-tryptophan was present in the bioactive sub-fraction *L. casei* W56-7 and could be responsible for the immunomodulatory activity observed in the bioassays.

Although the enantiomeric separation and detection technique used in this study seems nice at first glance, it had four major flaws for the project at that point in time: 1) the derivatization reaction is not specific to primary amino acids and other compounds present in the sample could be derivatized as well, causing major interferences in the detector or

misleading interpretation of results; 2) detection of D-Trp (and other D-AA) direct in crude supernatants or even after a SPE clean-up, i.e., without fractionation, was impossible due the high concentration of L-AA that overloaded the detector producing large squared peaks which probably hide smaller ones under it (**Figure 3.8** and **Figure 3.9**); 3) up-front dilution of crude supernatants to minimize interference of medium components could make low concentrations of bacteria produced D-Trp undetectable in FLD; and 4) even though the fluorescence detector is considered to be very selective and sensitive, the derivatization and identification of DL-AA is not specific enough to cover the quality standards required nowadays in many research projects (or by the research community), as for example, the mass spectrometer does.

With that in mind, it was of great interest to qualify a new method that combined the advantages offered by the chiral derivatization and reversed phase separation in C18 columns with the sensitivity and specificity offered by the mass spectrometry detection, which could support future research on D-AA.

A method development project was then started using standard solutions of DL-AA and the UPLC-FLD. The reasons for using FLD at the beginning were: great availability of the instrument in our laboratory routine, lower cost of operation than other instruments (there was no need of having a high-resolution mass spectrometry detector at that point), and possibility of data transfer into DryLab® software.

DryLab® is a commercial computer modelling software used to artificially create few hundred experiments in HPLC methods as a function of simultaneous changes in one or more variables that affect separation (e.g., pH, temperature, gradient, etc), all based on real data obtained from an average 4 to 12 runs only. Such method optimization could be potentially tedious in practice depending on the complexity and number of analytes (Dolan et al. 1989; Haber et al 2000). The software was developed based on the concept described in the "Solvophobic Theory" (Horváth et al, 1976) and is well-established software to model reversed phase separations.

Regarding the separation of the DL-AAs standard mixture, DryLab® provided a good indication on the gradient steps and column temperature to be used in the method. However, satisfactory peak resolution was not achieved (artificially) and the prediction of the separation was not as accurate as expected when confronted with the experimental run (**Figure 3.10**). Some factors may have contributed to an error in the computer simulation: 1) software version tested (DryLab 2000) which did not fully assist the modern retention behaviour of an UHPLC separation (i.e., sub-2µm particle size, ultra-high pressure, steep

gradients and high mobile phase velocities), 2) separation of DL-AA may not be 100% based in reversed phase mode interactions but also in a chiral mechanisms and secondary interactions (hypotheses no further examined), 3) the use of sodium acetate buffer in mobile phase A only, where mobile phase B was composed of 7% acetonitrile in methanol which adds complexity to the elution gradient, i.e., change in pH as the concentration of the solvent B increases and a system containing a "protic" or hydrogen bond donating solvent (methanol) and a polar aprotic solvent (acetonitrile). The most recent software versions (e.g., DryLab®4) claim to model UHPLC separations and several chromatographic modes with great accuracy (Kormánya et al. 2014; Tyteca et al. 2016).

Despite that, a promising separation method for DL-AA was achieved after few improvements on the gradient elution and served as the basis for a method transfer to UPLC-MS that was published thereafter.

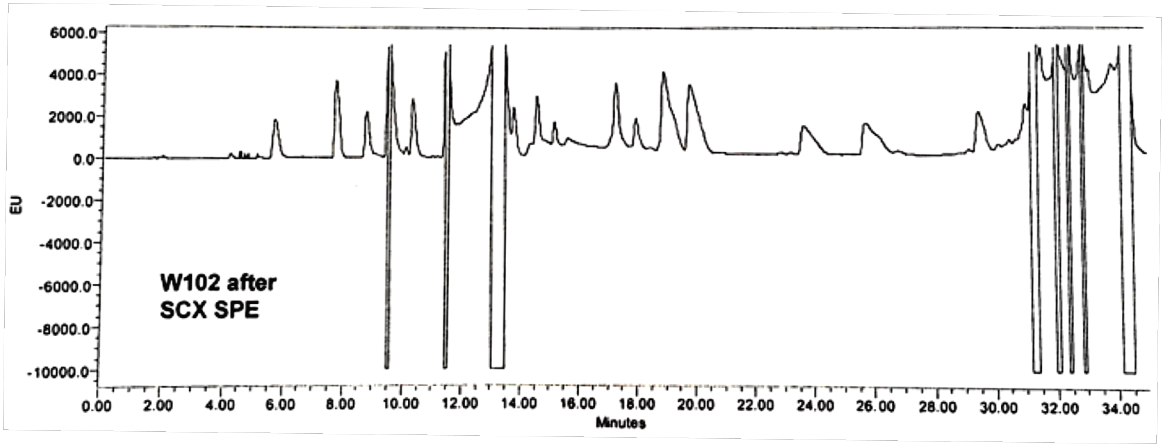

Figure 3.8. Representative FLD chromatogram of a L. rhamnosus W102 cell culture supernatant after a clean-up step with a strong cation exchanger SPE (Bond Elut SCX, Agilent Technologies) followed by derivatization with OPA-IBLC reagent. The flat-shaped peaks observed indicates detector overload.

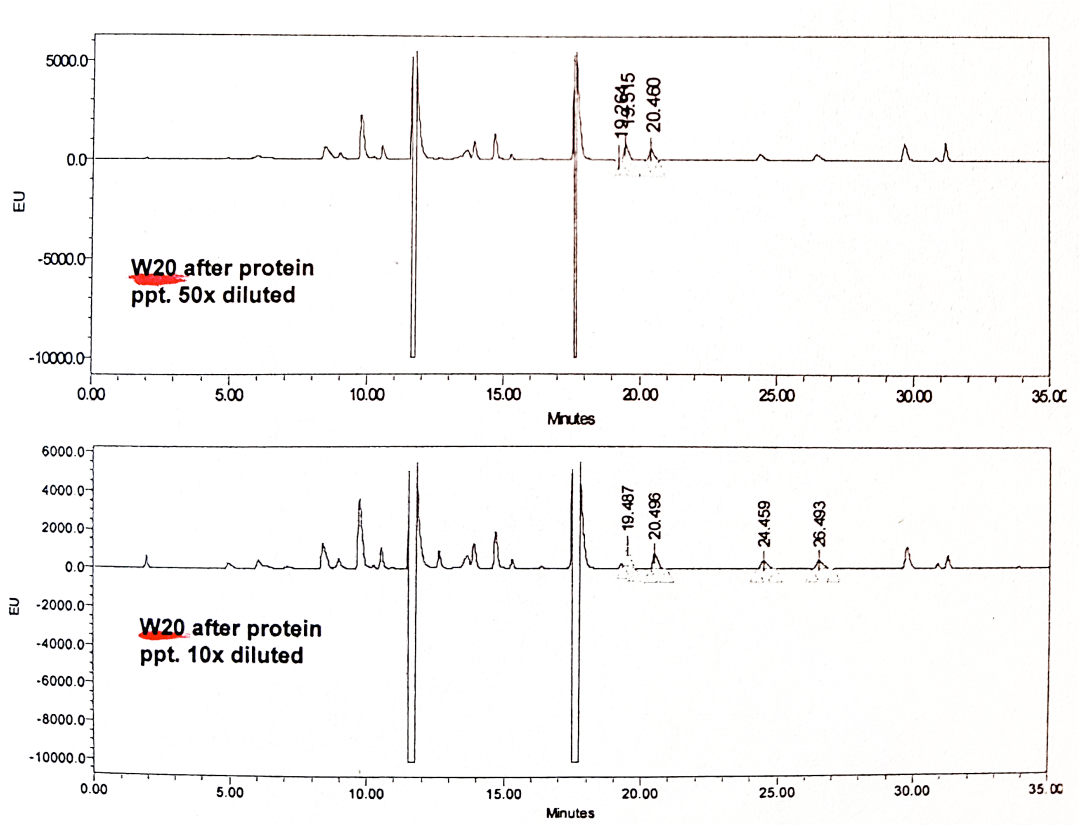

Figure 3.9. Representative FLD chromatogram of a *L. casei* W20 cell culture supernatant after pre-treatment by protein precipitation followed by dilution with aqueous mobile phase and derivatization with OPA-IBLC reagent. The flat-shaped peaks could be observed (detector overload) even after a 50-fold dilution of the sample.

Note: cell-free supernatant of L. rhamnosus W102 and L. casei W20 were randomly chosen from the non-bioactive group of strains to save samples from bioactive strains culture. Experiments only aimed to assess the method capabilities of analysing cell culture without any up-front fractionation.

A

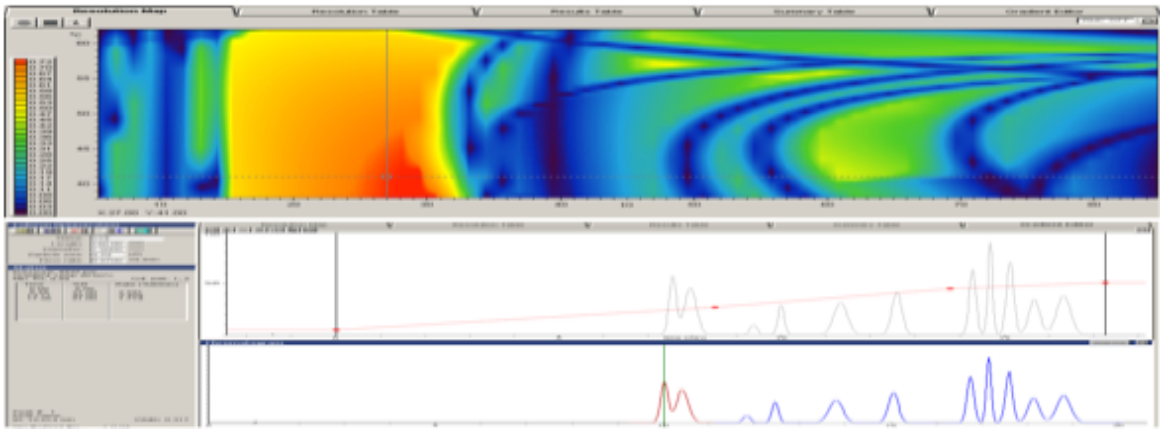

B

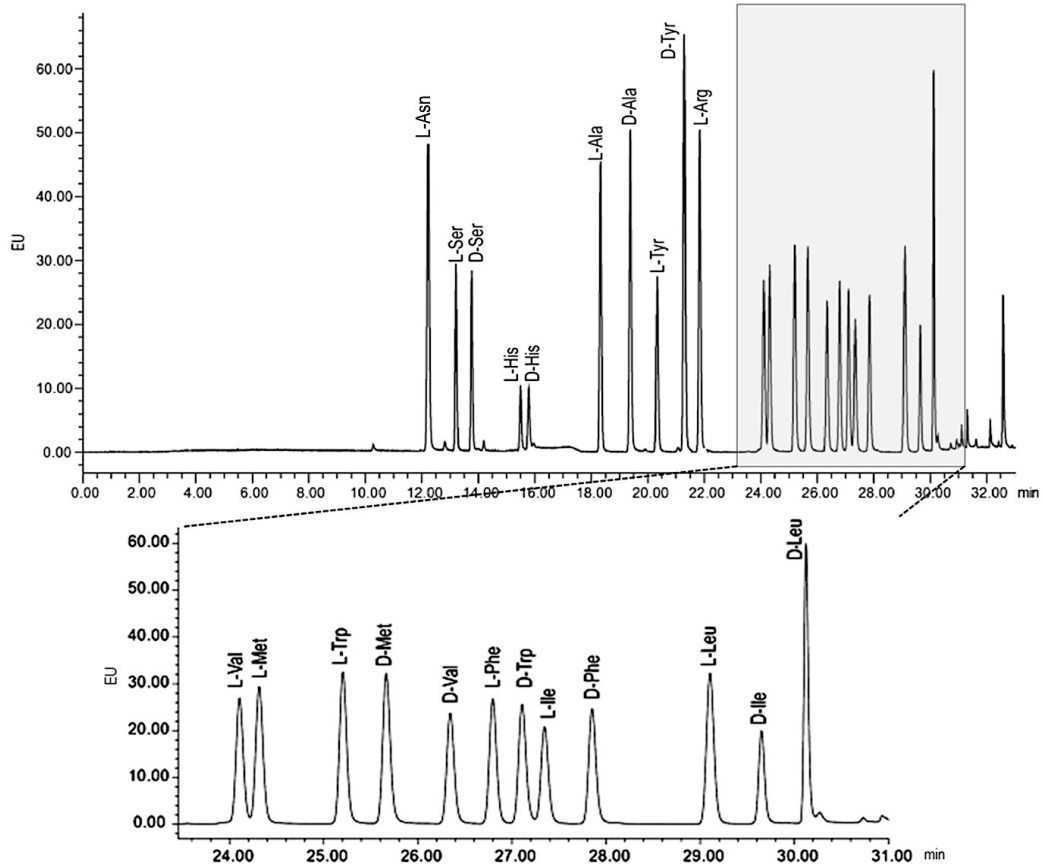

Figure 3.10. Enantiomeric separation of a standard mixture containing DL-amino acids by UPLC®-FLD. A: Representative two-dimensions resolution map for chromatographic simulation of the first group of DL-AA (tR 12-22 min) in DryLab®. The region in red colour defines the conditions of highest peak resolution and method robustness. The blue ones the lowest, where peaks overlap. By moving the cursor to a new position, the chromatogram is changing in its time scale and peak separation. By moving points of the red line that crosses the modelled chromatogram, gradient steps can be defined artificially. B: Representative chromatogram of the final method for OPA/IBLC - amino acids derivatives enantioseparation. This separation method has been the basis for the study using mass spectrometry detection in which additional AAs were included, as shown in Chapter 4.

3.4 Conclusions

Although laborious and time-consuming, the classical bioassay-guided fractionation approach was effective and suitable to the exploratory phase of our studies. This systematic strategy led to the discovery of D-tryptophan bioactivity and yet, left questions unanswered: what compounds are responsible for the immunomodulatory activity observed in the 40% and 50% MeOH/water extracts? It is also clear that this classical procedure deals with the risk of loosing potential bioactive compounds during subsequent bioassay-guided purification. Bioactive substances could be diluted to a non-active concentration level or lose bioactivity after being separated from other compounds that are only efficacious when combined. Poor long-term stability of bioactive metabolites has to be taken into consideration as well as the possibility of loosing very hydrophobic bioactive compounds that might be strongly retained in the SPE solid phase and could not be eluted.

The identification and structural analysis of D-Trp was quite straightforward. However, the lack of high sample volume for the bioactive sub-fraction made NMR analysis difficult as the technique is concentration sensitive. This encourages the extraction of a larger amount of cell culture supernatant in the future studies.

Even though only D-Trp showed immunomodulatory activitv in our bioassay among the proteinogenic amino acids, the establishment of a new UPLC-MS method to analyse D- and L-AA is of great importance since it is well known that microorganisms synthesize D-amino acids with innumerous unknown physiological properties. A selective and sensitive method can support research not only in the field of functional animal biology, but it can also be extended to different research areas, e.g., food chemistry, geochemistry, or cosmochemistry.

3.5 References

Brückner H., Westhauser T., 2003. Chromatographic determination of L- and D-amino acids in plants. *Amino Acids* 24: 43-55.

Brückner H., Westhauser T., Godel H. J., 1995. Liquid chromatographic determination of d- and l-amino acids by derivatization with o-phthaldialdehyde and N-isobutyryl-l-cysteine applications with reference to the analysis of peptidic antibiotics, toxins, drugs and pharmaceutically used amino acids. *Journal of Chromatography A* 711: 201-215.

Dolan J.W., Lommen D.C., Snyder L.R., 1989. DryLab computer simulation for high-performance liquid chromatographic method development. II. Gradient elution. *Journal of Chromatography A* 485: 91-112.

Haber P., Baczek T., Kaliszan R., Snyder L.R., Dolan J.W., Wehr C.T., 2000. Computer simulation for the simultaneous optimization of any two variables and any chromatographic procedure. *Journal of Chromatographic Science* 38: 386-92.

Horvath C., Melander W., Molnar I., 1976. Solvophobic interactions in liquid chromatography with nonpolar stationary phases. *Journal of Chromatography* 125: 129-56.

Horvath C., Melander W., Molnar I., 1977. Liquid chromatography of ionogenic substances with nonpolar stationary phases. *Analytical Chemistry* 49: 142-55.

Kepert, Ingeborg. 2013. Immunmodulatorische Aktivität von Überständen Probiotischer Bakterien Und Dem Darin Enthaltenen D-Tryptophan. Ludwig-Maximilians-Universität München.

Mengerink Y., Kutlán D., Tóth F., Csámpai A., Molnár-Perl I., 2002. Advances in the evaluation of the stability and characteristics of the amino acid and amine derivatives obtained with the o-phthaldialdehyde/3-mercaptopropionic acid and o-phthaldialdehyde/N-acetyl-l-cysteine reagents: High-performance liquid chromatography–mass spectrometry study. *Journal of Chromatography A* 949: 99-124.

Molnar-Perl I., 1999. Stability and characteristics of the O-Phthaldialdehyde / 3-Mercaptopropionic acid and O-Phthaldialdehyde / N-Acetyl- L -Cysteine reagents and their amino acid derivatives measured by High-Performance Liquid Chromatography. *Journal of Chromatography A* 835: 73–91.

Kormánya R., Feketeb J., Guillarme D., Fekete S., 2014. Reliability of simulated robustness testing in fast liquid chromatography, using state-of-the-art column technology, instrumentation and modelling software. *Journal of Pharmaceutical and Biomedical Analysis* 89: 67-75

Tyteca E., Veuthey J-L., Desmet G., Guillarmeb D., Fekete S., 2016. Computer assisted liquid chromatographic method development for the separation of therapeutic proteins. *Analyst*, DOI: 10.1039/c6an01520d.

Waters Corporation, 2007−2009. ACQUITY UPLC Fluorescence Detector Getting Started Guide, 71500142403/Revision B.

4
Enantioseparation and selective detection of D-amino acids by ultra-high-performance liquid chromatography/mass spectrometry in analysis of complex biological samples

Published as: *Juliano R. Fonseca, Constanze Müller, Theresa M. Rock, Susanne Krauss-Etschmann, Philippe Schmitt-Kopplin (2014). Journal of Chromatography A; 1324: 109-114.*

Author contributions

Juliano R. Fonseca identified the need for having a DL-AA quantification methodology as result of the studies already described in Chapter 2 and 3. Juliano conducted literature research and performed the method development for DL-AAs enatioseparation and detection using UHPLC-FLD as well as its method transfer to UHPLC-QqToF-MS.

Constanze Müller was of great support during method transfer to UHPLC-QqToF-MS and further method optimization for its application in different biological matrices, with great technical help from Theresa M. Rock on matrix interference and stability experiments.

Juliano R. Fonseca and Constanze Müller wrote the paper together (shared co-first authorship), with critical and intellectual contribution from Philippe Schmitt-Kopplin and other co-authors.

This chapter fully reproduces the content of the publication but includes few adaptations to align with the format of this thesis.

Abstract

The growing scientific attention in the biological function of D-amino acids leads to an increasing analytical interest for enantiomeric amino acid separation, which is still very challenging due to the lack of sufficiently sensitive, high-throughput analytical methods that can cope with often occurring matrix interferences and very low D-amino acid concentrations. Here, enantioseparation can benefit from improved resolution and chromatographic speed offered by modern UHPLC techniques and the precision of MS detection. We developed an RP-UHPLC-QqToF-MS method using pre-column OPA/IBLC derivatization for very precise discrimination of amino acids enantiomers. The method shows a superb sensitivity with limits of detection in the range of several pmol/l. It has neither shown matrix inferences in the tested very complex biological matrices (serum, plasma, urine and gut) nor stability or racemization problems.

4.1 Introduction

Amino acids (AA) are very important chiral biomolecules. They participate in gene expression, regulation of metabolism, cell signalling and immunity (Lamzin et al. 1995; Wu 2009). The predominantly present L-enantiomers function as building blocks of peptides and proteins or precursors for the synthesis of several important molecules. D-enantiomers are comparatively very low abundant. While even been believed to be absent in higher animals in the past (Corrigan 1969; Miyoshi et al. 2012), now D-AAs are the focus of several studies as they are considered to be new bioactive compounds and biomarkers (Hamase et al. 2009). An accumulation of D-isoleucine, D-valine, D-leucine, and D-methionine in culture media was reported to stimulate the conversion of rod-shaped into spherical bacteria, which illustrates how D-AA can influence peptidoglycan structure and composition (Lam et al. 2009). D-tryptophan, D-leucine, D-methionine and D-tyrosine can inhibit biofilm formation or even disrupt existing ones (Kolodkin-Gal et al. 2010). Additionally, D-AAs are used in nutritional industry as markers for contamination from microorganism or for food age because D-AAs, like D-alanine or D-glutamic acid, are natural components of bacterial cell walls (Cava et al. 2011). Moreover, the isomerization of L to less digestible D-enantiomers leads to a reduced dietary value in processed food products (Friedman 2010). Main natural sources of D-AAs are next to microorganisms' soils, seeds, fruits and tree leaves of several plants (Brückner and Westhauser 2003), but also meteorites have been extensively studied for D/L-AA ratio. This ratio is used to confirm an abiotic origin or possible terrestrial contamination of AAs in the analyzed material (Glavin et al. 2006; Glavin et al. 2012).

To further facilitate research on the presence and biological function of D-AA, sensitive and selective methods need to be developed. The aim of this work was to establish a UHPLC-QqToF-MS (ultra-high performance liquid chromatography–time of flight mass spectrometry) method for AA enantiomeric analysis, which combines the enhanced separation possibilities of sub-2 µm particles of UHPLCs with the sensitivity and accuracy of mass spectrometric detection (Glavin et al. 2012; Visser et al. 2011; Min et al. 2010), and that is directly applicable to biological samples. A pre-column derivatization using o-phthalaldehyde (OPA) in combination with the chiral thiol isobuteryl-l-cysteine (IBLC), a well-established tagging reagent (Figure 4.1) has been preferred and applied in UHPLC-FLD (fluorescence detection) and UHPLC-QqToF-MS. The challenges of fluorescence detection will be discussed as well as the need of detection method transfer from FLD to the more selective and therefore sensitive MS. The developed method and putative matrix

interferences were tested analyzing four very complex biological matrices. Stability issues of AA derivatives were addressed as well.

4.2 Materials and methods

4.2.1 Chemicals and reagents Methanol

Methanol (Chromasolv, Sigma–Aldrich, St. Louis, USA), acetonitrile (Chromasolv, Sigma–Aldrich) and water (MilliQ) were used in LC-MS quality. OPA, IBLC, IBDC, boric acid and sodium acetate were purchased from Sigma Aldrich, as well as all used amino acid standards (enantiomeric mixtures: D/L-Ala, D/L-Asn, D/L-Asp, D/L- Cys, D/L-Glu, D/L-His, D/L-Ile, D/L-Leu, D/L-Met, D/L-Pro, D/L-Ser, D/L-Val; enantiomer pure standards: L-Arg, L-Gln, L-Lys, L-Phe, L-Thr, L-Trp, L-Tyr, D-Arg, D-Gln, D-Lys, D-Phe, D-Thr, D-Trp, D-Tyr). Compounds are indicated according to IUPAC symbolism for amino acids (Suppl. **Table S 4**). Ammonium acetate buffer was bought from Biosolve (Valkerswaard, Netherlands) and an electrospray ionization (ESI) tuning mix from Agilent (Santa Clara, USA) for MS calibration.

4.2.2 Preparation of human serum, human plasma and urine

The developed UHPLC-FLD and UHPLC-QqToF-MS protocols were tested with human serum (HuS), EDTA-plasma and urine for general suitability and putative matrix interferences. Therefore, we took samples from several individual volunteers and pooled these aliquots. The samples were stored at -80 °C directly after sampling until analysis. The reason to test the method with such a mixture of samples taken from many individuals was the increased complexity of pooled samples. We wanted to capture as many possible interfering compounds as possible (e.g., different diets of different persons and therefore different putative interfering compounds). We did not intent to answer any biological question with these experiments. HuS and EDTA-plasma required furthermore protein precipitation prior analysis. After careful thawing on ice, 20 µl of each sample matrix were mixed with 80 µl ice-cold methanol and centrifuged (15,000 rpm, 4 °C, 15 min). The supernatant was taken, evaporated and resolved in water before injection. Urine was thawed on ice as well and centrifuged to avoid particle injection (15,000 rpm, 4 °C, 15 min).

4.2.3 Preparation of mouse gut

About 100 mg of frozen cecal content of 10-week-old C57BL/6J mouse was protein-precipitated by using 500 µl cold methanol (-20 °C) whereas ceramic beads were used for cell disruption (NucleoSpin bead Tubes, Macherey-Nagel GmbH & Co. KG). Subsequently, the sample was homogenized using TissueLyser II (Qiagen) for 5 min at a rate of 30 Hz. This procedure was repeated three times in order to increase the extraction efficiency. Afterwards, the sample was centrifuged at 14,000 rpm for 10 min at 4 °C and the supernatants were pooled for the analyses. The supernatants were kept in -20 °C conditions prior to experiments.

4.2.4 Derivatization

The derivatization reagent OPA/IBLC was freshly prepared based on a previously described HPLC-FLD method (Brückner et al. 1995). A methanolic solution of OPA (200 mM) was mixed with 200 mM IBLC prepared in 0.1 M borate buffer corresponding to the moles ratio OPA/IBLC 1/3, which is optimal for the stability of AA derivatives (Mengerink et al. 2002). The pH of the mixture was adjusted to 9 with 1 M sodium hydroxide. Derivatization of amino acids in standard solutions and samples were carefully carried out for 2 min under a fume hood by mixing 10 µl of standards/samples with 20 µl derivatization reagents prior injection. This corresponds to an excess of OPA molecules of approximately 1 × 10E8 (for the lowest tested amino acid concentration) and to 10 (for the highest tested amino acid concentration) compared to amino acids molecules in solution (0.0001–1.5 ppm). All glassware was heat sterilized before usage (Glavin et al. 2012). Blank samples consisting of pure solvents were included in all analyses.

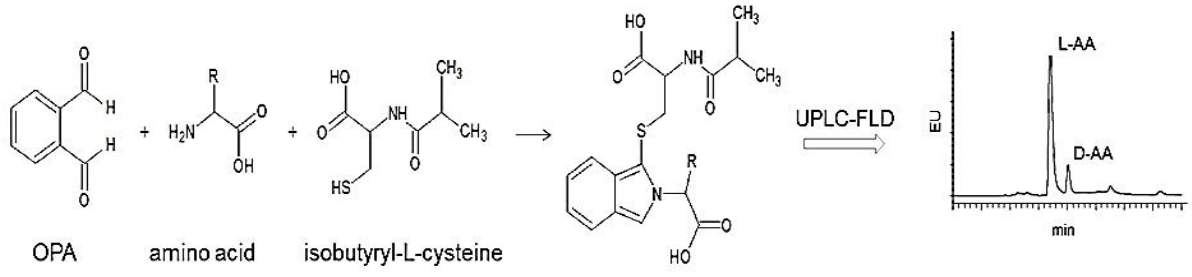

Figure 4.1. Derivatization reaction between OPA, primary amino acid and IBLC. Besides primary amino acids, their esters, amino alcohols, alkyl- and aryl-amines, heterocyclic amines react with OPA resulting in strong interferences for complex samples. The condensation between the amino group and the aromatic o-dicarboxaldehyde leads in a N-substituted isoindolin-1-one (phthalimidine) derivative (Gyimesi-Forrás et al. 2005). The use of N-isobutyryl-D-cysteine leads to a reversal in the elution order of derivatives, i.e., D-AA elutes before its respective L-form.

4.2.5 UHPLC-FLD

Enantiomeric separation was initially achieved using an ACQUITY UPLC® system (Waters, Milford, USA) coupled to a fluorescence detector, which has been set to λ = 300 nm for excitation and λ = 445 nm for emission. A BEH-C18 column with dimensions of 2.1 mm × 150 mm and 1.7 µm particle size (Waters) was applied with a column temperature of 30 °C. The autosampler was set to 25 °C. Mobile phase A consisted of 20 mM sodium acetate buffer that was adjusted to pH 6.2 with acetic acid. Mobile phase B was composed of 7% acetonitrile in methanol (Brückner et al. 1995). The gradient was optimized with a flow rate of 0.350 ml/min (**Table 5**).

Table 5: Optimized gradient for enatiomeric separation of AA.

Time (min)	Flow (ml/min)	%A	%B
0	0.350	100.0	0.0
15.00	0.350	70.0	30.0
28.00	0.350	50.0	50.0
31.00	0.350	20.0	80.0
32.00	0.350	20.0	80.0
33.00	0.350	10.0	90.0
34.00	0.350	10.0	90.0
34.50	0.350	100.0	0.0

4.2.6 UHPLC-QqToF-MS

The ACQUITY UPLC® was coupled to a QqToF-MS (maXis, Bruker Daltonics, Bremen, Germany) to allow mass spectrometric detection. The maXis mass spectrometer is a hybrid QqToF dual stage reflector instrument, which uses orthogonal ion acceleration. “Q” (capital letter) refers to a mass selective mass resolving quadrupole, whereas “q” indicates a quadrupole collision cell. It is therefore possible to isolated selected masses in the mass isolating quadruple and fragment these isolated masses of interest in the second quadrupole. The mass fragments can thereafter be measured according to their time of flight in the flight tube. Slight modifications of the UHPLC-FLD method were necessary to ensure compatibility with electrospray ionization. Sodium acetate was exchanged with ammonium acetate (2.5 mM). The flow rate was reduced to 0.200 ml/min for the same reason. Additional parameters were kept constant. Mass spectrometric parameters were optimized in order to

achieve highest sensitivity in the mass range of the amino acid derivatives (350–500 Da) within an acquisition window of 50–1500 Da and a scan rate of 2 Hz.

4.3 Results

4.3.1 UHPLC-FLD matrix interferences followed by method transfer Baseline

Baseline separation of enantiomeric amino acid standards could be achieved within 34 min using the sensitive UHPLC-FLD method. Nevertheless, separation of standard materials is so far easily achievable, but in daily routine the analyst has to deal with very complex samples. FLD detection turned out to be not well suited for such studies as e.g., strong interferences from derivatization reagents and samples themselves have been recognized (**Figure 4.2**). Since besides primary amino acids, amino esters, amino alcohols, alkyl- and aryl-amines, and heterocyclic amines react with OPA (Gyimesi-Forrás et al. 2005), a higher baseline and co-elution for some D-AA has been observed. This increases the limit of detection and might lead in missinterpretation if identification solely relies on retention time comparison with standard compounds. Extensive sample clean-up might overcome this problem but requires time and bargains the risk of contaminations and sample alterations. Thus, analytical methods insensitive for such interferences are on demand and consequently we transferred the method to UHPLC-QqToF-MS. The flow rate and buffer of mobile phase A were therefore adjusted. **Figure 4.3** shows the extracted ion chromatogram (EIC) obtained for a derivatized AA standard mixture. Proline as a secondary amine does not react with OPA/IBLC reagent, glycine is achiral and was consequently not included in our study, and cysteine could not be detected. Additionally, the early elution of aspartic acid (tR 4.1 min) resulted in poor resolution between its D and L forms showing a single peak. With these exceptions, baseline separation was achieved for all proteinogenic AA enantiomeric pairs. The high resolution ToF-MS allowed us to extract m/z values of each AA derivative with an accuracy of m/z ± 0.001 (except Asp 0.005, Glu 0.005, Phe 0.002 and Val 0.005), which provided clean chromatograms.

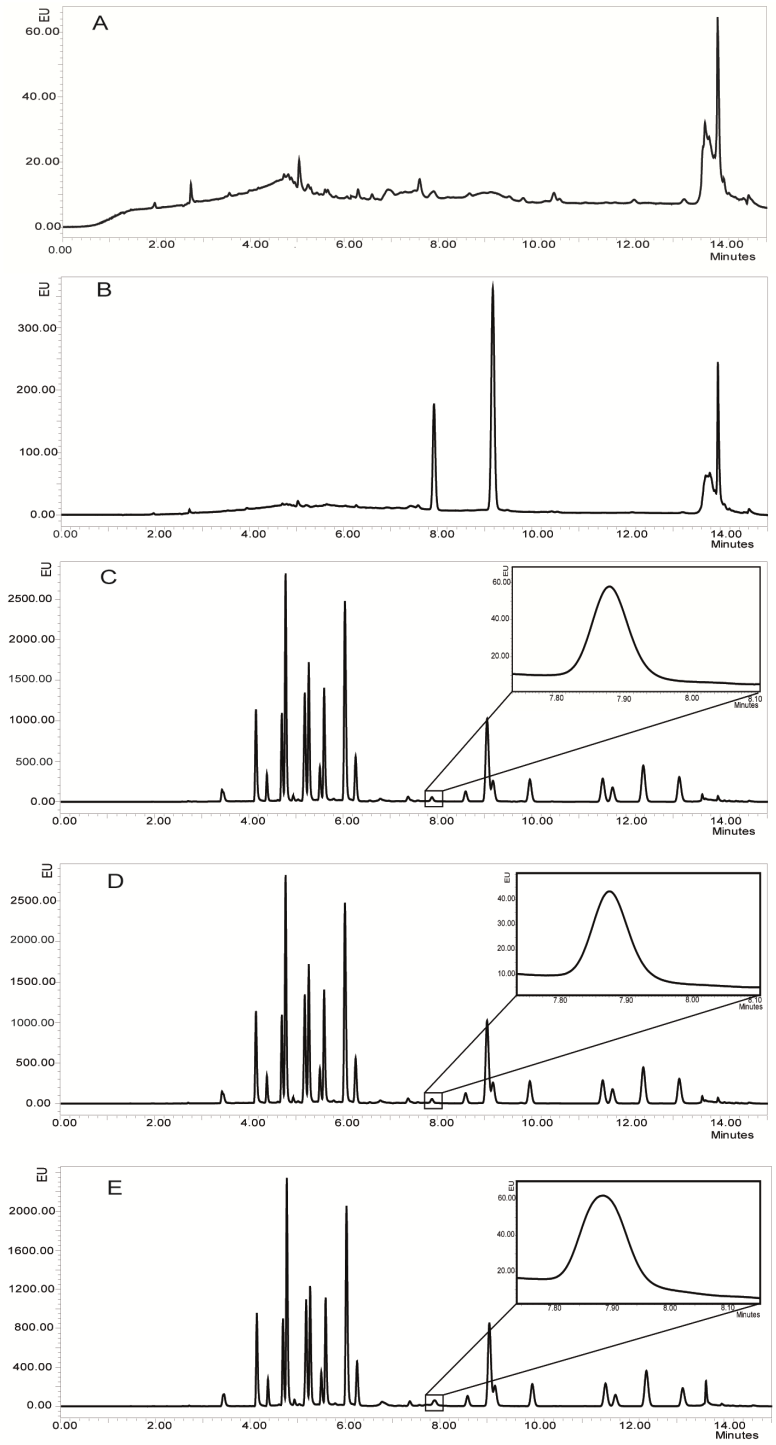

Figure 4.2. UHPLC-FLD chromatograms for the analysis of Tryptophan in human serum. A) water with derivatization reagent, B) 5 ppm D-Trp and 10 ppm L-Trp in water, Human serum spiked with C) 0.005 ppm, D) 0.02 ppm and E) 1.5 ppm D-Trp. Even though the method worked very well for pure standard solution, detection of D-Trp was disturbed by co-eluting matrix interference at t_R 7.8 min. No increase in the peak area with elevated D-Trp amounts can consequently be recognized (enlarged in box C, D, E). Such problems can be minimized when using more specific detection methods like MS, as the mass of derivatized D-Trp can be isolated from the interfering signal. This keeps the advantage of less method adaptation necessities and guarantees a less matrix-dependent sensitivity.

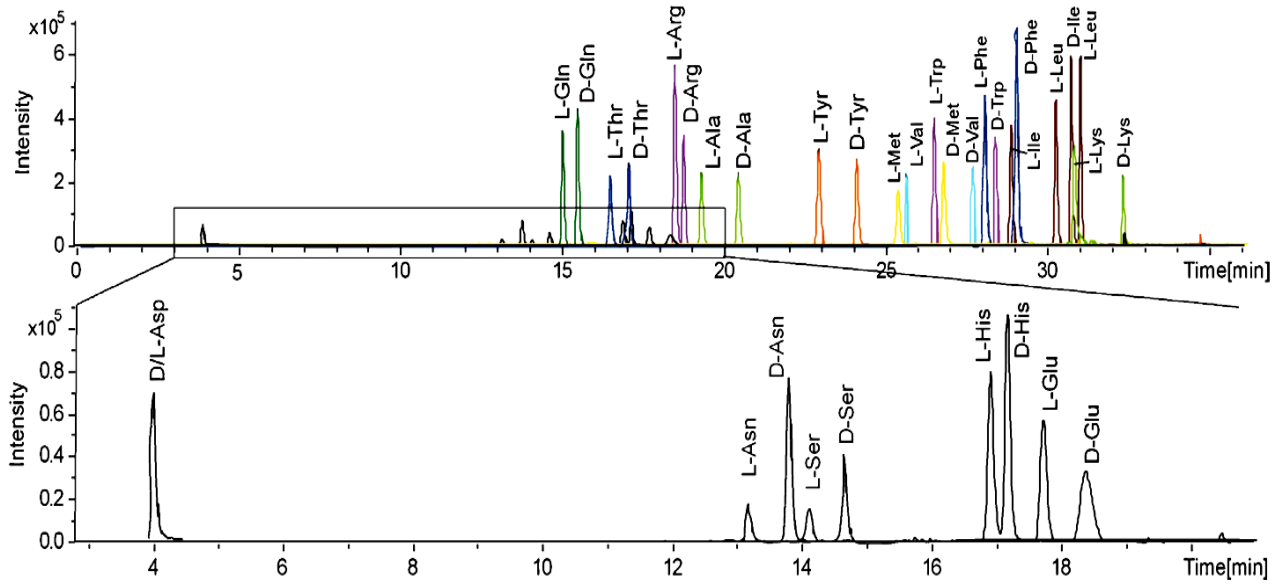

Figure 4.3: UHPLC-MS extract ion chromatogram (EIC) obtained for the reversed phase enantioseparation of OPA/IBLC derivatized amino acid standards with concentrations of 0.5 and 1 ppm (Thr, Asp, Lys, Phe, Arg, Glu, Tyr and Trp).

4.3.2 LOD and linearity in UHPLC-QqToF-MS

Amino acid standards of 0.5–1 ppm concentration were used to determine the limits of detection, which were calculated as LOD = conc. AA [mmol/l] × 3/SNR for pure standards solutions and as LOD = basic AA conc. + spiked conc. AA [mmol/l] × 3/SNR at spiked concentration for biological matrices. Signal to noise ratios (SNR) were elaborated with Bruker Daltonics Data Analysis 4.2. It needs to be considered that the LOD may vary when analysing different sample matrices. Here, we present data for pure standards (**Table 6**) and spiked plasma samples (**Table 7**). The signal-concentration response followed a linear relationship for both standard solution (data not shown) and plasma in the concentration range of 0.0001–1.5 ppm. Depending on the matrix and AA of interest it might be necessary to dilute the matrix before spiking due to high basic concentrations.

Table 6: Masses, retention time and limits of detection for D-amino acids standards measured by UHPLC-MS using OPA/IBLC derivatization.

D-AA	$[M + H]^{+}$[a] (m/z)	tR (min)	LOD (pmol/L)
Ala	379.1322	20.5	11.46
Arg	464.1962	18.8	8.27
Asn	422.1380	13.8	27.09
Asp[b]	423.1221	4.1	76.43
Gln	436.1537	15.4	8.93
Glu[b]	437.1377	15.3	29.33
His	445.1540	17.1	19.22
Ile	421.1792	30.7	2.79
Leu	421.1792	31.0	2.83
Lys	436.1901	32.4	24.75
Met	439.1356	26.6	12.25
Phe	455.1635	28.8	7.31
Ser	395.1271	14.6	62.52
Thr	409.1428	17.1	40.17
Trp	494.1744	28.2	10.47
Tyr	471.1584	22.2	3.82
Val	407.1635	27.7	6.87

[a] Calculated mass for protonated molecules of AA derivatives.
[b] Limited solubility in water under used conditions.

Table 7: Masses, LODs and calibration parameters for D-amino acids measured in plasma sample matrix by UHPLC-MS using OPA/IBLC derivatization (4 calibration points were used except for aspartic acid, glutamic acid and lysine).

D-AA	$[M + H]^{+}$[a] (m/z)	Calibration range (mg/L)	Calibration curve y = aC + b	R^2	LOD (pmol/L)
Ala	379.132	001-0.75	y = 2,003,274.81C + 294,580.47	0.9432	21.75
Arg	464.196	0.0002-1.0	y = 740,377.10C + 127,178.72	0.9807	19.6
Asn	422.138	0.01-0.75	y = 641,037.87C + 66,622.62	0.9577	28.37
Asp[b]	423.122	–	–	–	–
Gln	436.154	0.0002-1.0	y = 1,532,437.43C + 239,481.50	0.9808	16.83
Glu[b]	437.138	–	–	–	–
His	445.154	0.0001-0.5	y = 577,640.12C + 41,467.93	0.9865	61.23
Ile	421.179	0.0001-0.75	y = 3,519,703.40C + 326,974.14	0.9951	7.78
Leu	421.179	0.0001-0.75	y = 2,880,663.20C + 163,095.19	0.9965	7.08
Lys[c]	436.190	–	–	–	–
Met	439.136	0.0001-0.75	y = 1,856,244.56C + 53,060.88	0.9903	22.11
Phe	455.164	0.0002-1.0	y = 2,859,517C + 216,411.03	0.9988	20.63
Ser	395.127	0.0001-0.75	y = 794,772.77C + 51,842.50	0.9973	33.92
Thr	409.143	0.0002-1.5	y = 1,158,402.21C + 65,359.65	0.9969	79.43
Trp	494.174	0.0002-1.0	y = 1,237,427.67C + 37,510.10	0.9975	20.39
Tyr	471.158	0.0002-1.5	y = 248,853C + 54,497	0.9780	64.35
Val	407.164	0.01-0.75	y = 2,278,485.89C + 224,692.79	0.9830	159.18

[a] Calculated values for protonated molecules of AA derivatives.
[b] Limited soluble in water under used conditions.
[c] Basic concentration too high, LOD calculation possible with 10-fold dilution of the matrix.

4.3.3 Stability of derivatization product

An additional crucial point is the stability of the derivatization product. Derivatization is completed after 2 min at room temperature and has been known to be stable for at least 18 min (Brückner and Westhauser 1995). We tested the peak area response of the solutions of the standards after 2, 20, 40 and 60 min and observed stable signals of derivatization products for at least 40 min (97.5–101.8% of original detected value). Thereafter, the signal response decreased (**Figure 4.4**). Thus, we strongly suggest the derivatization directly prior injection. A lab robot might be useful for automation of this procedure. Putative racemization of amino acids during derivatization and chromatography can be excluded because we confirmed the absence (or very low abundance as indicated by the enantiomeric purity of the vender) of the other enantiomer for several amino acids in standard mixtures and in biological samples of various concentrations (exemplarily illustrated for L-Arg, L-Asp and L-Trp in **Figure 4.5**).

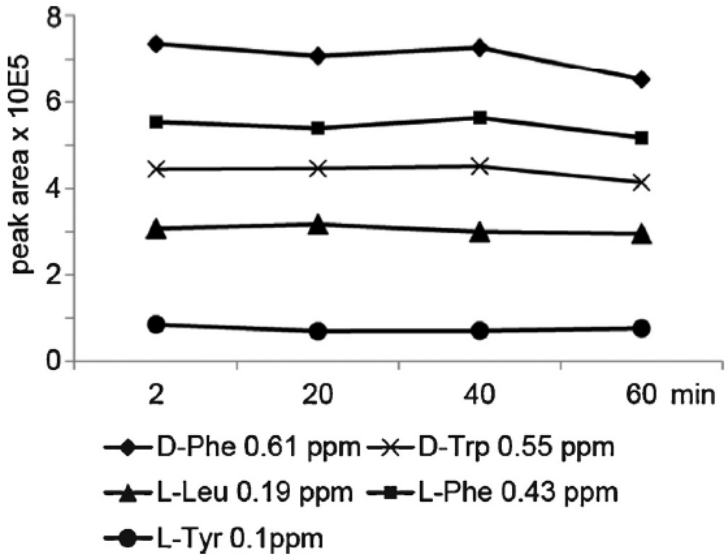

Figure 4.4. Stability of detected peak area after t0 + x min.

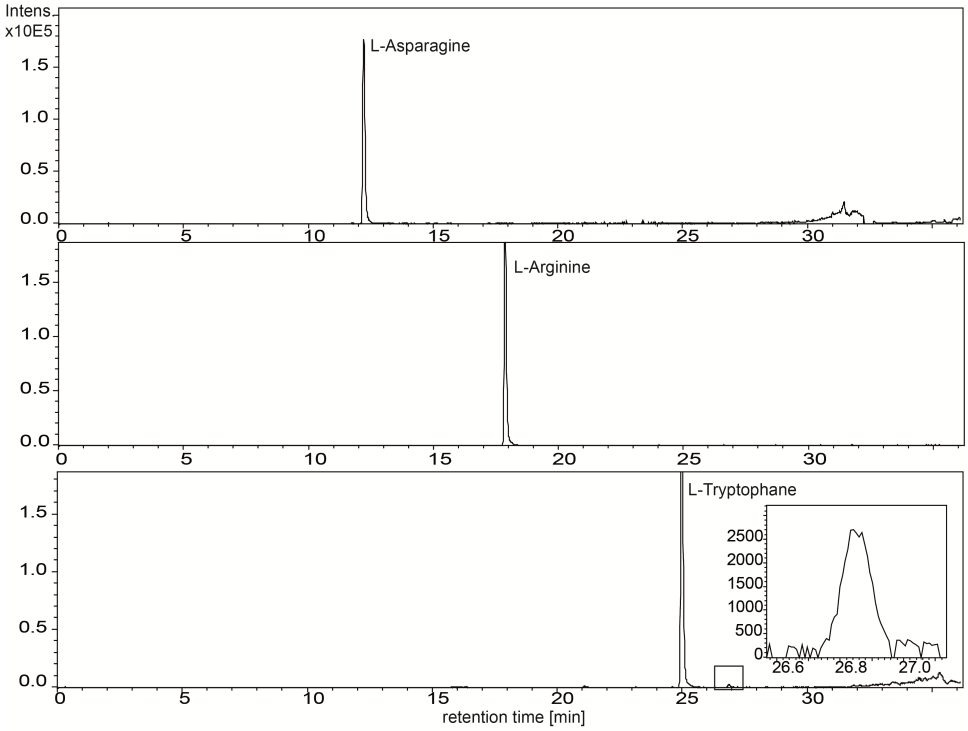

Figure 4.5. Enantiomeric stability of standards, exemplarily illustrated for 1 ppm solution of L-asparagine (99% purity), L-arginine (≥98% purity) and L-tryptophan (≥98% purity). While asparagine and arginine standards show a very high purity of the L-enantiomer (no D-AA has been detected), a small contamination of D-tryptophan (enlarged in box) in the L-tryptophan standard needs to be recognized. The contamination is however in the range of the vender given purity (< 1.12%). In consequence, racemization during the chromatographic analysis can be excluded.

4.3.4 Applicability to important biological matrices

The developed UHPLC-QqToF-MS method was finally tested in four different biological matrices to evaluate possible signal interferences caused by the sample matrix itself. Due to the application of QqToF-MS, specific detection of proteinogenic amino acids could be achieved without matrix interferences. Chromatograms for alanine, serine and methionine for standards and tested biological matrices are exemplarily illustrated in **Figure 4.6** as their derivatization and ionization behavior can be used as approximation of the other amino acids (Visser et al. 2011). Detection of the exact masses of AA derivatives and their retention time allow certain identification. We observed very small retention time shifts when injecting different matrices, e.g., retention time shifts for D-AA standards in water and plasma were between 0.1 and 0.3 min, which shows a high reproducibility. Additionally, MS^2 fragmentation information can be easily obtained by various MS instrument if uncertainties in the identity of any AA exist. Due to very presumable different matrix effects of each sample type in electrospray ionization, we relinquish to give absolute concentrations and

strongly suggest determining crucial quantification parameters for each specific application. The biological matrices were used here with the purpose to test the analytical protocol for putative inferences or any other analytical problem. Consequently, we repetitively analyzed pooled samples of the selected matrices. We did not intent to answer any biological question.

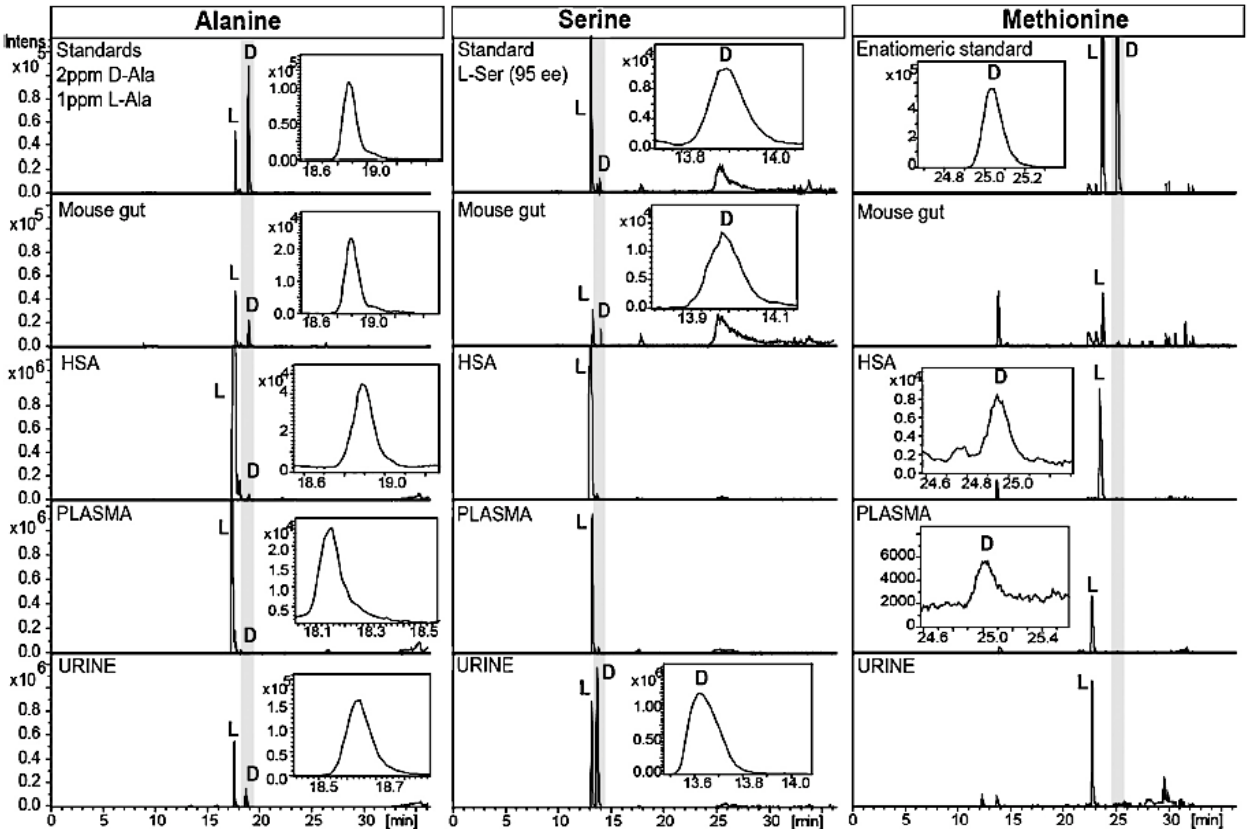

Figure 4.6: Extracted ion chromatograms (±0.01) of alanine, serine and methionine for standards, mouse gut, HuS, plasma and urine. Retention time windows of D-AA are marked in gray and enlarged illustrated, if the D-enantiomer has been detected.

4.4 Discussion

The increasing scientific interest in D-AA requires more and more sensitive and selective analytical protocols. Due to several facts, like the possibility for reliable chiral separation, coverage of a very high number of analytes and suitability for full automation, liquid chromatography (LC) has been applied for chiral separation (Miyoshi et al. 2012; Brückner and Westhauser 1995; Armstrong et al. 1993). Existing HPLC-FLD protocols are particularly challenged by matrix interferences, the very low abundances of D-AAs and huge concentration differences compared to their L-enantiomers. UHPLC, which offers a much higher separation efficiency and chromatographic speed due to the application of sub-2 µm

porous particles (Guillarme et al. 2010; Oláh et al. 2010), in combination with the precise and sensitive detection of mass spectrometry is one way to improve enantio separation and reach the analytical needs currently occurring.

Two strategies can be followed to resolve enantiomers in LC systems, first the application of chiral stationary phases and secondly enatioseparation based on a pre-column derivatization. Several facts led us to use pre-column derivatization for the development of our UHPLC method. The most important ones are a higher efficiency, which can be reached using chiral derivatization reagents followed by reversed phase (RP) chromatography (Miyoshi et al. 2012), the missing availability of chiral material with sub-2 µm particles for UHPLCs and a better sensitivity that can be reached with RP columns due to the high number of analytical plates. Commonly, pre-column derivatization uses fluorescence tagging for detection (Brückner and Westhauser 1995; Hanczkó et al. 2004; Kutlan et al. 2002; Brückner et al. 1994). Unfortunately, although fluorescence detection is one trustworthy detection method, complex biological samples contain endogenous compounds that are likely to cause signal interference or may co-elute with some D-AA, which is a source of variability and inaccuracy. Mostly primary amino acids, amino esters, amino alcohols, alkyl- and aryl-amines and heterocyclic amines react with OPA (Gyimesi-Forrás et al. 2005). Samples need consequently either an intensive clean-up or more precise detection methods are necessary. FLD applications have been therefore limited to few amino acids (Visser et al. 2011). We also observed such problems when we applied our developed UHPLC FLD method to differently composed biological matrices and decided thus to transfer the method to UHPLC-QqToF-MS, which allows to isolate the exact masses of the derivatization products of each amino acid and is in consequence insensitive for most matrix-interference signals. This leads eventually to a method that is much more extensive in its application. This potential of UHPLC applications in combination with pre-column derivatization for chiral separation of amino acids has been hardly described. Only three references could be found. Zhe Min developed a new florescence tagging reagent (DBD-PyPNCS) for the analysis of amino acids in human nails (Min et al. 2010). Visser compared NDB-PyNCS, GITC, AMBI, OPA/IBLC, S-NIFE, Marfeys- and Sangers reagent (Visser et al. 2011). In their publication it was shown that NIFE delivered best sensitivity for alanine, serine and methionine followed by OPA/IBLC. However, we decided to proceed with OPA/IBLC due to availability issues and achieved 10 times lower LOD for OPA/IBLC compared to the published method. One further argument to proceed with OPA/IBLC is the possibility to exchange the elution order of D and L enantiomers simply by using IBDC instead of IBLC, which allows verification

of the abundance of the D-AA and might be helpful in some rare cases in which a co-eluting peak has the same mass as the AA derivative. Additionally, the exchange is very advantageous if the L-form is present in much higher concentration than the D-AA, which might be the case of bacterial cell cultures or chemically defined medium. A third study using UHPLC for enantiomeric AA separation has been published recently (Glavin et al. 2012). Glavin et al. used OPA/NAC and combined three different analytical columns for sensitive identification of aspartic acid, glutamic acid, serine, threonine, glycine, alanine and GABA in meteorites.

The development of the presented method was motivated by the fact that traditional fluorescence detection alone cannot offer the level of certainty necessary to analyze D-AA in biological samples. Although there is still some place for improvement, our MS detection allows sensitive, specific targeted and relatively fast differentiation of proteinogenic AA enantiomers in complex matrices.

4.5 Conclusions

A simple applicable, specific and sensitive UHPLC-MS method for differentiation of AA using chiral derivatization with OPA/IBLC reagent and RP chromatography has been presented. The widely implemented stationary phase C18 prevents the analyst of buying special and more expensive chiral columns. It offers moreover a high number of analytical plates and consequently very good separation efficiency. The exchangeability of the elution order of L- and D-enantiomers simply by the usage of IBDC instead of IBLC might be very helpful for some applications. Most importantly, the very sensitive and selective MS detection overcomes misinterpretation of detected peaks, which can result from interference signals in complex samples when methods solely rely on fluorescence detection.

4.6 References

Armstrong D.W., Gasper M., Lee S.H., Zukowski J., Ercal N., 1993. D-amino acid levels in human physiological fluids. *Chirality* 5: 375-378.

Briickner H., Haasmann S., Langer M., Westhauser T., Wittner R., Godel H., 1994. Liquid chromatographic determination of d- and l-amino acids by derivatization with o-phthaldialdehyde and chiral thiols: Applications with reference to biosciences. *Journal of Chromatography A* 666: 259-273

Brückner H., Westhauser T., 2003. Chromatographic determination of L- and D-amino acids in plants. *Amino Acids* 24: 43-55.

Brückner H., Westhauser T., Godel H. J., 1995. Liquid chromatographic determination of d- and l-amino acids by derivatization with o-phthaldialdehyde and N-isobutyryl-l-cysteine applications with reference to the analysis of peptidic antibiotics, toxins, drugs and pharmaceutically used amino acids. *Journal of Chromatography A* 711: 201-215.

Cava F., Lam H., Pedro M.A. de., Waldor M.K., 2011. Emerging knowledge of regulatory roles of d-amino acids in bacteria. *Cellular and Molecular Life Sciences* 68: 817-831.

Corrigan J.J. 1969. D-amino acids in animals. *Science* 164:142-149.

Friedman F., 2010. Origin, Microbiology, Nutrition, and Pharmacology of D-Amino Acids. *Chemistry & Biodiversity* 7: 1491-1530.

Glavin D.P., Dworkin J.P., Aubrey A., Botta O., Doty III J.H., Martins Z., Bada J.L., 2006. Amino acid analyses of Antarctic CM2 meteorites using liquid chromatography-time of flight-mass spectrometry. *Meteoritics & Planetary Science* 41: 889-902.

Glavin D.P., Elsila J.E., Burton A.S., Callahan M.P., Dworkin J.P., Hilts R.W., Herd C.D.K., 2012. Unusual nonterrestrial l-proteinogenic amino acid excesses in the Tagish Lake meteorite. *Meteoritics & Planetary Science* 47: 1347-1364.

Guillarme D., Ruta J., Rudaz S., Veuthey J.-L., 2010. New trends in fast and high-resolution liquid chromatography: a critical comparison of existing approaches. *Analytical and Bioanalytical Chemistry* 397: 1069-1082.

Gyimesi-Forrás K., Leitner A., Akasaka K., Lindner W., 2005. Comparative study on the use of ortho-phthalaldehyde, naphthalene-2,3-dicarboxaldehyde and anthracene-2,3-dicarboxaldehyde reagents for α-amino acids followed by the enantiomer separation of the formed isoindolin-1-one derivatives using quinine-type chiral stationary phases. *Journal of Chromatography A* 1083: 80-88.

Hamase K., Morikawa A., Etoh S., Tojo Y., Miyoshi Y., Zaitsu K., 2009. Analysis of Small Amounts of D-Amino Acids and the Study of Their Physiological Functions in Mammals. *Analytical Sciences* 25: 961-968.

Hanczkó R., Kutlán D., Tóth F., Molnár-Perl I., 2004. Behavior and characteristics of the o-phthaldialdehyde derivatives of n-C6–C8 amines and phenylethylamines with four additive SH-containing reagents. *Journal of Chromatography A* 1031: 51-66.

Kolodkin-Gal I., Romero D., Cao S., Clardy J., Kolter R., Losick R., 2010. d-Amino Acids Trigger Biofilm Disassembly. *Science* 328: 627-629.

Kutlan D., Prestits P., Molnar-Perl I., 2002. Behavior and characteristics of amine derivatives obtained with o-phthaldialdehyde/3-mercaptopropionic acid and with o-phthaldialdehyde/N-acetyl-l-cysteine reagents. *Journal of Chromatography A* 949:

235-248.

Lam H., Oh D-C., Cava F., Takacs C.N., Clardy J., Pedro M.A. de., Waldor M.K., 2009. D-Amino Acids Govern Stationary Phase Cell Wall Remodeling in Bacteria. *Science* 325: 1552-1555.

Lamzin V. S., Dauter Z., Wilson K. S., 1995. How nature deals with stereoisomers. *Current Opinion in Structural Biology* 5: 830-836.

Mengerink Y., Kutlán D., Tóth F., Csámpai A., Molnár-Perl I., 2002. Advances in the evaluation of the stability and characteristics of the amino acid and amine derivatives obtained with the o-phthaldialdehyde/3-mercaptopropionic acid and o-phthaldialdehyde/N-acetyl-l-cysteine reagents: High-performance liquid chromatography–mass spectrometry study. *Journal of Chromatography A* 949: 99-124.

Min J.Z., Hatanaka S., Yu H., Higashi T., Inagakia S., Toyo'okaa T., 2010. First detection of free D-amino acids in human nails by combination of derivatization and UPLC-ESI-TOF-MS. *Analytical Methods* 2: 1233-1235.

Miyoshi Y., Koga R., Oyama T., Han H., Ueno K., Masuyama K., Itoh Y., Hamase K. 2012. HPLC analysis of naturally occurring free d-amino acids in mammals. *Journal of Pharmaceutical and Biomedical Analysis* 69: 42-49.

Oláh E., Fekete S., Fekete J., Ganzler K., 2010. Comparative study of new shell-type, sub-2 μm fully porous and monolith stationary phases, focusing on mass-transfer resistance. *Journal of Chromatography A* 1217: 3642-3653.

Visser W.F., Verhoeven-Duif N.M., Ophoff R., Bakker S., Klomp L.W., Berger R., Koning T.J. de., 2011. A sensitive and simple ultra-high-performance-liquid chromatography–tandem mass spectrometry-based method for the quantification of d-amino acids in body fluids. *Journal of Chromatography A* 1218: 7130-7136.

Wu G., 2009. Amino acids: metabolism, functions, and nutrition. *Amino Acids* 37: 1-17.

5
D-tryptophan from probiotic bacteria influences the gut microbiome and allergic airway disease

Published as: Juliano Fonseca, Inge Kepert, Constanze Müller, Katrin Milger, Kerstin Hochwind, Matea Kostric, Maria Fedoseeva, Caspar Ohnmacht, Stefan Dehmel, Petra Nathan, Sabine Bartel, Oliver Eickelberg, Michael Schloter, Anton Hartmann, Philippe Schmitt-Kopplin, and Susanne Krauss-Etschmann. Journal of Allergy and Clinical Immunology 2017; 139: 1525-35. © 2016 Published by Elsevier Inc. on behalf of the American Academy of Allergy, Asthma & Immunology.

Author contributions

This research project started with the work performed by Juliano Fonseca, Inge Kepert and Kerstin Hochwind under the supervision of Philippe Schmitt-Kopplin, Susanne Krauss-Etschmann and Anton Hartmann in their respective research groups and laboratories.
Juliano Fonseca designed and established the chromatographic fractionation workflow applied to cell culture supernatants using SPE and ultra-high performance liquid chromatography. Juliano Fonseca performed the isolation, purification and chemical characterizantion of the bioactive compound, and promoted the theory that D-Trp was the bioactive candidate encouraging further investigation.
Inge Kepert established and performed all in vitro immunomodulatory screening assays in which bioactivity of crude cell culture supernatants and synthetic D-Trp was tested.
Kerstin Hochwind studied the growth behavior of strains and selected the most suitable cultivation medium to perform the experiements, matching the needs of both bioassay and mass spectrometry analysis regarding medium composition.
Other co-authors fruther contributed to the study by performing experiments in mice, i.e., *in vivo* oral administration of D-Trp, evaluation of allergic airway inflammation, study of intestinal microbial diversity, and further T-cell differentiation assays in vitro to support the findings *in vivo*.

Juliano and Inge took the lead and wrote the first manuscript (shared co-first authorship). All other co-authors participate in further drafts, writing and revising it critically for important intellectual content until its final version.

The study was supported by grants provided by the Helmholtz Center Munich, the German Research Center for Environmental Health, Research Center Borstel, and the Leibniz Center for Medicine and Biosciences. Probiotic bacteria were provided by Winclove Bioindustry BV, The Netherlands; Chr. Hansen, Horsholm, Denmark; Daniscom Niebüll, Germany; and Ardeypharm GMbH, Herdecke, Germany. None of the providers had any influence on the design, analyses, or interpretation of the study.

This chapter fully reproduces the content of the publication, but few adaptations were done to align with the format of this thesis.

Abstract

Chronic immune diseases, such as asthma, are highly prevalent. Currently available pharmaceuticals improve symptoms but cannot cure the disease. This prompted demands for alternatives to pharmaceuticals, such as probiotics, for the prevention of allergic disease. However, clinical trials have produced inconsistent results. This is at least partly explained by the highly complex crosstalk among probiotic bacteria, the host's microbiota, and immune cells. The identification of a bioactive substance from probiotic bacteria could circumvent this difficulty. Objective: we sought to identify and characterize a bioactive probiotic metabolite for potential prevention of allergic airway disease. Methods: probiotic supernatants were screened for their ability to concordantly decrease the constitutive CCL17 secretion of a human Hodgkin lymphoma cell line and prevent upregulation of costimulatory molecules of LPS-stimulated human dendritic cells. Results: supernatants from 13 of 37 tested probiotic strains showed immunoactivity. Bioassay-guided chromatographic fractionation of 2 supernatants according to polarity, followed by total ion chromatography and mass spectrometry, yielded $C_{11}H_{12}N_2O_2$ as the molecular formula of a bioactive substance. Proton nuclear magnetic resonance and enantiomeric separation identified D-tryptophan. In contrast, L-tryptophan and 11 other D-amino acids were inactive. Feeding D-tryptophan to mice before experimental asthma induction increased numbers of lung and gut regulatory T cells, decreased lung T_H2 responses, and ameliorated allergic airway inflammation and hyperresponsiveness. Allergic airway inflammation reduced gut microbial diversity, which was increased by D-tryptophan. Conclusions: D-tryptophan is a newly identified product from probiotic bacteria. Our findings support the concept that defined bacterial products can be exploited in novel preventative strategies for chronic immune diseases (J. Allergy Clin. Immunol. 2017; 139:1525-35).

5.1 Introduction

Chronic immune diseases, such as allergies, inflammatory bowel disease, or diabetes, are highly prevalent in industrialized countries, and a further increase of burden caused by noncommunicable diseases is expected for the next decades (WHO, 2010). Currently available pharmaceuticals improve symptoms but cannot cure the disease. Accordingly, there is an increasing demand for proved alternatives to pharmaceutical products from both health care professionals and consumers (Jackson et al. 2014).

Probiotic bacteria have been shown to modify immune responses in vitro (Borthakur et al. 2010; Heuvelin et al. 2010; Mileti et al. 2009) and in animals (Kwon et al 2010; Fanning et al 2012) and are defined as ‘‘live microorganisms which when administered in adequate amounts confer a health benefit on the host’’. Accordingly, they have been proposed as an alternative to classical therapies for the treatment of immune diseases (FAO/WHO 2001). However, apart from acute infectious diarrhea (Allen et al. 2009) clinical trials for different indications, such as primary prevention of allergic diseases (see group of references: probiotics in clinical trials) or treatment of chronic inflammatory bowel disease (Butterworth et al. 2008) were highly inconsistent. Accordingly, a consensus paper (Fiocchi et al. 2012) and the European Food Safety Authority (EFSA 2010) stated that a role for probiotic microbes for prevention of allergic manifestations is not established.

One important reason for the conflicting results is most likely the complexity of the reciprocal crosstalk between probiotic bacteria and the host’s microbiota and immune cells. Even in healthy subjects, the gut microbiome differs remarkably among individual patients (Arumugam et al. 2011; van Baarlen et al. 2011). In addition, both the microbiome and immunity can be substantially altered under disease conditions (Candela et al. 2012). Thus, it is hard to predict the precise functionality of a probiotic strain in individual patients. In addition, there is a lack of mechanistic understanding that is important to establish biological plausibility for any claimed health effect.

The use of specified substances derived from probiotic microbes could provide an attractive alternative to overcome these problems. Other than living bacteria with complex fates and response patterns in the host, they should have definable properties with a provable mode of action. Thus far, only very few candidate structures or substances have been demonstrated as bioactive agents and even less with preclinical evidence for therapeutic effects (Yan et al. 2011).

Therefore, the aim of the present study was (1) to establish a screening tool for the detection of T_H2-decreasing immune activity in probiotic supernatants, (2) to identify a soluble bacterial molecule that mediates this activity, (3) to test the putative substance in a mouse model of allergic airway disease (AAI), and (4) to obtain insight into potential underlying mechanisms.

5.2 Methods

For detailed information on reagents, culture conditions of bacteria and human cells, generation of human monocyte-derived dendritic cells (DCs), structural elucidation of D-tryptophan (Sigma-Aldrich, St Louis, Mo), cytokine/chemokine quantification, murine T-cell differentiation, flow cytometry, quantitative RT-PCR, microbiota analysis, isolation of intestinal lamina propria cells, and animal experiments (induction of experimental asthma and lung function analyses), see Supplementary Information section.

5.3 Bacterial strains

Bifidobacteria, lactobacilli, lactococci, Escherichia coli Nissle 1917, *Enterococcus faecium*, and *Streptococcus thermophilus* were obtained from different providers (see Table E1). All strains were grown until stationary phase and a minimum cell number of 10^8 colony-forming units/mL. Cell-free supernatants were obtained by means of centrifugation (at 6000 rpm for 5 minutes at 20°C), followed by filtration through a 0.220 μm pore size surface-modified Polyethersulfone Membrane (Millipore, Darmstadt, Germany). No bacterial growth was observed when aliquots from supernatants were cultured in bacterial growth medium. Otherwise, supernatants were stored immediately after collection in aliquots at –80 °C until further use.

5.4 Bioassays for screening for immunomodulatory activity in probiotic supernatants

Two biological assays based on downmodulation of costimulatory molecules on human DCs and of CCL17 secretion by a human Hodgkin lymphoma T-cell line (KM-H2) were set up. Human immature DCs were matured with 0.1 μg/mL LPS from E coli (Sigma-Aldrich) in the presence or absence of 200 μL of bacteria-free supernatants for 24 hours, followed by flow cytometric analysis of costimulatory molecules.

Similarly, 200 µL supernatants were added to 3 to 5 x 10^6 KM-H2 cells for 24 hours. Supernatants were collected from KM-H2 cells by means of centrifugation and stored at -80 °C until quantification of CCL17. The corresponding amount of blank MRS medium was added to control for the dilution of KM-H2 culture medium with different volumes of bacterial supernatants. Blank bacterial growth medium and supernatants from Lactobacillus rhamnosus DSM 20021, which has no probiotic activity, were used as negative controls in both screening assays.

5.5 Animals and oral supplementation with D-tryptophan

All animal experiments were conducted under the Federal Guidelines for the Use and Care of Laboratory Animals (Az 55.2-1-54-2532-137-13) and approved by the Government of the District of Upper Bavaria and Schleswig- Holstein (V244-13313/2016 [7-1/10]). Six- to 8-week-old female BALB/c mice were obtained from Charles River (Sulzfeld, Germany) and housed in individually ventilated cages, with 2 mice each maintained in specific pathogen-free conditions. A standard extruded pellet diet and sterile filtered drinking water were provided *ad libitum*. For quantification of D-Tryptophan in mouse sera, D-Tryptophan was dissolved in drinking water at concentrations of 1.8 or 18 mg/dL (approximately 0.09 and 0.9 mg/d per mouse). Control animals received pure water (n=8 per group). No changes in behaviour or body weight were noted in the supplemented animals compared with control animals. Animals were killed after 14 days, and sera were immediately stored at -80 °C until analysis.

For testing prevention of AAI, mice received 50 mmol/L D-Tryptophan starting at least 3 days before the first sensitization until death on day 25. For microbiome analyses, the cecum was cut off and immediately stored at -80 °C until further processing.

5.6 Statistical analyses

5.6.1 Bioassays and animal experiments

Results of bioassays and animal experiments are presented as means with SDs. The Student *t* test with the Dunn multiple comparison test or 2-way ANOVA with the Bonferroni posttest was used, where appropriate. Tests applied are presented in the respective figure legends. *P* values of less than 0.05 were considered significant (version 5.0; GraphPad Prism Software, La Jolla, California).

5.6.2 Microbial diversity

Bacterial diversity was assessed by means of molecular barcoding of 16S rRNA genes in cecum samples of 6 animals per group. To this end, DNA was directly extracted from the cecum by using a kit-based protocol (PowerSoil DNA Isolation Kit; MO BIO Laboratories, Carlsbad, Calif). Fragments of 315 bp were amplified within the variable regions V5 and V6 of the 16S rRNA gene by using S-D-Bact-0785-a-S-18 (5'-GGMTTAGATACCCBDGTA-3') and S-*-Univ-1100-a-A-15 (5' GGGTYKCGCTCGTTR-3') as primers (Klindworth et al. 2013). Sequencing of amplicons was performed on the Illumina MiSeq platform (Illumina, San Diego, California) by using paired-end technology (see supplementary information). Sequences were deposited in National Center for Biotechnology Information accession no. PRJNA304109.

Reads were analysed with the software package QIIME (http://qiime.org). Operational taxonomic units (OTUs) were picked within the 13_8 version of the Greengenes reference database (McDonald et al. 2012) at a similarity level of 95% sequence identity. Sequences were subsampled to 15,000 reads per sample, which reflects the number of reads obtained in the sample with the lowest number of reads after quality control. This number was still sufficient to reach a plateau when collectors' curves were calculated based on of OTU_{95}. The taxonomy assignment was done with the RDP classifier 2.2 (Wang et al. 2007). Principal coordinate analysis was generated on the unweighted UniFrac distance matrix by using the ape package within the R software environment (http://www.r-project.org), and statistical significance was determined with the Student *t* test. The α-diversity of each sample was measured by using the Chao1 metric (Chao 1984) and compared between treatments by using the nonparametric 2-sample *t* test (i.e., with Monte Carlo permutations for significance testing). ß-Diversity was calculated by using the phylogenetic method UniFrac (Lozupone 2005). The nonparametric analysis of similarity was performed to examine the ß-diversity distance matrix for significant differences between groups of samples; differences in OTU abundance between groups were tested for significance by means of nonparametric ANOVA.

5.7 Results

5.7.1 Identification and characterization of a bioactive probiotic substance

5.7.1.1 Screening of crude probiotic supernatants for downregulation of CCL17

To develop a high-throughput screening system for the detection of T_H2-downregulatory activity in supernatants from probiotic bacteria, we made use of high constitutive secretion of the T_H2-associated CCL17 by the human Hodgkin lymphoma T-cell line KM-H2.

KM-H2 cells were incubated with increasing volumes of supernatants from *Lactobacillus rhamnosus* GG (LGG), *Bifidobacterium* BB-420, and *Lactobacillus casei* W56 to identify the threshold for downregulation of CCL17. Supernatants from all 3 probiotic strains led to a significant dose- and timedependent reduction of CCL17 concentrations to approximately 30% relative to supernatant from the nonprobiotic *Lactobacillus rhamnosus* DSM-20021 (**Figure 5.1**). The minimum volume (200 µL) leading to that reduction was used in all subsequent experiments.

Because the numerous ingredients of the bacterial culture medium interfered with the detection of specific signals in mass spectrometry, the bacteria were cultivated in less complex, chemically defined medium (CDM1). The potency of supernatants from probiotic strains cultivated in CDM1 versus standard medium to decrease CCL17 concentrations was comparable. Subsequent testing of supernatants from 37 probiotic strains revealed that 7 of 21 *Lactobacillus* species strains, 5 of 10 *Bifidobacterium* species strains, and 1 of 3 *Lactococcus* species strains decreased CCL17 secretion without affecting cell viability. In contrast, none of the *Streptococcus thermophilus*, *Enterococcus faecium*, or *E coli* Nissle 1917 strains influenced CCL17 levels.

5.7.1.2 *Verification of results from CCL17-based screening assays*

To confirm the observed immunomodulatory activity, we evaluated the efficacy of probiotic supernatants to decrease the expression of costimulatory molecules on human monocytederived DCs. On recognition of antigen, naive DCs undergo a complex maturation process (Banchereau and Steinman 1998). Although fully activated DCs induce adaptive immune responses, incomplete activation leads to tolerance (Probst et al. 2014). Therefore, we screened for reduced expression of costimulatory molecules in the presence of probiotic supernatants. All 13 supernatants that had already been preidentified as

‘‘immunomodulatory’’ in the CCL17-based screen also significantly decreased the percentages of LPS-induced CD83-, CD80-, CD86-, and CD40-expressing mature DCs, whereas the remaining supernatants were inactive on DCs (**Figure 5.1**). None of the supernatants affected the viability of DCs. Thus, both bioassays produced 100% concordant results. For a complete overview of the bioactivity of all strains, see Suppl. **Table S 4**.

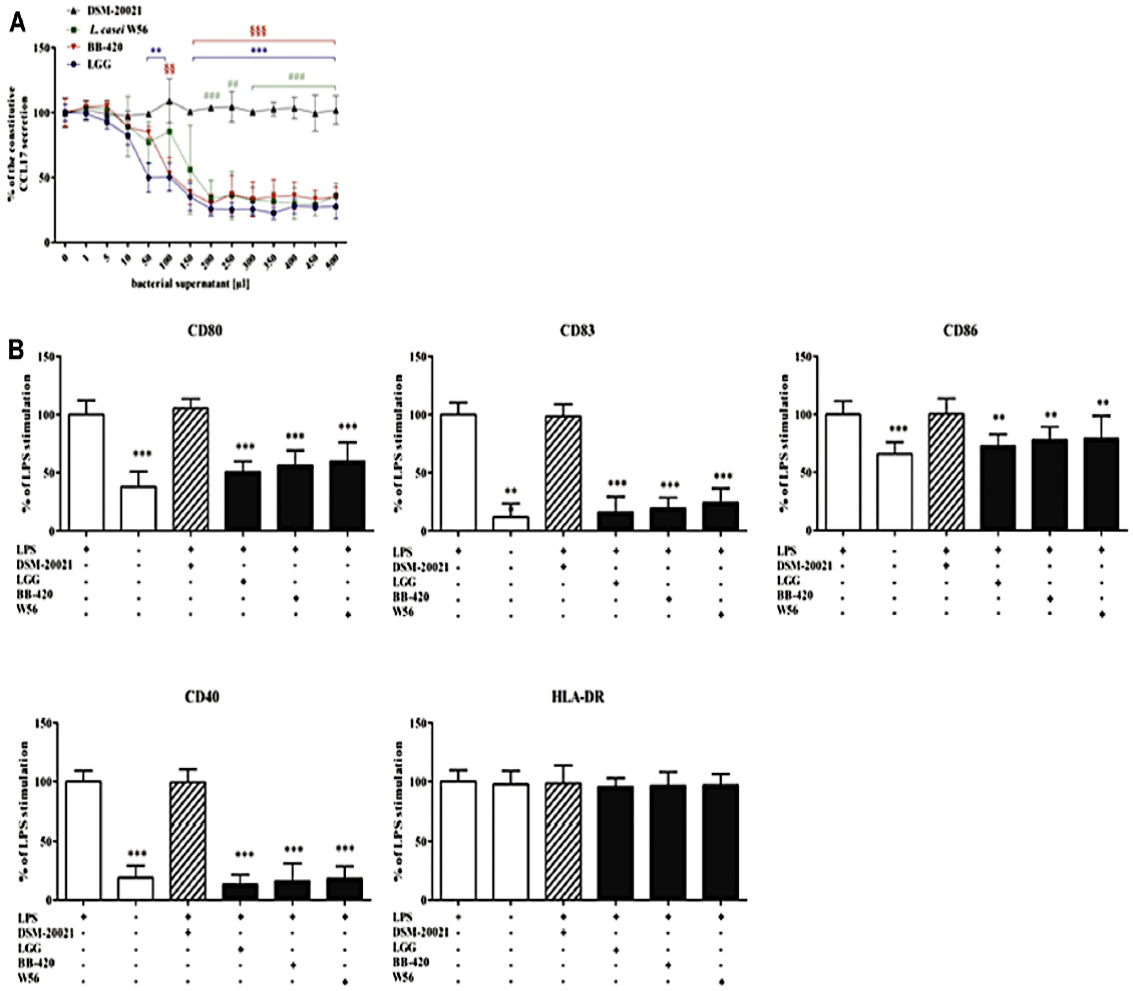

Figure 5.1. Screening of supernatants from different probiotic strains for immune activity on human cells. (A) Dose-dependent capacity of bacterial supernatants from LGG (*fx1*), *Bifidobacterium* BB-420 (*fx2*), and *Lactobacillus casei* W56 (*fx3*) to lower CCL17 secretion of human Hodgkin lymphoma KM-H2 cells. The negative control was nonprobiotic *Lactobacillus rhamnosus* DSM-20021 (*fx4*). Three independent experiments in duplicates are shown (mean ± SD percentages relative to CCL17 secretion of untreated KM-H2 cells). LGG: $^{**}P < .005$ and $^{***}P < .0005$, *L casei* W56: $\#\#P < .005$, $\#\#\#P < .0005$, BB-420: §§$P < .005$, §§§$P < .0005$, Student *t* test. (B) Capacity of supernatants from LGG, *Bifidobacterium* BB-420, *Lactobacillus casei* W56, or nonprobiotic *Lactobacillus rhamnosus* DSM-20021 to prevent full upregulation of costimulatory molecules and HLA-DR on LPS-stimulated human monocyte-derived DCs. +/-, With/without bacterial supernatant. Five independent experiments are shown (mean ± SD percentages relative to LPS alone). $^{**}P < .01$ and $^{***}P < .001$, Dunn multiple comparison test.

5.7.1.3 Fractionation of selected probiotic supernatants yields 3 bioactive fractions of different polarity.

LGG has been most frequently used in clinical studies (NHI, ClinicalTrials.gov) Therefore we selected supernatants from LGG and further supernatants of *L. casei* W56 for further enrichment and stepwise chemical characterization of the putative metabolite. During this procedure, each sub-fraction was retested for bioactivity in both the KM-H2 and DC bioassays.

Bacterial supernatants were subjected to semi-preparative chromatography, yielding 11 MeOH/H_2O extracts. The highest immunomodulatory activity was found in the 20% fraction, along with slightly lower activities in the 40% and 50% MeOH fractions (**Figure 5.2**). Therefore, we chose this fraction for further purification.

5.7.1.4 Isolation and identification of the bioactive substance in 20% MeOH/H_2O extracts

Chromatographic sub-fractionation of the 20% MeOH/H_2O fraction yielded 10 sub-fractions (**Figure 5.3**), 3 of which showed activity in bioassays. These sub-fractions and their closest neighbours were re-evaluated by means of reverse-phase; ultra performance liquid chromatography coupled to high-resolution time-of flight mass spectrometry to generate total ion chromatograms. By identifying similarities in the chromatograms, we identified a substance that, according to peak retention time and molecular mass information, was only present in the bioactive sub-fractions, being highest in sub-fraction 7 from *L. casei* W56 and sub-fraction 6 from LGG. The extracted mass spectrum strongly suggested that this substance was composed of the tryptophan ions $(2M+H)^+$ and $(M+H)^+$ and its fragment, $(M+H-NH_3)^+$ (see **Figure 3.4** in Chapter 3).

After careful enrichment of the bioactive substance by repeated chromatography runs, the isolated candidate substance of both strains showed bioactivity in both screening assays. High-resolution mass spectrometric analyses by using Fourier transform ion cyclotron resonance mass spectrometry confirmed $C_{11}H_{12}N_2O_2$ as the molecular formula of these ions (see **Figure 3.5** in Chapter 3). Further analyses by using proton nuclear magnetic resonance provided detailed information on the functional group distribution and molecular structure: the doublets and triplets (δ7.8-7.0) showed the occurrence of an indole ring. Resonance signals at the region of δ3.9-3.8 and δ 3.2-3.1 could also be assigned to ß-CH and α-CH

protons, respectively (see **Figure 3.6** in Chapter 3). Thus, there was a close agreement between standard tryptophan and our bioactive sub-fraction.

Because L-tryptophan is a standard component of the bacterial growth medium, we hypothesized that the bioactivity is related to the D-form of this amino acid. Indeed, enantiomeric separation of the purified sub-fraction confirmed the presence of D- and L-tryptophan, whereas the corresponding sub-fraction of blank medium contained only L-tryptophan (see **Figure 3.7** in Chapter 3).

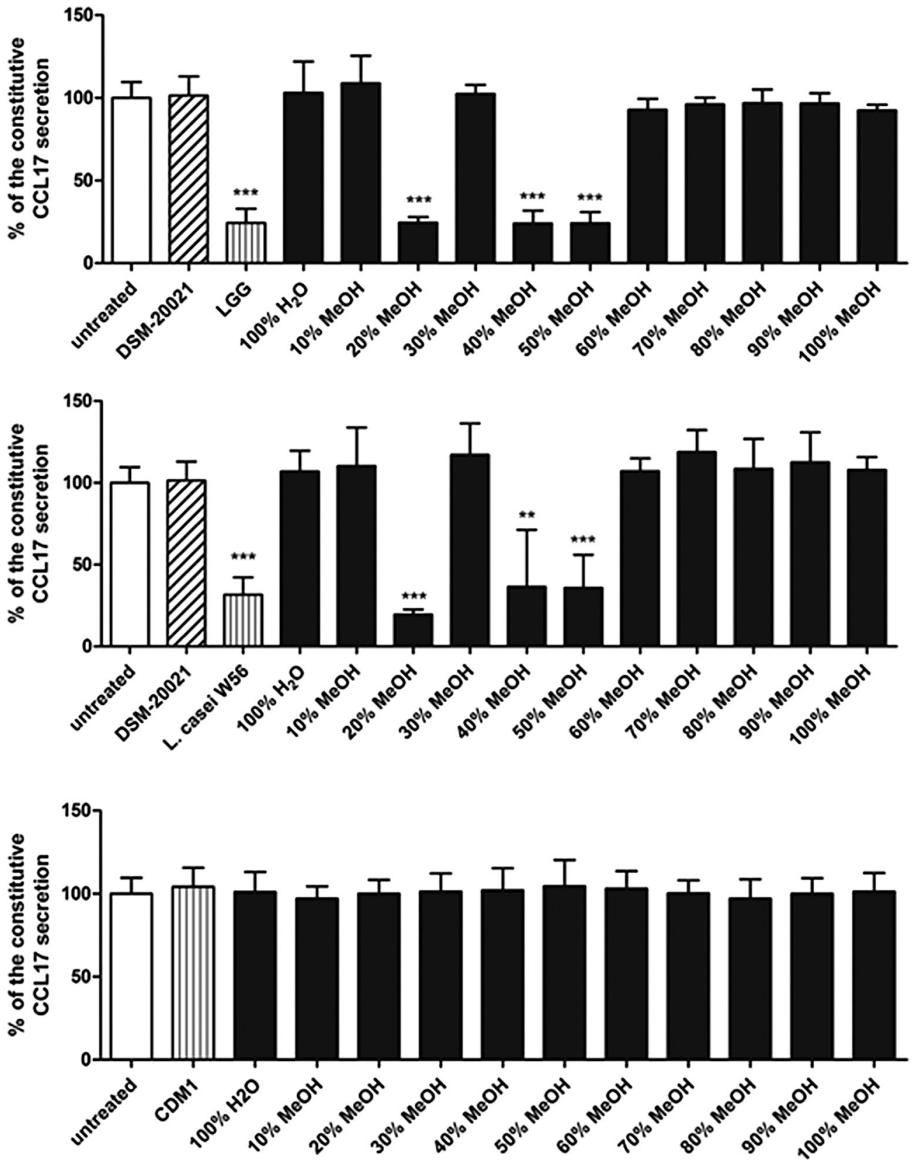

Figure 5.2. Capacity of subfractions of probiotic supernatants to decrease CCL17 secretion in KM-H2 cells. Subfractions with different polarity (MeOH/H_2O gradient chromatography) from supernatants of LGG (top) or *Lactobacillus casei* W56 (middle). Negative controls were nonprobiotic DSM-20021 and blank CDM1 medium (bottom). Three independent experiments in duplicates are shown (mean ±SD percentages relative to constitutive CCL17 secretion of untreated KM-H2 cells). $^{**}P < .005$ and $^{***}P < .0005$, Student *t* test.

Segment	Set Start Time (min)	Duration (min)
1	1.00	1.40
2	3.00	0.70
3	3.70	0.70
4	4.40	0.20
5	4.60	0.90
6	5.50	1.50
7	7.00	1.00
8	8.00	1.00
9	9.00	1.00
10	10.00	2.00

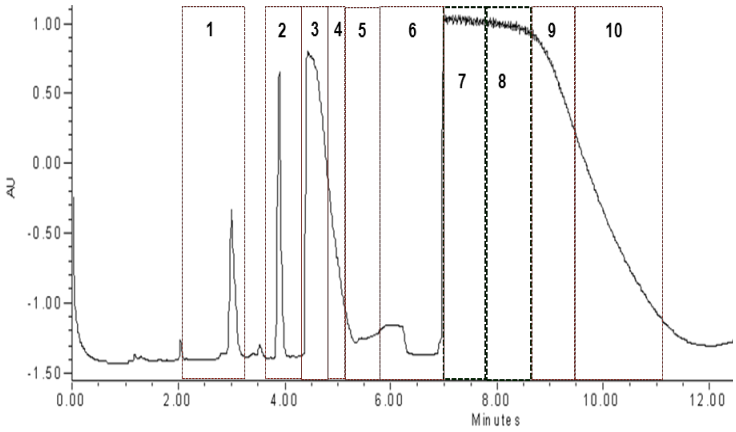

Figure 5.3. UPLC-PDA chromatogram of 20% MeOH/H_2O extract from *L. casei* W56 supernatant. Sub-fractions and their time of collection were decided based on the peaks observed in the chromatogram. Immune modulatory activity was observed for sub-fractions 7, 8 and 9. Chromatographic conditions: Kinetex PFP column 1.7 µm particle size, 2.1 x 150 mm. Nonlinear gradient in 10 min from 5 to 25% B, 14 min to 100% B at 40 °C and 0.180 mL/min flow rate (Mobile phase A: 10% MeOH/H_2O and B: 100% MeOH).

5.7.1.5 Immunomodulatory activity in probiotic supernatants is restricted to the D-form of tryptophan.

To verify whether bioactivity was indeed restricted to the D-isomer of tryptophan, we tested different concentrations of synthetic L- and D-tryptophan in the CCL17 bioassay. Only D-tryptophan showed dose-dependent immune activity (**Figure 5.4**). Moreover, none of 12 other polar and nonpolar neutral D-amino acids tested showed any bioactivity (Suppl. **Table S** 5).

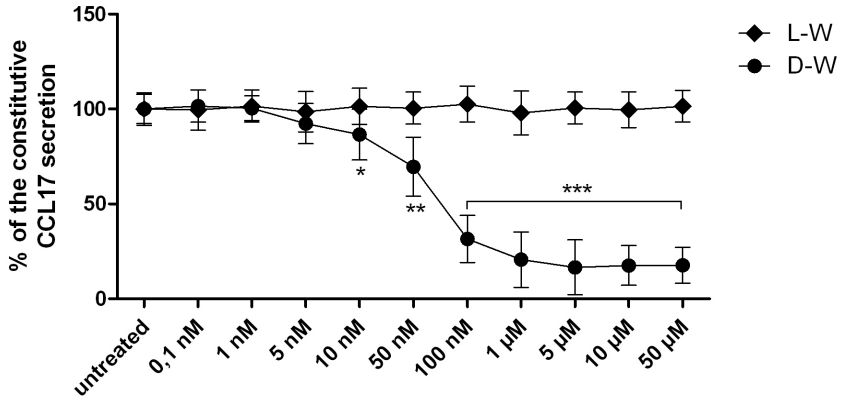

Figure 5.4. Effect of tryptophan L- and D-isomers on CCL17 secretion by KM-H2 cells. KM-H2 cells were stimulated with different concentrations of synthetic L- and D-isomers of tryptophan followed by CCL17 quantification in KM-H2 culture medium after 24 hours. Circles, D-tryptophan; diamonds, Ltryptophan. Three independent experiments in duplicates are shown (mean ± SD percentages relative to constitutive CCL17 secretion of untreated KM-H2 cells). **P* < .05, ***P* < .005, and ****P* < .0005, Student *t* test.

5.7.1.6 Bacterial supernatants and D-tryptophan modulate cytokine profiles of enriched human DCs.

To obtain a first insight into mechanisms underlying this bioactivity, we quantified the cytokines secreted by highly enriched DCs after treatment with the bacterial supernatants or synthetic D-tryptophan. All probiotic supernatants and D-tryptophan strongly induced IL-10 and decreased LPS-induced IFN-g, IL-12, and IL-5 in these cultures. In contrast, cytokine patterns were unaffected by the control supernatants and amino acids (Suppl. Table S 6). Overall, this resulted in increased IL-10/IL-12 ratios and, with the exception of BB-46, in decreased IL-5/IFN-g ratios.

5.7.2 Preclinical effects of oral D-tryptophan supplementation

5.7.2.1 D-tryptophan influences allergic airway inflammation and TH2 immune responses.

If it is to be used as an oral intervention in patients with allergic diseases, D-tryptophan needs to be absorbed from the gut. Oral supplementation of mice with 0.9 mg/d D-tryptophan increased D-tryptophan serum levels significantly (Suppl. **Figure S 1, A**), indicating enteric uptake and systemic distribution. Pretreatment of mice with D-tryptophan for 3 days and throughout experimental ‘‘asthma’’ induction decreased numbers of total bronchoalveolar lavage fluid cells, which was mainly caused by a reduction in eosinophil numbers (Suppl. **Figure S 1, B and C**). Furthermore, this supplementation improved airway hyperreactivity to methacholine (Suppl. **Figure S 1, D**). Because this suggested an involvement of T_H2 responses, we analysed lung T cells: D-tryptophan reduced Il-4–producing T cells and Il-4 levels in bronchoalveolar lavage fluid (trend, Suppl. **Figure S 1, E and F**, and **Figure S 4**) but not Ifn-g-producing T_H1 cells. Furthermore, D-tryptophan treatment significantly increased Helios-positive regulatory T (Treg) cell numbers, whereas total forkhead box p3 $(Foxp3)^+$ cell numbers remained unchanged (Suppl. **Figure S 1, G**).

To further substantiate these *in vivo* findings, we performed T-cell differentiation assays in vitro. In line with the *in vivo* observations, D-tryptophan reduced T_H2 cell differentiation, whereas T_H1 differentiation remained unaffected (Suppl. **Figure S 3, A and B**, and Suppl. **Figure S 4, A**). Consequently, *Il4* and *Gata3* expression and Il-13 secretion were reduced, whereas *Ifng* expression remained unaffected. However, Treg cells showed increased *Foxp3* expression on mRNA and protein levels (Suppl. **Figure S 3, C**, and see **Figure S 4, B**).

5.7.2.2 D-tryptophan induces gut Treg cells and increases intestinal microbial diversity in allergic airway inflammation.

In addition to the observed pulmonary immune response, the frequency of $Foxp3^+$ T cells was locally increased in the colons of supplemented mice with AAI compared with nonsupplemented mice with AAI (Suppl. **Figure S 5, A**). Altered gut immunity might be driven directly by D-tryptophan and/or indirectly through altered gut microbiota.

A diversity analysis of bacteria by 16S rRNA–based barcoding demonstrated a strongly reduced community richness and diversity at the level of OTU_{95} in mice with AAI (Suppl. **Figure S** 5**, B**). Supplementation with D-tryptophan increased the bacterial diversity of AAI mice, resulting in comparable α-diversity patterns compared with those of healthy animals. Although the original diversity was not completely restored after D-tryptophan application, its effect on microbial community composition was significant (Suppl. **Figure S 6**).

Independent of the health status of the animals' D-tryptophan supplementation, all samples were dominated by the phyla Bacteroidetes and Firmicutes (19.4% to 27.7% and 65.9% to 78.4% of the total sequences). As expected, the phylum Firmicutes mainly consisted of members of the order Clostridiales. Other phyla, including Actinobacteria and Proteobacteria, were also present, although at significantly lower abundance. At the family level, Lachnospiraceae, Odoribacteraceae, Rikenellaceae, Ruminococcaceae, S24-7, and an unclassified bacterial family belonging to the Clostridiales (Suppl. **Figure S 6, B**) dominated. The latter was mainly present in mice with AAI, forming 58.6% of the total community. However, Lachnospiraceae were less abundant in animals with AAI (5.5%) compared with control animals (13.7%), D-tryptophan–treated mice with AAI (20.6%), or D-tryptophan treated mice without AAI (27.5%). Odoribacteraceae were strongly affected by D-tryptophan because their relative abundance tripled in both groups of supplemented animals (3.9% vs approximately 1.1%). In contrast, Rikenellaceae showed a decreased abundance in the D-tryptophan groups (1.1% to 2.0%) compared with the control groups (4.6% to 7.7%). Interestingly, Ruminococcaceae, which were strongly reduced in the control mice affected with AAI (3.7%) recovered through application of D-tryptophan (8.9%): this was comparable with abundance in the control group of mice without AAI. Members of the S24-7 family were affected by neither AAI nor application of D-tryptophan. Overall, D-tryptophan supplementation increased intestinal bacterial diversity in D-tryptophan–treated mice with AAI, such that the bacterial diversity pattern was more comparable with healthy control mice (PBS/PBS; Suppl. **Figure S 5, B**). Thus, our results suggested that D-

tryptophan treatment re-establishes a healthy microbial community genotype in mice with AAI.

5.8 Discussion

In the present work, for the first time, we identified D-tryptophan as a bacterial substance produced by the probiotic strains LGG and *L casei* W56. We demonstrate that D-tryptophan decreases the production of T_H2 cytokines and chemokines in human peripheral and murine immune cells and, more importantly, prevents full development of AAI when fed to mice. Aside from immune modulation, this can occur also through maintenance of a diverse gut microbiota, which was otherwise lost in animals with experimental asthma.

Probiotic bacteria have been shown to modify immune responses in vitro (Borthakur et al. 2010; Heuvelin et al. 2010) and in animal studies (Mileti et al. 2009; Kwon et al. 2010) but clear evidence for clinical efficacy in the treatment of chronic inflammatory disorders is largely lacking. Because the reciprocal interaction of probiotic bacteria with the host's microbiota and immune system is extremely complex, use of defined small substances with a predictable mode of action might provide an interesting alternative for prevention of allergic disease in subjects at risk.

D-amino acids are nonproteinogenic enantiomers of L-amino acids. Until the discovery of free D-aspartate and D-serine in the mammalian brain as neurotransmitters in the late 1980s, D-amino acids were considered to play no role in higher organisms. Thus far, research on D-amino acids in mammals has been mainly restricted to the nervous system because of the relative abundance of D-aspartate and D-serine in the brain (Hashimoto et al. 1993) and the difficulty of detecting D-amino acids at trace levels (Visser et al. 2011). Thus, very little is known on D-tryptophan uptake (Lopez-Burillo et al. 1985) and metabolism in human subjects (Langner & Berg 1955), and it has been assumed that higher organisms use D-tryptophan poorly (Triebwasser et al. 1976). By developing highly sensitive assays, we demonstrated systemic distribution of D-tryptophan in mice after oral uptake.

In contrast to higher organisms, numerous bacteria, including probiotic bacteria, produce D-amino acids, such as D-glutamate and D-alanine, by using them mainly for cross-linking glycan chains in the peptidoglycan wall (Cava et al. 2011; Lam et al. 2009)

The regulation of bacterial L-tryptophan biosynthesis and degradation is well known (Yanofsky 2007). A role for D-tryptophan in bacterial communication was only recently discovered by demonstrating its requirement for disassembly biofilms in *Bacillus subtilis*

(Kolodkin-Gal 2010). Other soluble substances produced by probiotic bacteria are less investigated thus far (Heuvelin et al. 2010; Thomas et al. 2007).

Human subjects are potentially exposed to microbially generated D-amino acids (Friedman 2010) because body surfaces and the environment harbor an abundant and high diversity of microbes (Human Microbiome Project Consortium 2012). Similar to what has already been shown for acyl-homoserine lactones from gram-negative bacteria (Hooi et al. 2004; Smith et al. 2002; Richtie et al. 2003; Chhabra et al. 2003) means to recognize and interact with bacterial D-amino acids, including D-tryptophan, could have evolved.

This hypothesis is supported by several observations. First, human cells used in our bioassays responded to D-tryptophan but to neither L-Tryptophan nor any other tested D-amino acid.

Second, at least 2 surface receptors for D-tryptophan exist in human subjects: the G protein–coupled receptor GPR109B (Irukayama-Tomobe et al. 2009) is expressed on macrophages, monocytes, adipose tissue, and lung (Wise et al. 2003) and mediates attraction of neutrophils on binding of D-tryptophan or its metabolite, D-Kynurenine. Of note, when we extracted and analyzed published transcriptomic data (Kicic et al. 2010) GPR109B was significantly decreased in airway epithelial cells and T cells from patients with asthma as opposed to control subjects, indicating a potential role for this receptor in allergic disease.

The second receptor, solute carrier family 6 amino acid transporter member 14 (SLC6A14, alias $ATB^{0,+}$), transports D-tryptophan and 4 other D-amino acids across epithelial cells (Hatanaka et al. 2002). Because the receptor is expressed in the intestine, SLC6A14 is exposed to high microbial load and diversity. SLC6A14 is further expressed at exceptionally high levels in the fetal lung (based on our own data [see Fig E10 in the article's Online Repository at www.jacionline.org] and those of Su et al. (2004). The physiologic role of SLC6A14 in fetal life is unknown thus far. However, it is tempting to speculate a mechanistic link for prenatal intervention trials using probiotic bacteria.

Three enzymes, tryptophan 2,3-dioxygenase (TDO), indoleamine 2,3-dioxygenase (IDO) 1, and the more recently discovered IDO2, can metabolize tryptophan. Although tryptophan 2,3-dioxygenase is specific for L-tryptophan, IDO1 channels both D- and L-tryptophan into the kynurenine pathway. IDO activation leads to tryptophan depletion and thereby promotes peripheral tolerance (Munn & Mellor 2013), which contrasts our findings. However, IDO1 seems not to be important for the induction of immune tolerance in the airways but instead promotes T_H2 responses through effects on lung DCs (Xu et al. 2008), which we suggest could be counteracted by D-tryptophan. In addition, IDO2, which is also expressed on DCs

(Lob et al. 2008) and has slightly different substrate specificity, could further modulate D-tryptophan metabolism (Pantouris et al. 2014). Thus far, we concentrated on the 20% MeOH fraction for identification of the putative substance because this was the sub-fraction with the highest immunomodulatory activity and polarity. Bioactivity was further detected in the 40% and 50% MeOH fractions, holding the potential for the discovery of further small immunoactive substances. Our bioassays were designed to detect substances that induce a tolerogenic profile in DCs and decrease levels of the allergy-related chemokine CCL17. Therefore, it is possible that further immunoregulatory substances not related to allergic disease were overlooked.

D-tryptophan could influence immune homeostasis either directly, as shown in our screening assays, or indirectly by shifting the structure of the microbiome of the host. Apart from the observed immunomodulatory properties of D-tryptophan, we do not have direct mechanistic links explaining the altered gut microbiota or protection from AAI. However, in line with our own findings, Trompette et al. (2014) demonstrated that a change in the gut microbiota caused by dietary fermentable fibers induces production of metabolites involved in protection from AAI. These metabolites have further been associated with increased frequencies of $Foxp3^+$ Treg cells (Smith et al. 2013). The lung microbiota and a population of $Foxp3^+$ Treg cells have further been shown to protect neonatal mice from exaggerated type 2 immune responses in a murine model of house dust mice–induced AAI (Gollwitzer et al. 2014), which supports a role of both immune parameters also in adult mice.

In summary, for the first time, we identified that D-tryptophan acts as an immunomodulatory substance produced by probiotic strains. Our results suggest that tryptophan can potentially influence both immune responses and the constituents of intestinal microbiota and can conceivably reduce the degree of hyperactivity severity of AAI. In addition to immune modulation, this can occur through the maintenance of a diverse gut microbiota, which was otherwise lost in animals with AAI.

We conclude that bacteria-derived D-tryptophan can play a wider role in human health than previously thought. Overall, our findings support the concept that defined bacterial products can provide the basis for future development of preventive strategies for chronic inflammatory disorders.

5.9 References

Allen S.J., Martinez E.G., Gregorio G.V., Dans L.F., 2010. Probiotics for treating acute infectious diarrhoea. *Cochrane Database of Systematic Reviews* 11: CD003048.

Arumugam M., Raes J., Pelletier E., Le Paslier D., Yamada T., Mende D.R., et al., 2011. Enterotypes of the human gut microbiome. *Nature* 473: 174-80.

Banchereau J., Steinman R.M., 1998. Dendritic cells and the control of immunity. *Nature* 392: 245-52.

Borthakur A., Anbazhagan A.N., Kumar A., Raheja G., Singh V., Ramaswamy K., Dudeja P.K., 2010. The probiotic Lactobacillus plantarum counteracts TNF-{alpha}-induced downregulation of SMCT1 expression and function. *American Journal of Physiology-Gastrointestinal and Liver Physiology* 299: G928-34.

Butterworth A.D., Thomas A.G., Akobeng A.K., 2008. Probiotics for induction of remission in Crohn's disease. *Cochrane Database of Systematic Reviews* 3: CD006634.

Candela M., Rampelli S., Turroni S., Severgnini M., Consolandi C., De Bellis G., et al., 2012. Unbalance of intestinal microbiota in atopic children. *BMC Microbioly* 95: 2-9.

Cava F., de Pedro M.A., Lam H., Davis B.M., Waldor M.K., 2011. Distinct pathways for modification of the bacterial cell wall by non-canonical D-amino acids. *The EMBO Journal* 30: 3442-53.

Chao A., 1984. Nonparametric estimation of the number of classes in a population. *Scandinavian Journal of Statistics* 11: 265-70.

Chhabra S.R., Harty C., Hooi D.S., Daykin M., Williams P., Telford G. et al., 2003. Synthetic analogues of the bacterial signal (quorum sensing) molecule N-(3-oxododecanoyl)-L-homoserine lactone as immune modulators. *Journal of Medicinal Chemistry* 46: 97-104.

European Food Safety Authority 2010. EFSA delivers advice on further 808 health claims. EFSA in focus-food 8: 6-7. Available at: http://focalpointbg.com/images/stories/food01 11.pdf. Accessed in May 2018.

Fanning S., Hall L.J., Cronin M., Zomer A., MacSharry J., Goulding D., Motherway M. O´. et al., 2012. Bifidobacterial surface-exopolysaccharide facilitates commensal-host interaction through immune modulation and pathogen protection. *Proceedings of the National Academy of Sciences of the United States of America* 109: 2108-13.

FAO/WHO 2001. Evaluation of health and nutritional properties of probiotics in food including powder milk with live lactic acid bacteria. Available at: http://www.fao.org/3/a-a0512e.pdf. Accessed in May 2018.

Fiocchi A., Burks W., Bahna S.L., Bielory L., Boyle R.J., Cocco R., et al., 2012. Clinical Use of Probiotics in Pediatric Allergy (CUPPA): AWorld Allergy Organization position paper. *World Allergy Organ Journal* 5:148-67.

Friedman M., 2010. Origin, microbiology, nutrition, and pharmacology of D-amino acids. *Chemistry & Biodiversity* 7:1491-530.

Gollwitzer E.S., Saglani S., Trompette A., Yadava K., Sherburn R., McCoy K.D., et al., 2014. Lung microbiota promotes tolerance to allergens in neonates via PD-L1. *Nature Medicine* 20: 642-47.

Hashimoto A., Kumashiro S., Nishikawa T., Oka T., Takahashi K., Mito T., et al. 1993.

Embryonic development and postnatal changes in free D-aspartate and D-serine in the human prefrontal cortex. *Journal of Neurochemistry* 61: 348-51.

Hatanaka T., Huang W., Nakanishi T., Bridges C.C., Smith S.B., Prasad P.D., et al., 2002 Transport of D-serine via the amino acid transporter ATB(0,+) expressed in the colon. *Biochemical and Biophysical Research Communications* 291: 291-95.

Heuvelin E., Lebreton C., Bichara M., Cerf-Bensussan N., Heyman M., 2010. A Bifidobacterium probiotic strain and its soluble factors alleviate chloride secretion by human intestinal epithelial cells. *The Journal of Nutrition* 140: 7-11.

Hooi D.S.W., Bycroft B.W., Chhabra S.R., Williams P., Pritchard D.I., 2004. Differential immune modulatory activity of Pseudomonas aeruginosa quorum-sensing signal molecules. *Infection and Immunity* 72: 6463-70.

Human Microbiome Project Consortium 2012. Structure, function and diversity of the healthy human microbiome. *Nature* 486: 207-14.

Irukayama-Tomobe Y., Tanaka H., Yokomizo T., Hashidate-Yoshida T., Yanagisawa M., Sakurai T., 2009. Aromatic D-amino acids act as chemoattractant factors for human leukocytes through a G protein-coupled receptor, GPR109B. *Proceedings of the National Academy of Sciences of the United States of America* 106: 3930-34.

Jackson D.J., Hartert T.V., Martinez F.D., Weiss S.T., Fahy J.V., 2014. Asthma: NHLBI workshop on the primary prevention of chronic lung diseases. *Annals of the American Thoracic Society* 11(suppl 3): S139-45.

Kicic A., Hallstrand T.S., Sutanto E.N., Stevens P.T., Kobor M.S., Taplin C. et al. 2010. Decreased fibronectin production significantly contributes to dysregulated repair of asthmatic epithelium. *American Journal of Respiratory and Critical Care Medicine* 181: 889-98.

Klindworth A., Pruesse E., Schweer T., Peplies J., Quast C., Horn M., Glockner F.O., 2013. Evaluation of general 16S ribosomal RNA gene PCR primers for classical and next-generation sequencing-based diversity studies. *Nucleic Acids Research* 41: No 1 e1.

Kolodkin-Gal I., Romero D., Cao S., Clardy J., Kolter R., Losick R., 2010. D-amino acids trigger biofilm disassembly. *Science* 328: 627-29.

Kwon H-K., Lee C-G., So J-S., Chae C-S., Hwang J-S., Sahoo A., Nam J.H., Rhee J.H., Hwang K-C., Im S-H., 2010. Generation of regulatory dendritic cells and CD4+Foxp3+ T cells by probiotics administration suppresses immune disorders. *Proceedings of the National Academy of Sciences of the United States of America* 107: 2159-64.

Lam H., Oh D.C., Cava F., Takacs C.N., Clardy J., de Pedro M.A., et al., 2009. D-amino acids govern stationary phase cell wall remodeling in bacteria. *Science* 2009 325: 1552-55.

Langner R.R., Berg C.P., 1955. Metabolism of D-Tryptophan in the normal human subject. *Journal of Biological Chemistry* 214: 699-707.

Lob S., Konigsrainer A., Schafer R., Rammensee H.G., Opelz G., Terness P., 2008. Levobut not dextro-1-methyl tryptophan abrogates the IDO activity of human dendritic cells. *Blood* 111: 2152-54.

Lopez-Burillo S., Garcıa-Sancho J., Herreros B., 1985. Tryptophan transport through transport system T in the human erythrocyte, the Ehrlich cell and the rat intestine. *Biochimica et Biophysica Acta* 820: 85-94.

Lozupone C, Knight R., 2005. UniFrac: a new phylogenetic method for comparing microbial communities. *Applied and Environmental Microbiology* 71: 8228-35.

McDonald D., Price M.N., Goodrich J., Nawrocki E.P., DeSantis T.Z., Probst A., et al. 2012. An improved Greengenes taxonomy with explicit ranks for ecological and evolutionary analyses of bacteria and archaea. *The ISME Journal* 6: 610-18.

Mileti E., Matteoli G., Iliev I.D., Rescigno M., 2009. Comparison of the immunomodulatory properties of three probiotic strains of lactobacilli using complex culture systems: prediction for in vivo efficacy. *PLoS One* 4: e7056.

Munn D.H., Mellor A.L., 2013. Indoleamine 2,3 dioxygenase and metabolic control of immune responses. *Trends in Immunology* 34: 137-43.

NHI, U.S. National Library of Medicine. Search of: Lactobacillus. Results on map ClinicalTrials.gov. Available at: https://clinicaltrials.gov/ct2/results/map?term5Lactobacillus. Accessed May, 2018.

Pantouris G., Serys M., Yuasa H.J., Ball H.J., Mowat C.G., 2014. Human indoleamine 2,3-dioxygenase-2 has substrate specificity and inhibition characteristics distinct from those of indoleamine 2,3-dioxygenase-1. *Amino Acids* 46: 2155-63.

Probst H.C., Muth S., Schild H., 2014. Regulation of the tolerogenic function of steadystate DCs. *European Journal of Immunology* 44: 927-33.

Ritchie A.J., Yam A.O.W., Tanabe K.M., Rice S.A., Cooley M.A., 2003. Modification of in vivo and in vitro T- and B-cell-mediated immune responses by the Pseudomonas aeruginosa quorum-sensing molecule N-(3-oxododecanoyl)-L-homoserine lactone. *Infection and Immunity* 71: 4421-31.

Smith P.M., Howitt M.R., Panikov N., Michaud M., Gallini C.A., Bohlooly-Y M., et al., 2013. The microbial metabolites, short-chain fatty acids, regulate colonic Treg cell homeostasis. *Science* 341: 569-73.

Smith R.S., Kelly R., Iglewski B.H., Phipps R.P., 2002. The Pseudomonas autoinducer N-(3-oxododecanoyl) homoserine lactone induces cyclooxygenase-2 and prostaglandin E2 production in human lung fibroblasts: implications for inflammation. *The Journal of Immunology* 169: 2636-42.

Su A.I., Wiltshire T., Batalov S., Lapp H., Ching K.A., Block D., et al., 2004. A gene atlas of the mouse and human protein-encoding transcriptomes. *Proceedings of the National Academy of Sciences of the United States of America* 101: 6062-67.

Thomas C.M., Hong T., van Pijkeren J.P., Hemarajata P., Trinh D.V., Hu W., et al., 2012. Histamine derived from probiotic Lactobacillus reuteri suppresses TNF via modulation of PKA and ERK signaling. *PLoS One* 7: e31951.

Triebwasser K.C., Swan P.B., Henderson L.M., Budny J.A., 1976. Metabolism of D- and L-Tryptophan in dogs. *The Journal of Nutrition* 106: 642-52.

Trompette A., Gollwitzer E.S., Yadava K., Sichelstiel A.K., Sprenger N., Ngom-Bru C., et al., 2014. Gut microbiota metabolism of dietary fiber influences allergic airway disease and hematopoiesis. *Nature Medicine* 20: 159-66.

van Baarlen P., Troost F., van der Meer C., Hooiveld G., Boekschoten M., Brummer R.J.M., Kleerebezem M., 2011. Human mucosal in vivo transcriptome responses to three lactobacilli indicate how probiotics may modulate human cellular pathways. *Proceedings of the National Academy of Sciences of the United States of America* 108: 4562-69.

Visser W.F., Verhoeven-Duif N.M., Ophoff R., Bakker S., Klomp L.W., Berger R., Koning T.J., 2011. "A sensitive and simple ultra-high-performance-liquid chromatography–tandem mass spectrometry based method for the quantification of d-amino acids in body fluids". *Journal of Chromatography* A 1218: 7130-36.

Wang Q., Garrity G.M., Tiedje J.M., Cole J.R., 2007. Naive Bayesian classifier for rapid assignment of rRNA sequences into the new bacterial taxonomy. *Applied and Environmental Microbiology* 73: 5261-67.

Wise A., Foord S.M., Fraser N.J., Barnes A.A., Elshourbagy N., Eilert M. et al. 2003. Molecular identification of high and low affinity receptors for nicotinic acid. *The Journal of Biological Chemistry* 278: 9869-74.

World Health Organization (WHO) 2010. Global status report on noncommunicable diseases. Available at: http://www.who.int/nmh/publications/ncd_report2010/en/. Accessed in May 2018.

Xu H., Oriss T.B., Fei M., Henry A.C., Melgert B.N., Chen L., et al., 2008. Indoleamine 2,3-dioxygenase in lung dendritic cells promotes Th2 responses and allergic inflammation. *Proceedings of the National Academy of Sciences of the United States of America* 105: 6690-95.

Yan F., Cao H., Cover T.L., Washington M.K., Shi Y., Liu L., et al., 2011. Colon-specific delivery of a probiotic-derived soluble protein ameliorates intestinal inflammation in mice through an EGFR-dependent mechanism. *The Journal of Clinical Investigation* 121: 2242-53.

Yanofsky C., 2007. RNA-based regulation of genes of Tryptophan synthesis and degradation in bacteria. *RNA* 13: 1141-54.

References: probiotics in clinical trials

Abrahamsson T.R., Jakobsson T., Böttcher M.F., Fredrikson M., Jenmalm M.C., Björksten B., Oldaeus G., 2007. Probiotics in prevention of IgE-associated eczema: a double-blind, randomized, placebo-controlled trial. *Journal of Allergy and Clinical Immunology* 119: 1174-80.

Bertelsen R.J., Brantsæter A.L., Magnus M.C., Haugen M., Myhre R., Jacobsson B., et al., 2014. Probiotic milk consumption in pregnancy and infancy and subsequent childhood allergic diseases. *Journal of Allergy and Clinical Immunology* 133: 165-71.

Boyle R.J., Ismail I.H., Kivivuori S., Licciardi P.V., Robins-Browne R.M., Mah L-J., et al., 2011. Lactobacillus GG treatment during pregnancy for the prevention of eczema: a randomized controlled trial. *Allergy* 66: 509-16.

Brouwer M.L., Wolt-Plompen S.A., Dubois A.E., van der Heide S., Jansen D.F., Hoijer M.A., et al, 2006. No effects of probiotics on atopic dermatitis in infancy: a randomized placebo-controlled trial. *Clinical & Experimental Allergy* 36: 899-906.

Cuello-Garcia C.A., Brozek J.L., Fiocchi A., Pawankar R., Yepes-Nunez J.J., Terracciano L., et al., 2015. Probiotics for the prevention of allergy: a systematic review and meta-analysis of randomized controlled trials. *Journal of Allergy and Clinical Immunology* 136: 952-61.

Dotterud C.K., Storrø O., Johnsen R., Oien T., 2010. Probiotics in pregnant women to prevent allergic disease: a randomized, double-blind trial. *British Journal of*

Dermatology 163: 616-23.

Kalliomaki M., Salminen S., Arvilommi H., Kero P., Koskinen P., Isolauri E., 2001. Probiotics in primary prevention of atopic disease: a randomised placebo-controlled trial. *Lancet* 357: 1076-79.

Kopp M.V., Hennemuth I., Heinzmann A., Urbanek R., 2008. Randomized, double-blind, placebo-controlled trial of probiotics for primary prevention: no clinical effects of Lactobacillus GG supplementation. *Pediatrics* 121: e850-6.

Kukkonen K., Savilahti E., Haahtela T., Juntunen-Backman K., Korpela R., Poussa T., et al., 2007. Probiotics and prebiotic galacto-oligosaccharides in the prevention of allergic diseases: a randomized, double-blind, placebo-controlled trial. *Journal of Allergy and Clinical Immunology* 119: 192-98.

Soh S.E., Aw M., Gerez I., Chong Y.S., Rauff M., Ng Y.P., et al., 2009. Probiotic supplementation in the first 6 months of life in at risk Asian infants - effects on eczema and atopic sensitization at the age of 1 year. *Clinical & Experimental Allergy* 39: 571-78.

Szajewska H., Shamir R., Turck D., van Goudoever J.B., Mihatsch W.A., Fewtrell M., 2015. Recommendations on probiotics in allergy prevention should not be based on pooling data from different strains. *Journal of Allergy and Clinical Immunology* 136:1422.

Taylor A.L., Dunstan J.A., Prescott S.L., 2007. Probiotic supplementation for the first 6 months of life fails to reduce the risk of atopic dermatitis and increases the risk of allergen sensitization in high-risk children: a randomized controlled trial. *Journal of Allergy and Clinical Immunology* 119:184-91.

Wickens K., Black P.N., Stanley T.V., Mitchell E., Fitzharris P., Tannock G.W., et al., 2008. A differential effect of 2 probiotics in the prevention of eczema and atopy: a doubleblind, randomized, placebo-controlled trial. *Journal of Allergy and Clinical Immunology* 122: 788-94.

6 Concluding Remarks

Non-targeted metabolomics was applied to uncover a potential bioactive candidate class of bacterial secreted compounds as well as discriminating metabolic pathways that differenciates bioactive from non-bioactive probiotic cell culture supernatants. The results obtained by non-targeted metabolomics are in close agreement with the results observed after bioassay-guided fractionation followed by in vitro and *in vivo* experiements (and with the literature), which suggests that trypthopahn metabolism play a pivotal role in the regulation of immune responses. This result can be used to generate new hypothesis and provides the basis for further investigations. Unknown metabolites (and unique metabolic pathways) that discriminate the two groups of supernatants have also the potential to be the primary cause of the immunomodulation observed *in vitro* and are yet to be fully characterized, which sparks curiosity and motivates further research. In this regard, ultrahigh resolution mass spectrometry plays an important role in maximizing the chances of compound identification.

The use of traditional reductionist methods such as bioassay-guided fractionation was successful at bringing this research into the next level with the identification of potential postbiotic, i.e., a bacteria secreted metabolite that can alone act as therapeutics in the treatment of diseases as observed for the amino acid D-trypthopan *in vitro* and *in vivo*. Also, the bioactivity detected in the 40% and 50% MeOH fractions leave the door open to the discovery of immunoactive substances.

It is well known that microorganisms synthesize D-amino acids and that there are no intestinal barriers for absorption of D-Trp. Thus, after proper safety assessment in animal models, D-tryptophan activity in patients with allergic diseases could be evaluated in clinical studies. This research emphasizes the importance and need for understanding the functions of D-AA in the human body. Highly sensitive and selective analytical methods for the quantification of D- and L-amino acids as the one described in this dissertation are extremely necessary to support studies not only associated with D-AA production in bacterial cell culture, but also to analyse biological samples originated from *in vivo* studies (biofluids, tissues, etc.), where D-AA action may take place.

Both holistic and traditional reductionist approaches are complementary. Considering the vast number of metabolites that might be present in bacteria cell cultures, with huge molecular mass and polarity ranges, the loss of bioactive compounds during fractionation can not be excluded. Metabolomics overcomes this obstacle by allowing a systematic study

of such complex mixture of compounds, which was then linked to results obtained in both *in-vitro* test systems without the need of the time consuming and expensive bioassay-guided fractionation. On the other hand, the large amount of data generated from FT-ICR-MS requires sophisticated computational processing and analysis tools, and time (including technical expertise) to explore and interpret the data. Adittionaly, a limitation of direct infusion FT-ICR/MS analysis is the inability to distinguish identical monoisotopic masses and ion suppression effects that may camouflage potential discriminat compounds. Thus, one approach does not exclude the other.

Lastly, a simple experiemental setups is rare in such interdisciplinary research and effective interaction between expertes from different fields is crucial to success. This dissertation describes practical problem-driven research that found a special answer to a scientific question, and it still leaves a lot of open opportunities for new discoveries. The results presented in this work may support discussions with health authorities on probiotics health claims and autorizathion of clinical trials by providing data on the metabolic footprint of strains. In a long term, the data generated here may support the design of more disease targeted/personalized probiotics and postbiotics products.

7 Annex - Alternatives in sample preparation: development of hybrid magnetic particles for micro solid-phase extraction

7.1 Introduction

This Annex describes a parallel work performed in the field of solid phase extraction. Hybrid magnetic particles shynthesis and prelimiray tests are shown. The knowledge aquired on set-up and optimization of sample extraction and analytical methods to quantify N-acylhomoserine lactones was used in two interdisciplinary research projects that originated two scientific publications (Buddrus-Schiemann et al. 2014; Cataldi et al. 2013).

Samples obtained from cell cultures studies are not always ready for direct introduction into analytical instruments such as chromatography systems and mass spectrometers. They might contain bacterial cells, extracellular products, proteins, and components of the growth media at high concentration. Thus, sample pre-treatment prior chemical analysis is usually required to isolate and pre-enrich metabolites to a concentration level at which the analysis can be carried out. In some instances, the volume of cell culture available for extraction might be limited or not available at all, and an alternative approach to metabolite extraction may be required. An example of such situation is the study bacterial colony dynamics where kinetics of metabolite production is of interest and a low-invasive and non-exhaustive method for in situ monitoring is mandatory as the colony could be impacted by the removal of large volumes of cell culture.

The growth of nanotechnology has offered an excellent alternative to conventional sample preparation methods. Surface functionalized magnetic nanoparticles (matrix@MNP) were successfully applied to DNA extraction (Zhang et al. 2006; Shi et al. 2009), protein isolation using antibody-conjugated MNPs (Chou et al. 2005), enrichment of peptides in biological samples for MALDI-TOF-MS analysis (Yao et al. 2008), pesticides extraction from water samples prior HPLC-ESI-MS (Song et al. 2007), and selective enantioseparation of amino acids (Chen et al. 2011). Regarding that, iron oxide nanoparticles are the most used material due its biocompatibility, high magnetization values and narrow particle size distribution; where a variety of magnetic beads and automatic separation devices are commercially available (Berensmeier 2006; Cardoso et al. 2017).

Several synthetic strategies have been proposed for preparation of iron-based magnetic nanoparticles (Wu et al. 2008; Aguilar-Arteaga et al. 2010; Tartaj et al. 2003). Coprecipitation of ferric and ferrous salts in aqueous solution containing NH_4OH or NaOH is perhaps the simplest method, but alterantives have been used to obtain a higher level of size and shape control, e.g., thermal decomposition in boiling solvent of organometallic precursors and carboxyls (iron (III) acetylacetonate, iron pentacarbonyl, etc.) and hydrothermal processes in in reactors or autoclaves at high temperatures and high pressure (Cardoso et al. 2017; Ajinkya et al. 2020).

Therefore, the aimed of this project was to synthesize hybrid particles combining magnetic nano-sized ferrite spheres with Si-C18 sorbent material obtained from SPE cartridges and to investigate its potential application as micro solid phase extraction. For that, a mixture of N-acylhomoserine lactones (AHLs), covering a wide range of polarity, was chosen as test solution to study the performance characteristic of the particles regarding extraction.

7.2 Material and methods

7.2.1. Synthesis of hybrid magnetic particles

The fabrication of magnetite (Fe_3O_4) nanospheres was set based on the previously described method of iron (III) chloride solvothermal reduction (Deng et al. 2005). Using glass vials, 0.270g of $FeCl_3$ (Santa Cruz Biotechnology, Heidelberg, Germany) was dissolved at room temperature in 8 mL ethylenglycol PA (Serva Electrophoresis, Heidelberg, Germany) followed by addition of 0.720g of sodium acetate crystals (Merck, Darmstadt, Germany). The mixture was then sonicated for 5 minutes. To optimize the synthesis of hybrid MPs, different weighty ratios between the sorbent matrix (Si-C_{18}) and $FeCl_3$ were tested in the production process. Thus, amounts varying from 0.027g (1/10) to 0.270g (1/1) of material obtained from SPE cartridges (Bond Elut C18, Agilent Technologies) were introduced into the glass vials and the mixture was stirred until became homogenous. The vials were sealed in Teflon-lined stainless steel autoclave vessels and were maintained in an oven at 200 ºC for 12 hours (Figure A1). Once the reaction was finished, hybrid particles of Si-C_{18}@MNPs were separated from the solvent using an external magnet and were washed 3 times with ethanol followed by 3 times methanol (5 mL solvent each time). Finally, the synthesized particles were dried at 60 ℃.

The shape and the size of the hybrid microparticles were verified using a Scanning Electron Microscope SEM where images were taken after coating the materials with gold (Figure A 3).

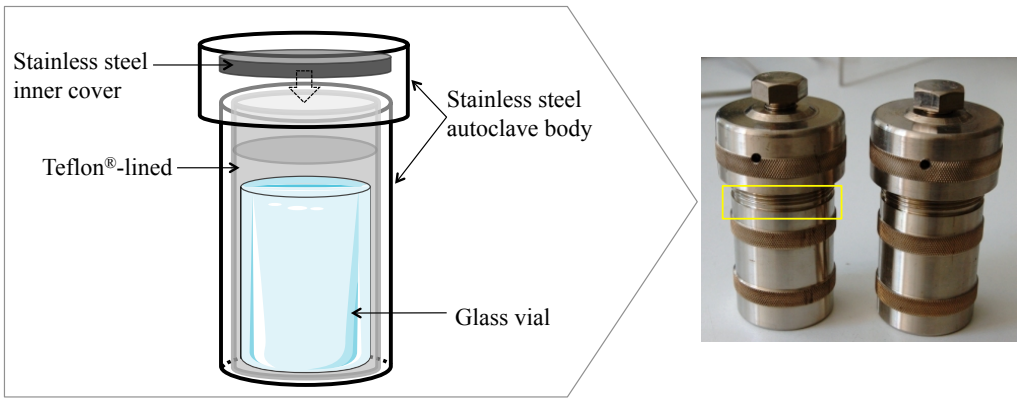

Figure A 1. Scheme and photography of the teflon®-lined stainless steel autoclave system. The parts of the autoclave fit into each other perfectly preventing the flasks of toppling over. Glass vial capacity: 10 mL. Stainless steel cap and container have a *screw* closure system (yellow square; photo) that maintains the inner pressure high during solvothermal reduction of $FeCl_3$. Hybrid magnetic particles were synthetized after reaction at 200 ºC for 12 hours.

7.2.2. Evaluation of hybrid magnetic particles adsorption capacity

A standard mixture of N-acylhomoserine lactones compounds (AHLs) contained C4−, oxo-C6−, C6−, C7−, oxo-C8−, C8−, C9−, OH-C10−, oxo-C10−, C10−, C11−, oxo-C12−, C12−, oxo-C14−, and C14−AHL dissolved in 10% acetonitrile/water solution was used. Calibration curves were constructed for each AHL present in the mixture by plotting chromatographic peak area against its concentration, varying from 0.5 to 10 mg/L. At first, the adsorption percentage of each AHLs to the particles were calculated by analysing 1 mL standard mixture solution (5 mg/L) before and after extraction with the hybrid MPs. Like the extraction procedure applied for SPE cartridges, particles of Si-C18@MNPs were conditioned with 1 mL methanol followed by 1 mL water before interaction with the test-solution. Long and short interaction time and the influence of the amount of material used to adsorb AHLs were investigated, and extraction capacity was evaluated according to the percentage of recovery of the analites. The micro solid phase extraction procedure using hybrid magnetic particles is shown in Figure A2.

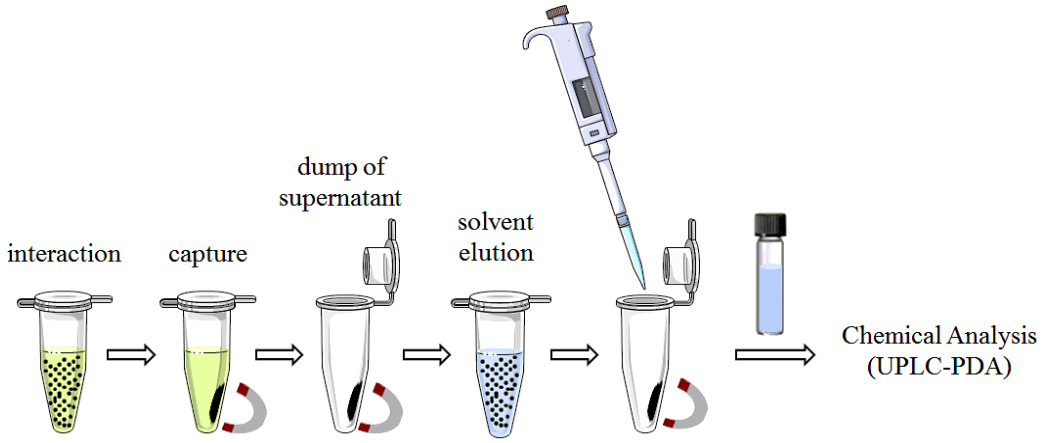

Figure A 2. Solid-phase extraction using hybrid magnetic particles. Before interaction with samples, Si-C18@MNPs were conditioned with 1mL MeOH followed by 1mL H2O. Hybrid magnetic particles can be manipulated and separated from solution using an external magnet.

7.2.3. Chromatographic conditions

Based on a previously described method (Fekete et al. 2007), the separation and determination of homoserine lactones was conducted on a Waters Acquity UPLC System (Waters, Darmstadt, Germany) coupled to a 2996 PDA detector. Standard mixtures of AHLs and eluates were injected into a reversed phase UPLC BEH C18 column (Waters) with dimensions of 100 mm x 2.1 mm and 1.7 µm particle size. Gradient elution was applied starting from 100% Eluent A (Water - 10% Acetonitrile) to 48% Eluent B (Acetonitrile) in 2.55 min; increasing to 100% B in 3.5 min. The flow rate was set to 800 µL/min and the injection volume was 5 µL via full loop. The column and the auto sampler temperature were set to 60 ºC and 27 ºC respectively. The choose detection wavelength was 196.5 nm with scan rate of 20 Hz.

7.3. Results and discussion

7.3.2. Synthesis of hybrid magnetic particles

The solvothermal reduction method showed to be efficient in producing iron oxide nanoparticles on the porous surface of the nosorbent matrix originating a black precipitate. According to Deng et al. (2005), time of reaction and concentration of $FeCl_3$ can influence nanoparticles diameter when temperature is constant, but is hard to describe a straightforward correlation between those parameters. The nanoparticles can be magnetite (Fe_3O_4) or maghemite (Fe_2O_3) with superparamagnetic properties.

Figure A3 shows electron microscopy images obtained in this study. The pure Si-C18 particles are non-uniform in shape and have a porous surface. Iron oxide nanoparticles have

regular spherical shape and diameter distribution smaller than 500 nm; obtained after 12 hours reaction at 200 ºC. Magnetic nanospheres were deposited on the surface of Si-C18 particles in a non-homogenous way but giving then the paramagnetic properties needed to be handled by external magnetic force.

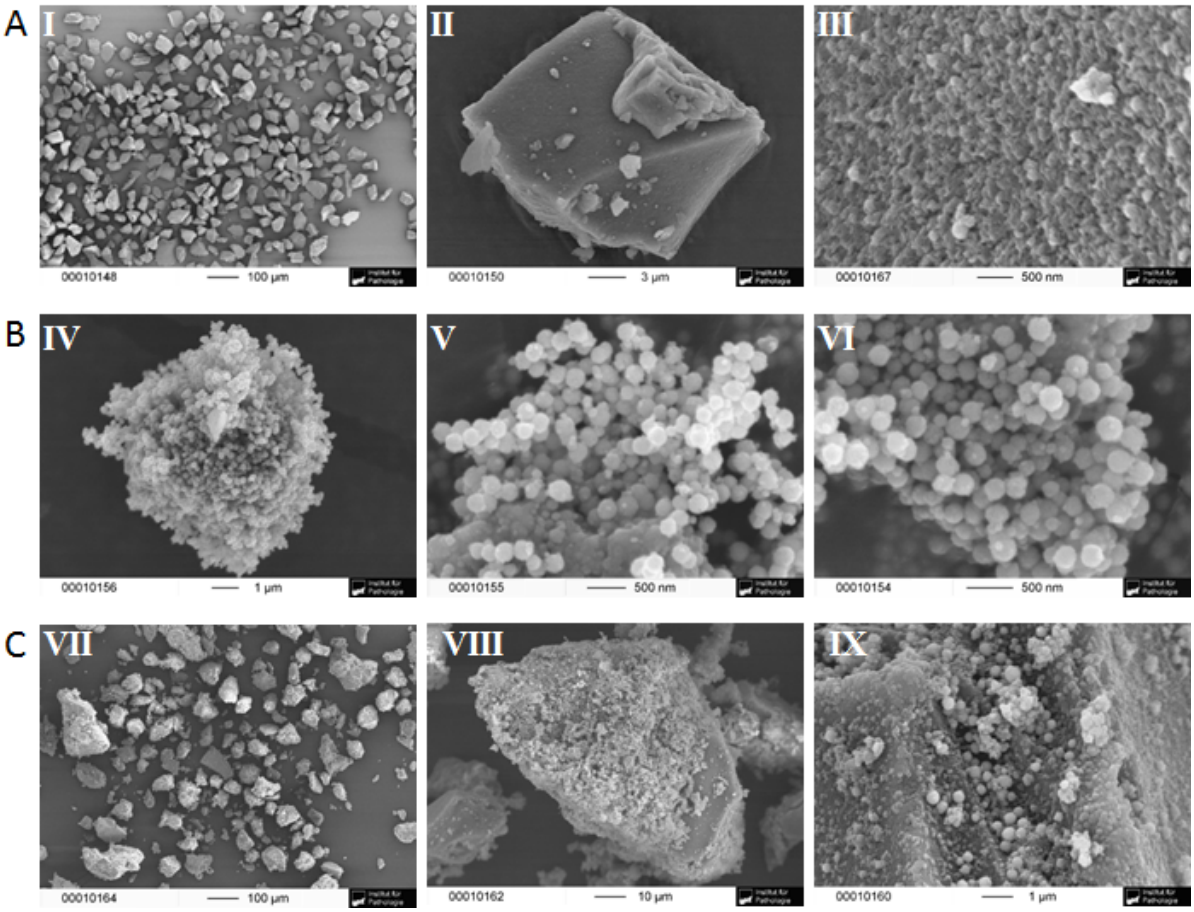

Figure A 3. Scanning Electron Microscope images of the particles in study. (A) Non-uniform Si-C18 microparticles obtained from a SPE cartridge (I-II) and its porous surface (III). (B) Agglomeration of ferrite nanospheres produced by the solvothermal reduction method. The particles have regular rounded shape and diameter smaller than 500 nm (V, IV). (C) Magnetic nanoparticles deposited on the surface of the porous non-magnetic Si-C_{18} matrix.

Under the chosen reaction conditions (200 ºC; 12 h), the amount of $FeCl_3$ was fixed to 0.270g in all synthesis to maximized production of nanospheres using 8 mL solvent; keeping the proportions published by Deng *et al*. (2005) and considering the glass vial volume capacity of 10 mL. Only the amount of Si-C18 particles was variable. The hybrid Si-C18@MPs got a greenish colour and showed less paramagnetism with the increase of the amount of sorbent material in the synthesis (Figure A4); and the handling of those particles with an external magnet became difficult. Those characteristics were observed for Si-C18/$FeCl_3$ weight ratios 1/1 and 1/1.5. The biggest amount of hybrid particles produced that

kept good paramagnetic properties were observed when using 1/2 (w/w) of Si-C18/$FeCl_3$; in this case 0.135g of Si-C18 to 0.270g $FeCl_3$. Thus, these values were considered for further synthesis.

Four stainless steel autoclaves allowed the production of 4 batches of Si-C18@MPs particles simultaneously. It is important to highlight that iron-based nanoparticles did not interact with each other when dispersed in solution and in the absence of magnetic field. Thus, homogenization between hybrid magnetic particles produced in different batches is easily done by mixing them in methanol or water solution and washing all together as a single batch. It is a very useful information once the amount of particles obtained in one single production batch is not enough for sample preparation of studies involving high number of samples. It can reduce analytical variation that could appear by using hybrid particles produced in different batches for extraction of samples of the same set.

The hybrid-MPs were stored at room temperature in polypropylene Eppendorf test tubes for more than 1 year and still showed magnetic properties, been nicely handled by the magnet. This characterizes a certain chemical stability of the iron nanoparticles against oxidation, which could cause loss of paramagnetism.

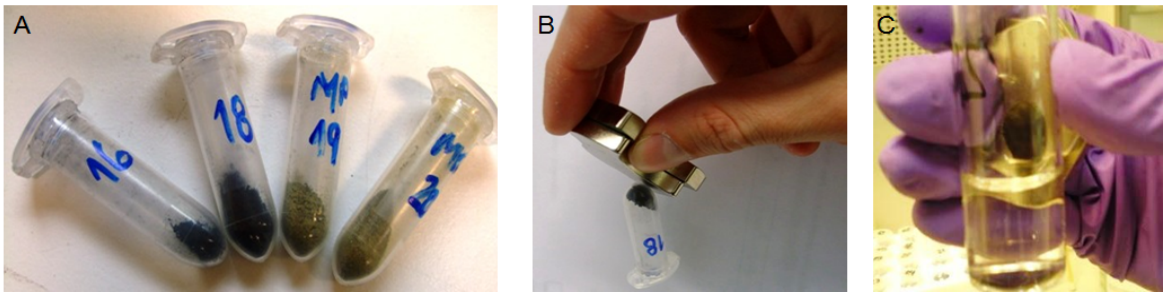

Figure A 4. Photography of in-house prepared Si-C18@MNPs. (A) Different Si-C18/$FeCl_3$ weighty mass ratios: (16) 1/10, (18) 1/2, (19) 1/1.5 and (20) 1/1. Greenish color and loss of magnetic properties was observed in 19 and 20 tubes (numbers in the tubes does not have any scientific meaning besides experiments identification. Not all production batchs and ratios Si-C18/$FeCl_3$ are show in the pictures).

7.3.3. Chromatographic analysis of the N-acylhomoserine lactones standard mixture for the evaluation of hybrid magnetic particles as micro solid phase extraction

Besides the broad range of polarity covered by AHLs bacterial metabolites, this class of compounds was chosen to form the test-solution due our in-house expertise and interest in quorum sensing research (Englmann *et al*, 2007; Fekete *et al*, 2010; Cataldi *et al*, 2013).

Derivatives of N-acylhomoserine lactones (AHLs, also referred to as HSLs or acyl-HSLs) occur as autoinducer in cell-to-cell signalling among Gram-negative bacteria and regulate the infection process based on the local bacterial cell density beyond a wide variety of collective behaviour (Hartmann and Schikora 2012; Van Delden and Iglewski 1998). The chemical structure of AHLs consist of a furen-2-one moiety linked to a variable acyl side-chain containing 4 to 14 carbon atoms (less frequently up to 18). Common variations of the side-chain include keto or hydroxyl functional group located at the β-carbon, unsaturated fatty acid side-chain , and more rarely, *p*-coumaroyl group derived from *p*-coumaric acid; an example of non-fatty side chain (Thiel *et al*, 2009; Schaefer *et al*, 2008). Classical techniques such as liquid-liquid extraction (LLE) (Morin et al. 2003) and column solid-phase extraction (SPE) (Li et al. 2006) have been proposed to isolate AHLs and were reviewed elsewhere (J. Wang et al. 2011). Moreover, both techniques require collection of large volume of cell culture supernatant and may limit their application in studies when kinetic of AHL production is the focus of the research disturbs long term growth. The development of a simple method for in situ and small volume sampling is of high interest not only in quorum sensing research but also to other applications in bioanalytical and metabolomics.

Using an UPLC-PDA system, it has been possible to separate fifteen AHLs in 3.5 min by reverse phase chromatography with less than 10% relative standard deviation for peak area and less than 1% and for retention time (data not show). The number of AHLs detected in this method is increased when compared to previous published data (Li et al. 2006).

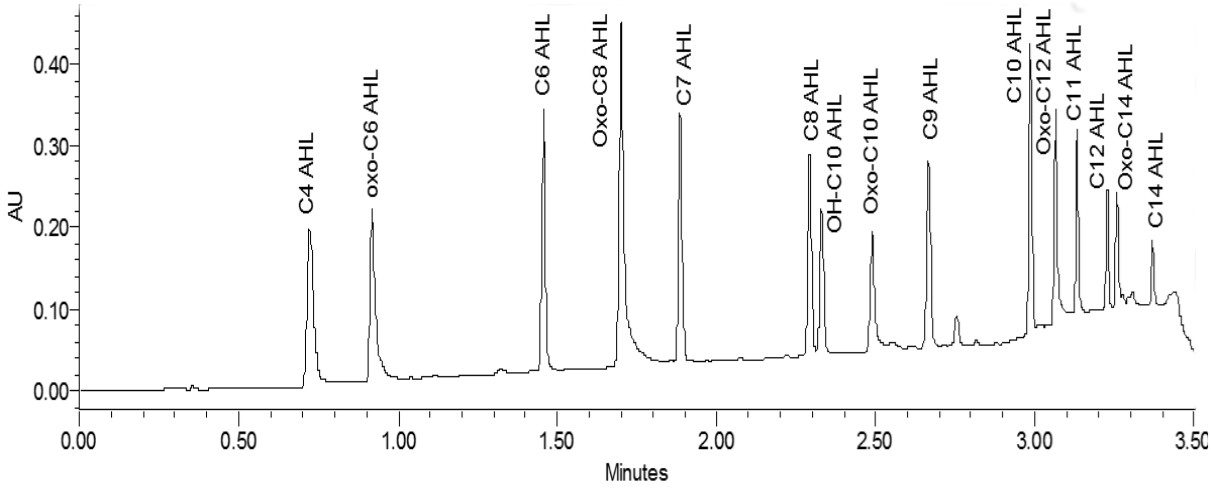

Figure A 5. UPLC-PDA Chromatogram of the AHLs test-solution. Baseline separation was achieved in 3.5 min run time using RP-C18. Column dimensions: 100 mm x 2.1 mm and 1.7 µm particle size. Gradient elution went from 100% Eluent A (Water - 10% Acetonitrile) to 48% Eluent B

(Acetonitrile) in 2.55 min; increasing to 100% B in 3.5 min. Flow rate: 0.8 mL min^{-1}. Column temperature was set to 60ºC and the auto sampler to 27ºC. Detection wavelength: 196.5 nm (adapted from Cataldi et al. 2013).

Extraction experiments using 1mL AHL mix solution (5 mg/L concentration each) and different amounts of Si-C18@MNPs suggest that 20 mg particles after 20 minutes interaction led already to a good percentage of adsorption and chromatograms without interference peaks. Long side chain AHL were highly adsorbed and therefore were less detected in the solution. Figure A 6 shows the concentrations measured in the AHL standard mix solution after interaction with C18@MNPs, while Figure A 7 shows the recovery of AHLs after elution from MNPs.

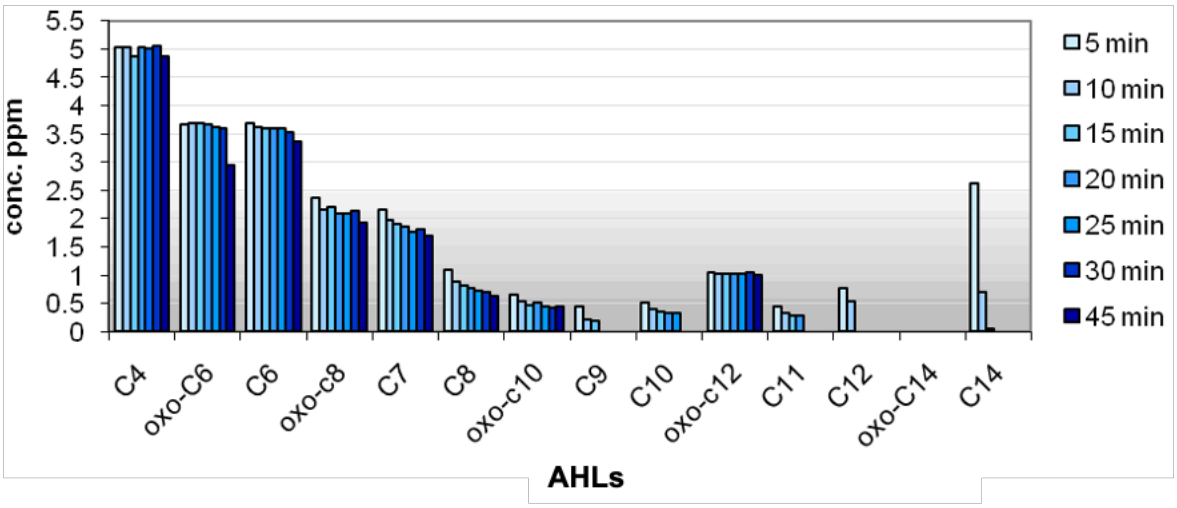

Figure A 6. AHLs concentrations measured in the standard mix solution as a function of time after interaction with Si-C18@MNPs.

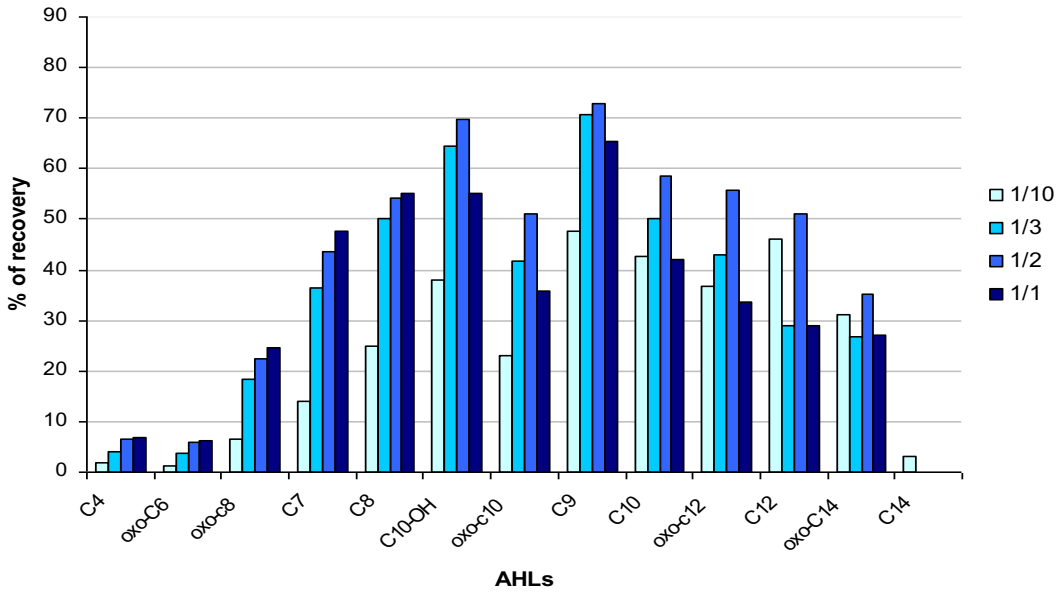

Figure A 7. Comparision of recovery of AHLs in solution after interaction with C18@MNPs produced with different C18/$FeCl_3$ weighty ratios. The ratio 1/2 (Si-C18/$FeCl_3$) showed the best recovery while particles obtained with ratios 1/1.5 (not shown) and 1/1 lost magnetic properties and were difficult to handle (recovery measurements have been made only using 1/1 material).

The longest carbon chain AHLs could not be fully recovered, probably due to strongest binding to the C18 material and AHLs with short side chain stayed preferentially in the original solution and thus, had low percentage of recovery in the elution step.

Pure iron-oxide nanoparticles were also tested and as expected, did not adsorb AHLs from the standard mix solution. For all UPLC-PDA measurements, a calibration curve was built with standard solutions. In addition, the use of C18@MNPs to extract compounds direct from growth medium has been investigated and first results were favorable to the use of this sample extraction technique confirming no presence of cells in the eluted portion. It means that the filtration procedure which requires big amount of cell culture to obtain supernatant for chemical analyses can be avoided and hybrid magnetic particles can be applied into few milliliters of growth medium only.

7.3.4. Attempt using HLB sorbent material

HLB sorbent material is a resin made from a co-polymer of divinybenzene and vinyl pyrrolidinone that is widely used in SPE cartiridges. Based on the experience with C18@MNPs, the same experimental set up was applied to the preparation and evaluation of HLB@MNPs particles. The 1/3, 1/2 and 1/1.5 weighty mass ratios for HLB/$FeCl_3$ were used to obtain the hybrid magnetic particles, which were evaluated for the extraction of AHLs (Figure A 8). Scanning Electron Microscope images were not obtained for HLB@MNPs.

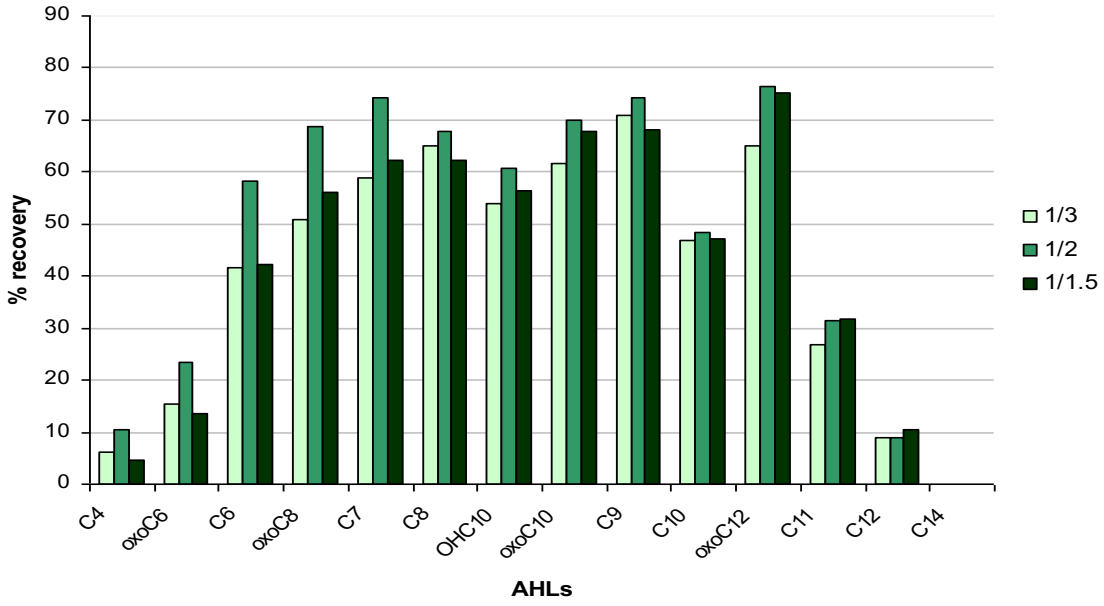

Figure A 8. Comparision of recovery of AHLs in solution after interaction with HLB@MNPs produced with different HLB/ FeCl3 weighty ratios.

Figure A 8 shows a decrease in capacity of recovery when 1/1.5 ratio was used to produce the hydrid MNPs. Contrary to C18@MPs, no unusual color of the final product was realized when using HLB material, but a loss of magnetism was also observed when increasing de amount of the HLB material during synthesis. This suggests that an excess of sorbent material in the reaction system can disturbs the formation of iron oxide nanoparticles during solvothermal reduction.

Also, differences in recovery characteristics between both C18@ and HLB@ MNPs are observed and are associated with the polarity of the respective solid phases. Overall, HLB@MNPs showed better recoveries when compared to C18@MNPs. The longest side chain AHL was highly adsorbed in both MNPs and was therefore not detected after elution solution. Thus, the results showed that HLB material can be also used for the isolation of homeserine lactones in solution and biological samples.

Conclusion

The advantage of the hybrid magnetic particles includes the ability to easly handle them in solution (or sample) using external magnetic field. The experiments presented here suggest that hybrid-MNPs can be washed and used again several times for analyte extraction in samples, in opposition to SPE cartridges. The composite with functionalize silica gel was

chosen at the first stage since mostly C18-SPE has been applied for AHL analysis. Many experiments on the production of hybrid magnetic particles, characterization and adsorption-desorption tests were done. The solvothermal reduction method to obtain iron nanoparticles was set in one simple step. By varying temperature of the oven, time of reaction and choosing the best reactor flask, nanoparticles was obtained at 200ºC during a 12h reaction. This production method can be extended to other adsorbent materials available on the market after careful feasibility studies as performed for HLB, i.e., the stability of the adsorbent matrix at reaction conditions must be evaluated. The AHL standard mix can be defined as a quality control solution to evaluate extraction properties of hybrid-MNPs.

References

Aguilar-Arteaga, K.; Rodriguez, J.A.; Barrado, E., 2010. Magnetic solids in analytical chemistry: a review. *Analytica chimica acta* 674: 157–65.

Ajinkya, N.; Yu, X.; Kaithal, P.; Luo, H.; Somani, P.; Ramakrishna, S., 2020. Magnetic Iron Oxide Nanoparticle (IONP) Synthesis to Applications: Present and Future. *Materials* 13: 4644.

Berensmeier, S., 2006. Magnetic particles for the separation and purification of nucleic acids. *Applied microbiology and biotechnology* 73: 495–504.

Buddrus-Schiemann, Katharina, Martin Rieger, Marlene Mühlbauer, Maria Vittoria Barbarossa, et al. (2014). Analysis of N-Acylhomoserine Lactone Dynamics in Continuous Cultures of Pseudomonas Putida IsoF by Use of ELISA and UHPLC/qTOF-MS-Derived Measurements and Mathematical Models. Analytical and Bioanalytical Chemistry 406: 6373–83

Cardoso, V.F.; Francesko, A.; Ribeiro, C.; Banobre-López, M.; Martins, P.; Lanceros-Mendez, S., 2017. Advances in Magnetic Nanoparticles for Biomedical Applications. *Advanced Healthcare Materials* 7: 1700845.

Cataldi, T.R.I.; Bianco, G.; Fonseca, J.; Schmitt-Kopplin, P., 2013. Perceiving the chemical language of Gram-negative bacteria: listening by high-resolution mass spectrometry. *Analytical and bioanalytical chemistry* 405: 493–507.

Chen, X.; Rao, J.; Wang, J.; Gooding, J.J.; Zou, G.; Zhang, Q., 2011. A facile enantioseparation for amino acids enantiomers using β-cyclodextrins functionalized Fe3O4 nanospheres. *Chemical communications* 47: 10317–19.

Chou, P.-H.; Chen, S-H.; Liao, H-K.; Lin, P-C.; Her, G-R.; et al. 2005. Nanoprobe-based affinity mass spectrometry for selected protein profiling in human plasma. *Analytical chemistry* 77: 5990–97.

Deng, H.; Li, X.; Peng, Q.; Wang, X.; Chen, J.; Li, Y., 2005. Monodisperse magnetic single-crystal ferrite microspheres. *Angewandte Chemie* 44: 2782–85.

Englmann, M.; Fekete, A.; Kuttler, C.; Frommberger, M.; Li, X.; et al., 2007. The hydrolysis of unsubstituted N-acylhomoserine lactones to their homoserine metabolites. Analytical approaches using ultra performance liquid chromatography. *Journal of chromatography. A* 1160: 184–93.

Fekete, A.; Kuttler, C.; Rothballer, M.; Hense, B.A.; Fischer, D.; et al., 2010. Dynamic regulation of N-acyl-homoserine lactone production and degradation in Pseudomonas putida IsoF. *FEMS microbiology ecology* 72: 22–34.

Fekete, A.; Frommberger, M.; Rothballer, M.; Li, X.; Englmann, M.; et al., 2007. Identification of bacterial N-acylhomoserine lactones (AHLs) with a combination of ultra-performance liquid chromatography (UPLC), ultra-high-resolution mass spectrometry, and in-situ biosensors. *Analytical and bioanalytical chemistry* 387: 455–67.

Hartmann, A.; Schikora, A., 2012. Quorum sensing of bacteria and trans-kingdom interactions of N-acyl homoserine lactones with eukaryotes. *Journal of chemical ecology* 38: 704–13.

Li, X.; Fekete, A.; Englmann, M.; Götz, C.; Rpthballer, M.; et al., 2006. Development and

application of a method for the analysis of N-acylhomoserine lactones by solid-phase extraction and ultra high pressure liquid chromatography. *Journal of chromatography A* 1134: 186–93.

Morin, D.; Grasland, B.; Vallée-Réhel, K.; Dufau, C.; Haras, D., 2003. On-line high-performance liquid chromatography-mass spectrometric detection and quantification of N-acylhomoserine lactones, quorum sensing signal molecules, in the presence of biological matrices. *Journal of chromatography A* 1002: 79–92.

Schaefer, A.L., Greeberg, E.P.; Oliver, C.M.; Oda, Y.; Huang, J.J.; et al., 2008. A new class of homoserine lactone quorum-sensing signals. *Nature* 454: 595–9.

Shi, R.; Wang, Y.; Hu, Y.; Chen, L.; Wan, Q-H., 2009. Preparation of magnetite-loaded silica microspheres for solid-phase extraction of genomic DNA from soy-based foodstuffs. *Journal of chromatography A* 1216: 6382–86.

Song, Y.; Zhao, S.; Tchounwou, P.; Liu, Y-M., 2007. A nanoparticle-based solid-phase extraction method for liquid chromatography-electrospray ionization-tandem mass spectrometric analysis. *Journal of chromatography A* 1166: 79–84.

Tartaj, P.; Morales, M.P.; Veintemillas-Verdaguer, S.; González-Carreño, T.; Serna, C.J., 2003. The preparation of magnetic nanoparticles for applications in biomedicine. Journal of Physics D: *Applied Physics* 36: R182–R197.

Thiel, V.; Kunze, B.; Verma, P.; Wagner-Döbler, I.; Schulz, S., 2009. New structural variants of homoserine lactones in bacteria. *Chembiochem* 10: 1861–68.

Van Delden, C.; Iglewski, B.H., 1998. Cell-to-cell signaling and Pseudomonas aeruginosa infections. *Emerging infectious diseases* 4: 551–60.

Wang, J.; Quan, C.; Wang, X.; Zhao, P.; Fan, S., 2011. Extraction, purification and identification of bacterial signal molecules based on N-acyl homoserine lactones. *Microbial biotechnology* 4: 479–90.

Wu, W.; He, Q.; Jiang, C., 2008. Magnetic iron oxide nanoparticles: synthesis and surface functionalization strategies. *Nanoscale research letters* 3: 397–415.

Yao, N.; Chen, H.; Lin, H.; Deng, C.; Zhang, X., 2008. Enrichment of peptides in serum by C(8)-functionalized magnetic nanoparticles for direct matrix-assisted laser desorption/ionization time-of-flight mass spectrometry analysis. *Journal of chromatography A* 1185: 93–101.

Zhang, Z.; Zhang, L.; Chen, Lei; Chen, Liong; Wan, Q-H., 2006. Synthesis of novel porous magnetic silica microspheres as adsorbents for isolation of genomic DNA. *Biotechnology progress* 22: 514–18.

8 Supplementary Information

Chapter 2: Mining for Active Molecules in Probiotic Supernatant by Combining Non-Targeted Metabolomics and Immunoregulation Testing

Table S 1: Chemically defined medium (CDM1) used for growing probiotic bacteria for metabolomics.

Component	**[g/L]**	**[mmol/l]**	**Component**	**[g/l]**	**[mmol/l]**
L-Cystine	0,05	0,208	Folic acid	0,005	0,011
Thiamine	0,005	0,015	Adenine	0,01	0,074
Riboflavin	0,005	0,013	Guanine	0,01	0,066
Niacin	0,004	0,032	Uracil	0,01	0,089
Ca-Pantothenic acid	0,005	0,023	Xanthine	0,01	0,066
Pyridoxine	0,004	0,023	Myo-Inositol	0,005	0,028
Cyanocobalamin	0,005	0,004	$MnSO_4$ x H_2O	0,01	0,059
$FeSO_4$ x $7H_2O$	0,01	0,036	NaCl	0,01	0,171
p-Aminobenzoic acid	0,005	0,036	D(+) Biotin	0,005	0,020
DL-Alanine	0,5	5,6	L-Tryptophan	0,56	2,7
Bacto Asparagine	1,1	8,3	L-Aspartate	0,8	6,0
L-Cysteine	1,5	12,4	L-Tyrosine	0,4	2,2
L-Glutamine	1,0	6,8	L-Threonine	0,5	4,2
Glycine	0,4	5,3	L-Glutamate	1,2	8,2
L-Histidine	0,44	2,8	L-Valine	1,0	8,5
L-Isoleucine	0,5	3,8	$MgSO_4$ x $7H_2O$	0,2	0,8
L-Leucine	0,5	3,8	Na-Acetate	20	243,8
L-Lysine	1,05	7,2	NH_4Cl	3,0	56,1
L-Methionine	0,2	1,3	KH_2PO_4	0,6	4,4
L-Phenylalanine	0,5	3,0	K_2HPO_4	0,6	3,4
L-Proline	0,4	3,5	D(+) Glucose	25	138,8
L-Serine	1,55	14,7			

Table S 2: Instrumental parameters used for the analyses of cell-free supernatant extracts. Single MS acquisition mode and ESI ionization.

Parameters	**(-) FT-ICR-MS**	**(+) FT-ICR-MS**
HLB and CN-E extracts		
Mass range	147.4 – 2000 Da	147.4 – 1500 Da
Source accumulation	0.01 sec	0.05 sec
Ion accumulation time	0.30 sec	0.50 sec
Acquired scans	500	300
Capillary voltage	4000 V	4000 V
Drying gas flow rate	4.0 L/min	4.0 L/min
Drying gas temperature	180 °C	200 °C
Nebulizer gas flow rate	1.0 bar	1.0 bar
Spray shield	-500 V	-500 V
Excitation pulse time	5.0 µsec	5.0 µsec
Analyzer entrance	4.0 V	-5.0 V
Sidekick offset	1.5 V	-1.5 V
Trap	-20 V	20 V
Front trap plate	-0.4 V	0.4 V
Back trap plate	-0.5 V	0.5 V
Transient time domain	2 MW	2 MW
Syringe flow rate	120 µL/h	240 µL/h
Run time	10.0 min	10.0 min
Non-extracted supernatants	**(-) FT-ICR-MS**	**(+) FT-ICR-MS**
Mass range	73.7 – 1000 Da	73.7 – 1000 Da
Source accumulation	0.01 sec	0.01 sec
Ion accumulation time	0.30 sec	0.30 sec
Acquired scans	500	400
Capillary voltage	3600 V	3600 V
Drying gas flow rate	4.0 L/min	4.0 L/min
Drying gas temperature	180 °C	180 °C
Nebulizer gas flow rate	2.0 bar	2.0 bar
Spray shield	-500 V	-500 V
Excitation pulse time	15.0 µsec	15.0 µsec
Analyzer entrance	4.0 V	-10.0 V
Sidekick offset	10.0 V	-1.5 V
Trap	-20 V	20 V
Front trap plate	-0.4 V	0.4 V
Back trap plate	-0.5 V	0.5 V
Transient time domain	2 MW	2 MW
Syringe flow rate	120 µL/h	120 µL/h
Run time	10.0 min	10.0 min

Chapter 4: Enantioseparation and selective detection of D-amino acids by ultra high-performance liquid chromatography/mass spectrometry in analysis of complex biological samples

Table S 3: Name and symbol of proteinogenic amino acids (IUPAC-IUB 1984).

Amino Acid	**Symbols**	
Alanine	Ala	A
Arginine	Arg	R
Asparagine	Asn	N
Aspartic Acid	Asp	D
Cysteine	Cys	C
Glutamic Acid	Glu	E
Glutamine	Gln	Q
Glycine	Gly	G
Histidine	His	H
Isoleucine	Ile	I
Leucine	Leu	L
Lysine	Lys	K
Methionine	Met	M
Phenylalanine	Phe	F
Proline	Pro	P
Serine	Ser	S
Threonine	Thr	T
Tryptophan	Trp	W
Tyrosine	Tyr	Y
Valine	Val	V

Chapter 5: D-Tryptophan from probiotic bacteria influences the gut microbiome and allergic airway disease

Materials and Methods

Reagents

L-Tryptophan and D-amino acids (A, F, H, I, L, M, P, S, T, V, W, Y) were purchased from Carl Roth GmbH, Karlsruhe, Germany.

Growth conditions of bacteria and collection of supernatants

For the primary screen of bioactivity, probiotic strains were grown in complex de Man-Rogosa-Sharpe (MRS) medium (Applichem, Darmstadt, Germany) at 37 °C under microaerobic conditions in an Incubator (Thermo Fisher Scientific, Waltham, USA). For metabolite analyses, the strains were grown in modified defined medium CDM1 (1) which contains L-Tryptophan among 19 other L-amino acids, at 37 °C. In contrast to the original medium, we omitted Tween 80, as it is known to interfere with mass spectrometric analyses (2). E. Coli Nissle 1917 was grown aerobically in Luria-Bertani (LB)-Medium on a rotary shaker (New Brunswick Scientific, Enfield, USA) (200 rpm) at 37 °C.

(1) Savijoki K., Suokko A., Palva A., Varmanen P., 2006. New convenient defined media for [(35)S] methionine labelling and proteomic analyses of probiotic lactobacilli. Letters in Applied Microbiology 42(3): 202–9.

(2) Müller C., Fonseca J.R., Rock T.M., Krauss-Etschmann S., Schmitt-Kopplin P., 2014. Enantioseparation and selective detection of D-amino acids by ultra-high-performance liquid chromatography/mass spectrometry in analysis of complex biological samples. J Chromatogr A. 1324:109–14.

Table S 4: Probiotic bacterial strains evaluated in this study.

Bacterial strain	**Provider**	**Bioactivity on[1]**	
		KM-H2	**DC**
Lactobacillus rhamnosus DSM-20021	Leibniz Institute DSMZ	-	-
Lactobacillus rhamnosus GG	Valio Ltd, Helsinki, Finland	+	+
Lactobacillus acidophilus W22	Winclove Bioindustries BV	+	+
Lactobacillus acidophilus W37	Winclove Bioindustries BV	-	-
Lactobacillus acidophilus W50	Winclove Bioindustries BV	-	-
Lactobacillus acidophilus W74	Winclove Bioindustries BV	-	-
Lactobacillus acidophilus DSM-20079	Leibniz Institute DSMZ	-	-
Lactobacillus acidophilus LA-2	Chr. Hansen	+	+
Lactobacillus acidophilus LA-5	Chr. Hansen	+	+
Lactobacillus casei W56	Winclove Bioindustries BV	+	+
Lactobacillus casei W79	Winclove Bioindustries BV	+	+
Lactobacillus paracasei DSM-20312	Leibniz Institute DSMZ	-	-
Lactobacillus paracasei subsp. *paracasei* LC-01	Chr. Hansen	+	+
Lactobacillus gasseri W44	Winclove Bioindustries BV	-	-
Lactobacillus gasseri DSM-20077	Leibniz Institute DSMZ	-	-
Lactobacillus helveticus W60	Winclove Bioindustries BV	-	-
Lactobacillus plantarum W21	Winclove Bioindustries BV	-	-
Lactobacillus plantarum W62	Winclove Bioindustries BV	-	-
Lactobacillus plantarum DSM-20174	Leibniz Institute DSMZ	-	-
Lactobacillus rhamnosus W102	Winclove Bioindustries BV	-	-
Lactobacillus salivarius W24	Winclove Bioindustries BV	-	-
Lactobacillus salivarius W57	Winclove Bioindustries BV	-	-
Bifidobacterium animalis subsp. *lactis* BB-12	Chr. Hansen, Horsholm, Denmark	+	+
Bifidobacterium breve W25	Winclove Bioindustries BV, Amsterdam, Netherlands	-	-
Bifidobacterium breve DSM-20091	Leibniz Institute DSMZ-German Collection of Microorganisms and Cell Cultures, Braunschweig, Germany	-	-
Bifidobacterium bifidum DSM-20456	Leibniz Institute DSMZ	-	-
Bifidobacterium lactis BB-420	Danisco, Niebüll, Germany	+	+
Bifidobacterium lactis W51	Winclove Bioindustries BV	-	-
Bifidobacterium lactis W52	Winclove Bioindustries BV	+	+
Bifidobacterium longum BB-46	Chr. Hansen	+	+
Bifidobacterium longum W108	Winclove Bioindustries BV	+	+
Bifidobacterium longum subsp. infantis DSM-20088	Leibniz Institute DSMZ	-	-
Enterococcus faecium W54	Winclove Bioindustries BV	-	-

Bacterial strain	Provider	Bioactivity on[1]	
		KM-H2	DC
Lactococcus lactis W19	Winclove Bioindustries BV	-	-
Lactococcus lactis W32	Winclove Bioindustries BV	-	-
Lactococcus lactis W58	Winclove Bioindustries BV	+	+
Streptococcus thermophilus W69	Winclove Bioindustries BV	-	-
Escherichia coli Nissle 1917	Ardeypharm GMbH, Herdecke, Germany	-	-

[1]Ability of bacterial cell-free supernatants to lower CCL17 secretion by KMH2 cells (left) and to reduce LPS-induced up-regulation of costimulatory molecules on human monocyte derived dendritic cells (DC, right)

Table S 5: Percentage of surface marker–expressing mature DCs treated with synthetic D-amino acids

	D-Alanine	D-Histidine	D-Isoleucine	D-Leucine	D-Methionine	D-Phenylalanine
CD83	97.67 ± 2.29	103.09 ± 0.33	100.51 ± 1.18	97.07 ± 2.39	102.40 ± 2.19	99.55 ± 2.02
CD86	99.24 ± 2.13	102.49 ± 0.43	99.84 ± 1.19	101.94 ± 1.34	102.22 ± 2.53	99.19 ± 3.33
CD80	98.34 ± 2.64	102.02 ± 0.88	98.23 ± 1.48	100.28 ± 1.55	100.39 ± 0.15	92.40 ± 3.45
CD40	102.34 ± 3.36	101.44 ± 3.22	100.43 ± 2.41	100.37 ± 1.72	102.66 ± 0.60	100.35 ± 2.72
HLA-DR	98.06 ± 1.06	99.85 ± 0.93	100.08 ± 0.33	98.95 ± 9.97	98.91 ± 2.02	98.02 ± 3.17
	D-Proline	**D-Serine**	**D-Threonine**	**D-Tryptophan**	**D-Tyrosin**	**D-Valine**
CD83	100.98 ± 0.40	100.78 ± 0.29	102.62 ± 0.46	**7.63 ± 3.31**	101.63 ± 0.56	102.06 ± 1.20
CD86	101.18 ± 1.85	101.08 ± 2.76	102.09 ± 0.68	**24.14 ± 2.67**	102.23 ± 0.85	101.77 ± 0.87
CD80	100.32 ± 0.10	100.13 ± 2.78	100.76 ± 0.35	**12.11 ±1.68**	101.62 ± 0.37	99.62 ± 2.03
CD40	99.19 ± 1.33	100.78 ± 1.12	100.56 ± 1.49	**15.18 ± 6.51**	100.37 ± 1.25	101.42 ± 2.35
HLA-DR	98.39 ± 2.60	98.64 ± 0.58	97.06 ± 3.91	88.85 ± 2.96	98.43 ± 2.42	100.02 ± 1.02

Three independent experiments are shown (mean 6 SD percentages relative to LPS-induced expression). DCs were stimulated with LPS (0.1 mg/mL) in the presence of the indicated D-amino acids (10 mmol/L). Percentages of CD83-, CD86-, CD80-, or CD40-expressing DCs were assessed.

Table S 6: Cytokine regulation by probiotic supernatants or D/L-tryptophan in human LPS-treated DCs

	IL-10 (pg/mL)		IL-5 (pg/mL)		IFN-g (pg/mL)		IL-12 (pg/mL)		Ratios			
									IL-10/IL-12		IL-5/IFN-g	
	-	LPS	-	LPS	-	LPS	-	LPS	-	LPS	-	LPS
Medium	3.20	2.90	14.70	68.30	112.50	2238.80	102.10	2092.80	0.031	0.001	0.131	0.031
DSM-20021	6.80	4.80	33.60	55.90	330.00	2520.50	447.80	2217.30	0.015	0.002	0.102	0.022
LGG	432.90	787.90	9.10	5.40	372.70	105.70	79.20	106.90	5.466	7.370	0.024	0.051
LA-2	107.30	591.70	8.00	10.30	111.60	437.70	89.30	238.00	1.202	2.486	0.072	0.024
LA-5	81.30	305.70	7.60	8.00	113.30	531.80	87.50	331.10	0.929	0.923	0.067	0.015
LC-01	452.40	924.50	7.90	2.40	109.30	211.30	76.90	67.80	5.883	13.636	0.072	0.011
BB-12	234.90	735.70	11.00	10.90	75.40	437.00	91.50	228.20	2.567	3.224	0.146	0.025
BB-46	813.50	1230.70	14.00	13.60	13.50	637.90	95.10	202.30	8.554	6.084	1.037	0.021
BB-420	450.40	915.40	8.80	8.40	81.50	783.70	102.50	356.90	4.394	2.565	0.108	0.011
L-Tryptophan	5.70	4.90	12.00	61.40	45.00	2031.50	88.30	1993.00	0.065	0.002	0.267	0.030
D-Tryptophan	56.90	202.50	10.30	20.60	21.90	1129.50	82.50	871.90	0.690	0.232	0.470	0.018
L-Proline	†	6.00	14.80	57.70	88.90	2133.90	99.80	1938.00	†	0.003	0.166	0.027
D-Proline	5.90	4.00	15.80	69.10	92.60	2295.40	90.60	1911.90	0.065	0.002	0.171	0.030

DCs were stimulated in the presence or absence of LPS (0.1 mg/mL) with supernatants from 200 mL of bacterial cell-free supernatants or tryptophan enantiomers (10 mmol/L) for
14 hours. Nonprobiotic DSM-20021 and blank medium (CDM1) were used as negative controls. D/L-proline and L-Tryptophan were used as controls for D-tryptophan.
Less than the detection limit.

Generation of human monocyte-derived dendritic cells

Peripheral venous blood was obtained from healthy volunteers aged between 20 and 50 years after informed consent. Individuals with allergic disease, acute infection or taking any medication 20 days prior to blood sampling or any history of smoking smokers (personal interview) were excluded prior to blood sampling. All experiments were conducted according to the principles expressed in the Declaration of Helsinki. Peripheral blood mononuclear cells (PBMC) were isolated from heparinized whole blood by density gradient centrifugation (2000 rpm, 22 °C, 20 min) (Biocoll, Biochrom AG, Berlin, Germany). Adherent monocytes were obtained from PBMC via plastic adherence in 12-well plates (Nunc, Wiesbaden, Germany) in 1.5 mL very low endotoxin (VLE) RPMI 1640 medium (Biochrom AG, Berlin, Germany) supplemented with 5% human serum type AB (CELLect®, MP Biomedicals™, Eschwege, Germany) and 1% glutamine (Gibco® Invitrogen, Karlsruhe, Germany) for 1 h. Granulocyte macrophage colony-stimulating factor (GM-CSF) and Interleukin (IL)-4 (CellGenix, Freiburg, Germany) were added on days 1, 3, and 6 at 100 ng/mL and 20 ng/mL, respectively, yielding 2-3 x 10^6 immature DCs per well. Purity and viability of DCs was assessed by flow cytometry.

Human T cell line KM-H2

The human Hodgkin lymphoma T cell line (KM-H2) was purchased from the Leibniz Institute DSMZ-German Collection of Microorganisms and Cell Cultures, Braunschweig, Germany. 3-5 x 10^6 KM-H2 cells were grown in 4 mL RPMI 1640 per well in 6-well-plates (Nunc, Wiesbaden, Germany). All eukaryotic cells were cultured in 5% CO_2 at 37 °C (HeraCell 240 and Heraeus BDD 6220, Thermo Fisher Scientific, Waltham, USA). Viability of cells after treatment with bacterial supernatants was assessed by trypan blue, 7-AAD and Cell Titer-Blue® staining.

Isolation of intestinal lamina propria cells

Total colons were excised from mice, removed from mesenteries, opened longitudinally and cut into 2 cm long pieces that were incubated for 30 min in 30 mM EDTA in PBS on ice and then shaken vigorously with PBS to remove epithelial cells. After further cutting into small pieces with sharp scissors these were digested at 37 °C in RMPI supplemented with 1 mg/mL collagenase D (Roche Diagnostics, Mannheim, Germany) and 10 mg/ml DNAse I (Sigma-Aldrich, St. Louis, USA). Cells were separated by a 40/80% (w/v) Percoll (GE Healthcare,

Chalfont St. Giles, UK) density centrifugation step and washed prior to staining for flow cytometry analysis.

Differentiation of murine primary T cells

Murine spleens from female Balb/c mice were filtered through a 40 µm filter to generate single cell suspensions. These were then subjected to red blood cell lysis by using RBC lysis buffer (Biolegend, San Diego, USA) according to the manufacturer's recommendations. Afterwards, naïve $CD4^+$ T cells were isolated via magnetic-activated cell sorting (MACS) using the naïve $CD4^+$ T cell isolation kit (Miltenyi Biotec, Bergisch-Gladbach, Germany). The resulting naïve $CD4^+$ T cells were cultured in 96 wells plates ($1x10^6$ cells/ml Medium) in TexMACS medium supplemented with 10% FCS, 0.01 mM 2-Mercaptoethanol, rIL-2 (10 ng/ml) as well as MACSiBead particles with anti-CD3 and anti-CD28 ($1x10^6$ beads per $1x10^6$ cells) (all Miltenyi Biotec). Cells were differentiated over a period of 6 days towards Th1 (10 ng/ml IL12 and 10 µg/ml anti-IL4, derived from Cytobox Th1), Th2 (10 ng/ml Il4 and 10 µg/ml anti-Ifnγ, derived from Cytobox Th2) and Treg (5 ng/ml) (all Miltenyi Biotec). Differentiation of cells was assessed by flow cytometry, enhanced cytometric bead array (CBA) from cell culture supernatants and qRT-PCR. Prior to CBA and flow cytometry, cells were stimulated with monensin (0.7 µL/mL, BD Golgi Stop, BD Bioscience, Heidelberg, Germany) for 4 h at 37 °C in the presence of Ionomycin (500 ng/ml, Sigma Aldrich, Missouri, USA) and PMA (5 ng/ml, Sigma Aldrich, Missouri, USA).

Flow cytometry

Costimulatory molecules on human DCs

The following primary monoclonal antibodies were used: CD83 fluorescein isothiocyanate (FITC); CD1a phycoerythrin (PE); CD86-FITC; CD80-PE; CD14 allophycocyanine (APC); CD40-APC; CD3-peridinin chlorophyll protein (PerCP); HLA-DR-PerCP; mouse immunoglobulins G_1 (IgG_1) mouse immunoglobulins G_1 (IgG_1) κ were used as isotype controls using the corresponding fluorochromes (all purchased from BD Biosciences, Heidelberg, Germany). To account for donor dependent variability of DC surface markers, all data were normalized to the expression induced by LPS, which was set to 100% after subtraction of background values (FACS Canto, FACS DIVA software, Version 5.0.3, BD Biosciences, Heidelberg, Germany).

Murine DC subsets and CD4+ T cells

Single cell suspensions of splenocytes were obtained by filtering spleens through a 70 µm strainer. Samples were stained with CD3-PB (1:200, Biolegend, San Diego, USA), CD4-APC-H7 (BD, 1:400), CD11c- APC-Cy7 (1:100), Mhc-II-Percp-Cy5 (1:100), CD11b-FITC (1:100), CD80-AF647, CD40-APC (1:100). For intracellular cytokines, total spleen cells were stimulated with anti-CD3 (4 µg/mL, BD Bioscience, Heidelberg, Germany) and anti-CD28 (30 ng/mL, BD Bioscience, Heidelberg, Germany) for 16 h. $1x10^6$ of total lung cells were stimulated for 16 h with MACSiBead particles coated with anti-CD3 and anti-CD28 using the T cell activation/expansion kit (Miltenyi Biotec, Bergisch Gladbach, Germany) in TexMACS medium (Miltenyi Biotec) according to the manufactures recommendations. Prior to staining, cells were treated with monensin (0.7 µL/mL, BD Golgi Stop, BD Bioscience, Heidelberg, Germany) for 6 h at 37 °C and intracellularly stained for Il-4-PE (1:100, eBioscience, Vienna, Austria according to the manufacturer's protocols. Intracellular staining for Foxp3 was performed by using the Foxp3/Transcription Factor Staining buffer set (eBiosciences, Vienna, Austria) according to the manufacturer's recommendations.
The analysis was performed on an LSRII, with DIVA TM Software v8.0 (BD Bioscience, Heidelberg, Germany), kindly provided by the core unit fluorescence cytometry of the Research Center Borstel.

Assessment of cytokines by cytometric bead array

Levels of Il4, Il5 and Il13 were analysed in BALF and cell culture supernatants using an enhanced cytometric bead array (eCBA, Fex Set Kits, BD Biosciences, Franklin Lakes, New Jersey, USA) according to the manufacturer's guidelines.

Murine regulatory T cells

Cells were preincubated with Fc-Block (BD Bioscience, Heidelberg, Germany) for 5 min and stained for 20 min with the following antibodies: FITC-conjugated anti-CD3, Alexa-Fluor700-conjugated anti-CD4 and APC-eFluor780-conjugated CD45.2. For intracellular staining, cells were fixed and permeabilized with a commercially available fixation/permeabilization buffer (eBioscience, Vienna, Austria). LIVE/DEAD fixable Aqua dead stain kit (Invitrogen, Carlsbad, USA) was used prior to fixation. Intracellular staining was performed with PerCP-Cy5.5-conjugated anti-Foxp3 and Helios. Gates were set on live CD45+CD3+CD4+ T cells. All antibodies were from eBioscience (Vienna, Austria). Cells

were analyzed with a flow cytometer (Fortessa and LSRII, BD Bioscience, Heidelberg, Germany) and analyzed with Flowjo software (Flowjo LLC, Ashland, USA).

Quantification of CCL17 and cytokines in eukaryotic cell culture supernatants

CCL17 was quantified in cell culture supernatants of KM-H2 cells using ELISA reagent Quantikine CCL17/TARC, (R&D Systems, Minneapolis, USA) according to the manufacturer's instructions (ELISA reader MRXII, Thermo Fisher Scientifc, Waltham, USA).

For cytokine analyses, cell-free culture supernatants were collected from DCs after 24 h incubation with either probiotic supernatants or D-Tryptophan and were stored in aliquots at −80 °C before analysis. For probiotic supernatants, blank CDM1 was used as medium control. For D-Tryptophan we used L-Tryptophan, D- and L-Prolin as control. IL-5, IFN-gamma, IL-12, and IL-10, were quantified by a multiplex assay (Milliplex Human Cytokine Immunoassay, Millipore GMbH Schalbach, Germany) as described by the manufacturer.

Bioassay-guided fractionation of probiotic supernatants and structural elucidation of D-Tryptophan

A detailed description of the methods used is shown in Chapter 3 of this thesis.

Enantiomeric separation of D-Tryptophan in murine sera

The investigator (C.M.) was blinded to the murine intervention groups. Due to the abundance of interfering proteins a protein precipitation was done. For this purpose, the sera were thawed on ice and 20 µL of each sample were vigorously shaken with 80 µL at 4 °C methanol (Chromasolve, Fluka, St. Louis, USA) and centrifuged (15,000 x g at 4 °C for 15 min). The supernatants were taken, evaporated and resolved in water before injection. The derivation was performed as described for bacterial supernatants with some modifications as published (2). For quantification human serum was spiked with different concentrations (0.005-0.15 µg/mL) of D-Tryptophan and randomly analyzed. The enantiomeric ratio (peak area D-Tryptophan/peak area L-Tryptophan) was calculated and was observed to follow a linear regression ($y=0.0406x+0.0102$, $R^2>0.98$).

(2) Fonseca J.R., Müller C., Rock T.M., Krauss-Etschmann S., Schmitt-Kopplin P., 2014. Enantioseparation and selective detection of D-amino acids by ultra-high-performance liquid chromatography/mass spectrometry in analysis of complex biological samples. J Chromatogr A. 1324:109–14.

Induction of allergic airway inflammation

Female 6–8-week-old Balb/c mice (Charles River Laboratories, Wilmington, USA) were sensitized i.p. using 10 µg of ovalbumin (grade VI; Sigma Aldrich, St. Louis, USA) or PBS (controls) in alum (Pierce Chemical Co, Rockfort, USA) at day 0, 7 and 14 and challenged intranasally under isoflurane narcosis with 10 µg of ovalbumin in 20 µl PBS or PBS only (controls).

Lung Function

Animals were anesthetized i.p. with ketamine (140 mg/kg) and xylazine (7 mg/kg), tracheostomized, intubated (18G tube), placed on a warming plate and ventilated with a tidal volume of 10 mL/kg at a frequency of 150 breaths/minute and a positive end-expiratory pressure of 2 cm H_2O on a Buxco R/C system (Buxco Reseach Systems, Wilmington, USA). To assess airway hyperreactivity, the mice were challenged with metacholine in physiological saline generated with an in-line nebulizer and administered directly with increasing concentrations (0, 12.5, 25, 50 mg/mL) by the ventilator for 20 seconds. Resistance (R) and Compliance (C) were measured continuously for 2 min and the average was calculated and plotted against concentration.

Gene expression analysis in murine fetal lungs

Fetal lungs were collected from animals delivered via cesarean section at embryonic day 18.5 (Balb/c). Total RNA was isolated employing the miRNeasy Mini (Qiagen, Venlo, Netherlands) including digestion of remaining genomic DNA. The Agilent 2100 Bioanalyzer (Agilent Technologies, Santa Clara, USA) was used to assess RNA quality and only high-quality RNA (RIN $\geq$ 8.7) was used for microarray analysis. For mRNA profiling, 30 ng total RNA was amplified using the Ovation PicoSL WTA System V2 in combination with the Encore Biotin Module (Nugen, San Carlos, USA). Amplified cDNA was hybridized on an Affymetrix Mouse Gene ST 2.1 array plate. Staining and scanning was done according to the Affymetrix expression protocol including minor modifications as suggested in the Encore® Biotin protocol (NuGen, San Carlos, USA).

Bacterial 16S rRNA gene amplification and diversity analysis

Diversity analysis of 16S rRNA genes was performed by amplicon sequencing. In the first PCR reaction, bacterial genomic DNA was subjected to 16S rRNA gene amplifications using the primer S-D-Bact-0785-a-S-18[5'-GGMTTAGATACCCBDGTA-3'] and S-*-Univ-

1100-a-A-15 [5'-GGGTYKCGCTCGTTR-3'] as already mentioned. The reaction mixture of 25 µL in total was composed of 5 ng x µL-1 template DNA, 10 µM of each primer, 10 mM dNTPs (Fermentas, Vilnius, Lithuania), 5% of dimethyl sulfoxide (Sigma-Aldrich, St. Louis, USA), 5 U x µL-1 of FastStart High Fidelity Polymerase (Roche Diagnostics, Mannheim, Germany), 10x FastStart Buffer, and nuclease-free water (Life Technologies, Carlsbad, CA, USA). The PCR started with an initialization at 95 °C for 5 min, followed by 28 cycles of denaturation at 94 °C for 45 sec, annealing at 44 °C for 45 sec, and elongation at 72 °C for 45 sec. A final elongation step at 72 °C for 5 min completed the PCR reaction. To minimize contamination with primer dimers, generated fragments were cut out of the gel after standard agarose gel electrophoresis and purified with the NucleoSpin Gel and PCR Clean-up Kit (Macherey-Nagel, Düren, Germany).

During the second PCR, Illumina sequencing adapters as well as dual indices were attached to the purified amplicons using the Nextera XT Index Kit (Illumina, San Diego, CA, USA). The reaction volume was 50 µL in total and contained 5 µL of genomic DNA, 5 µL of each Nextera XT Index Primer, 25 µl 2x KAPA HiFi HotStart ReadyMix (Kapa Biosystems, Wilmington, MA, USA), and 10 µL of nuclease-free water (Life Technologies, Carlsbad, CA, USA). The PCR reaction was performed according to the following thermal profile: 95 °C for 3 min, followed by 8 cycles of 95 °C for 30 sec, 55 °C for 30 sec, 72 °C for 30 sec, and finalized by 72 °C for 5 min. The PCR products were cleaned up with the Agencourt AMPure XP system (Beckman Coulter, Brea, CA, USA), DNA was quantified and the DNA quality was controlled using the 2100 Bioanalyzer Instrument (Agilent Technologies, Santa Clara, CA, USA), and sequenced with the MiSeq instrument (Illumina, San Diego, CA, USA).

Gene expression analysis

Total RNA was isolated from homogenized lung tissue or cell culture using the miRNeasy Micro Kit according to manufacturer´s instructions (Qiagen, Venlo, Netherlands). Concentrations were determined using a NanoDrop® ND-1000 (NanoDrop Technologies, Erlangen, Germany) spectrophotometer. mRNA was transcribed to cDNA with the QuantiTect Rev. Transcription kit (Qiagen, Venlo, Netherlands) and PCR for specific genes was performed on a LightCycler 480 platform with Light Cycler 480 SYBR Green I Mastermix (Roche, Mannheim, Germany).

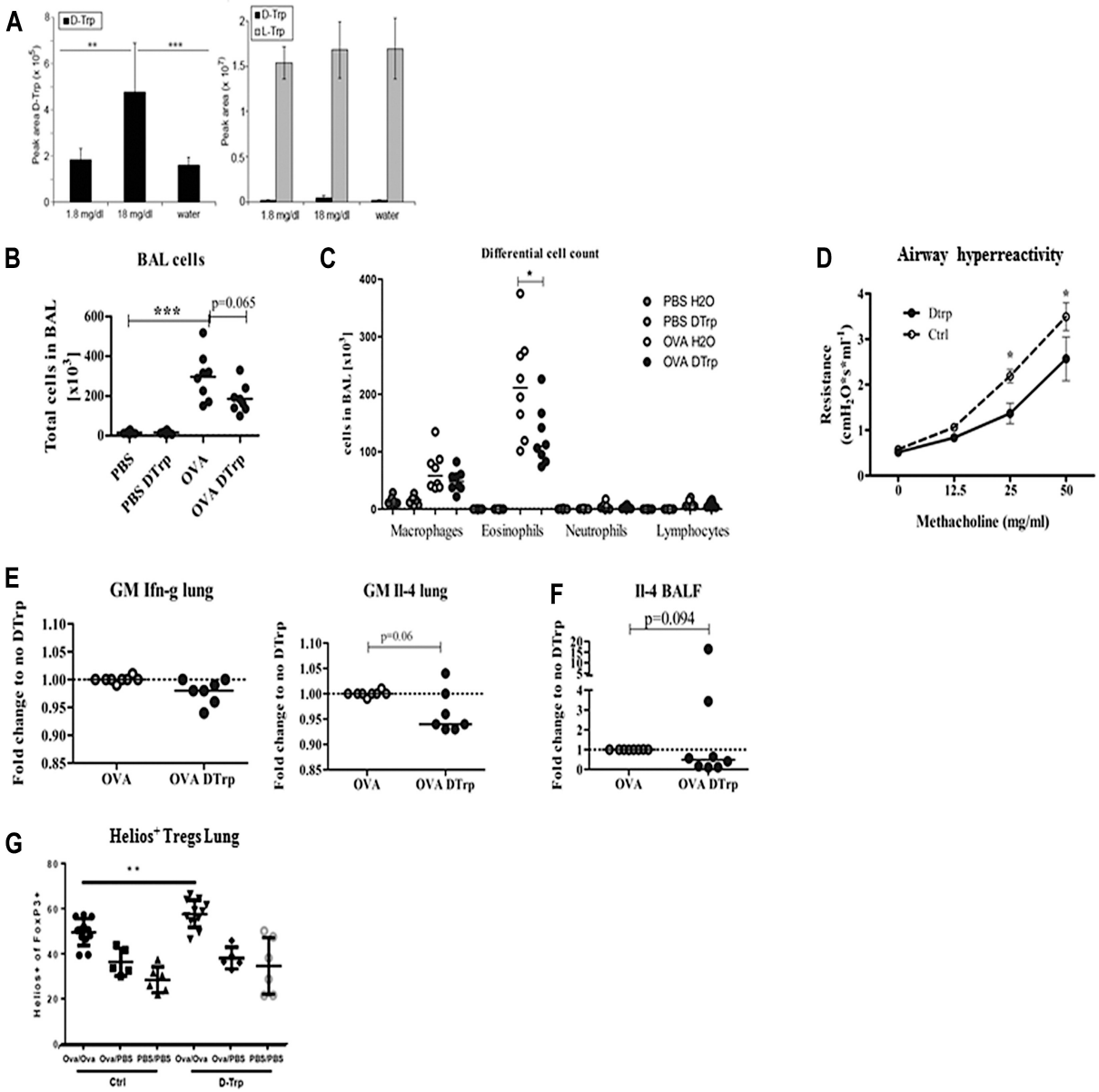

Figure S 1. Oral D-tryptophan reduces allergic airway inflammation. A, Serum D-tryptophan in mice receiving D-tryptophan (50 mmol/L) in drinking water or water only (ultraperformance liquid chromatography mass spectrometry peak areas). Note the different scales for D-tryptophan (solid bars) and L-tryptophan (shaded bars). ***P* = .006 and ****P* = .004, Welch Test, mean ± SD. B, Total number of cells in bronchoalveolar lavage fluid (*BAL*). C, Differential cell count. D, Measurement of airway resistance to increasing doses of methacholine (2-way ANOVA with the Bonferroni posttest). E, Geometric mean (fold change) of Ifn-g and Il-4 in lung-derived $CD3^+CD4^+$ lymphocytes. F, Il-4 levels in bronchoalveolar lavage of mice, as assessed by using a Cytometric Bead Array. G, Helios-positive Treg cells of lung-derived $CD3^+CD4^+Foxp3^+$ lymphocytes. Student *t* test: **P* < .05, ***P* < .01, and ****P* < .001. Fig 5, *B, C, E* and *F*, n = 8 mice per group, Mann-Whitney *U* test, median ± SD, **P* < .05, ****P* < .001, and Fig 5, *D* and *G*, n = 6 to 12 mice per group.

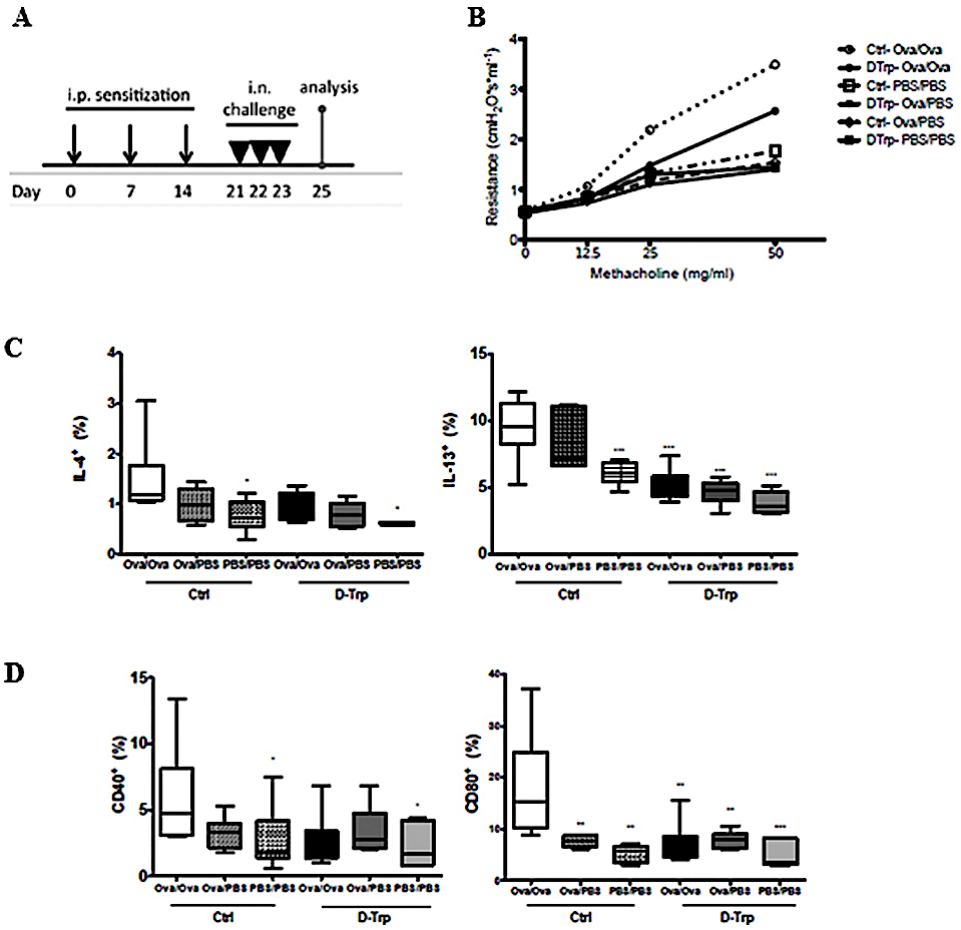

Figure S 2. Oral D-Tryptophan supplementation ameliorates allergic airway inflammation. A, Treatment scheme for induction of allergic airway inflammation, D-Trp was supplied in drinking water from day -3 in respective groups. B, Measurement of airway resistance to increasing doses of methacholine. C, Percent Il-4^{+} and Il-13^{+} cells within spleen CD3^{+}CD4^{+} T cells. D, CD40^{+} and CD80^{+} on spleen CD11b^{high}DCs, Box and whisker plots: Maximum and minimum values (whiskers), the upper and lower quartiles (boxes) and median (horizontal line). (A) 7-8 mice/group, mean ± SD, Two-way ANOVA with Bonferroni post-test. **P*<0.05, ****P*<0.001.

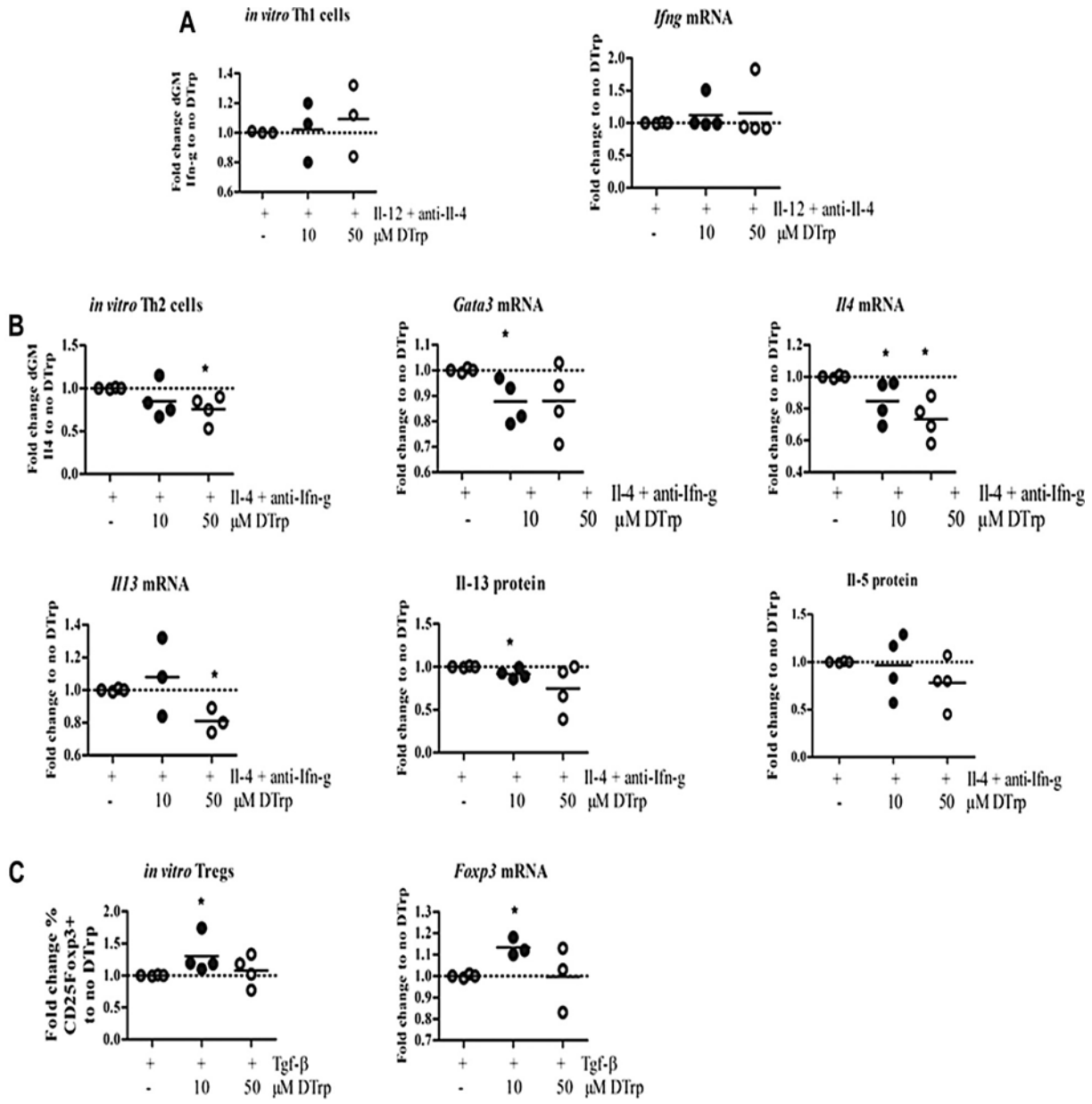

Figure S 3. D-tryptophan (DTrp) influences *in vitro* primary T-cell differentiation. Primary murine splenocytes were differentiated toward T_H1 (A), T_H2 (B), and Treg (C) cells with respective cytokine mixes in the presence of 0, 10, or 50 µmol/L D-tryptophan (dissolved in water). Differentiation was assessed by means of flow cytometry, quantitative RT-PCR, and the Cytometric Bead Array for Il-13 and Il-5 protein levels from culture supernatants. Graphs depict fold changes to differentiated cells not treated with D-tryptophan. $*P < .05$, n = 3 to 4 independent experiments, Mann-Whitney *U* test.

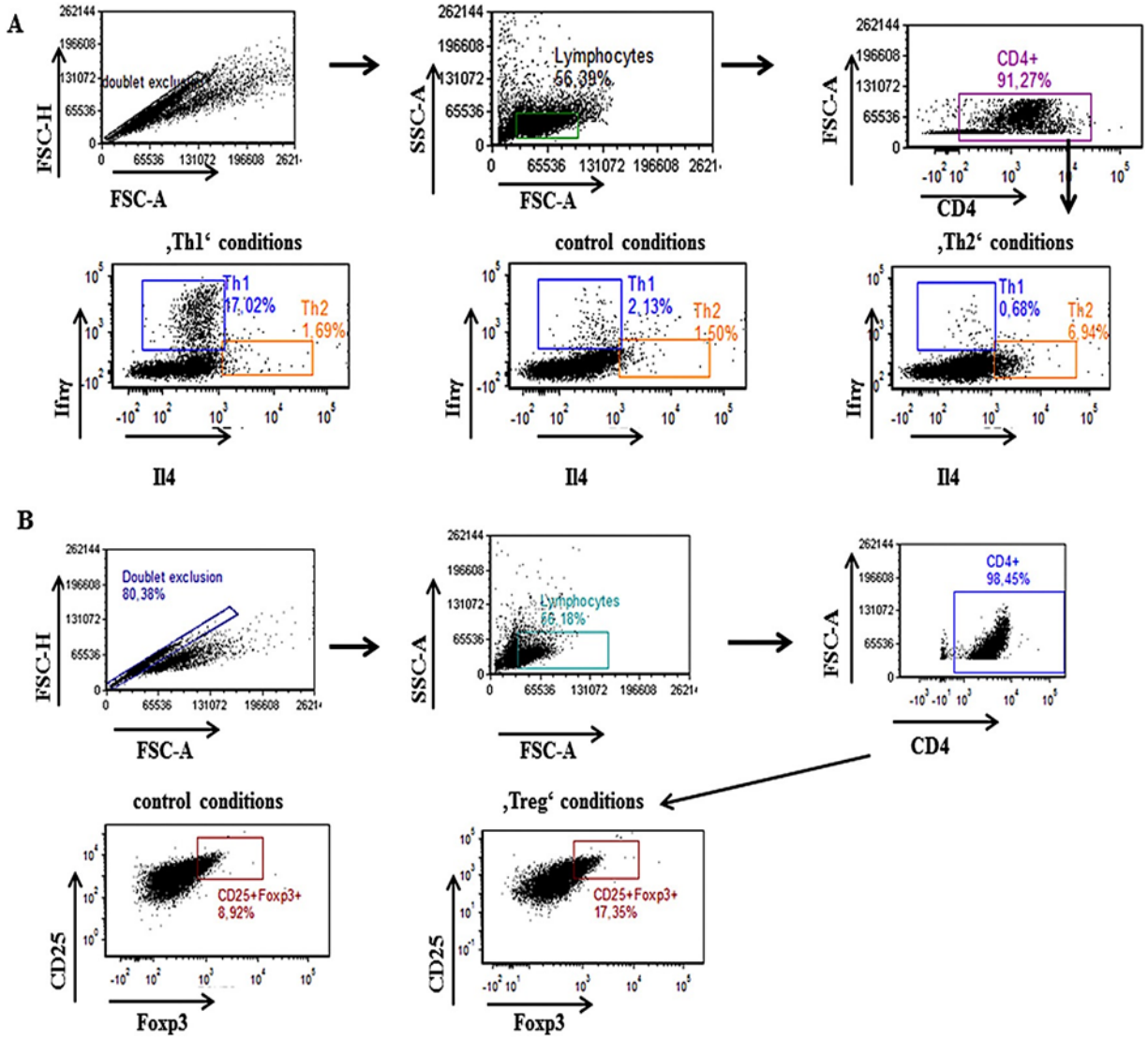

Figure S 4. *In vitro* differentiation of primary T cells. Murine naïve $CD4^+$ cells were differentiated *in vitro* for 6 days with respective cytokines. Gating strategy for analysis of (A) Th1 & Th2 cells as assessed by $CD4^+Ifny^+$ or $CD4^+Il4^+$, respectively, and induced Tregs as $CD4^+CD25^+Foxp3^+$ cells (B). Representative images of n=4 independent experiments.

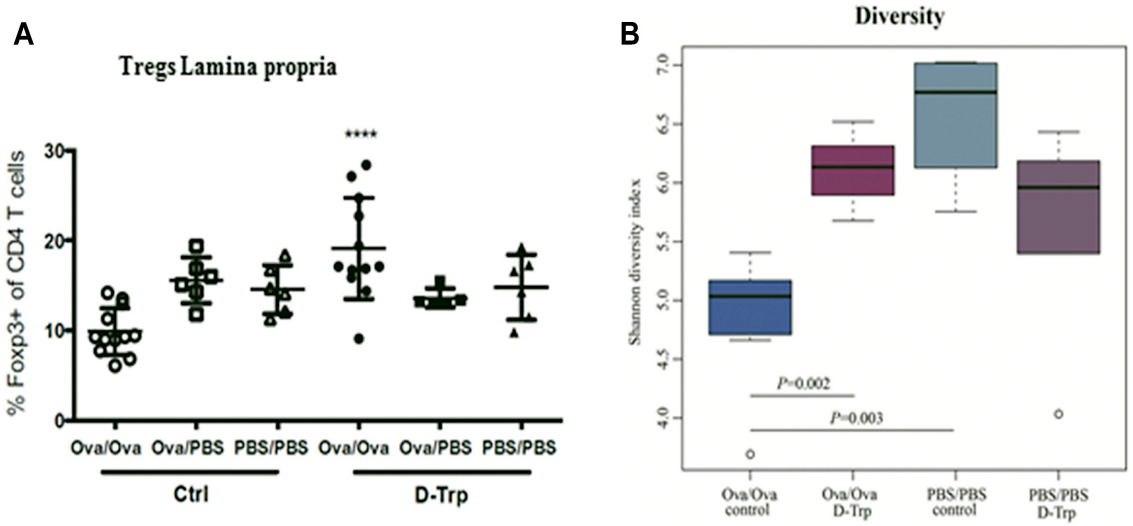

Figure S 5. Oral D-tryptophan (DTrp) supplementation increased gut Treg cell numbers and the intestinal bacterial community in mice with AAI. A, Percentage of Foxp3$^+$ cells within CD3$^+$CD4$^+$ T cells in the lamina propria of the colon. ****$P < .0001$, n = 6 to 12 mice per group, Student *t* test. B, α-Diversity of bacterial communities. Shannon diversity index was used to estimate bacterial diversity for each treatment (Wilcoxon rank sum test).

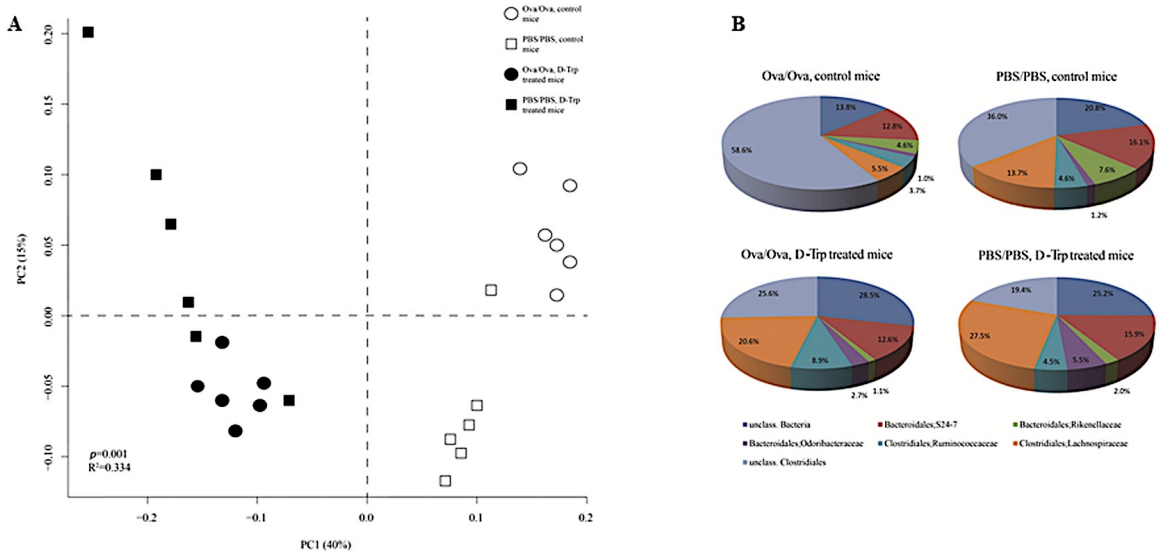

Figure S 6. Influences of D-Tryptophan supplementation on the intestinal bacterial composition in healthy and diseased mice. A, an unweighted UniFrac distance matrix based on OTU counts was used to perform Principal Coordinate Analysis (PCoA). The generated scatterplot indicates dissimilarities between individual samples. Statistical significance was determined with Student's *t* test, P=0.001. All results are based on 95%-similarity OTUs. OTU, operational taxonomic unit. PC, principal coordinate. Ova, ovalbumin. PBS, phosphate buffered saline. B, Proportion of dominant bacteria (>0.05% abundance) in the intestinal tract of healthy and diseased mice. Pie charts were generated to visualize the relative distribution of the most abundant bacteria at the family level